Universidade de Aveiro Departamento de Engenharia Civil
Ano 2013

ANA FRAGATA DA COSTA

REVESTIMENTOS COMPATÍVEIS PARA ALVENARIAS ANTIGAS SUJEITAS A AÇÃO SEVERA DA ÁGUA

Universidade de Aveiro Departamento de Engenharia Civil
Ano 2013

ANA FRAGATA DA COSTA

REVESTIMENTOS COMPATÍVEIS PARA ALVENARIAS ANTIGAS SUJEITAS A AÇÃO SEVERA DA ÁGUA

Tese elaborada no Laboratório Nacional de Engenharia Civil (LNEC) e apresentada à Universidade de Aveiro para cumprimento dos requisitos necessários à obtenção do grau de Doutor em Engenharia Civil, realizada sob a orientação científica da Doutora Engenheira Maria do Rosário da Silva Veiga, Investigadora Principal com Habilitação do Laboratório Nacional de Engenharia Civil e da Professora Doutora Ana Luísa Lomelino Velosa, Professora Associada do Departamento de Engenharia Civil da Universidade de Aveiro

Apoio financeiro da FCT e do FSE no âmbito do III Quadro Comunitário de Apoio e da FRADICAL Lda.

o júri

presidente

Prof. Doutora Ana Isabel Couto Neto da Silva Miranda
professora catedrática da Universidade de Aveiro

Prof. Doutor Rob van Hees
professor catedrático da Universidade Técnica de Delft - Holanda

Prof. Doutora Maria Paulina Santos de Faria Rodrigues
Professora associada da Universidade Nova de Lisboa

Prof. Doutor Victor Miguel Carneiro de Sousa Ferreira
professor associado da Universidade de Aveiro

Doutora Maria do Rosário da Silva Veiga
investigadora principal com habilitação do Laboratório Nacional de Engenharia Civil

agradecimentos

À Fundação para a Ciência e Tecnologia (FCT) e à Fabrica de Transformação de Cal Lda. (Fradical Lda.) pelo financiamento no âmbito da bolsa de doutoramento em empresa da FCT.

À Direção do Laboratório Nacional de Engenharia Civil (LNEC), por me colocar à disposição todas as condições necessárias para a realização deste trabalho. Em particular agradeço ao Departamento de Edifícios e ao seu Diretor, Engenheiro Jorge Grandão Lopes pelos oportunos conselhos e pelo rigor na correção de trabalhos desenvolvidos.

À Reitoria da Universidade de Aveiro e ao Departamento de Engenharia Civil, por me permitirem realizar este trabalho no âmbito do Doutoramento em Engenharia Civil dessa Universidade.

Às minhas orientadoras científicas Engenheira Maria do Rosário Veiga e Professora Ana Luísa Velosa, um especial agradecimento, pela constante disponibilidade, incansável orientação científica, exigência, incentivo, otimismo e por me disponibilizarem as condições para o desenvolvimento do trabalho. Em especial agradeço a amizade que constituiu um valoroso incentivo e estímulo.

Ao meu orientador empresarial Engenheiro Fernando Cartaxo, pela atitude construtiva, debate científico e técnico, constante disponibilidade pessoal e de meios e por ter encetado valiosas perspetivas e dimensões no desenvolvimento do trabalho.

Às colegas Dr.ª Martha Tavares e Eng.ª Sofia Malanho, pelo persistente apoio, críticas, comentários, sugestões, correções e conselhos que me foram dando ao longo da tese. Acima de tudo, agradeço a grande amizade.

Aos colegas Sr. Bento Sabala, Sr.ª Ana Maria Duarte e Sr. Luís Carmo, que muito me ajudaram na execução da campanha experimental desde o seu início.

Aos colegas Eng.º Cláudio Cruz e Eng.º Hildebrando Cruz pelo apoio e conselhos que foram dando ao longo deste trabalho.

Aos colegas Dr. Giovanni Borsoi, Eng.º Sandro Botas e Dr.ª Sílvia Costa que partilharam sugestões e ideias.

Ao Eng.º Carlos Pina dos Santos, Dr. Luís Matias e Eng.º António Vilhena pela disponibilidade na partilha de ideias e pela ajuda no desenvolvimento da monitorização de alguns ensaios deste trabalho.

Aos restantes colegas do NRI e do DED do Laboratório Nacional de Engenharia Civil.

agradecimentos

No Núcleo de Materiais Metálicos (NMM) do LNEC, ao Dr. Santos Silva pelo auxílio, colaboração científicos e disponibilidade demonstrada ao longo deste trabalho. À Dr.ª Paula Menezes agradeço a disponibilidade na execução e interpretação dos resultados das observações ao MEV. À Dr.ª Luzia Barracha e Sr.ª Fátima Meneses pela colaboração prestada durante as diversas análises químicas efetuadas.

Ao Departamento de Engenharia Civil da Universidade Técnica da Dinamarca (DTU), por ter permitido o estágio na instituição disponibilizando meios, equipamentos e instalações.

À Professora Lisbeth Ottosen da DTU, agradeço o empenho e disponibilidade constante, ajuda na interpretação de resultados, assim como a disponibilização dos recursos e meios para a realização dos ensaios de dessalinização eletrocinética. À Professora Iben Christensen e à Ebba Schneel pela disponibilidade e auxílio na realização dos ensaios na DTU.

Ao Ricardo, amigo e companheiro que se viu privado da minha disponibilidade e companhia.

Aos meus pais, por tudo e por terem cuidado com carinho da minha filha na minha ausência.

palavras-chave humidade ascensional, revestimentos compatíveis, sais solúveis, degradação salina, alvenarias antigas.

resumo

Uma das maiores causas de degradação dos revestimentos é a presença de sais solúveis, tanto nas zonas costeiras como nas zonas continentais. Estes sais podem ter origens distintas, tais como: humidade ascensional, nevoeiro salino, inundações ou ainda estarem presentes nos próprios materiais, como é o caso da utilização de areias mal lavadas. O local onde os sais cristalizam é dependente do tipo de transporte entre a alvenaria e o revestimento, assim como da severidade da envolvente ambiental (temperatura e humidade relativa).

Com esta tese pretende-se desenvolver revestimentos de substituição compatíveis, eficazes e duráveis para alvenarias antigas sujeitas à ação severa da água (humidade ascensional através das fundações com elevada concentração de NaCl); desenvolver ensaios de envelhecimento acelerado baseados em ciclos de dissolução e cristalização que permitam simular a ação severa da água; perceber a influência de revestimentos com caraterísticas extremas de permeabilidade ao vapor de água aplicados nas duas faces do mesmo suporte (argamassas de cimento e resina versus argamassas de cal), e sujeitos à ação severa da água; perceber a influência de vários fatores, tais como : rasgos verticais contínuos executados no emboço e a utilização de hidrófugo no reboco no desempenho dos vários sistemas de revestimento desenvolvidos, quando sujeitos à ação severa da água;; utilizar a remoção eletrocinética de sais, em provetes simulando a influência da alvenaria e dos revestimentos, com o objetivo de reduzir a sua concentração de NaCl, para que no futuro possa ser aplicado de forma eficaz em paredes de edifícios antigos, enquanto ação de manutenção, e desta forma aumentar a durabilidade dos revestimentos.

Para atingir os objetivos descritos, foram considerados: i) o desenvolvimento de provetes que permitam considerar os sistemas de revestimento desenvolvidos nesta tese e o suporte, e que simulem uma alvenaria revestida em ambas as faces, e com os quais seja possível a simulação da ação severa da água em laboratório e, ii) o desenvolvimento ciclos de dissolução e cristalização numa parede de grandes dimensões existente em laboratório, que permitam simular a ação severa da água em condições tão reais quanto possível.

O objetivo final deste estudo é o desenvolvimento de um revestimento de substituição denominado “emboço ventilado” para paredes de edifícios antigos com revestimentos degradados devido à presença de humidade ascensional e sais solúveis. Pretende-se que este sistema de revestimento, composto por duas camadas de revestimento (camada base e reboco), seja compatível, durável e eficaz, e que funcione como um sistema de acumulação no qual os sais cristalizem na camada base do sistema de revestimento (executada com rasgos verticais) e não na alvenaria ou na camada exterior.

keywords rising damp, compatible renders, soluble salts, salt damage, historic masonry.

abstract

Salt damage is one of the major causes of render decay, not only near the sea but also in continental areas. These salts can appear in the walls from different sources: from the ground due to rising damp, carried by the wind as salt spray, by flooding, or they can originally be present in materials as is the case of unwashed beach sand. Salts can crystallize depending on the salt transport behaviour of the substrate/render and the surrounding environmental conditions (temperature and relative humidity).

In the present thesis the following objectives were drawn: the development of compatible, efficient and durable replacement renders for historic constructions when submitted to severe action of water (capillary rising water through foundations with high content of NaCl); the improvement of dissolution and crystallization ageing tests able to simulate the severe action of water; to understand the influence of renders with water vapour extreme characteristics applied in the same support (cement and resin renders vs lime renders), submitted to severe action of water; to understand the influence of several factors, such as: vertical grooves in base layer and water repellent in the outer layer in the render systems performance when submitted to the severe action of water; application of electrocinetic removal of salts method to small scale specimens in order to reduce the NaCl content, as a way to allow in the future an efficient use in old buildings masonry walls, as a maintenance action to improve renders durability.

In order to achieve the drawn objectives, were considered: i) the development of small scale specimens considering the render systems developed in this thesis and the support, simulating a rendered masonry in both larger faces, when submitted to severe action of water and ii) the development of dissolution-crystallization cycles in a full scale masonry wall existent in laboratory, able to simulate the severe action of water in real conditions.

The final goal of this study is the development of a replacement render system called “ventilated render” (“*emboço ventilado*” in Portuguese) for historic constructions with renders damaged due to high moisture content and the presence of soluble salts. The ventilated render has two layers (base and external layer) which are supposed to act as an accumulating system in which the salt is induced to crystallize in the base layer (executed with vertical grooves) of the render and not in the masonry nor in the external layer.

ÍNDICE DE TEXTO / LIST OF CONTENTS

ÍNDICE DE TABELAS / LIST OF TABLES

ÍNDICE DE FIGURAS / LIST OF FIGURES

1. INTRODUÇÃO

1.1 Importância e justificação do tema

Esta tese insere-se na área de revestimentos de paredes de edifícios, focando o desenvolvimento de um sistema de revestimento para alvenarias antigas, resistente à ação severa da água. Este sistema de revestimento, denominado por “emboço ventilado”, foi desenvolvido para aplicação, como revestimento de substituição, em alvenarias de edifícios antigos na presença de humidade ascensional e elevado teor de sais (NaCl).

A humidade ascensional pode ser considerada uma das maiores causas da degradação das paredes de edifícios antigos. A humidade ascensional surge devido à sucção dos materiais porosos das paredes (alvenarias e revestimentos). A afinidade da água com os materiais porosos e a inexistência de cortes capilares permitem que a humidade presente no terreno ascenda facilmente através das paredes. A presença de humidade ascensional com elevados teores de sais (dissolvidos ou presentes nos materiais com os quais entra em contato) torna a humidade ascensional um dos maiores mecanismos de degradação. O tratamento da humidade ascensional num edifício antigo é muito complexo principalmente devido à elevada heterogeneidade e espessura das paredes e ao caráter estrutural dessas paredes. Existem várias técnicas desenvolvidas para minimizar os efeitos da humidade ascensional; no entanto muitas delas apresentam-se de difícil aplicação e, portanto, ineficazes.

Os sais solúveis podem estar presentes nas paredes em elevadas quantidades, tendo como origem a humidade ascensional quando existe elevado teor de sais no solo (em edifícios antigos, monumentos ou fortes em zonas costeiras), transportados como nevoeiro salino pelo vento (como é o caso dos edifícios localizados em zonas marítimas) ou ainda presentes nos próprios materiais (como é o caso na presença de ligantes com elevados teores de sais solúveis e utilização de areias mal lavadas ou água proveniente de fontes com elevado teor de sais). Em Portugal a degradação associada à presença de sais e humidade ascensional (considerada aqui uma ação severa da água), como é o caso de edifícios localizados em zonas costeiras, tem-se demonstrado especialmente severa ao nível dos revestimentos das alvenarias.

Nos edifícios localizados em zonas próximas da costa, facilmente são desenvolvidas condições favoráveis à cristalização dos sais (em especial o NaCl) – variações na humidade relativa e temperatura -, originando ciclos repetidos de dissolução e cristalização. A cristalização dos sais acontece na zona de evaporação e pode ocorrer sob a forma de: i) eflorescências originando perda de coesão do material ou lacunas, ou ii) sob a forma de criptoflorescências o que poderá dar origem ao destacamento de várias camadas do revestimento ou mesmo ao destacamento do revestimento do suporte.

Os sais podem continuar a cristalizar devido a variações da humidade relativa e da temperatura da envolvente (sendo que este último fator promove a evaporação e consequente cristalização) originando efeitos estéticos nefastos no revestimento ou mesmo a degradação da alvenaria.

A utilização de revestimentos de substituição incompatíveis (como é o caso da utilização de ligantes hidráulicos) pode originar tensões excessivas na alvenaria, introduzir sais solúveis ou ainda reduzir a evaporação, retendo a humidade e os sais na alvenaria o que poderá originar aí a sua cristalização e assim desenvolver a degradação precoce. Estes revestimentos (preferencialmente com base em ligantes aéreos, sempre que possível) devem ser compatíveis com os materiais pré-existentes, o mais duráveis possível tendo em consideração a ambiência da envolvente, e eficazes no seu desempenho. No entanto estes revestimentos compatíveis demonstram ser pouco duráveis quando sujeitos à cristalização de sais e, consequentemente, à ação severa da água descrita no âmbito desta tese.

Para lidar com as situações de ação severa da água, em que existe humidade ascensional e sais solúveis, acrescidas de condições ambientais favoráveis à cristalização dos sais, como é o caso de muitos edifícios antigos localizados em zonas costeiras ou próximos dela, surgiu a necessidade de se desenvolver um sistema de revestimento de acumulação compatível, durável e eficaz. Existem alguns revestimentos de acumulação disponíveis no mercado e com princípios de funcionamento que poderão ser considerados adequados (compatíveis), quando testados em laboratório, mas cuja eficácia e durabilidade carece ainda de ser testada tendo em conta o suporte e a ação severa da água considerada nesta tese.

Pretende-se desenvolver, no âmbito desta tese, um sistema de revestimento de acumulação de sais inovador para alvenarias de edifícios antigos, denominado por “emboço ventilado”, e testá-lo quanto à sua compatibilidade com os elementos pré-existentes, eficácia na acumulação de sais e na prevenção da cristalização na alvenaria e durabilidade, considerando outras soluções de revestimento igualmente compatíveis com os materiais pré-existentes, contribuindo para a boa aparência exterior. Este sistema é composto por duas camadas (emboço e reboco), sendo o emboço executado com rasgos verticais contínuos com o objetivo de aumentar a evaporação e consequente cristalização de sais na superfície exterior dos rasgos em contato com o ambiente, e reduzir a cristalização no suporte e na superfície do reboco exterior.

O desenvolvimento desta tese, pela sua pertinência, foi co-financiada pela Fradical – Fábrica de Transformação de Cal – e pela FCT – Fundação para a Ciência e Tecnologia -, no âmbito do doutoramento em empresa, com a referência SFRH/33800/2009.

1.2 Objetivos

Com esta tese pretende-se desenvolver revestimentos de substituição compatíveis, eficazes e duráveis para alvenarias de edifícios antigos, localizados em Portugal, quando sujeitas à ação severa da água.

Para atingir este objetivo principal são definidos três objetivos parciais:

- Definição das principais anomalias e determinação das causas, em revestimentos de edifícios antigos Portugueses;

- Estudo da possibilidade de aplicação de uma ação de manutenção com vista ao aumento da durabilidade de revestimentos quando sujeitos à ação severa da água;

- Desenvolvimento de um revestimento de substituição durável, eficaz e compatível para edifícios antigos,sujeitos à ação severa da água.

A metodologia seguida para atingir os objetivos é:

- Aplicação de uma metodologia de diagnóstico para determinação das anomalias e respetivas causas, em revestimentos de edifícios antigos Portugueses;

- Utilizar a remoção eletrocinética de sais, em provetes simulando a influência da alvenaria e dos revestimentos, com o objetivo de reduzir a sua concentração de NaCl, para que no futuro possa ser aplicado de forma eficaz em paredes de edifícios antigos, enquanto ação de manutenção, e desta forma aumentar a durabilidade dos revestimentos.

- Desenvolver provetes (maquetas de pequenas dimensões – tijolos maciços revestidos em ambas as faces de maiores dimensões) que permitam considerar não apenas os sistema de revestimento, mas também o suporte e que simulem uma alvenaria revestida em ambas as faces, e com os quais seja possível a simulação da ação severa da água (humidade ascensional através das fundações com elevada concentração de NaCl), em laboratório;

- Desenvolver ensaios de envelhecimento acelerado baseados em ciclos de dissolução e cristalização que permitam simular a ação severa da água (humidade ascensional através das fundações com elevada concentração de NaCl) e posterior secagem, dando origem a ciclos de dissolução/cristalização do NaCl com os quais se consiga obter, por um lado, a degradação acelerada dos revestimentos e, por outro lado, representar a degradação real que seria obtida com a ação severa da água.

- Perceber a influência de revestimentos com caraterísticas extremas de permeabilidade ao vapor de água aplicados em conjunto no mesmo suporte (revestimentos com base em argamassas de

cimento versus argamassas de cal), e sujeitos à ação severa da água (humidade ascensional através das fundações com elevada concentração de NaCl) quanto: i) à cristalização no suporte e degradação deste e ii) à cristalização e degradação dos próprios revestimentos.

- Perceber a influência dos rasgos verticais contínuos executados no emboço, a utilização de hidrófugo no reboco e a utilização de pó de tijolo na argamassa, no desempenho dos vários sistemas de revestimentos (constituídos por duas camadas de argamassas de cal – emboço e reboco) desenvolvidos no âmbito desta tese, quando sujeitos à ação severa da água;

- Desenvolver ciclos de dissolução e cristalização numa parede de grandes dimensões existente em laboratório, que permitam simular a ação severa da água em condições tão reais quanto possível.

- Desenvolver o sistema de revestimento de acumulação denominado “emboço ventilado” para alvenarias antigas sujeitas à ação severa da água e aferir a sua compatibilidade, durabilidade e eficácia;

1.3 Organização da tese

A dissertação está organizada em oito capítulos:

Capítulo 1 (Introdução) – Apresenta um texto introdutório, fundamenta o tema selecionado, assim como os objetivos que se pretendem alcançar no final do estudo.

Capítulo 2 (Revestimentos para alvenarias antigas sujeitas à ação severa da água: Revisão da literatura) – Inclui pesquisa bibliográfica e compilação de informação sobre a área de revestimentos compatíveis para alvenarias antigas sujeitas à ação severa da água. Neste capítulo ainda é apresentado o levantamento das principais formas de anomalias em revestimentos de alvenarias antigas, assim como as soluções conhecidas para minimização dos efeitos da ação severa da água nos revestimentos e alvenarias antigas.

Capítulo 3 (Damage due to the severe action of salt laden water: Results of case studies) – Apresenta os casos de estudo sobre revestimentos de edifícios antigos sujeitos à ação severa da água. Neste capítulo é apresentada uma metodologia de diagnóstico para determinar as causas das anomalias nos revestimentos antigos (pré-existentes) assim como nos novos revestimentos degradados devido à ação severa da água (elevado teor de humidade e sais solúveis). Finalmente apresentam-se soluções para minimização dos efeitos da ação severa da água que passam pela introdução de barreiras físicas assim como pela seleção dos revestimentos de paredes mais adequados em cada caso.

Capítulo 4 (Electric DC field for removal of NaCl from rendered bricks) – Inclui a aplicação de um método inovador para remoção de sais através da aplicação de corrente elétrica. Este método foi aplicado em maquetas de pequenas dimensões (tijolos maciços revestidos com algumas das soluções de revestimento definidas nos capítulos 4 e 5). Esta parte do trabalho experimental foi desenvolvida na Universidade Técnica da Dinamarca sob orientação da Prof.ª Lisbeth Ottosen.

Capítulo 5 (Influence of substituion renders) – É o primeiro capítulo referente à campanha experimental em laboratório. Incluí soluções de revestimento com caraterísticas extremas em termos de permeabilidade à água sujeitas à ação severa da água. São apresentados os ensaios definidos para simular a ação severa da água, em maquetas de pequenas dimensões compostas por tijolos furados revestidos com as soluções de revestimento, através dos quais é possível concluir sobre a sua ação na degradação dos próprios revestimentos assim como do suporte.

Capítulo 6 (Definition of a substituion render system “emboço ventilado” - Laboratorial work) – Apresentam-se as formulações de argamassas da Fradical Lda estudadas, compatíveis com alvenarias antigas. São definidas as formulações a incluir em sistemas de revestimento a estudar, com vista ao desenvolvimento do sistema de revestimentos “emboço ventilado”, composto por duas camadas (camada base e reboco) cujo objetivo é permitir a acumulação dos sais no seu interior e evitar a sua acumulação no suporte e na superfície do reboco. Estes sistemas de revestimento foram desenvolvidos em maquetas de pequenas dimensões (tijolos maciços e sistemas de revestimento) em que a ação severa da água é simulada através de ensaios em laboratório específicos para o efeito, e determinados e quantificados os efeitos dessa degradação, em cada sistema de revestimento.

Capítulo 7 (Performance of the render system “emboço ventilado” - Laboratorial work) – Selecionou-se o sistema de revestimento de alvenarias antigas que, de entre os estudados, apresenta maior durabilidade e eficácia na presença da ação severa da água. Este sistema de revestimento, “emboço ventilado” da Fradical Lda assim como mais três sistemas de revestimento distintos para comparação, são neste capítulo testados à ação severa da água numa maqueta de grandes dimensões (alvenaria de pedra) existente no Laboratório de Ensaios de Revestimentos e Pavimentos do Laboratório Nacional de Engenharia Civil. A ação severa da água é simulada através de ensaios específicos para o efeito, e determinados e quantificados os efeitos dessa degradação, em cada sistema de revestimento como forma de aferir a eficácia e durabilidade do sistema de revestimento “emboço ventilado”.

Capitulo 8 (Conclusões) – São reunidas as principais conclusões obtidas no estudo, apresentadas as questões que foram sendo levantadas ao longo do trabalho e apresentados os assuntos a desenvolver no futuro.

2. REVESTIMENTOS PARA ALVENARIAS ANTIGAS SUJEITAS À AÇÃO SEVERA DA ÁGUA: REVISÃO DA LITERATURA

2.1 Introdução

Em Portugal as intervenções de reabilitação e conservação em edifícios antigos têm vindo a assumir uma relevância crescente. Os revestimentos desempenham uma função decorativa e de proteção das alvenarias antigas (de pedra, de tijolo, de adobe ou de taipa) e por estarem particularmente expostos a ações externas, são considerados os elementos mais vulneráveis destes edifícios. Na maioria dos casos os revestimentos são executados com base em cal e apresentam bom estado de conservação (boa coesão e boa aderência ao suporte); no entanto, por vezes, podem apresentar alguma degradação superficial com o aparecimento de colonização biológica, destacamentos superficiais e cristalização de sais (envelhecimento natural)..

Numa estratégia de intervenção, sempre que possível, os revestimentos antigos devem ser conservados através de ações de consolidação e restituição da aderência. No entanto, em muitos casos a conservação destes revestimentos antigos não é possível e estes deverão ser substituídos por novos revestimentos que se apresentem duráveis e compatíveis com os materiais pré-existentes. A compatibilidade significa que os novos materiais (e a intervenção em si própria) não provocam a degradação dos materiais pré-existentes, e promovem a durabilidade e eficácia da intervenção. Este conceito de compatibilidade é dependente das características da alvenaria antiga e das condições específicas a que o edifício ou o elemento do edifício está sujeito. Em cada caso específico será necessário ter em consideração as fontes de humidade existentes (humidade ascensional e chuva), as condições climáticas (humidade relativa, variações de temperatura, vento, intensidade da chuva) e questões ambientais relacionadas com a poluição e ambiente marítimo. A utilização de materiais incompatíveis com o suporte e com os materiais pré-existentes e inadequados para as ações ambientais envolventes pode originar o aparecimento prematuro de anomalias [Vei08a, Vei09a, Vei10a].

As alvenarias antigas são muito espessas e a evaporação da humidade nelas contida poderá demorar vários meses ou até mesmo anos a acontecer. Nos casos em que existem fontes ativas de água (tais como a humidade ascensional) torna-se ainda mais difícil a sua evaporação devido à existência de uma fonte ativa e contínua de humidade. Quando esta fonte já transporta sais ou os sais estejam contidos na alvenaria e sejam transportados pela água, e a eliminação de fontes ativas de humidade não for possível, a utilização de revestimentos incompatíveis que reduzem a evaporação e contribuem para a sua acumulação na alvenaria pode acelerar a degradação prematura das paredes.

Num edifício antigo, os materiais porosos podem acumular elevados teores de sais. Os sais que se acumulam nas paredes destes edifícios podem ter várias origens: externas (humidade ascensional, poluição, nevoeiro salino) ou internas (existência de sais nos materiais utilizados), ou ainda inerentes ao uso (tipo de utilização do edifício no passado – existência de salgadeiras ou estábulos). Quando dissolvidos em água, os sais podem migrar através das paredes por capilaridade e originar degradação devido à sua cristalização.

A humidade ascensional é uma das fontes de humidade mais difíceis de eliminar, sendo uma das maiores origens de sais nas alvenarias antigas. Por outro lado, o cloreto de sódio (NaCl) é um dos sais mais comuns em edifícios localizados na costa Portuguesa e origina elevada degradação dos revestimentos.

A determinação da distribuição da humidade existente nas paredes e o teor de sais solúveis são fatores chave a ter em consideração na definição das novas argamassas de revestimento (em condições de ação severa da água) para que se consiga um adequado desempenho e durabilidade das intervenções.

O trabalho experimental desenvolvido nesta tese pretende comprovar a compatibilidade, durabilidade e eficácia de um sistema de revestimento de substituição para edifícios antigos "emboço ventilado" quando sujeito à ação severa da água (humidade ascensional e elevado teor de NaCl). Pretende-se que este sistema acumule sais no seu interior sem que se degrade e evite a sua acumulação no suporte e também a sua cristalização na superfície exterior do revestimento. Este sistema de revestimento foi desenvolvido em conjunto com a Empresa Fradical Lda.

2.2 Degradação dos materiais de construção porosos

A cristalização de sais é considerada uma das maiores causas de degradação dos materiais porosos. A extensão deste fenómeno é dependente das fontes de humidade e do tipo e quantidade de sais presentes, do comportamento face ao transporte de sais na alvenaria, do tipo de revestimento e do sistema alvenaria/revestimento, assim como das condições ambientais da envolvente (principalmente temperatura e humidade relativa). Condições ambientais variáveis podem originar ciclos de dissolução/cristalização e a degradação prematura dos materiais de construção [Lub06].

No entanto, a presença de sais não é condição suficiente para que ocorra a degradação dos materiais. A presença de humidade, na forma de vapor ou na forma líquida, permite o transporte dos sais (até ao local onde estes se acumulam até atingirem a concentração critica) e os consequentes ciclos de cristalização-dissolução.

Elevadas concentrações de sais solúveis em zonas críticas poderão ter uma maior influência na degradação do material poroso do que o teor total de sais nele contido; a localização crítica é

dependente do material (distribuição do tamanho dos poros, por ex.) e das condições envolventes (temperatura, humidade relativa, vento) [Gro12].

A degradação dos revestimentos tem origem em: causas exógenas devidas a agentes externos ambientais, físico-químicos, mecânicos e biológicos; causas endógenas intrínsecas resultantes do envelhecimento dos próprios materiais; causas mistas com origem na combinação de ações externas e processos endógenos [Vei07c]. A degradação devida à presença de sais pode ocorrer na superfície do revestimento ou no interior do próprio revestimento. No primeiro caso os sais acumulam-se na superfície devido ao transporte da solução salina do interior da alvenaria (humidade ascensional) ou do exterior (nevoeiro salino) e consequentemente os ciclos de dissolução/cristalização podem originar a degradação superficial. A acumulação de sais no interior do revestimento (criptoflorescências) pode originar maior degradação, estando a frente de secagem no seio do revestimento ou entre o suporte e o revestimento. Este fenómeno tem como causa primordial a utilização de materiais com propriedades hidrófugas [Gro09a] ou com baixa permeabilidade, como é o caso das argamassas com base cimentícea.

A degradação de materiais porosos devido à presença de sais desenvolve-se tanto em ambientes interiores como em ambientes exteriores, tendo nos últimos anos este tipo de degradação vindo a ser amplamente estudada em diferentes materiais, quer em laboratório quer *in situ*: i) Em edifícios na zona litoral diretamente expostos à ação das marés: em alvenarias de tijolo de fortes do século XVIII na Finlândia onde se verificaram de acordo com Konow [Kno02]; “Some of the bricks on the wall are almost completely deteriorated... The bricks nearby have weird white whiskers on them”; em revestimentos de fortes do século XVII em Portugal expostos a ambiente marítimo agressivo [Tav08b, Vei05a]; em revestimentos de alvenarias de pedra e de tijolo de faróis expostos a ambiente marítimo muito agressivo [Pap08]; ii) Em edifícios localizados em zonas Costeiras de Portugal onde se verifica uma degradação acelerada das telhas cerâmicas expostas a ambiente marítimo [Cru10]; iii) Em edifícios próximos de zonas costeiras em Portugal com fontes ativas de água (principalmente humidade ascensional) com degradação de revestimentos de antigos conventos [Vei09b, Vei10b, Gon07].

Neste contexto têm surgido várias linhas de investigação que visam: i) o desenvolvimento de novos revestimentos de substituição para alvenarias com elevados teores de sais solúveis [Gon07, Hee07a]; ii) o desenvolvimento de novos revestimento para aplicação em fortes e outros edifícios Portugueses [Vei08a, Vei09c] e iii) estudos laboratoriais por forma a determinar os revestimentos mais compatíveis para edifícios antigos em função da agressividade do ambiente envolvente [Vei10a].

Na Fig. 2.1 apresentam-se os principais fatores que influenciam a degradação associada à presença de sais solúveis: as fontes de humidade presentes (frequência de ocorrência, atividade e quantidade de água introduzida), as condições ambientais (velocidade de secagem, insolação,

temperatura, humidade relativa), os sais solúveis presentes (tipo de sais, quantidade e distribuição) e as características dos materiais (distribuição do tamanho dos poroso, caraterísticas mecânicas e físicas) (Fig. 2.1).

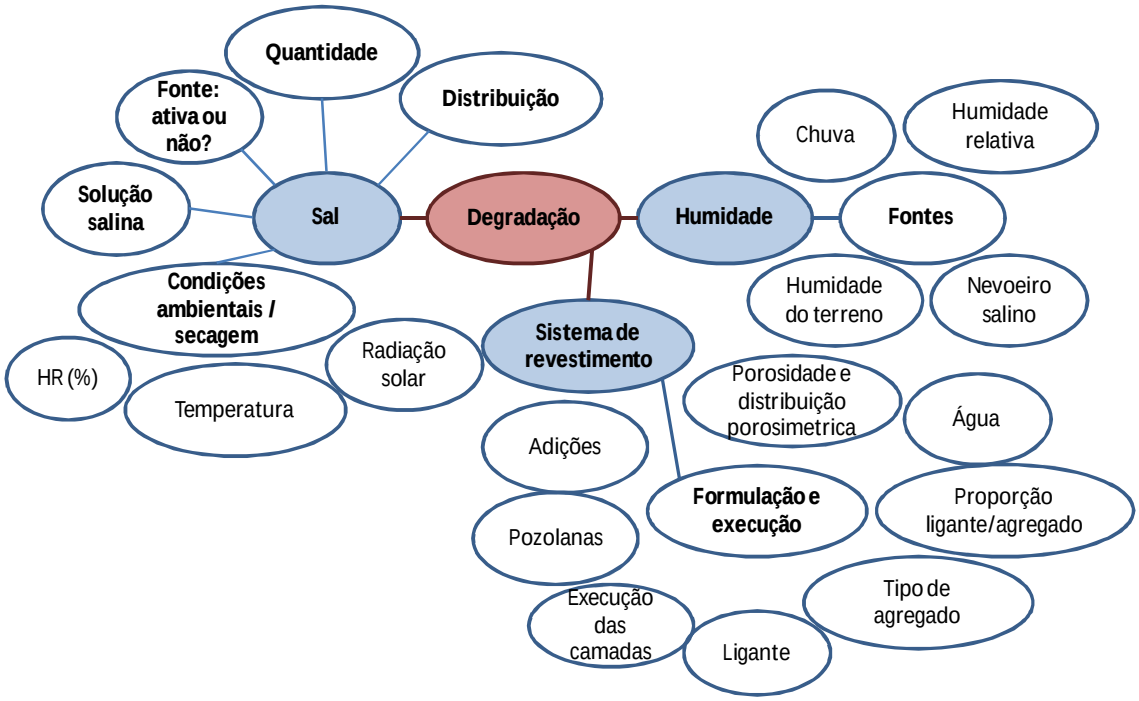

Fig. 2.1 Representação esquemática dos principais fatores que influenciam a degradação dos revestimentos

Os materiais de construção podem conter sais na sua constituição (utilização de água com sais na sua execução ou areias mal lavadas, ou aditivos com sais) ou os sais podem ser introduzidos mais tarde através do sistema poroso por forças capilares devido à existência de humidade ascensional ou infiltrações. A água evapora devido a alterações das condições ambientais e os sais podem cristalizar no interior da estrutura porosa dos materiais ou em interfaces (criptoflorescências) ou à superfície do material (eflorescências) com um aumento de volume e consequente degradação do material [Pav11]. O comportamento de um tipo de sal em particular depende da quantidade de humidade no material, da solubilidade do sal, assim como da temperatura e da humidade do ambiente envolvente.

Para a seleção de argamassas adequadas que minimizem a degradação devida aos sais, da alvenaria assim como dos revestimentos pré-existentes, deve ser determinada a composição da alvenaria e o seu estado de conservação, assim como a causa da degradação do material e o tipo e a severidade do ambiente envolvente. Para reduzir a degradação associada à cristalização de sais solúveis devem ser tidas em conta as fontes de sais solúveis incluindo a atmosfera, os constituintes das argamassas, os sais existentes na alvenaria e a humidade presente no terreno [Mau12].

2.2.1 Condições ambientais

A cristalização dos sais é uma das maiores causas de degradação dos materiais de construção porosos. A evaporação é um fator chave no processo da cristalização de sais o qual portanto, depende das condições ambientais. Quando um objeto histórico é mantido no interior, as condições climáticas podem ser controladas mantendo, na envolvente do objeto, a humidade relativa constate e a ventilação em níveis mínimos de forma a prevenir ciclos de dissolução/cristalização; no exterior os monumentos e edifícios são frequentemente expostos ao vento e variações da humidade relative, o que origina elevada taxa de evaporação [Pel04]. Para reduzir a degradação devida à presença de sais é necessário limitar as fontes de sais e de humidade, como por exemplo a humidade ascensional.

Alguns sais podem causar maior degradação do que outros sob as mesmas condições e um tipo de sal inócuo pode originar degradação quando sujeito a condições ambientais mais severas (secagem rápida e variações na humidade relativa). As principais condições ambientais capazes de degradar os materiais porosos são: chuva incidente, ciclos de gelo-degelo, nevoeiro salino, utilização de sais para eliminação da formação de gelo, condições do solo, condições de secagem rápidas, ataque biológico, ciclos de secagem e molhagem e ação mecânica e do vento [Hees12].

Ciclos de dissolução e cristalização que resultem de condições severas (evaporação rápida) como é o caso da elevada insolação, vento ou elevada ventilação e aquecimento originam frentes de secagem localizadas no seio do revestimento e a degradação pode ser severa, associada a grande perda de material (por exemplo desintegração); em condições moderadas (evaporação lenta) a frente de evaporação localiza-se à superfície do revestimento e a degradação aparece geralmente em menor grau, sob a forma de eflorescências e destacamento do revestimento por pintura [Gro12]. Rijniers [Rij04] fundamenta estas observações, referindo que:

i) Se a secagem é muito rápida os sais tendem a cristalizar nos poros de pequenas dimensões e a degradar o material. Inicialmente a solução salina é transportada até ao local onde ocorre a evaporação e precipitação (na interface entre o material e o ar). Devido à ação capilar os poros de maiores dimensões secam primeiro e depois o transporte de vapor começa a dominar o processo, deixando a fase líquida de ser contínua;

ii) Se a secagem é lenta não se espera a degradação do material. O filme líquido permite o transporte da solução por difusão a partir dos poros de pequenas dimensões para os poros de maiores dimensões, onde a cristalização poderá ocorrer [Rij04].

Pel [Pel04] observou num tijolo de cerâmica que após uma secagem inicial rápida durante a qual os sais são transportados, a secagem diminuiu e a difusão do sal igualou a concentração no tijolo.

Na prática os sistemas podem ser constituídos por vários materiais existindo a interação entre os diferentes sistemas porosos, como é o caso de uma alvenaria de argamassa e tijolo. Durante a secagem da alvenaria, os poros de pequenas dimensões são os das argamassas e os de maiores dimensões são os dos tijolos. Iniciada a secagem no interior dos poros de pequenas dimensões da argamassa, o teor em sais destes poros aumenta comparado com o teor inicial de sais, o que origina degradação. Analogamente o mesmo processo acontece quando um substrato é revestido com reboco com diferente distribuição de poros [Pet04].

Perceber o transporte da humidade e a capacidade de secagem do sistema é crucial para o desenvolvimento de um sistema de revestimento durável, eficaz e compatível com os elementos pré-existentes, quando submetido à ação severa da água (humidade ascensional e elevado teor de sais solúveis, especialmente NaCl).

2.2.2 Sais solúveis e sua origem

Os materiais alcalinos fornecem muitos sais às paredes e podem ocorrer processos de transformação que geram sais mais prejudiciais (os álcalis-carbonatos podem reagir com a atmosfera ácida e originar álcalis-sulfatos, álcalis-nitratos ou alkalis-cloretos); o cimento Portland contém teores de álcalis solúveis que originam eflorescências salinas de álcalis-carbonatos que em grandes concentrações, podem originar degradação severa e irreversível; as águas do terreno podem conter nitratos e cloretos; a cal dolomítica poderá reagir com os sulfatos e originar $MgSO_4$ [Arn91].

Quando os sais solúveis estão presentes, pode aparecer degradação na superfície dos revestimentos devido a variações na humidade relativa do ambiente envolvente. Um dos sais mais frequentes em edifícios localizados em ambientes marítimos é o NaCl, que origina elevada degradação dos revestimentos e alvenarias dos edifícios. A degradação devida à presença de NaCl surge quando a humidade relativa varia em torno dos 75% (Tabela 2.4 na secção 2.4.3) [Lub06]. No caso da existência de outros sais solúveis, ou mistura de sais, a degradação acontece a diferentes humidades relativas [Cha00, Arn91].

Os sais solúveis podem ter origem no terreno (solos salinos e humidade do terreno com sais solúveis), nos materiais de construção (sais presentes em areias mal lavadas ou na água utilizada na mistura das argamassas), na atmosfera poluída e no metabolismo dos organismos, que circulam em soluções aquosas através das paredes e nos materiais porosos. Um elevado teor de sais pode não originar degradação, tal como acontece no caso de “sais não destrutivos”, tais como o carbonato de cálcio que forma eflorescências de calcite sem degradação do material; no entanto os nitratos, sulfatos e cloretos são considerados sais “mais destrutivos” que originam degradação. Os nitratos podem estar presentes no ambiente como resultado da oxidação biológica por microorganismos de compostos orgânicos ou através de fertilizantes; os sulfatos podem ter origem

em fertilizantes e mais frequentemente na ação do SO_2 na atmosfera (chuva ácida) ou fazerem parte de alguns materiais de construção; os cloretos encontram-se na água do mar e nos sais utilizados na manutenção de inverno de passeios e estrada em climas frios. Todos os sais mencionados são encontrados na água do terreno [Pav11]. Acima do nível do terreno a que a água evapora, o soluto concentra-se e os sais acumulam-se. Onde e quando ocorre a supersaturação, os sais precipitam numa sequência temporal de acordo com a atividade do ião correspondente à fase salina presente no sistema. Eles concentram-se localmente como eflorescências na superfície ou como criptoflorescências por baixo da superfície dos materiais porosos [Arn91].

Os sais solúveis podem estar presentes nas alvenarias desde a sua construção ou serem introduzidos mais tarde nos materiais porosos absorvidos da atmosfera ou da humidade do terreno. Os sulfatos podem estar presentes nos tijolos (se não forem adequadamente cozidos), nas rochas e no cimento Portland ou na água absorvida do terreno [Bak09, Cha00]; os cloretos podem ter origem no nevoeiro salino, na água utilizada na preparação das argamassas ou água do terreno [Bak09], na utilização de areias mal lavadas [San10a, Vei10b]; os nitratos podem indicar o contato com esgotos ou usos anteriores relacionados com estábulos de animais [You08]. O tipo de sais pode servir como guia para a sua origem e como os sais solúveis podem entrar nos materiais porosos apenas se dissolvidos em água, eles indicam também a existência de uma fonte de humidade.

2.2.3 Fontes de humidade

A humidade é absorvida pelos materiais de construção porosos quer na forma líquida, quer na forma de vapor. Na forma liquida, esta absorção ocorre devido à ação de capilaridade resultante da tensão superficial através da qual a água entra através dos poros capilares do material, movendo-se devido a diferenças na pressão hidrostática, dependente da permeabilidade do material [Cha00, Hen01]. Na fase de vapor pode ocorrer a condensação superficial ou capilar nos poros ou até mesmo higrospicidade, que depende do tipo de material, porosidade e superfície interna [Cha00].

A humidade que ascende por capilaridade através das paredes tem origem em águas superficiais e águas do terreno (mais ou menos profundas) e a humidade existente na base das paredes tem como origem a chuva ou a neve que derrete (esta última em climas mais frios). Exteriormente a evaporação começa acima do solo e internamente acima do nível do pavimento. A humidade nas paredes ascende ao nível em que existe um equilíbrio entre a evaporação e a absorção de humidade. A água no estado líquido, presente no terreno assim como nos materiais porosos, é considerada uma solução salina mais ou menos diluída [Arn91], independentemente da sua origem. A chuva, as águas superficiais, as águas freáticas ou a humidade de condensação podem transportar iões (de sais solúveis), e percolam através dos materiais porosos [Arn91].

2.2.4 Humidade ascensional e sais solúveis

A humidade ascensional deve-se à ação da capilaridade da água do terreno através dos poros dos materiais. A sucção capilar é mais forte em poros pequenos. Em edifícios verifica-se que a altura que a água atinge nas paredes é limitada pela taxa de evaporação. A taxa de evaporação através da superfície da parede é influenciada pelos materiais da alvenaria, rebocos exteriores e interiores, soluções de pintura, condições ambientais e condições de humidade [You10]. A humidade ascensional humedece os materiais com os quais contata e pode provocar odores, mas a degradação associada da alvenaria e dos revestimentos é limitada (exceto quando na presença de materiais mais suscetíveis tais como argilas provenientes de solos) [You10].

Quando existem sais solúveis, o transporte, acumulação e cristalização dos sais pode ocorrer devido à presença de humidade ascensional através das paredes dos edifícios. Arnold e Zehnder [Arn91] observaram que a maioria dos edifícios históricos e monumentos apresentam maior ou menor degradação na base das paredes devido à presença de água superficial ou no terreno. As observações realizadas em zonas com humidade do terreno mostraram que a humidade se concentrou e acumulou entre 0.5 m e 2.5-3 m acima do nível do terreno, correspondendo à zona C (Fig 2.2 e Tabela 2.1).

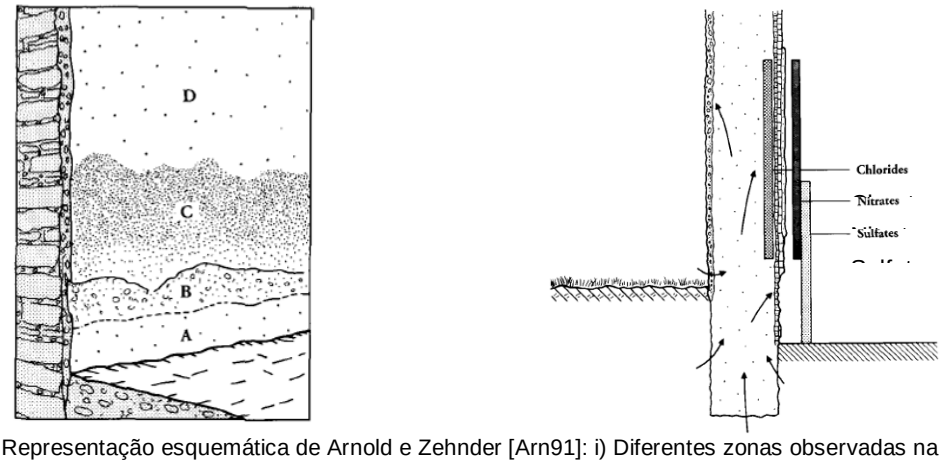

Fig. 2.2 Representação esquemática de Arnold e Zehnder [Arn91]: i) Diferentes zonas observadas na parede devidas à presença de humidade ascensional – alçado (esquerda) e ii) evolução dos perfis verticais de sais em relação à humidade ascensional (direita).

Tabela 2.1 Tipificação das zonas das paredes e dos tipos de sais onde pode ocorrer cristalização [Arn91]

Zona	Principais iões e tipo de degradação	Solubilidade e higrospicidade
Zona C	Cloretos e nitratos: humidade e manchas mais escuras que em outras zonas.	Muito higroscópicos
Zona B	Sulfatos: perda de coesão, desintegração e escamação. Sais sob a forma de eflorescências.	Baixa a moderada
Zona A	Sulfatos: degradação menor do que na zona B.	Baixa a moderada

As observações realizadas por Arnold e Zehnder [Arn91] demonstraram que: a maior degradação pode surgir em zonas onde não se verifica a maior concentração de sais; a maior concentração de sais foi verificada na zona C e a maior degradação na zona B, que pode ser justificada pela maior

higroscipidade dos sais presentes na zona C que não cristalizam facilmente em condições ambientais exteriores normais; os sulfatos e carbonatos que são sais menos solúveis e menos higroscópicos e encontrar-se-ão na base das paredes enquanto nas zonas mais elevadas das paredes encontrar-se-ão os cloretos e nitratos, formando soluções altamente higroscópicas.

Na Fig. 2.3 apresentam-se casos de degradação associados à presença de sais solúveis e humidade ascensional.

Fig. 2.3 (a) Destacamento do acabamento interior composto por reboco/pintura impermeável (a parede é revestida com mármore até 1,2 m, acima da qual ocorreu o destacamento da pintura); (b) destacamento do reboco de cimento e pintura impermeável exteriores devido à dificuldade de evaporação.

À medida que a humidade evapora da superfície, e nos casos em que a fonte de humidade está ativa, mais humidade é absorvida através da base das paredes, sendo este um processo dinâmico. Assim, a humidade que atinge as paredes é dependente da humidade absorvida, da evaporação e da permeabilidade dos materiais de construção. Quando existe uma fonte ativa de água e a humidade ascende através das fundações e paredes na presença de sais solúveis, origina degradação.

A degradação das alvenarias está frequentemente associada à presença de humidade no terreno. Nas alvenarias afetadas por humidade ascensional, os sais solúveis aparecem sob a forma de crostas nas zonas mais baixas e húmidas das paredes; as zonas das paredes a cotas mais elevadas e menos húmidas apresentam desagregação. Existindo um aumento de humidade nas zonas com perda de coesão poderão surgir crostas de sais devido à sua recristalização [Arn87].

A humidade ascensional é considerada a mais gravosa das fontes de humidade que atingem as alvenarias. Quando uma elevada quantidade de humidade é introduzida na alvenaria combinada com sais solúveis pode originar a cristalização nos revestimentos ou na alvenaria devido à evaporação [Lub08a]. A sua nocividade é essencialmente devida à elevada quantidade de humidade introduzida na alvenaria e ao facto da humidade ascensional, normalmente ser uma grande fonte de sais. A introdução de grandes quantidades de sais na alvenaria superior à quantidade de sais existente no solo, e a sua elevada concentração ajuda a manter os materiais humedecidos, aumentando o problema [You10]. A quantidade de água absorvida pode saturar a alvenaria. A dificuldade em prevenir a humidade ascensional é devida essencialmente à

heterogeneidade da alvenaria, que torna ineficazes alguns dos sistemas usados, como a injeção de produtos químicos [Lub06b].

2.3 Tipos de degradação

De acordo com as definições do ICOMOS [Ver08], adotadas no desenvolvimento do presente trabalho de investigação, a degradação pode ser definida como a perceção humana da perda de valor e pode ser definida como uma modificação química e física das propriedades intrínsecas que originam a perda de valor e a impossibilidade de utilização. A presença de sais pode originar a degradação do reboco, quer à superfície (eflorescências, delaminação, escamação) quer mais em profundidade (desintegração e pulverulência). Na tabela 2.2 estão definidos os principais tipos de degradação da pedra com base nas definições do ICOMOS-ISCS, tendo sido adaptadas para rebocos no âmbito do presente trabalho de investigação (ver capítulos 4, 5 e 7).

Tabela 2.2 Tipos de degradação na superfície dos rebocos e definições (com base em ICOMOS-ISCS [Ver08], adaptadas para rebocos)

Tipo de degradação	Definição (adaptadas para rebocos, com base em ICOMOS-ISCS [Ver08])
Destacamento/ detachment	
	Delaminação/ delamination (layering): Separação física em uma ou várias camadas (espessura e forma das camadas são variáveis).
	Escamação fina/ peeling: Destacamento parcial de uma camada superficial (espessura da ordem do mm ou inferior) que aparece como uma camada na superfície exterior do revestimento.
	Escamação média/ scaling: Destacamento como escamas de peixe (espessura da ordem do milímetro ao centímetro e é negligenciável em relação à dimensão da superfície).
	Desintegração/ crumbling: Destacamento da camada exterior (limitada a 2 cm de espessura).
	Pulverulência/ sanding: Desintegração granular com perda de coesão.

Tabela 2.2 (Cont.) Tipos de degradação na superfície dos rebocos e definições (com base em ICOMOS-ISCS [Ver08], adaptadas para rebocos)

Deposito /Deposit	
	Crosta de sal/ salt crust: Acumulação de sais solúveis na superfície, desenvolvidos na presença de elevada quantidade e que resultam de ciclos de dissolução/cristalização.
	Eflorescência/ efflorescence: Geralmente sob a forma de cristais na superfície brancos, tipo pó e fracos (pouco coesivos).

2.4 Mecanismos de degradação devido à presença de sais solúveis

A presença de sais solúveis nos materiais porosos pode originar vários tipos de degradação: tais como a perda de material, humedecimento devido à presença de sais higroscópicos. A perda de material pode acontecer quando o cristal contido no sistema poroso aumenta de tamanho como resultado da cristalização ou hidratação. As eflorescências resultam do crescimento de cristais longos e fracos na superfície dos materiais porosos, sem que ocorra a quebra na estrutura porosa. O humedecimento da parede pode estar relacionado com a presença de sais higroscópicos que retêm humidade suficiente do ar para tornar a parede visivelmente húmida, mesmo em clima seco ou na ausência de fontes de humidade. Este humedecimento é um dos fatores que provoca a degradação dos revestimentos.

Existem propriedades importantes e factores que influenciam o processo de cristalização de sais. O grau de saturação e a localização do cristal são considerados fatores chave para a degradação [Doe02]. As propriedades e fatores que mais influenciam a saturação: taxa de evaporação (área da superfície, temperatura, humidade e vento), taxa de arrefecimento (temperatura e vento), sais pré-existentes e as suas taxas de crescimento; localização onde ocorre a formação dos cristais: taxa de evaporação, capacidade de transporte da solução, propriedades da solução (tensão superficial e viscosidade), distribuição do tamanho dos poros (poros mais pequenos = maior degradação) [Doe02].

2.4.1 Pressão de cristalização e outros mecanismos

Os mecanismos e fatores que controlam a formação dos cristais de sais nos materiais porosos e a evolução da degradação associada ao crescimento dos sais não estão ainda totalmente explicados. É necessário compreender o movimento da água e dos iões durante a evaporação e a

formação dos cristais nos materiais porosos para explicar a degradação dos diferentes materiais e condições [Pel04].

O crescimento dos sais nos materiais de construção porosos é uma das maiores causas de degradação. Encontrar uma teoria única relativa à degradação dos sais nos materiais porosos é impossível principalmente devido à complexidade das variáveis envolvidas. As reações químicas entre os iões na solução desenvolvem-se até atingirem o equilíbrio. As variações da humidade relativa associadas à variação da temperatura, dos teores de humidade nas paredes dos edifícios antigos e ainda dos sistemas de sais presentes contribuem para alterar o equilíbrio.

Existem várias teorias relativas aos mecanismos de degradação da estrutura porosa dos materiais de construção. A degradação associada à pressão de cristalização nos poros é a teoria mais aceite [Cor49, Eve61, Wel65, Zeh89, Rod99, Sch99, Sch04, Ste05a, Ste05b]. No entanto outros mecanismos de degradação também têm vindo a ser propostos: a pressão de hidratação [Wil81], a dilatação hídrica diferencial [Lub06a, Lub07] e a dilatação térmica diferencial [Gou97].

Na tabela 2.3 estão descritas, de acordo com a literatura, as principais teorias associadas à cristalização dos sais que origina a degradação dos materiais porosos. É unanimemente aceite que a cristalização de sais origina degradação dos materiais porosos; no entanto definir o principal mecanismo de degradação ainda é controverso.

Tabela 2.3 Mecanismos de degradação: teorias da cristalização de sais

Pressão de cristalização: O sal preenche os poros onde cristaliza e origina pressão contra as paredes dos poros. A degradação surge quando a pressão é maior que a resistência do material.	
[Cor49]	No caso dos sais mais comuns (como é o caso do NaCl), a pressão de cristalização é desenvolvida devido ao maior volume ocupado pela precipitação dos cristais e pela solução saturada residual, quando comparado com o volume da solução supersaturada. Esta cristalização é diretamente proporcional à supersaturação. Com o desenvolvimento da pressão de cristalização, a solubilidade do sal aumenta (de acordo com o principio de Le Chatelier) e a supersaturação diminui.
[Eve61]	O crescimento de pequenos cristais em poros pequenos não é termodinamicamente favorável; em poros maiores os cristais crescem e exercem pressão até o potencial químico ser igual ao dos cristais pequenos.
[Wel65]	A cristalização inicia-se nos poros de maiores dimensões (formando grandes cristais, que crescem em detrimento dos mais pequenos) a partir da solução absorvida dos pequenos capilares. Quando os poros de grandes dimensões estão preenchidos, os cristais não crescem nos poros mais pequenos porque isto necessita de um aumento significativo da área superficial em relação ao pequeno aumento de volume, resultando um grande aumento do potencial químico do cristal.
[Wel65, Zeh89]	O modelo termodinâmico indica que a cristalização ocorre primeiro nos poros maiores (crescimento de cristais maiores) a partir da solução fornecida dos pequenos capilares; os materiais porosos com capilares maiores ligados a pequenos capilares são mais suscetiveis à degradação.

Tabela 2.3 (Cont.) Mecanismos de degradação: teorias da cristalização de sais

Pressão de cristalização: O sal preenche os poros onde cristaliza e origina pressão contra as paredes dos poros. A degradação surge quando a pressão é maior que a resistência do material (cont.)	
[Rod99]	No caso do NaCl os sais cristalizam primeiro nos poros de pequenas dimensões. Observa-se degradação embora se verifique um baixo índice de supersaturação atingido antes da nucleação do NaCl, baixo índice de precipitação da halite e de crescimento. Referem ainda que uma elevada supersaturação não pode ser sustentada por uma solução de NaCl na presença de uma área de superfície elevada.
[Sch99]	A cristalização é menor em poros de maiores dimensões, sendo que em poros de menores dimensões a supersaturação é maior.
[Ste05a, Ste05b]	O desenvolvimento de forças no sistema poroso é um processo dinâmico, numa situação de não equilíbrio, controlado pela dinâmica associada à evaporação, difusão e taxa de crescimento. Não existe pressão de cristalização constante e a pressão e elevada supersaturação evolui temporariamente. O equilíbrio da pressão de cristalização suficiente para degradar os materiais porosos só pode ser atingido nos poros muito pequenos.
[Sch04]	Numa situação em que não existe equilíbrio, durante o processo de evaporação, o filme líquido pode ser rompido e a solução ficar retida entre a superfície do cristal e as paredes dos poros, podendo passar a funcionar como poros de pequenas dimensões.
Pressão de hidratação: Pressão resultante da expansão do sal durante a hidratação	
[Wil81]	O NaCl não apresenta formas hidratadas a temperaturas superiores a 0.1°C e por isso este mecanismo não se aplica na cristalização do NaCl.
[Rod00]	A hidratação do sulfato de sódio pode acontecer devido à dissolução da fase anidra e re-precipitação num estado mais hidratado, em vez da absorção direta de humidade.
Dilatação hídrica diferencial: A variação da humidade relativa resulta em diferentes coeficientes de expansão hídrica entre as zonas dos materiais contaminadas com sais e as não contaminadas, nos materiais porosos.	
[Sne97]	NaCl, $NaNO_3$ ou KCl podem originar retração devido ao aumento da espessura da camada formada na superfície dos cristais. Os materiais contaminados podem expandir durante baixa humidade relativa e retrair quando sujeitos a baixas humidades relativas; o oposto acontece em materiais isentos de sais.
[Rod99, Sch06]	Rodriguez-Navarro e Doehne apresentam dúvidas quanto à existência deste mecanismo, Scherer considera que mais do que a dilatação hídrica a pressão de cristalização pode originar a expansão dos materiais contaminados com sais durante a secagem.
[Lub06a]	Nos materiais degradados quando os sais se encontram na superfície de evaporação, podem ser desenvolvidas tensões na envolvente do material contaminado e do material não contaminado com sais, resultando em destacamentos dos materiais contaminados com perda de coesão e fragmentação na superfície. Estas observações foram justificadas através do comportamento oposto entre os materiais contaminados e não contaminados.
Dilatação higrica diferencial: Tensão desenvolvida em materiais contaminados com sais devido à dilatação diferencial das zonas com mais sais e com menos sais.	
[Lub06a]	Este mecanismo pode produzir destacamentos, mesmo quando não é evidente a presença de sais, em argamassas de cal e cimento após vários ciclos de humedecimento e secagem.
Dilatação térmica diferencial: Degradação com origem na expansão térmica dos sais e do material durante as variações de temperatura.	
[Gou97, Wij04]	Goudie refere que o NaCl expande aproximadamente 0.9% entre 0 e 100°C e Wijffels refere que este fato não é suficiente para explicar a degradação severa devida à cristalização verificada nos materiais de construção.

A degradação devida à cristalização dos sais é dependente da saturação da solução e da localização da cristalização, sendo estes dois fatores chave relacionados com as propriedades da

solução; a evaporação depende da composição da solução, condições ambientais, propriedades do substrato e padrões de crescimento dos cristais [Rod99]. A solução tem que estar saturada para que se dê a cristalização nos materiais porosos [Sch99]. A supersaturação pode ser conseguida através da capilaridade ascensional, seguida de evaporação ou através de ciclos de molhagem e secagem [Sch04].

A degradação associada à presença de sais é um dos principais problemas em revestimentos e alvenarias de tijolo e pedras e esculturas de pedra. De um modo geral os materiais porosos expandem quando absorvem humidade (dilatação hígrica) ou água no estado líquido (dilatação hídrica) e contraem na secagem; na presença de sais solúveis este efeito poderá ser contrário [Cha00].

2.4.2 Combinação de sais solúveis

A degradação dos materiais porosos pode ser atribuída à combinação de dois ou mais sais e a sua presença simultânea afeta a solubilidade individual de cada tipo de sal. Este efeito foi compilado por Charola [Cha00]: i) se a solução salina contiver sais que não apresentem iões em comum (como é o caso do cloreto de sódio e do sulfato de cálcio – gesso desidratado) a solubilidade de ambos os sais aumenta devido ao aumento da força iónica da solução; o aumento de solubilidade será maior na presença de sais menos solúveis, como é o caso do gesso; ii) em soluções salinas que contenham sais com iões em comum, como é o caso do cloreto de sódio e o do sulfato de sódio, a solubilidade de ambos decresce; a solubilidade de sais menos solúveis será mais afetada, neste caso a do sulfato de sódio. De acordo com a autora, alguns sais poderão não se comportar deste modo tal como, será o caso do nitrato de potássio que, na presença de outros nitratos, aumenta a sua solubilidade.

2.4.3 Higrospicidade / cristalização

De um modo geral atribui-se o termo higroscópico a sais capazes de absorver humidade sob a forma de vapor. Se os sais estão presentes na matriz dos materiais porosos, a humidade poderá ser absorvida por capilaridade e higrospicidade [Mas93].

Os sais solúveis poderão absorver humidade quando a humidade relativa do ar aumenta acima da sua humidade relativa de equilíbrio. Os sais muito solúveis podem deliquescer – tornar-se líquidos (absorver quantidade de água suficiente para a formação de uma solução saturada). Por outro lado uma solução salina concentrada apresenta pressão de vapor de água menor que a água no estado puro e terá uma maior tendência para condensar o vapor de água do ambiente para atingir o equilíbrio.

Cada solução salina saturada está em equilíbrio com a humidade relativa do ar, HR_{eq}. A humidade relativa do ar em contato com a solução salina saturada é RH_{eq} e a humidade relativa do ar é $HR_{air.}$

Quando a humidade evapora, aumenta a concentração da solução salina até atingir a saturação e o início da cristalização do sal. Para que tal aconteça é necessário que a humidade relativa do ar seja inferior à humidade relativa de equilíbrio de uma dada fase salina presente no sistema: a saturação e consequente precipitação é atingida quando $HR_{air} \leq HR_{eq}$. Caso a $HR_{air} < HR_{eq}$ a humidade evapora e aumenta a concentração até à saturação até que, finalmente, o sal começa a cristalizar. O sal absorve humidade do ar devido à sua higrospicidade, tornando a solução mais diluída. Na tabela 2.4 apresenta-se a humidade relativa de alguns dos sais mais comuns, presentes em paredes de edifícios antigos, em função da temperatura.

Tabela 2.4 HR_{eq} dos principais sais encontrados nos materiais das paredes (cloretos, sulfatos e nitratos) a diferentes temperaturas. Dados de Arnold e Zehnder [Arn87]

T (°C)	0 °C	5 °C	10 °C	15 °C	20 °C	25 °C	30 °C
NaCl HReq (%)	75.5	75.7	75.7	75.6	75.5	75.3	75.1
$NaNO_3$ HReq (%)		78.6	77.5	76.5	75.4	74.3	75.1
Na_2SO_4 HReq (%)					82	82.8	84.3
KCl HReq (%)	88.6	87.7	86.8	85.9	85.1	84.3	83.6
KNO_3 HReq (%)	96.3	96.3	96	95.4	94.6	93.6	92.3
K_2SO_4 HReq (%)	98.8	98.5	98.2	97.9	97.6	97.3	97.0

Em edifícios em vez de um tipo de sais encontram-se diferentes tipos de misturas de sais. As misturas de sais apresentam diferentes valores de HR_{eq} que os sais na sua forma pura. O conhecimento da temperatura e condições de humidade críticas é crucial para a conservação das alvenarias antigas. Os diagramas de solubilidade das misturas de sais solúveis são referidos na literatura [Ste96] como resultado de estudos experimentais e modelos de cálculo onde normalmente todas as combinações de sais apresentam HR_{eq} inferiores aos sais na sua forma pura [Cha00].

A cristalização poderá ocorrer: quando a temperatura diminui, quando ocorre evaporação da humidade e/ou devido à combinação destes dois efeitos. A solubilidade de uma solução salina depende da temperatura do ar (Tab. 2.4). No caso do NaCl – considerando que foi o sal utilizado no âmbito do desenvolvimento experimental do presente trabalho de investigação - a sua cristalização ocorre essencialmente devido à evaporação da humidade até que se atinja a saturação, uma vez que a solubilidade do NaCl não é muito afetada pela temperatura (Tabela 2.4). Uma solução saturada de NaCl a 20°C está em equilíbrio com uma humidade relativa de 75.5%. A solubilidade de uma solução salina é também dependente da pressão (Tabela 2.5): um cristal sob pressão apresenta maior solubilidade do que um cristal não sujeito a pressão [Rie94].

Tabela 2.5 Efeito da pressão na solubilidade do NaCl – Dados de Lubelli [Lub06a]

Pressão (atm)	0	250	500	750	1000	1250	1500
Gramas de NaCl por 100g de solução	26.42	26.59	26.74	26.88	27.01	27.11	27.20
Gramas de NaCl por 100g de água	35.91	36.22	36.50	36.76	36.99	37.18	37.37

De acordo com Rijniers [Rij04] em alguns materiais de construção, a deliquescência do sal inicia-se quando a HR_{air} é inferior à HR_{eq}, devido à combinação entre a higrospicidade e a presença de

poros de pequenas dimensões (na escala do nanómetro), originando condensação capilar. Como resultado, se existirem sais solúveis que absorvam humidade do ar, a parede poderá manter-se húmida mesmo caso não existam fontes de humidade. Se existirem sais ou outros materiais higroscópicos (capazes de absorver humidade sob a forma de vapor) na alvenaria então a quantidade de água introduzida (e retida) na parede poderá ser suficiente para que a parede apareça visivelmente húmida, mesmo em clima seco [You08].

A solução terá que estar supersaturada para que ocorra a degradação do material poroso [Sch99]. A supersaturação atinge-se a partir da absorção e secagem, ou a partir de ciclos de molhagem e secagem [Sch04]. Os ciclos de molhagem e secagem originam a dissolução e cristalização dos sais existentes no sistema poroso. Cada tipo de sal apresenta diferente capacidade de absorver humidade sob certas condições climáticas, dependendo da humidade relativa do ar e da quantidade de humidade que cada tipo de sal pode absorver. O teor de sais nos materiais influencia a sua capacidade em reter água. Os sais higroscópicos contribuem para o humedecimento dos materiais, não sendo possível atingir a secagem completa da alvenaria quando os sais estão presentes [Pav11].

2.5 Influência da estrutura porosa na degradação devida à cristalização de sais

O tamanho dos poros e a sua distribuição é referido na bibliografia [Dei99, Sch06, Ste05a, Ste05b, Yu10] como um dos principais fatores que influenciam a absorção de sais e a degradação associada: i) a porosidade total apresenta um papel fundamental na absorção do sal; ii) a distribuição do tamanho dos poros é fundamental, tanto na absorção dos sais, como na degradação associada à cristalização.

Scherer [Sch99] afirma que a quantidade de solução/sal que preenche os poros de diferentes tamanhos depende da sua interconetividade e da supersaturação que é atingida. De acordo com o autor, se os poros de grandes dimensões estão dispersos pelo material, eles são os primeiros a preencher-se com a solução, pois o fluxo é mais rápido nos poros de maiores dimensões, e só depois a solução é drenada para os poros mais pequenos (de acordo com a equação de Laplace e de Washburn, a sucção da capilaridade e a pressão são inversamente proporcionais ao raio dos poros). Durante a secagem, enquanto a evaporação progride, a solução é drenada dos poros de maiores dimensões para os poros de menores dimensões, onde se concentra. A cristalização pode ocorrer nos poros de menores dimensões e não nos poros maiores quando a supersaturação crítica é atingida [Rod99]. Se a supersaturação aumenta, a cristalização pode aumentar e mesmo os poros com dimensões inferiores a 0.1 μm poderão ser preenchidos com sais [Rod99, Yu10]. Caso os poros de grandes dimensões não estejam dispersos no material poroso, os poros de menores dimensões serão preenchidos com solução salina, enquanto os poros de maiores dimensões permanecem vazios [Sch99].

Stainer [Ste05b] refere que os sais podem cristalizar nos poros de maiores dimensões com pequenos capilares (com dimensões inferiores a 0.05 μm), em condições de equilíbrio, originando tensões elevadas. No entanto as tensões elevadas podem também ser obtidas em poros maiores, quando não existem condições de equilíbrio, quando a pelicula da solução supersaturada é descontínua e, como resultado da evaporação durante a secagem, a solução fica em contato com os cristais apenas em alguns pontos [Sch06]. Durante a imersão, o mecanismo de dissolução e cristalização induz uma supersaturação similar nos poros com qualquer dimensão [Ste08]; por isso cristais de grandes dimensões em poros de grandes dimensões, mesmo que não contenham entradas com pequenos capilares, podem originar pressões.

Dei et al. [Dei99] refere que após a cristalização de sais, a oclusão dos poros de pequenas dimensões não é detetada na determinação da porosidade pois esta apenas deteta poros interconectados.

Os testes de absorção e secagem podem induzir o crescimento de cristais, tanto durante a secagem, como durante a absorção [Ste08]. A contribuição do crescimento do cristal durante a secagem é confirmada pelo destacamento imediato de partículas após a imersão parcial dos provetes em solução; é provável que os grãos desintegrados sejam cimentados pelos sais. Durante a secagem quando a solução utilizada inicialmente é saturada, a supersaturação pode ser atingida logo no início da evaporação. Os sais podem assim precipitar principalmente no interior de poros de maiores dimensões (maiores que 0.1 μm); após os cristais preencherem estes poros de maiores dimensões, a sua cristalização é inibida nos micro-poros vazios envolventes, continuando a desenvolver-se e a gerar tensões nos poros de maiores dimensões, até que as paredes dos poros rompem e os poros de dimensões inferiores a 0.1 μm serão dificilmente preenchidos com sais [Sch04].

Yu [Yu10] refere que os materiais porosos com baixa porosidade são mais propensos ao ataque por sais se apresentarem substancial microporosidade, ou seja o grau de degradação de materiais porosos com a mesma porosidade total pode ser diferente se a distribuição de poros, especialmente ao nível dos microporos, for diferente. Os autores observaram que materiais pétreos com diferentes quantidades substanciais de poros de grande dimensão (entre 0.1 e 5 um de raio) interconectados com grande quantidade de pequenos microporos (inferiores a 0.1 um de raio) são muito suscetíveis à absorção de sais. Os materiais com poros maiores são mais resistentes aos sais porque materiais com distribuição de poros de maiores dimensões parecem não facilitar a absorção de sais e a promoção de tensões associadas à cristalização. Estas observações estão de acordo com outros estudos, que consideram que a presença de microporos aumentam as tensões associadas à cristalização; no entanto diferentes gamas de microporos têm vindo a ser associadas à degradação devida à presença de sais [Sch06, Ste05b, Rij04, Ben04, Zeh89]. É bem aceite que os microporos estão associados a elevadas tensões como resultado da cristalização; no entanto vários estudos teóricos e laboratoriais atribuem a degradação à presença

de diferentes intervalos de microporos (P): P < 0.05 μm [Ste05b, Sch06], P < 0.1 μm [Rij04], P < 1 μm [Ben04], 0.05 μm < P < 0.1 μm [Yu10] e 0.5 μm <P < 5 μm [Zeh89].

Alguns estudos demonstram que os sais em condições de equilíbrio podem cristalizar em poros de dimensões inferiores a 0.05 μm de raio [Sch06, Ste05b, Ben04]; no entanto, em condições em que não existe equilíbrio, os poros de maiores dimensões também podem originar tensões de cristalização. Este último caso é devido à evaporação durante a secagem, na qual a pelicula formada pela solução supersaturada é descontínua e pode manter-se apenas em contato pontual com os cristais [Sch06], originando cristais de maiores dimensões em poros de maiores dimensões que não estejam ligados a pequenos poros mas que apresentam entradas com poros pequenos; tanto em equilíbrio como em condições de não equilíbrio os poros de menores dimensões apresentam-se mais eficazes no desenvolvimento de tensões devido à cristalização de sais.

Rijniers [Rij04] refere que uma pressão de 3MPa pode ser desenvolvida na presença de alite em poros de dimensões inferiores a 5.2 μm e para a ternadite em poros de dimensões inferiores a 100 μm, em materiais de construção como o betão, tijolos de silicato de cálcio e argamassas.

Yu e Oguchi [Yu10] estudaram a distribuição de poros em materiais pétreos de construção e concluíram que os poros entre 0.1 e 5 μm de raio são mais eficazes na absorção da solução devido a uma fácil saída de ar nos poros de maiores dimensões, permitindo a penetração da solução que preenche os poros; poros maiores que 5 μm e menores que 0.1 μm dificilmente estavam preenchidos com sais. Os autores demonstraram que microporos de pequenas dimensões (inferiores a 0.1 μm) são importantes no desenvolvimento de maiores tensões de cristalização, enquanto os microporos de maiores dimensões (pequenos capilares entre 0.1 μm e 5 μm) são mais eficazes na captação dos sais. Estas observações estão de acordo com os estudos desenvolvidos por Zehnder e Arnold [Zeh89] que observaram que a cristalização dos sais ocorria essencialmente em poros entre 0.5 e 5 μm, embora os poros com dimensões inferiores a 0.1 μm também estivessem preenchidos com sais.

Considerando poros de grandes e pequenas dimensões, no início do processo assume-se que o volume total dos poros é saturado com solução salina e não existe a formação de cristais. Os poros de maiores dimensões secam primeiro, seguidos dos poros de menores dimensões [Pel02]. Uma argamassa apresenta dimensões de poros desde 10 μm a 100 μm, os tijolos de silicato de cálcio apresentam poros entre 1 μm e 100 μm e os tijolos de barro entre 0.1 μm e 100 μm [Pel95]. Nas rochas porosas, a pressão de tensão de cristalização efetiva devida ao crescimento dos sais pode ser considerada em poros com dimensões entre 0.1 e 10 μm. Um cristal necessita de um grau de saturação considerável para poder penetrar nos poros com fração inferior a 0.1 μm. Estes graus de saturação não são frequentes em rochas para construção, podendo no entanto ser conseguidos em laboratório, com testes de cristalização de sais [Ben11].

2.6 Ensaios de cristalização de sais

Existindo sais nas paredes o seu transporte e cristalização serão dependentes das condições ambientais, tais como a temperatura e a humidade relativa. A degradação devida aos sais é influenciada pela variação da humidade. Esta secção não pretende apresentar de forma exaustiva os procedimentos de teste existentes, mas justificar, com base na literatura, os testes de cristalização adotados, considerados efetivos em laboratório, para testar a eficácia e durabilidade dos revestimentos estudados no âmbito desta tese, na presença de NaCl.

Em laboratório podem ser utilizados testes de envelhecimento acelerado para avaliar, quer o transporte de humidade, quer a degradação devida aos sais em materiais porosos. Estes testes incluem, de uma forma geral, elevadas concentrações de solução salina e variação das condições ambientais, conseguidas através de ciclos de molhagem (por ascensão de água por capilaridade) e posterior secagem a elevadas temperaturas (por forma a aumentar a velocidade de secagem e desta forma reduzir o tempo necessário, em laboratório, para que ocorra aparecimento da degradação devida à cristalização de sais).

Para tal podem ser utilizados diferentes provetes: i) argamassas de revestimento [Gon07, Lub06a, Gro09a], maquetas de pequenas dimensões constituídas por tijolos revestidos com argamassa [Fra10a, Vel06a, Mar09] e alvenarias de pedra revestidas com argamassas que simulam sistemas reais [Fra13a], em laboratório.

Numa primeira abordagem, e tal como já foi referido por Lubelli [Lub06], de acordo com a literatura os dois fatores principais que influenciam a degradação devido ao NaCl são: a rápida secagem obtida na presença de elevadas temperaturas, baixa humidade relativa ou elevada ventilação e variações da humidade relativa. A degradação na presença de sais solúveis não é resultado apenas de um evento em que ocorre cristalização, mas sim de ciclos repetidos de cristalização, que originam tensões de cristalização que vão degradando o material [Lub08a]. Nos materiais contaminados com sais higroscópicos, alterações na temperatura e humidade relativa do ar originam ciclos de dissolução e de cristalização dos sais que promovem a degradação. No caso específico do cloreto de sódio (o sal utilizado na presente investigação) a variação da temperatura não produz degradação considerável, pois a solubilidade deste sal não é afetada pela temperatura; no entanto, variações na humidade relativa podem originar ciclos de dissolução/cristalização e aumentar a degradação; assim a secagem em estufa poderá aumentar a evaporação e consequente degradação

Os testes de cristalização são testes de absorção (ascensão de solução salina) e secagem a que os provetes ou sistemas compostos por tijolos e sistema de revestimento, ou ainda as alvenarias de tamanho real com os sistemas de revestimento aplicados, são sujeitos. Nestes testes é utilizada uma elevada concentração de solução salina, repetição de contaminações e alteração

das condições ambientais, de modo a simular condições reais e gerar degradação. Os testes de cristalização de sais adotados no âmbito deste trabalho experimental simulam de forma tão real quanto possível, as piores condições de humidade ascensional continua e não apenas a presença de sais solúveis na alvenaria. Assim, foi definido que em cada ciclo a solução salina (27g/l) (similar à concentração do Oceano Atlântico Fig. 2.6) foi absorvida até massa constante e posterior secagem rápida a elevadas a temperaturas (60ºC) (ver capítulos 4, 5 e 7). Este procedimento foi adotado nos vários ciclos de dissolução/cristalização até à degradação. A eficácia destes testes é comprovada pelo transporte dos sais e acumulação na superfície do revestimento observada.

Tabela 2.6 Concentração dos principais sais presentes no Oceano Atlântico e no Mar Mediterrâneo [Aug90]

Sal	Oceano Atlântico (gramas/litro)	Mar Mediterrâneo (gramas/litro)
NaCl	28.14	30.76
KCl	0.69	0.66
$MgCl_2$	3.44	3.74
$CaSO_4$	1.42	1.64
$MgSO_4$	2.28	2.39

A cristalização de sais é uma das maiores causas da degradação de revestimentos, e depende do comportamento ao transporte de sais do sistema alvenaria/revestimento, da temperatura da envolvente e da humidade relativa. Condições ambientais desfavoráveis poderão originar ciclos repetidos de dissolução/cristalização, originando a rápida degradação dos materiais de construção [Lub06b]. Outros estudos referem que, com os testes de cristalização, a degradação foi conseguida, em laboratório, após vários meses e em provetes contaminados com sais muito agressivos, tal como é o caso do sulfato de sódio [Wij02]. No entanto, alguns revestimentos em edifícios podem apresentar degradação alguns anos após a aplicação [Hee03].

2.7 Medidas de reparação – Eliminação das causas das anomalias

Para eliminar as causas das anomalias poder-se-ão utilizar técnicas de tratamento que inibam a humidade ascensional, atuando na estrutura da parede (através da criação de uma barreira física ou química) ou no revestimento da alvenaria. Identificadas as caraterísticas das alvenarias, será importante identificar as limitações dos tratamentos utilizados. Algumas técnicas que atuam na estrutura da alvenaria têm vindo a ser estudadas; no entanto a sua eficácia é por vezes limitada devido à elevada heterogeneidade e espessura das paredes de alvenaria dos edifícios antigos.

As técnicas de tratamento contra a humidade ascensional na presença de sais solúveis podem ser conseguidas atuando na estrutura da alvenaria destes edifícios. Técnicas com base na aplicação de barreiras físicas, químicas ou eletroosmoticas [Mass93, Hen01, Vei09b, Fre02a, Hen01, Tor07] são utilizadas para reduzir os efeitos da humidade ascensional, mas apresentam-se por vezes ineficazes devido à elevada heterogeneidade e espessura destas paredes antigas. Mesmo nos casos em que é possível eliminar ou reduzir a humidade ascensional, a presença de sais

higroscópicos nas paredes pode continuar a produzir efeitos nefastos devido às alterações na humidade relativa.

Na tabela 2.7 apresenta-se a compilação dos principais tratamentos contra a humidade ascensional, por forma a minimizar a degradação na presença prolongada de elevados teores de humidade.

Tabela 2.7 Tratamento para alvenarias antigas para minimizar os efeitos da humidade ascensional

Tratamento (atuação na estrutura da parede) / Definição	
Criação de uma barreira física ou química	
Redução da secção absorvente [Mass93, Hen01]	Consiste na redução da secção absorvente através da substituição de parte do material por espaços vazios, com base na possibilidade da água absorvida evaporar facilmente através das aberturas criadas. Esta técnica pode ser pouco eficaz devido à elevada espessura das paredes e por questões estruturais.
Execução de corte hídrico [Mass93, Hen01]	Consiste na abertura de roços nas paredes ou remoção das juntas das paredes (este último caso pressupõe que a alvenaria seja executada com elementos regulares, com juntas contínuas e bem definidas) através dos quais é inserida a barreira estanque. A introdução deste tipo de barreira física poderá originar vibrações e problemas de estabilidade do edifício.
Injeção de produtos hidrófugos [Mass93, Hen01]	Impregnação química por injeção ou difusão de produtos hidrófugos ou tapa-poros, através dos drenos colocados na alvenarias com um determinado espaçamento entre si, por forma a produzir uma barreira impermeável. Este tipo de tratamento é muitas vezes ineficaz devido á elevada espessura e heterogeneidade das paredes de edifícios antigos.
Criação de drenos atmosféricos /tubos de arejamento [Vei09b, Fre02a, Mass93]	O princípio na base da colocação dos sifões de drenagem atmosférica é o fato de o ar húmido ser mais pesado que o ar seco. A colocação na posição obliqua destes drenos nas paredes liberta o ar húmido (no interior da parede), e facilita o processo de secagem das paredes.
Ocultação das anomalias [Vei09b, Hen01]	Execução de uma nova parede separada da original por uma caixa-de-ar, de forma a ocultar as anomalias, pode ser efetiva se realizada de forma adequada, embora reduza a área útil.
Ventilação da base das paredes [Vei09b, Fre02, Tor07]	Consiste na ventilação da base das paredes (através da criação de valas de ventilação na base das paredes), controlando a humidade ascensional através da promoção da evaporação ao nível mais baixo possível da parede e deste modo reduzindo os teores de humidade na base. Tanto em laboratório como *in situ* conduz à diminuição da humidade ascensional, aumentando a secagem das paredes.

2.8 Medidas de reparação – Minimização dos efeitos

Para reduzir ao mínimo a quantidade de água introduzida nas alvenarias deve-se considerar a ação dos seguintes elementos: soleiras, cobertura, beirais, caleiras, algerozes, etc. Uma adequada drenagem da água proveniente do solo é essencial para reduzir a água absorvida através das fundações para as alvenarias. Além disso, em climas frios, a utilização de sal para eliminar o gelo existente nos passeios ou nas estradas poderá ser transportado para as alvenarias através do contato desta humidade do solo com as alvenarias [Mau12]. O tratamento da humidade

ascensional em edifícios antigos é complexo devido à elevada espessura das suas paredes e heterogeneidade de soluções construtivas: quando os sais solúveis estão presentes o seu tratamento torna-se ainda mais complexo e é crucial estudar outras soluções que possibilitem a minimização dos efeitos associados à presença de humidade ascensional e sais solúveis (tabela 2.8).

Tabela 2.8 Tratamento das paredes de edifícios antigos contra a humidade ascensional na presença de sais solúveis

Tratamento de paredes de alvenarias – ação sobre o sistema de revestimento de argamassa	
Sistema de revestimento com porosidade controlada [Gon07, Pet10a, Pet10b, Hui07]	Reboco que promove a evaporação da humidade do interior das paredes e não permite que os sais cristalizem no exterior do revestimento. Este tipo de revestimentos de acumulação utiliza uma camada base (emboço) com dimensão de poros inferiores aos da camada exterior (reboco) e da alvenaria. Tem por base a teoria da secagem, segundo a qual o transporte da humidade está relacionado com a pressão capilar e a dimensão dos poros do material, considerando que a humidade e os sais permanecem no material com poros de menores dimensões. No entanto, de acordo com Huinik et al. [Hui07] os sais modificam as propriedades de secagem do reboco (essencialmente a diminuição da humidade relativa de equilíbrio na presença de sais solúveis), evitando a sua secagem completa e assim os sais migram facilmente do emboço para o reboco, devido à existência de continuidade líquida. Como resultado, criar um revestimento de acumulação apenas com base em diferenças de porosidade é impossível.
Sistema de revestimento de acumulação [Gon07, Pet10a, Pet10b, Rod05]	Um revestimento de acumulação pode ser conseguido através da aplicação de um agente hidrófugo na camada mais exterior (reboco), e assim prevenir a acumulação de água e de sais no reboco, acumulando-se os sais no emboço com maior porosidade. Esta solução pode induzir a cristalização sem que se degrade a superfície do revestimento, mas pode ter outras desvantagens associadas à maior dificuldade de evaporação da água que se encontra no interior da parede.
Sistema de revestimento de transporte [Gon07, Pet10a, Pet10b, Rod05]	Este sistema de transporte permite o transporte da solução líquida para a superfície exterior (reboco) onde as eflorescências aparecem, como é o caso de um revestimento tradicional de cal.
Remoção de sais através de revestimentos sacrificiais [Saw08a, You08]	Consiste na utilização de materiais absorventes com poros muito pequenos que induzem elevada sucção quando em contato com a alvenaria. A água contida no material absorvente é introduzida na parede e dissolve os sais, e o material absorvente retrai e absorve os sais na superfície da parede. O sucesso deste tratamento depende da ligação entre o material absorvente e a alvenaria, das condições de secagem e da distribuição de sais inicial na alvenaria. No entanto a sua eficiência é difícil de medir especialmente devido à elevada espessura das paredes antigas.
Remoção eletrocinética de sais [Fra10b, Fra10f, Ott07a, Ott08a, Ott12a, Rör09a]	É baseado na remoção eletrocinética de sais através da aplicação de um campo elétrico aos materiais porosos na presença de humidade. Embora os resultados laboratoriais demonstrem resultados que apontam para a eficácia deste método de remoção de sais, mais estudos devem ser desenvolvidos para testar a sua eficácia em alvenarias de edifícios.
Revestimento “Emboço ventilado” (desenvolvido no âmbito desta tese) [Fra10a, Fra10c, Fra10e, Fra12a, Fra13a]	Este sistema baseia-se no fato de que o ar húmido é mais pesado do que ar seco. Este sistema é executado com rasgos verticais na camada de emboço, que poderão ajudar a libertar a humidade existente na alvenaria, e portanto facilitar o processo de secagem da parede, favorecendo a acumulação de sais nestes rasgos. Previne a acumulação de sais na alvenaria (devido à existência dos rasgos verticais), assim como no reboco (quando é utilizada argamassa de cal hidrófuga no reboco) aumentando a durabilidade do sistema de revestimento quando comparado com outros sistemas de revestimento “resistentes aos sais”.

Quando se utilizam argamassas de substituição espera-se que estas tenham um adequado tempo de vida útil (ou seja que sejam duráveis).

Uma durabilidade adequada de uma argamassa de substituição compreende: resistência à ambiência envolvente (por exemplo, ciclos de gelo-degelo, sais, erosão associada ao vento, chuva ácida, elementos biológicos). A distribuição granulométrica das areias e a introdução de ar tem uma importância relevante na sua resistência ao gelo. Uma argamassa de substituição não deve promover tensões excessivas nos elementos pré-existentes (alvenaria e argamassas em bom estado de conservação): não deve ser mais forte do que o necessário em termos de requisitos estruturais e de durabilidade, deve ter resistência inferior à resistência dos materiais constituintes da alvenaria, não deve conter elevados teores de sais, deve permitir a secagem da alvenaria (quer por capilaridade, quer por difusão de vapor de água) [Mau12].

Outro tipo de rebocos utilizados em ações de reabilitação são os denominados “rebocos sacrificiais” que são rebocos porosos com elevada sucção e que são utilizados durante um curto espaço de tempo (alguns meses até 2 anos). Eles removem elevadas quantidades de sais da alvenaria durante este período, sendo depois removidos e substituídos por revestimentos de substituição [Pav11].

Com base nas anomalias observadas na presença de humidade ascensional e sais solúveis e na dificuldade associada à sua resolução, têm vindo a ser desenvolvidas novas soluções de revestimento adequadas a cada tipo de caso. A escolha dos revestimentos compatíveis que permitam a evaporação é um princípio básico; por outro lado, revestimentos que permitam a cristalização dos sais no revestimento poderão ser uma boa escolha (ver capítulos 5 e 7). A remoção eletrocinética de sais, com base na aplicação de um campo elétrico nos materiais porosos na presença de humidade, através do qual a corrente é transportada por eletrões nos elétrodos metálicos e por iões nos poros do material na presença de humidade, é uma solução possível quando o NaCl é o sal presente. Este tratamento permite a remoção dos iões Cl dos revestimentos (ver capítulo 6).

2.8.1 Argamassas de substituição para alvenarias antigas – formulações e requisitos gerais

A durabilidade de um revestimento de substituição é fundamental para o sucesso da intervenção e para o seu desempenho durante o tempo de vida útil esperado. A qualidade do revestimento depende do ligante, traço da mistura, porosidade total e distribuição da porosidade. Para além da porosidade total, a sua distribuição dimensional é um parâmetro importante pois poros com diâmetros superiores a 60 μm não são considerados eficazes na absorção de água por capilaridade [Pav11]. Os revestimentos são os constituintes mais vulneráveis dos edifícios antigos. A sua função de proteção da alvenaria e a sua exposição aos agentes externos, tais como as

ações climatéricas (chuva, vento, nevoeiro salino, etc.), a poluição e as ações mecânicas tornam-nos suscetíveis à degradação. A falta de manutenção e de conhecimentos técnicos sobre as técnicas de conservação podem originar elevada degradação, sendo necessária a sua substituição [Vei08a, Vei10a].

Uma estratégia de conservação é sempre a melhor opção a considerar quando a degradação afeta alvenarias antigas: pequenas reparações, preenchimento de lacunas e fissuras, consolidação da perda de coesão (através da utilização de um produto consolidante fluido – consolidantes orgânicos sintéticos ou inorgânicos) e restituição da perda de aderência (através da injeção de caldas de cal compostas por ligantes aéreos, hidráulicos e aditivos – grouts) [Tav09a]. No entanto, caso a degradação seja generalizada ou existam elevadas áreas com destacamentos, poderá ser necessária a substituição parcial ou total dos revestimentos antigos por novos. Nestes casos, a definição de novas argamassas de substituição, duráveis e compatíveis com os materiais pré-existentes, é essencial para a manutenção da imagem e integridade do edifício [Vei08a, Vei09a].

Os revestimentos com base em cal foram utilizados em Portugal até à 1ª metade do séc. XX altura em que começaram a ser substituídos por revestimentos com base em cimento. As vantagens aparentes do cimento, tais como a sua maior resistência e rápida presa, levaram ao desuso dos revestimentos de cal e à consequente falta de conhecimento das suas propriedades e caraterísticas. Entretanto a utilização de revestimentos de substituição com base em cimento, em alvenarias de edifícios antigos, tem efeitos adversos, pois apresentam-se demasiado rígidos e impermeáveis à água no estado líquido e de vapor; para além de apresentarem uma tendência para a fissuração através da qual a água migra para o interior do revestimento e da alvenaria sendo difícil a sua subsequente evaporação e, assim, aumentando a degradação [Hug03a, Mos06a].

Os revestimentos de substituição devem ser menos resistentes do que a alvenaria antiga para que possam acomodar as pequenas variações dimensionais dessas alvenarias, o que não acontece quando são utilizados revestimentos de cimento. Os revestimentos de cimento apresentam maior coeficiente de dilatação térmica que as argamassas de cal da alvenaria e sais solúveis [Mos06a, Gon06a].

Pelo menos desde o período Romano, são utilizadas pozolanas naturais e artificiais nas argamassas de cal com o intuito de melhorar a resistência à água e a durabilidade destas argamassas. O teor em sílica, a distribuição granulométrica e a superfície específica são fatores intrínsecos que influenciam a reatividade da pozolana. As pozolanas naturais são essencialmente de origem vulcânica e são produzidas pelo aquecimento a elevadas temperaturas de materiais naturais tais como argilas, conchas e algumas rochas siliciosas [Hug03a, Mor04a, Vel01a]. As argamassas de cal com pozolanas são física e quimicamente compatíveis com as argamassas

antigas devido à sua composição idêntica, e são capazes de acomodar o movimento das alvenarias. Numa intervenção a escolha dos materiais, textura, cor da camada de acabamento deve ter em conta os requisitos funcionais, o clima, a localização e as matérias-primas existentes no local [Hug03a, Mor04a].

Atualmente existem no mercado vários tipos de revestimentos de substituição para alvenarias com elevado teor de sais solúveis; no entanto o comportamento destes revestimentos nem sempre é o esperado. Este facto é essencialmente devido à falta de conhecimento sobre o transporte da humidade e dos sais solúveis através da alvenaria, através do revestimento, entre a alvenaria e o revestimento, assim como das condições da envolvente (teores de sais solúveis presentes, fontes de humidade, condições ambientais) [Lub06].

Requisitos gerais

A durabilidade e eficácia dos revestimentos de substituição dependem de vários fatores tais como: a escolha dos materiais, o traço da argamassa, a execução e aplicação e o tipo de exposição ao ambiente envolvente [Hug03a, Mar03a, Von97a, Mal88a, Far04].

A compatibilidade dos revestimentos de substituição deve ser assegurada considerando: i) a compatibilidade mecânica (resistência à flexão e compressão e módulo de elasticidade devem ser semelhantes às dos materiais pré-existentes); ii) compatibilidade física especialmente em termos de comportamento à água (permeabilidade ao vapor de água e coeficiente de capilaridade); e iii) compatibilidade química entre as argamassas de substituição e os materiais pré-existentes [Bar95a, Pap98a, Mor98, Rod98a, Val00a, Cal00a, Gro00a, Vei01a, Lan03a, Pap03a, Far04].

De um modo geral, por questões de compatibilidade, devem ser recomendados revestimentos com base em cal para edifícios antigos, para os quais existe uma grande diversidade de misturas possíveis para se conseguir obter revestimentos duráveis, tendo em conta a especificidade do ambiente envolvente e ações exteriores em cada caso. Para a seleção dos materiais é necessário conhecer as caraterísticas gerais, tendo em conta o caso específico sempre que possível, assim como os materiais pré-existentes e as condições envolventes.

As argamassas a utilizar em revestimentos de substituição em paredes de edifícios antigos – como argamassa de rebocos ou de juntas para alvenarias de pedra ou tijolo ou ainda como argamassas de ligação de revestimentos cerâmicos – devem estar de acordo com um conjunto de requisitos físicos, mecânicos e químicos, para além dos requisitos estéticos que incluem não descaraterizar o edifício.

Os requisitos estabelecidos para argamassas de edifícios antigos são muito diferentes dos definidos para edifícios recentes, devido aos critérios de compatibilidade subjacentes: menor resistência, maior deformabilidade, maior capilaridade e permeabilidade ao vapor de água e menor

teor de sais solúveis. Para além do referido, a diversidade de parâmetros que é necessário ter em consideração é maior no caso dos edifícios antigos de modo a garantir a preservação dos materiais pré-existentes. Os revestimentos de substituição não devem contribuir para aumentar a degradação dos elementos pré-existentes com os quais estão em contato, o que implica que não transmitam tensões elevadas, não contribuam para reter água no interior da parede ou alterar o seu transporte (sendo que alguma impermeabilização à água no estado liquido deve ser assegurada, embora mantendo elevada permeabilidade ao vapor de água), não contenham elevado teor em sais solúveis [Pap98a, Mor98a, Val00a, Vei01a].

A compatibilidade física deve ser assegurada em termos de comportamento à água: coeficiente de capilaridade e permeabilidade ao vapor de água (semelhantes aos das argamassas pré-existentes e inferior ao suporte) de forma a permitir a evaporação da água absorvida; os revestimentos de substituição não devem reduzir o transporte do vapor de água que circula devido a diferenças de pressão entre o exterior e o interior do edifício, evitando a sua acumulação no interior da alvenaria. A compatibilidade mecânica deve ser assegurada através de resistências à tração, compressão e módulo de elasticidade semelhantes aos das argamassas pré-existentes e inferiores aos do suporte, evitando a introdução de tensões elevadas nos elementos pré-existentes. A compatibilidade química será assegurada pelo baixo teor de sais solúveis e através da definição de soluções de revestimento resistentes à cristalização de sais e que minimizem os seus efeitos.

Em estudos anteriores [Vei01a, Vel05a, Adr07a, San06a, Tav08a, Tav08b, Mag09a], várias argamassas de diferentes períodos, regiões e usos, de edifícios antigos portugueses foram caraterizadas em laboratório e *in situ*. Algumas alvenarias também foram testadas, essencialmente através de testes *in situ*, para quantificar as características de compatibilidade consideradas mais importantes: resistência (ensaios de choque de esfera, esclerómetro Schmidt), módulo de elasticidade (através de ultra-sons) e absorção de água (através de Tubos de Karsten). A quantificação dos requisitos gerais apresentados na tabela 2.9 tem por base os resultados obtidos nestes estudos, tendo em conta uma análise conservativa e considerando os seguintes requisitos gerais: os revestimentos de substituição devem ser mais fracos e apresentar maior absorção do que o suporte; quando as características do suporte não são conhecidas, devem ser selecionados revestimentos de substituição com características semelhantes aos revestimentos pré-existentes; quando não são conhecidos nem as caraterísticas do suporte, nem as dos materiais pré-existentes devem ser escolhidos revestimentos de substituição com caraterísticas moderadas para evitar a degradação da alvenaria.

As exigências gerais a ter em conta em revestimentos de substituição para edifícios antigos devem incluir [Vei07c]: resistência à flexão e compressão e módulo de elasticidade semelhantes aos das argamassas originais e inferiores aos do suporte; resistência ao arrancamento inferior à resistência à tração do suporte (a rotura não deve ser coesiva pelo suporte); a permeabilidade ao

vapor de água e coeficiente de capilaridade semelhantes às argamassas originais e superiores às do suporte.

Na Tabela 2.9 são quantificadas as exigências para as características consideradas mais relevantes para o cumprimento dos critérios de compatibilidade no âmbito deste trabalho. Estas exigências foram quantificadas por Veiga em conjunto com outros investigadores [Vei02a, Vei04a, Vei07c], tendo por base a experiência adquirida no estudo de argamassas antigas e de argamassas de cal preparadas em laboratório.

Tabela 2.9 Requisitos estabelecidos para as características mecânicas e de comportamento à água das argamassas de substituição

Argamassa	Características mecânicas aos 90 dias			Comportamento à água aos 90 dias	
	Rt (N/mm^2)	Rc (N/mm^2)	E (N/mm^2)	Sd (m)	C ($kg/m^2/min^{1/2}$)
Reboco exterior	0.2–0.7	0.4–2.5	2000–5000	< 0.08	< 1.5; > 1.0
Reboco interior	0.2–0.7	0.4–2.5	2000–5000	< 0.10	-
Juntas	0.4–0.8	0.6–3.0	3000–6000	< 0.10	< 1.5; > 1.0

C, coeficiente de capilaridade; E, modulo de elasticidade; Rc, resistência à compressão; Rt, resistência à tração; Sd, espessura da camada de ar de difusão equivalente (valor relacionado com a permeância).

De um modo geral, os requisitos estabelecidos representam uma simplificação da definição de compatibilidade de revestimentos de substituição. Estes requisitos surgem como uma primeira abordagem quando não são conhecidas as caraterísticas do suporte nem dos materiais pré-existentes. No entanto, sempre que possível, deve-se proceder à caraterização do suporte, assim como dos materiais pré-existentes.

Formulações das argamassas para revestimentos de substituição

Foi realizada uma compilação de resultados com o objetivo de obter caraterísticas comparativas de diferentes formulações, como uma primeira abordagem para a seleção de argamassas de conservação e substituição. A compilação referida foi elaborada com base nos resultados obtidos por um grupo de investigação do Laboratório de Revestimentos e Isolamentos do LNEC entre os quais se encontra a autora deste trabalho [Vei08a, Vei10a].

Os testes foram realizados em diferentes alturas, por isso alguma heterogeneidade nos resultados para composições semelhantes pode ser explicada devida aos diferentes materiais utilizados (principalmente na granulometria dos agregados) e a pequenas diferenças nos procedimentos [Vei09c, Vei94a, Mag05a, Vei07a, Vei07b, Fra07a, Fra07b, Mag06a, Mar97a, Mar06a, Vel05a, Vel07a, Vel07b, Vel06].

A seleção dos revestimentos foi realizada com base em dois critérios: i) materiais mais utilizados em Portugal nas intervenções, por empresas de construção e profissionais da conservação e ii) materiais semelhantes aos identificados em alvenarias antigas.

Relativamente ao primeiro critério, a abordagem às intervenções por parte das empresas de construção e dos profissionais da conservação são distintas devidas essencialmente às diferentes culturas, sensibilidades e escala da intervenção. As empresas de construção utilizam essencialmente materiais comuns tais como cimento e cal hidráulica nacional (NHL classe 5) e areias comuns, enquanto os profissionais da conservação realizam de uma forma geral intervenções de menor envergadura e mais especializadas com materiais selecionados, tais como cal hidráulica importada (HL classe 3.5), materiais industriais pré-doseados e areias calibradas. As designações apresentadas referentes às cais hidráulicas foram definidas de acordo com a classificação da versão antiga da norma NP EN 459: 2002 [IPQ2002].

A seleção de formulações em que se utilizam materiais e/ou características similares com as das argamassas antigas, embora utilizando versões mais recentes e fáceis de obter, tais como cal aérea (em pó) e adições pozolânicas (pozolanas artificiais, incluindo resíduos da indústria), preenchem o segundo critério definido.

As argamassas selecionadas foram formuladas com diferentes ligantes: cimento, cal hidráulica das classes 5 e 3.5 segundo a norma NP EN 459: 2002 [IPQ2002], cal aérea hidratada (em pó); varias adições pozolânicas (duas pozolanas naturais e seis pozolanas artificiais); alguns aditivos; diferentes dosagens e diferentes distribuições de agregados. Algumas argamassas pré-doseadas com base em cal hidráulica e cal aérea também foram selecionadas.

As formulações foram baseadas na proporção volumétrica definida por Vitrúvio de 1:3 (ligante: agregado em volume) com base em hipóteses científicas (Vitrúvio referiu esta proporção e o volume de vazios de uma areia bem graduada é próximo de 1/3) e no facto de outras proporções testadas até ao momento não apresentarem melhorias significativas [Mar97a]. Relativamente às argamassas de cimento, a formulação referida é considerada demasiado rica e a proporção de 1:4 foi utilizada (muito comum para argamassas em Portugal); a mesma proporção (1:4) foi definida para argamassas com cal hidráulica NHL 5.

As formulações das argamassas selecionadas estão descritas nas tabelas 2.10 a 2.12: para argamassas com base em cimento (Tabela 2.10) [Vei94a, Mag05a, Vei07a], argamassas com base em cal hidráulica (Tabela 2.11) [Vei94a, Mag05a, Vei07a] e argamassas com base em cal aérea (Tabela 2.12) [Vei09, Vei94a, Mag05a, Vei07b, Fra07a, Fra07b, Mag06a, Mar97a, Mar06a, Vel05a, Vel06a, Vel07a, Vel07b].

Tabela 2.10 Composição das argamassas com cimento ou cimento e cal aérea.

Argamassa	Referência	Cimento	Cal aérea	Areia	Composição
C 1:4	C-1a	1	-	4	Cimento; areia T
	C-1b	1	-	4	Cimento; areia C
	C-1c	1	-	2+2	Cimento; areia C
C-AL 1:1:6	C-AL1a	1	1	6	Cimento branco; cal aérea; areia T
	C-AL1b	1	1	5.5+0.5	Cimento; cal aérea; areia M
C-AL 1:2:9	C-AL 2a	1	2	9	Cimento branco; Cal aérea; Areia siliciosa bem graduada
	C-AL 2b	1	2	4.5+4.5	Cimento; Cal aérea; areia C
C-Al 1:3:12	C-AL3	1	3	12	Cimento; Cal aérea; areia T

C - Areia de Corroios (areia siliciosa com alguma argila);M - areia siliciosa, T - areia siliciosa do Rio Tejo

Tabela 2.11 Composição das argamassas com cal hidráulica ou cal hidráulica e cal aérea.

Argamassa	Referência	Cal hidráulica	Cal aérea	Areia	Composição
HL-1:3	HL-1ª	1	-	3	HL 3,5; areia siliciosa bem graduada
	HL-1b	1	-	1.5 + 1.5	HL 3,5; areia T e areia C
HL-1:3.5	HL-2	1		3.5	NHL 5; areia T
HL-1:4	HL-3ª	1		4	NHL 5; areia T
	HL-3b	1		4	NHL 5; areia C
	HL-3c	1		2+2	NHL 5; areia T e areia C
HL-AL 1:1:6	HL-AL1	1	1	3+3	HL 3,5; areia T e areia C
HL-PD	HL-PD	-	-	-	Pré-doseada com base em cal hidráulica
HLAL-PD	HLAL-PD	-	-	-	Pré-doseada com base em cal hidráulica e cal aérea

C - Areia de Corroios (areia siliciosa com alguma argila); T - areia siliciosa do Rio Tejo

Tabela 2.12 Composição das argamassas com cal aérea e cal aérea e pozzolanas e outros aditivos

Argamassa	Referência	Cal aérea	Poz. Nat.	Poz. Art.	Areia	Composição
AL 1:3	AL-1a	1	-	-	3	Cal aérea; areia T
	AL-1b	1	-	-	3	Cal aérea; areia siliciosa bem graduada
	AL-1c	1	-	-	1,5+1,5	Cal aérea; areia T e areia C
	AL-1d	1	-	-	3	Cal aérea; areia M
	AL-1e	1	-	-	3	Cal aérea; 2/3 areia M (grossa) e ½ areia M (fina)
H-AL 1:3	H-AL	1	-	-	1,5+ 1,5	Cal aérea hidrófuga; areia T e areia C
AL-PD	PD-AL	-	-	-	-	Pré-doseada com base em cal aérea com adição acrílica
AL-PCV 1:1:4	AL-PCV1	1	1	-	4	Cal aérea; Pozolana Cabo Verde; areia T
AL-PCV 1:0.5:2.5	AL-PCV2	1	0,5	-	2,5	Cal aérea; Pozolana Cabo Verde; areia T
AL-PA 1:1:4	AL-PA	1	1	-	4	Cal aérea; Pozolana Açores; areia T
AL-M 1:1:4	AL-M1	1	-	1	4	Cal aérea; metacaulino; areia T
AL-M 1:0.5:2.5	AL-M2	1	-	0,5	2,5	Cal aérea; metacaulino; areia T
AL-PT/AL-CV 1:1:4	AL-PT	1	-	1	4	Cal aérea; pó de tijolo; areia T
	AL-CV	1	-	1	4	Cal aérea; cinzas volantes; areia T
AL-RAE 1:1:4	AL-RAE	1	-	1	4	Cal aérea; argila expandida; areia T
AL-SF 1:0.25:2.5	AL-SF	1	-	0,25	2,5	Cal aérea; sílica de fumo ; areia T
AL-G 1:1:4	AL-G	1	-	1	4	Cal aérea; pó de vidro; areia T

T – areia siliciosa do rio Tejo; C – areia de Corroios (areia siliciosa com alguma argila); M – areia siliciosa; Poz. Nat. – Pozolana natural; Poz. Art. – Pozolana artificial

Execução e condições de cura

As argamassas foram preparadas e misturadas de acordo com os procedimentos descritos na EN 1015-2 e as condições de cura de acordo com as condições especificadas pela EN 1015-11.

As condições de cura foram modificadas em alguns casos: i) para as argamassas cujo ligante é apenas a cal aérea foram utilizadas condições de cura seca (23ºC e 50% HR) que representam as condições de primavera e/ou verão frequentes em Portugal; algumas argamassas de cal aérea e pozolanas – argamassas de cal aérea e pozolanas naturais de Cabo Verde (AL-PCV1, AL-PCV2) e cal aérea e pó de vidro (AL-G) para além das condições especificadas na EN 1015-11, foram adicionalmente submetidas a diferentes condições de cura para tentar simular as condições de cura em obra. As condições de cura definidas pela EN 1015-11 consistem em 20ºC e 95% RH após moldagem até 5 dias, após os quais foram mantidos a 20ºC e 65% RH até à data em que foram realizados os ensaios.

Ensaios

Os ensaios realizados consistiram num conjunto de testes em laboratório escolhidos para determinar as características básicas que definem os requisitos gerais (Tabela 2.9) das argamassas tendo em conta uma primeira abordagem em termos de compatibilidade.

A caraterização laboratorial for definida para avaliar as características mecânicas e físicas das argamassas formuladas incluindo: i) resistência mecânica (Rc) e resistência à tração por flexão (Rt), com base no método prescrito na norma EN 1015-11; ii) módulo de elasticidade E, determinado pela frequência de ressonância definida pelo método da Norma Francesa NF B10-511 (1975); iii) coeficiente de absorção de água devido à ação capilar (C), com base no método prescrito na norma EN 1015-18; e iv) permeabilidade ao vapor de água, através da espessura da camada de ar de difusão equivalente (Sd), com base na norma EN 1015-19. Foram feitos alguns ajustamentos às normas Europeias (EN 1015) dependendo dos materiais utilizados: argamassas de cal aérea e cal hidráulica foram testadas aos 90 dias e não aos 28 dias devido ao tempo necessário para o seu endurecimento. Os resultados são apresentados nas figuras 2.4 a 2.8.

Análise dos resultados

As argamassas de cimento estabilizam as suas características por volta dos 28 dias, sendo que as argamassas com base em cal endurecem lentamente e apenas aos 90 dias é considerado um período adequado para o compromisso entre a carbonatação completa (que poderá estender-se por alguns anos, mas em curva assimptótica) [Mor05a, Mor05b], e o tempo de aceitável para a investigação. Para as argamassas com base em cal é esperada que a resistência mecânica aumente ao longo do tempo e a absorção diminua; no entanto a sua quantificação não é possível, com exceção de alguns casos específicos, tendo em conta a variabilidade de fatores subjacentes.

Características mecânicas

Nas Figuras 2.4 a 2.6 são apresentados os intervalos de valores para as caraterísticas mecânicas das argamassas estudadas. As linhas coloridas horizontais apresentadas nas figuras indicam os limites dos requisitos gerais propostos.

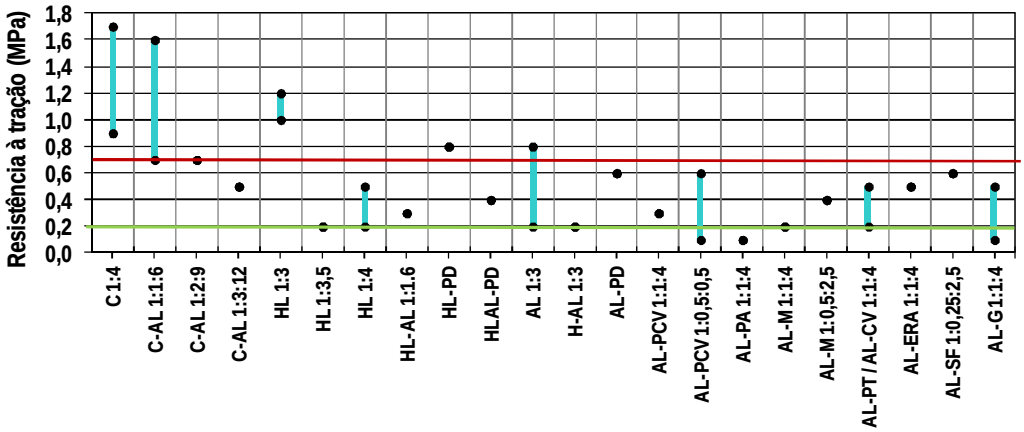

Fig. 2.4 Intervalos de valores para a resistência à tração – Rt (MPa)

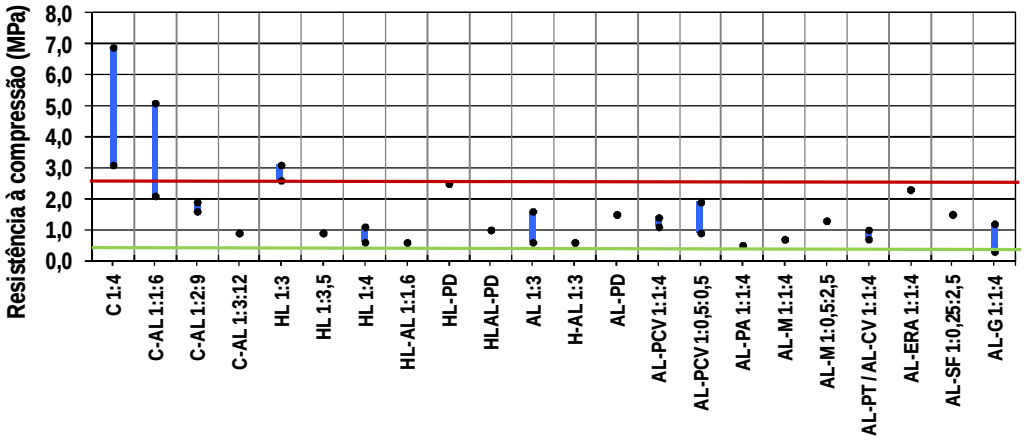

Fig. 2.5 Intervalo de valores para as resistências à compressão – Rc (MPa)

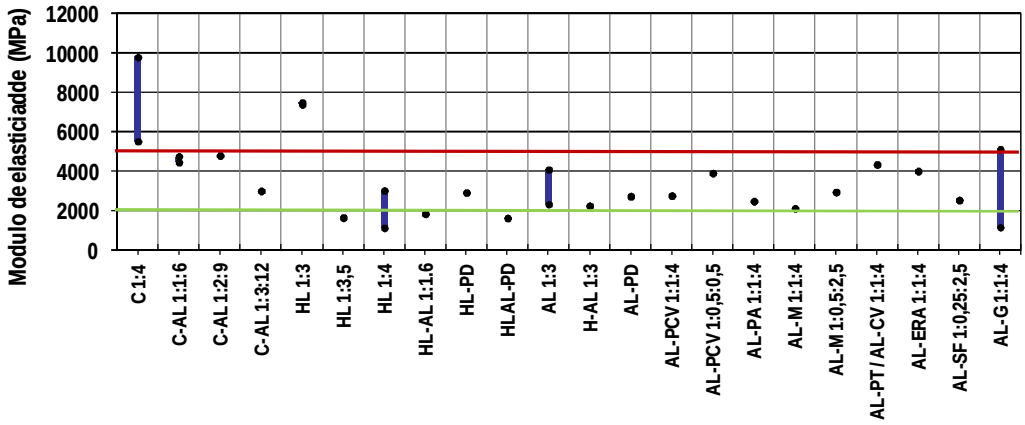

Fig. 2.6 Intervalo de valores para os módulos de elasticidade – E (MPa)

Verifica-se, relativamente à resistência mecânica, que as argamassas de cimento são demasiado rígidas e resistentes para serem utilizadas como argamassas de substituição para edifícios antigos. As argamassas compostas por cimento e cal em proporções volumétricas idênticas consideram-se igualmente demasiado resistentes para a maioria dos suportes, embora as restantes características possam ser consideradas adequadas.

As argamassas com menores quantidades de cimento poderão ter caraterísticas mecânicas adequadas: os traços volumétricos 1:2:9 e 1:3:12 correspondem a caraterísticas mecânicas moderadas e preenchem os requisitos.

As argamassas com base em cal hidráulica com traço volumétrico 1:3 parecem ser demasiado rígidas. As restantes argamassas com base em cal hidráulica e cal aérea apresentam boas caraterísticas, em termos de comportamento mecânico. Os resultados não são diretamente comparáveis pois foram utilizadas duas cais hidráulicas diferentes e em diferentes proporções. Foi assumido que a cal hidráulica NHL 5 confere maior resistência mecânica à argamassa, tendo sido utilizados menores traços ligante: agregado; no entanto esta hipótese não foi confirmada através dos resultados obtidos. Estudos recentes também confirmam esta incongruência [Pen08a]. Embora os resultados obtidos permitam a inclusão da argamassa NHL 5 no intervalo de compatibilidade, também apontam para alguma imprevisibilidade e assume-se que as argamassas com este ligante devem ser mais estudadas antes da sua ampla utilização em edifícios antigos. Estes resultados foram obtidos a partir de cal hidráulica definida segundo a normalização antiga NP EN 459-1:2002 [IPQ2002], segundo a qual classificavam-se como cais hidráulicas naturais (NHL), as cais que continham adições hidráulicas, podendo essas ser constituídas por materiais pozolânicos ou hidráulicos apropriados ou reguladores de presa, adicionados até 20% em massa. Segundo a nova normalização NP EN 459-1:2011 [IPQ2011] as cais hidráulicas naturais passam a ter características diferentes dos restantes ligantes minerais e com uma maior homogeneidade na qualidade (conseguidas através do maior controlo dos constituintes e processo de fabrico) comparativamente às anteriormente designadas pelo mesmo nome [Fra12a, Far12b].

As argamassas com base em cal, com ou sem adições pozolânicas, estão incluídas, tal como esperado, nos intervalos de valores de compatibilidade e serão as argamassas com caraterísticas mais semelhantes às dos materiais pré-existentes. A maior resistência mecânica foi obtida para argamassas com cal aérea e pozolana de Cabo Verde (com o traço volumétrico 1:0.5:2.5) e com cal aérea e argila expandida (com traço volumétrico 1:1:4). Relativamente às argamassas de cal e metacaulino, a maior resistência mecânica foi obtida com o traço volumétrico 1:0.5:2.5.

Características físicas

Nas Figuras 2.7 e 2.8 apresentam-se os intervalos de valores para as características de comportamento à água estudadas. As linhas coloridas horizontais apresentadas nas figuras indicam os limites dos requisitos gerais propostos.

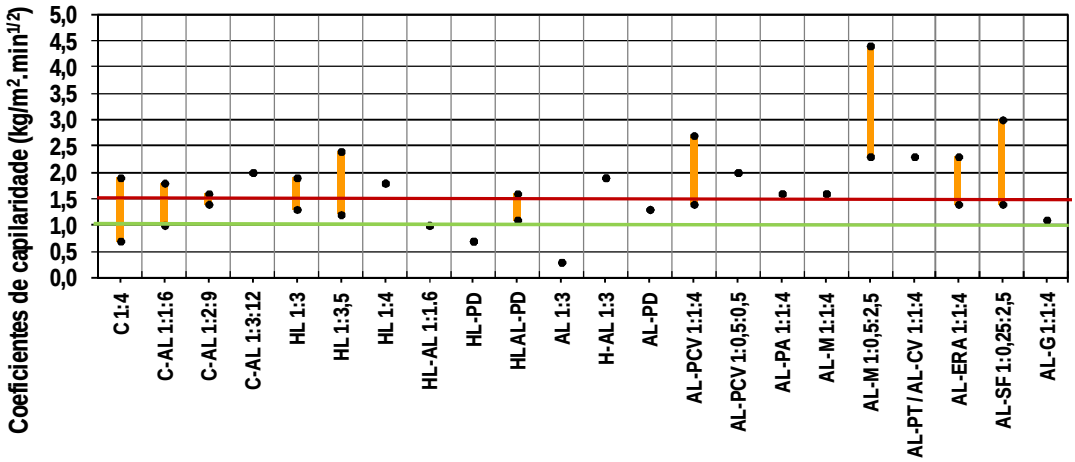

Fig. 2.7 Intervalo de valores para os coeficientes de capilaridade à água - C (Kg/m^2.min$^{1/2}$)

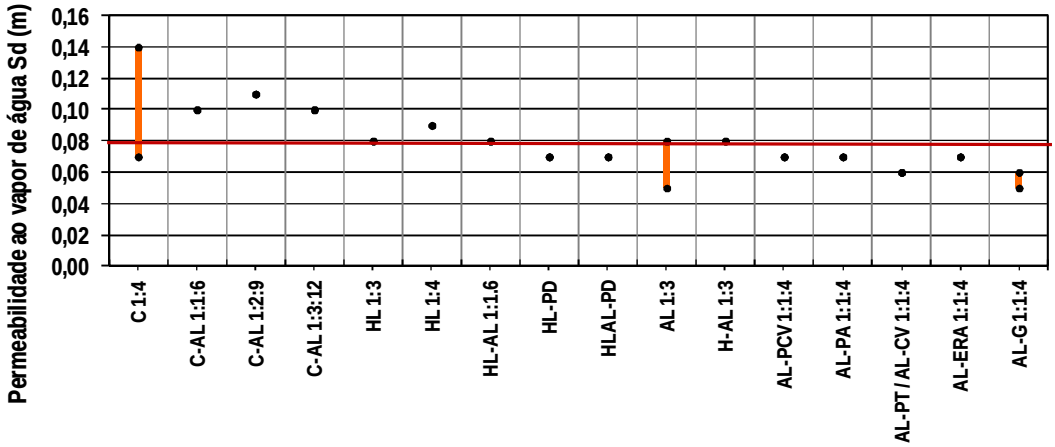

Fig. 2.8 Intervalos de valores para a permeabilidade ao vapor de água - Sd (m)

As argamassas com base em cimento estão fora dos limites definidos pelos requisitos quanto à permeabilidade à água no entanto, relativamente ao coeficiente de capilaridade à água a formulação 1:2:9 é adequada embora as restantes formulações 1:4, 1:1:6 e 1:3:12 já se encontrem fora dos limites.

De um modo geral, as argamassas com base em cal hidráulica encontram-se dentro dos limites aceitáveis quanto à permeabilidade ao vapor de água (exceto para a formulação 1:4); relativamente ao coeficiente de capilaridade será necessário controlar esta característica pois algumas formulações apresentam coeficientes de capilaridade fora dos limites estipulados.

Praticamente todas as argamassas estudadas com base em cal aérea estão dentro dos limites definidos pelos requisitos em termos de comportamento à água. Existem algumas exceções, em que o coeficiente de capilaridade está acima do limite estipulado, quando estas formulações incluem alguns tipos de adições pozolânicas, como é o caso: da pozolana de Cabo Verde (traço em volume 1:0.5:2.5); pó de tijolo (traço em volume 1:1:4), argila expandida (traço em volume 1:1:4) e pozolana dos Açores (traço em volume 1:1:4)

Análise final

As argamassas com pozolanas de baixa reatividade devem ter uma cura cuidada; caso contrário poderá ocorrer a carbonatação da cal antes da reação da pozolana com a cal, funcionando a pozolana como um agregado, não sendo possível obter-se o acréscimo de resistência pretendida com a incorporação da pozolana; no entanto caso seja utilizada uma pozolana de elevada reatividade este risco será muito menor [Hees12].

O intervalo de valores obtido para formulações semelhantes (o mesmo tipo de ligante e a mesma proporção ligante/agregado) foi essencialmente devida aos diferentes agregados utilizados – diferentes distribuições e à presença ou ausência de argila – e para as argamassas com adições pozolânicas foi devido essencialmente às diferentes condições de cura a que estas foram submetidas. Esta heterogeneidade nos valores pode também ser imputada aos diferentes operadores envolvidos ao longo do tempo; poderão na verdade ser consideradas úteis pois representam as diferenças também encontradas em obra, onde no final não é possível saber os valores exatos de cada característica em cada formulação. Na verdade, as condições existentes em obra e a mão-de-obra influenciam e muito a variação das características, mais do que em laboratório, por isso apresentar apenas um valor para uma dada característica de uma formulação não corresponderá a uma abordagem realística [Vei08a, Vei10a].

Testes complementares continuam a ser realizados em laboratório (tais como a estrutura porosa, aderência, retração restringida e capacidade de proteção à água) e *in situ* através da aplicação em painéis [Vei09c, Tav08a, Tav08b] e, para algumas formulações, através da aplicação em casos de estudo (ver Capítulo 3).

Considerando as argamassas com base em cal, verificou-se que para a argamassas com cal aérea e metacaulino a maior resistência mecânica foi obtida para a proporção 1:0.5:2.5, no entanto com alguma suscetibilidade à fissuração. Esta formulação tem sido estudada com o intuito de melhoria das suas caraterísticas (ver secção 2.8.2).

2.8.2 Argamassas de substituição para alvenarias antigas – teores de sais solúveis

Em revestimentos de substituição para edifícios antigos é importante garantir ao mínimo o teor de sais solúveis nas novas argamassas. Embora os revestimentos possam ser considerados física e mecanicamente compatíveis com os materiais pré-existentes, poderão ser considerados quimicamente incompatíveis caso contenham elevado teor em sais solúveis.

De acordo com a norma Austríaca ÖNORM B 3355-1 "Trockenlegung von Feuchtem Mauerwerk – Bauwerksdiagnostik und Planungsgrundlagen" ou seja "Desumidificação de alvenarias: diagnóstico e planeamento em edifícios" são definidos os limites de concentrações em sais solúveis para cloretos, sulfatos e nitratos de acordo com três categorias (Tabela 2.13): i) sem risco, ii) é recomendada uma avaliação em cada caso e iii) é recomendada a remoção de sais.

Tabela 2.13 – B 3355-1 ÖNORM B 3355-1 "Desumidificação de alvenarias – princípios de diagnóstico e planeamento" em mg/kg

Requisito	Cloretos (Cl^-)	Sulfatos (SO_4^{2-})	Nitratos (NO_3^{2-})
Sem risco	< 0,03	< 0,10	< 0,05
É recomendada a avaliação individual	0,03 – 0,10	0,10 – 0,25	0,05 – 0,15
É recomendada a remoção de sais	> 0,10	> 0,25	> 0,15

Na tabela 2.14 apresenta-se uma compilação de algumas argamassas tradicionais com base em cal e pré-doseadas (estas últimas existente no mercado português) supostamente adequadas para ações de conservação de alvenarias de edifícios antigos. Os resultados foram obtidos com base em resultados da investigação programada do LNEC "Revestimentos Históricos submetidos à ação severa da água 2009-2012" e do trabalho experimental de Margalha [Mar09].

Tabela 2.14 – Concentrações (em mg/kg) de alcalis, cloretos e sulfatos solúveis e resíduo insolúvel

Composição da argamassa	Sódio Na_2O	Potássio K_2O	Cloretos Cl^-	Sulfatos SO_4	Resíduo insolúvel
1:3 (HL-S : areia)	0.01	0.12	< 0.010	0.630	85.0
1:3 (HL-C : areia)	0.01	0.06	< 0.010	0.280	85.0
1:3 (HL-L1 : areia)	0.01	0.03	< 0.01	0.240	84.0
1:3 (HL-L2 : areia)	0.05	0.05	0.008	0.120	n.d.
PD-W (cal e cimento)	0.02	0.02	< 0.010	0.420	51.0
1:3:10 (cimento: cal: areia)	0.04	0.05	0.007	0.229	n.d
1:5 (L: areia)	0.05	0.02	0.007	0.085	n.d
1:3 (AL-BMC: areia)	0.04	0.04	0.010	0.079	n.d
1:3 (AL-WMC: areia)	0,05	0.04	0.007	0.070	n.d
1:3 (AL: areia) em massa	n.d.	0.01	0.030	0.480	71.0

HL – cal hidráulica; AL – cal aérea hidratada; L – cal em pasta; PD – argamassa pré-doseada; HL-S, HL-C, HL-L1 e HL-L2 cal hidráulica de diferentes produtores.
N.D. – não detetado

Comparando os resultados da Tabela 2.14 com as concentrações definidas na norma ÖNORM B 3355-1 verifica-se que as argamassas com cal hidráulica devem ser cuidadosamente selecionadas para intervenções de conservação especialmente devido ao seu elevado teor em sulfatos que

excedem os limites definidos na norma. Devem ser determinados os teores de álcalis e sulfatos das novas argamassas para minimizar a sua introdução nas alvenarias de edifícios antigos. Nesta compilação a seleção das areias foi cuidada pois os teores de cloretos encontram-se dentro dos limites definidos na norma.

2.8.3 Argamassas de substituição para alvenarias antigas – influência do uso de metacaulino, pó de tijolo e cal hidrófuga

Existem várias pozolanas artificiais (escórias de alto forno, metacaulino, sílica de fumo, pó de tijolo, cinzas volantes) que têm vindo se ser testadas em argamassas de cal [Vel06a]. O metacaulino e pó de tijolo têm vindo a demonstrar bons resultados quando adicionados a argamassas de cal.

O pó de tijolo, quando obtido a partir de tijolos recentes cozidos a elevadas temperaturas, pode apresentar muito baixa pozolanicidade, podendo funcionar como filler e não como pozolana nas argamassas. O pó de tijolo, com origem em tijolos tradicionais, cozidos a baixas temperaturas, poderá originar um aumento da resistência mecânica à flexão e compressão da argamassa e de acordo com Hees [Hees12] poderá ainda aumentar a impermeabilização e favorecer a retenção de água da argamassa.

O metacaulino é considerado uma pozolana eficaz quando introduzida em argamassas de cal: altera a estrutura porosa das argamassas, melhorando a sua resistência ao transporte de água e à difusão de iões solúveis através da estrutura das argamassas [Sab01a], quando pozolânico poderá originar um acréscimo da resistência das argamassas quando comparado com a utilização de outros materiais pozolânicos tradicionais [Hees12, Vei10a, Far04, Vel06a], embora, quando introduzido em argamassas de cal, possa apresentar uma tendência para a fissuração [Vei09c]. A reação entre o metacaulino, o hidróxido de cálcio e a água resulta na formação de produtos hidráulicos. No entanto, de acordo com a literatura, ainda não há uma explicação consistente sobre a estabilidade das fases hidratadas em função da razão cal/metacaulino, da temperatura e do tempo de cura [Gam12a, Gam12b, Ser87, Sil93]. A instabilidade das fases hidratadas poderá produzir efeitos indesejados na argamassa com o tempo – redução do volume, aumento da porosidade e perda de compacidade – resultando na diminuição da resistência mecânica e durabilidade das argamassas [Sil93]. Estudos recentes em pastas de cal e metacaulino [Gam12a, Gam12b], têm demonstrado que o uso de elevados teores de metacaulino (na ordem dos 50 % de substituição da cal): i) originam fases com *hydrogarnet* com baixo teor de sílica (responsável pelo decréscimo acentuado na resistência mecânica das pastas de cal e metacaulino) com o aumento do tempo de cura e ii) originam alguma stratlingite (responsável pelo aumento da resistência mecânica das pastas de cal e metacaulino) que se apresenta mais estável para menores teores de metacaulino.

Formulações

Algumas argamassas pré-doseadas da Fradical Lda., desenvolvidas em estudos anteriores e que se inserem no âmbito deste estudo são descritas na Tabela 2.15. Foi utilizada cal hidrófuga (cal aérea preparada de forma a apresentar um certo grau de hidrofugação) e adicionada pozolana artificial (composta por dois componentes e que inclui metacaulino) em duas proporções, 5 % e 10 % do volume da mistura total. Em algumas argamassas foi utilizado um "secante" (produto seco mineral) – 10 % do total da mistura no estado fresco – que, ao contribuir para o aumento da velocidade da reação pozolânica (através do aumento da temperatura), origina um aumento da resistência mecânica pelo menos durante os primeiros meses [Mag06a]. Para comparação foi ainda utilizada uma argamassa formulada com cal aérea hidratada comercial, aditivo pozolânico e areia siliciosa de rio.

Tabela 2.15 Composição das argamassas com cal aérea, cal aérea e pozolanas e outras adições da Fradical Lda, definidas em estudos anteriores [Mag08a, Mag06a]

Argamassa	Cal aérea	Cal hidrófuga	Adição pozolânica	Secante	Areia do rio
H-AL 1:0.4:3		1	0.40 (10%of 4)	-	3
H-AL 1:0.20:3		1	0.20 (5%of 4)	-	3
H-AL 1:(0.40+0.1):3		1	0.40 (10%of 4)	10% do volume	3
H-AL 1:(0.20+0.1):3		1	0.20 (5%of 4)	total da argamassa no estado fresco	3
AL 1:0.4:3	1	-	0.40 (10%of 4)	-	3

Execução e condições de cura

As argamassas foram preparadas de acordo com o especificado na norma EN 1015-2 e considerando as recomendações do fabricante. As condições de cura seguiram as especificações da norma EN 1015-11 (20°C e 65% RH durante os primeiros 5 dias, seguidas de 20°C e 65% HR até à data dos ensaios).

Ensaios

A caraterização laboratorial foi realizada para determinar as características mecânicas e físicas das argamassas formuladas e incluíram: resistência à tração por flexão (Rt) e à compressão (Rc), de acordo com a norma EN 1015 –11; módulo de elasticidade (E) [LNEC2005], determinado pelo método da frequência de ressonância da norma Francesa NF B10-511 (1975) e o coeficiente de absorção de água capilar (C) de acordo com a norma EN 1015-18. Estes testes estão representados nas figuras 2.10 e 2.11.

Caraterísticas mecânicas

Nas Figuras 2.9 e 2.10 estão apresentados os valores de resistência mecânica à tração por flexão e à compressão [Mag08a, Mag06a]. As linhas coloridas horizontais apresentadas nas figuras indicam os limites dos requisitos gerais propostos (Tabela 2.9).

Todas as argamassas demonstram uma tendência para o aumento da resistência à compressão com o tempo; no entanto, apenas as argamassas com adição de secante apresentam este comportamento para a resistência à tração.

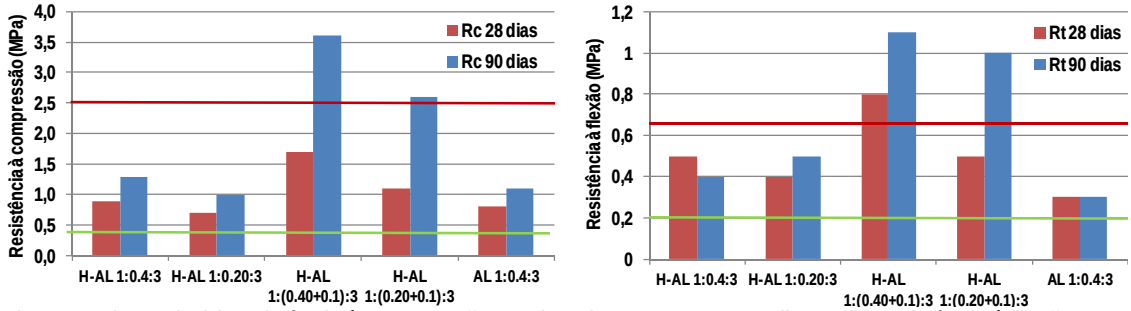

Fig. 2.9 Valores de (a) resistência à compressão, Rc (MPa) aos 28 e aos 90 dias, e (b) resistência à flexão, Rt (MPa) aos 90 dias.

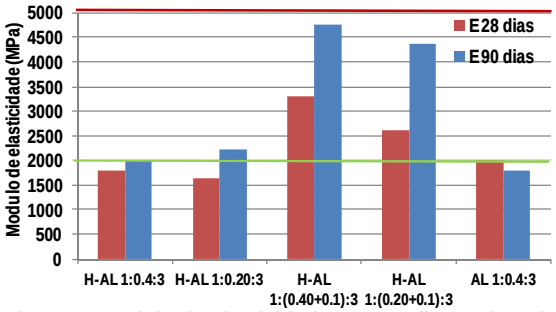

Fig. 2.10 Modulo de elasticidade aos 90 dias–E (MPa).

As argamassas com adição pozolânica e sem adição de secante apresentam valores de resistência à flexão, à compressão e módulo de elasticidade semelhantes entre si e dentro dos limites dos requisitos propostos.

No entanto, as argamassas com adição pozolânica e secante apresentam valores para as resistências à flexão e à compressão superiores aos limites definidos e com um aumento significativo dos 28 para os 90 dias; o módulo de elasticidade encontra-se dentro dos limites estabelecidos, embora superior do que os obtidos na generalidade das argamassas de cal. Estas argamassas atingem elevada resistência embora mais lentamente que as argamassas de cimento [Mag06a].

A argamassa comercial de cal com adição pozolânica (Al 1:0.4:3) apresenta características mecânicas inferiores e sem um aumento dos 28 para os 90 dias.

Caraterísticas físicas

Na figura 2.11 estão apresentadas os coeficientes de capilaridade e a permeabilidade ao vapor de água [Mag08a, Mag06a]. As linhas coloridas horizontais apresentadas nas figuras indicam os limites dos requisitos gerais propostos (Tabela 2.9).

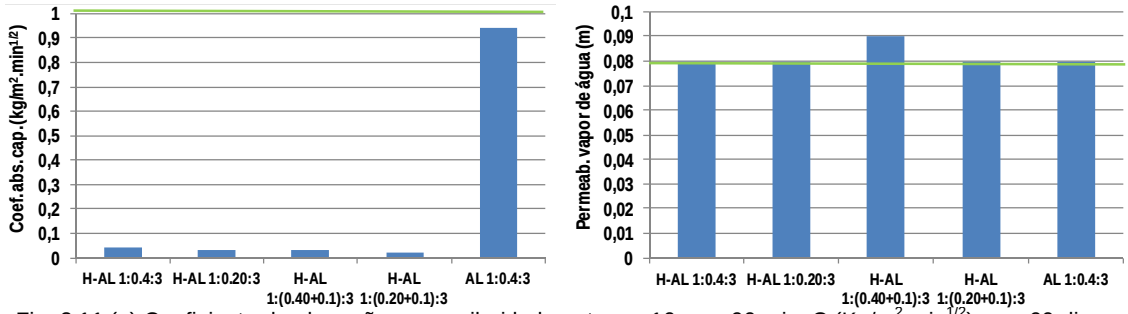

Fig. 2.11 (a) Coeficiente de absorção por capilaridade entre os 10 e os 90 min, C (Kg/m^2.min$^{1/2}$), aos 90 dias e (b) permeabilidade ao vapor de água, Sd (m), aos 90 dias.

A permeabilidade ao vapor de água apresenta-se similar para as argamassas com cal hidrófuga e argamassas com cal aérea (ver secção 2.6.2) e dentro do limite proposto (embora junto ao limite inferior); o coeficiente de capilaridade é bastante inferior nas argamassas com cal hidrófuga quando comparado com argamassas de cal aérea e abaixo do limite mínimo proposto. As argamassas testadas com cal hidrófuga, embora apresentem repelência à água no estado líquido, não podem ser consideradas impermeáveis.

A argamassa de cal aérea comercial (AL 1:04:3) apresenta o maior coeficiente de capilaridade entre as argamassas estudadas nesta secção, embora inferior às argamassas de cal tradicionais. O coeficiente de capilaridade encontra-se próximo do limite mínimo definido provavelmente devido à incorporação de adições pozolânicas.

Viabilidade para a sua utilização

As argamassas com base em cimento, cal hidráulica, cal aérea, cal aérea e ligante hidráulico – cimento ou cal hidráulica –, cal aérea e pozolanas e cal aérea com outras adições têm vindo a ser testados em vários estudos [Vei09c, Vei94a, Mag05a, Vei07a, Vei07b, Fra07a, Fra07b, Mar97a, Mar06a, Vel05a, Vel07a, Vel07b, Vel06, Mag06a, Mag08a].

Os intervalos de valores quanto às suas características mecânicas e comportamento à água foram estabelecidos para as diferentes formulações com diferentes ligantes, agregados e adições e sintetizados (ver secção 2.6.2). Esta compilação serve de base para, numa primeira abordagem, se definirem as soluções de revestimento mais compatíveis com as alvenarias de edifícios antigos e posteriormente aferir os sistemas de revestimento (compostos por várias camadas com diferentes soluções de revestimento) mais eficazes e duráveis na presença de sais solúveis e humidade ascensional ou seja, à ação severa da água (ver capítulo 4, 5 e 7).

As formulações com cal hidrófuga e com diferentes proporções de aditivos pozolânicos da Fradical Lda., foram também compiladas com base num estudo anterior (ver secção 2.6.3) e serviram de base à definição da solução de revestimento a utilizar como camada exterior num dos sistemas de revestimento resistentes à ação severa da água, desenvolvidos no âmbito desta tese (ver capítulo 5 e 7).

De um modo geral as argamassas com ligante só de cal aérea são materiais compatíveis com as alvenarias de edifícios antigos, mas na maioria dos casos apresentam valores próximos dos limites inferiores de compatibilidade, por isso devem ser utilizadas em alvenarias pouco resistentes e em condições ambientais pouco agressivas. A carbonatação da cal aérea é um processo moroso, sendo-o também o desenvolvimento da resistência e da compacidade destas argamassas de cal aérea. A longo prazo, será previsível que estas argamassas adquiram resistência adequada a condições climatéricas mais severas, tal como se tem vindo a observar em muitas das argamassas de cal aérea pré-existentes que se apresentam, ainda hoje, duráveis e resistentes. No entanto, estimar o tempo necessário para que tal aconteça será difícil aferir, pois o processo de carbonatação depende de vários fatores e a influência de cada um dos fatores não está completamente identificada [Mor05a, Mor05b]. Na decisão dever-se-á ter em conta que as argamassas apenas de cal aérea poderão ser sujeitas a ações que as degradem antes de atingirem uma resistência adequada; para além disso sabe-se que estas argamassas não se apresentam resistentes em ambientes propícios à cristalização de sais.

Quando se trata de alvenarias sujeitas a ações agressivas, a utilização de revestimentos formulados com cal aérea e adições pozolânicas pode ser adequada. Argamassas compostas por cal aérea e pozolana natural de Cabo Verde, cal aérea e argila expandida, cal aérea e metacaulino e cal aérea e sílica de fumo parecem ter uma boa prestação em vários tipos de ambientes, especialmente quando se utilizam formulações otimizadas. Não existem grandes desvantagens na utilização destas formulações, para além de alguma dificuldade na sua aplicação essencialmente relacionada com o aparecimento de fissuração devido à falta de conhecimento quanto aos cuidados na cura e na dosagem deste tipo de materiais [Vei09c]. A utilização de argamassas de cal aérea e resíduos de vidro, quando submetidos a uma cura adequada, poderão apresentar-se também como uma solução possível. No entanto estes materiais devem ser mais estudados, essencialmente ao nível das formulações e condições de cura, para melhorar o seu desempenho. Investigações recentes têm vindo a demonstrar que a utilização de metacaulino em volume causa variações nas propriedades das argamassas devido a diferenças na sua densidade aparente. A reação pozolânica destes materiais depende do consumo da sílica na sua reação com o hidróxido de cálcio, por isso a proporção destes materiais deve ser otimizada [Vel07a]. De acordo com Velosa [Vel09a] o tipo de metacaulino utilizado é determinante; o metacaulino obtido de diferentes lotes apresenta diferentes caraterísticas devidas ao processo de produção e às matérias-primas utilizadas. A utilização de metacaulino em argamassas com melhor qualidade e maior reatividade pozolânica, resultantes da melhoria do processo de produção deste material (temperatura de calcinação mais adequada), poderá originar argamassas com melhores desempenhos essencialmente ao nível da resistência mecânica.

Outros materiais pozolânicos e resíduos industriais são recursos que têm vindo a ser explorados com vista à sua utilização em argamassas: i) a adição de pequenas adições de micro-sílica e

metacaulino têm demonstrado aumentar a resistência à compressão das argamassas de cal aérea mas aumentam ou diminuir a sua resistência à tração, dependendo do tipo e quantidade de material pozolânico utilizado [Bos01, Mag06a] e ii) a adição de resíduos de tijolo cozido a baixas temperaturas com o intuito de aumentar a porosidade das argamassas têm demonstrado contribuir para diminuir a suscetibilidade destas argamassas à cristalização de sais solúveis (através do aumento do espaço disponível para a cristalização dos sais) e por outro lado, aumentar a retenção de água na argamassa durante a mistura e aplicação, que é essencial à reação pozolânica, melhorando, a longo prazo, características destas argamassas [Fra13a, Vel06a, You08]. O grau de finura do pó de tijolo, as condições e o tempo de cura da argamassa com este aditivo são os principais fatores a ter em conta contribuindo para o desenvolvimento das características mecânicas das argamassas.

A utilização de argamassas com cal hidrófuga poderá ser uma solução viável em sistemas de revestimento resistentes aos sais, reduzindo a degradação do revestimento em alvenarias com elevados teores de sais solúveis e humidade [Fra13a]. A utilização de argamassas hidrófugas previne o transporte da humidade para a superfície do sistema de revestimento, e é preferível a utilização da argamassa hidrófuga à aplicação de um tratamento hidrófugo na superfície, para evitar que se percam as propriedades hidrófugas com o tempo [Lux07a]. Nos casos em que existe uma fonte ativa de humidade (como é o caso da humidade ascensional) e em que esta humidade evapora lentamente através da parede, poderá ser recomendado um sistema de revestimento de substituição que possibilite a acumulação de sais, composto por duas camadas: a camada base absorve a solução salina e é onde os sais se acumulam, e a camada exterior com propriedades hidrófugas [Wij07a, Fra13a]. As adições pozolânicas (tais como o metacaulino e o pó de tijolo) melhoram as características das argamassas de cal [Fra13a, Vel06a] e este efeito poderá ser ainda mais rápido quando é utilizado “secante”. A utilização deste produto exige alguns cuidados pois poderá levar a um aumento excessivo da resistência da argamassa e originar tensões excessivas no suporte; no entanto os resultados obtidos com este aditivo em argamassas mostram que o módulo de elasticidade foi inferior ao limite inferior, o que poderá minimizar o efeito da transmissão das tensões excessivas devidas ao excessivo acréscimo da resistência [Mag06a]. A utilização de argamassas de cal e pozolanas com adição do “secante” apresenta-se bastante vantajosa em refechamento de juntas sendo que, para além das características apresentadas, as argamassas apresentam boa coesão. A resistência mecânica das argamassas com cal hidrófuga e adições pozolânicas é superior a uma argamassa com cal aérea corrente e adições pozolânicas, na mesma proporção, indicando que a utilização de cal hidrófuga pode levar a uma maior retenção da água e favorecer a reação pozolânica [Mag06a]. Para verificar a viabilidade quanto à utilização destas argamassas com cal hidrófuga nos sistemas de revestimento para alvenarias antigas, quando sujeitas à ação severa da água (elevado teor em sais solúveis e humidade ascensional), desenvolvidos no âmbito do presente trabalho de investigação, é fundamental testar a o seu comportamento à água nos sistema de revestimento estudados (já que existe tendência natural

para a retenção de água por parte do suporte), o seu comportamento na presença de sais solúveis e a sua aderência à camada de base do sistema de revestimento ao longo do tempo, para que se possa aferir quanto à eficácia e viabilidade de aplicação em alvenarias de edifícios antigos (ver Capítulos 5 e 7).

As argamassas com cal hidráulica apresentam uma vasta gama de características devido aos diferentes tipos de cal hidráulica utilizados, sendo que necessitam de ser mais estudadas. Existe uma vasta gama de produtos denominados cal hidráulica, quando comparados com produtos denominados cal área ou cimento. A cal hidráulica é obtida da calcinação do calcário e argila e na sua produção os diferentes fabricantes utilizam diferentes proporções de matérias-primas, temperaturas e tratamentos, o que origina cal hidráulica com diferentes características. No estudo das argamassas com base em cal hidráulica será necessário identificar o tipo de cal hidráulica utilizado e estudar cada tipo separadamente. A nova versão da norma para cais de construção, NP 459-1:2011 [IPQ2011], redefiniu a constituição das cais com propriedades hidráulicas e estabelece três tipos distintos destas cais: as cais hidráulicas naturais (NHL), as cais hidráulicas (HL) e as cais formuladas (FL). Relativamente às cais naturais (NHL) são estabelecidas três classes, na nova versão da norma (NHL2, NHL3.5 e NHL5) relacionadas com a resistência à compressão (MPa) aos 28 dias, não são permitidas adições e é exigido um teor mínimo de hidróxido de cálcio e máximo de sulfatos; as cais formuladas (FL) são constituídas por cais hidráulicas naturais ou cal aéreas com adições; e as cais hidráulicas (HL) são um ligante constituído por cal e outros materiais como o cimento, cinzas volantes, filer calcário ou outros materiais, desde de que dentro dos limites da norma. De acordo com a normalização anterior, NP 459-1:2002 [IPQ2002], as cais que continham adições hidráulicas (constituídas por pozolânicos ou hidráulicos apropriados ou reguladores de presa, adicionados até 20% em massa) eram classificadas como cais hidráulicas naturais.

A utilização de argamassas com base em cal e cimento (bastardas) são uma possibilidade em alvenarias resistentes e sob condições ambientais mais severas, em especial quando existe humidade ascensional; no entanto será necessário ter em consideração o risco associado à possibilidade da introdução de sais solúveis na alvenaria.

A análise dos intervalos de resultados possíveis e a comparação com os requisitos gerais de compatibilidade estabelecidos para alvenarias de edifícios antigos, assim como as exigências quanto aos diferentes tipos de alvenarias, as condições físicas, climáticas e ambientais específicas, limitam a seleção dos materiais mais eficazes a utilizar em cada caso. A compatibilidade com os elementos pré-existentes, a durabilidade do edifício no seu todo e, por ultimo, a durabilidade da argamassa devem servir de guia para a escolha dos revestimentos. No entanto, é sempre necessário ter em consideração que, para além das caraterísticas intrínsecas dos materiais, a qualidade da mão-de-obra e o cuidado na execução, aplicação e as condições de

cura dos revestimentos é crucial para o desenvolvimento das caraterísticas pretendidas dos revestimentos, influenciando fortemente a sua compatibilidade, eficácia e durabilidade.

Esta compilação, sobre características dos revestimentos e a sua possível aplicação em alvenarias de edifícios antigos, serve de base para a definição e otimização das formulações utilizadas no desenvolvimento do sistema de revestimento "emboço ventilado" desenvolvido no âmbito desta tese.

2.8.4 Utilização de argamassas de revestimento de substituição para alvenarias antigas com elevados teores de sais solúveis

Sistemas de revestimento – princípios de funcionamento quando na presença de sais solúveis

No âmbito do projeto Europeu Compass [Hee07a] – Compatibility of Plasters and renders with salt loaded substrates in historic buildings (Compatibilidade de rebocos exteriores e interiors com suportes sujeitos à ação de sais solúveis, em edifícios históricos) – foram definidos quatro princípios de funcionamento básicos, considerando o transporte e a evaporação da solução salina [Hee09a, Wij97a, Ver07a, Rod09a, Rod07a e Gon06a] (Fig. 2.12):

- Rebocos de transporte de sais: permitem o transporte da solução salina até à superfície onde ocorre a evaporação e, consequentemente, a cristalização dos sais sob a forma de eflorescências. Este é o comportamento geral dos rebocos tradicionais de cal aérea (em pó ou em pasta).

- Rebocos de acumulação de sais: permitem o transporte no estado líquido da solução salina desde o suporte até ao reboco, impedindo que esta atinja a superfície do reboco. A cristalização tende a ocorrer no seio do reboco e não na superfície. Vários rebocos industriais apresentam este princípio de funcionamento.

- Rebocos de bloqueio de sais: permitem o transporte no estado de vapor, impedindo o transporte no estado liquido. A cristalização tende a ocorrer na interface entre o reboco e o suporte. Este é o princípio de funcionamento de rebocos totalmente hidrófugos, tradicionais ou industriais.

- Rebocos selantes: não permitem o transporte nem de líquido nem de vapor, evitando o transporte de sais para o reboco. Os sais acumulam-se na alvenaria, contribuindo para a sua degradação e caso exista fissuração no reboco a degradação deste poderá progredir muito rapidamente. Este é o princípio de funcionamento de rebocos impermeáveis à água líquida e pouco permeáveis ou impermeáveis ao vapor.

Os rebocos de bloqueio de sais e selantes não são considerados adequadas para alvenarias antigas, quando estas paredes são submetidas a elevados teores de humidade na presença de

sais solúveis, por favorecerem a cristalização dos sais na alvenaria e assim promoverem a degradação da alvenaria antiga.

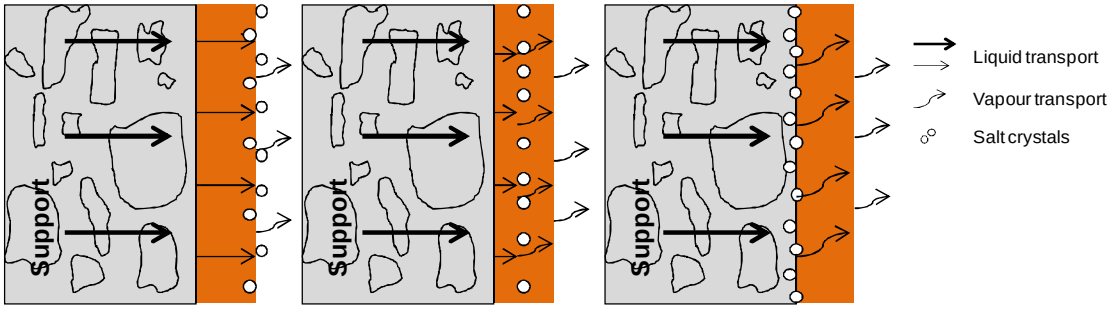

Fig. 2.12 Representação dos princípios de funcionamento principais para rebocos exteriores e interiores: (a) Sistema de transporte de sais - esquerda; (b) Sistema de acumulação de sais (meio); (c) Sistema de bloqueio de sais – direita (adaptado de [Gon06a]).

No âmbito deste trabalho pretende-se o desenvolvimento de um sistema de acumulação de sais para alvenarias sujeitas à ação severa da água, pelo que o princípio de funcionamento de acumulação será mais aprofundado.

Revestimentos de acumulação de sais

De acordo com a bibliografia o princípio de funcionamento de acumulação poderá ser conseguido através da aplicação de um agente repelente na camada exterior do sistema de revestimento, evitando o transporte e acumulação de sais na superfície da camada exterior. Como resultado, um sistema de revestimento composto por camada base (emboço) e camada exterior (reboco), sendo a camada base com elevada porosidade, permitirá a cristalização dos sais sem que ocorra degradação do revestimento [Hui07].

Huinink e Wijffels [Hui07, Wij05] estudaram a possibilidade de se obter um revestimento de acumulação sem a utilização de reboco com características hidrófugas através da utilização da camada de base (emboço) com dimensão de poros inferior à do suporte e à da camada exterior (reboco). Os autores concluíram que não será possível criar um revestimento de acumulação apenas com base na diferença da dimensão dos poros entre as camadas do revestimento e, consequentemente, será necessário utilizar uma camada exterior (reboco) com caraterísticas hidrófugas para induzir a cristalização de sais no seio do revestimento para que não ocorra a degradação superficial. Ainda de acordo com os autores e para além do que já foi referido acima, para se evitar a acumulação de sais no suporte antigo, este deverá secar primeiro do que o revestimento [Hui07].

Critérios de avaliação de desempenho

Foram definidos critérios de avaliação de desempenho para revestimentos resistentes aos sais por Rodrigues et al. [Rod07a], com base nos primeiros sinais de degradação como critério de classificação, no âmbito do projeto Compass [Hee07a] (Tabela 2.16). Estes critérios foram

adaptados para o presente trabalho de investigação por forma a avaliar o desempenho e classificar os sistemas de revestimento desenvolvidos, durante a campanha experimental, com o objetivo final de definir o revestimento de acumulação "emboço ventilado", para alvenarias antigas sujeitas à ação severa da água.

Tabela 2.16 Critério de avaliação de desempenho para revestimentos de paredes resistentes aos sais [Rod07a]

Princípio de funcionamento	Classe da argamassa	Tipo de degradação e número de ciclo até ao aparecimento dos primeiros sinais de degradação
Transporte	Degradação rápida	Eflorescências e/ou perda de coesão durante o primeiro ou segundo ciclos. Importante perda de massa nos ciclos seguintes.
	Moderada	Eflorescências e/ou perda de coesão durante o terceiro ou quarto ciclos. Importante perda de massa nos ciclos seguintes.
	Lenta	Eflorescências e/ou perda de coesão durante no quinto ciclo. Pequena perda de massa nos ciclos seguintes.
	Sem degradação	Sem grande degradação superficial após 5 ciclos. Perda de massa pouco significativa nos ciclos seguintes.
	Degradação rápida	Ocorrência de fissuração ou destacamento no primeiro ou segundo ciclos. Outras alterações significativas podem surgir nos ciclos seguintes.
Acumulação	Moderada	Ocorrência de fissuração ou destacamento no terceiro ou quarto ciclo. Outras alterações significativas podem surgir nos ciclos seguintes.
Bloqueio	Lenta	Ocorrência de fissuração ou destacamento no quinto ciclo. Alterações pouco significativas nos ciclos seguintes.
	Sem degradação	Sem ocorrência de fissuração ou destacamento significativa até ao quinto ciclo. Alterações pouco significativas nos ciclos seguintes.
Selagem		Devido ao princípio em que são baseados, estes sistemas não foram estudados.

2.9 Conclusões

A degradação devida aos sais é uma das maiores causas de degradação dos revestimentos e das alvenarias antigas. O transporte dos sais da alvenaria para o revestimento e as condições ambientais desfavoráveis poderão originar ciclos repetidos e dissolução-cristalização, que levam à acumulação e crescimento dos cristais e degradação dos materiais [Fra10b]. O cloreto de sódio pode ser considerado um dos tipos de sais mais comuns e abundantes, presentes em alvenarias antigas. A degradação pode ocorrer na superfície do revestimento (eflorescências) ou no seio do revestimento (criptoflorescências); este último caso apresenta geralmente maior degradação [Gro09a].

Estimar as condições ambientais existentes (microclima ou macroclima) às quais o revestimento está exposto é essencial para a seleção do revestimento de substituição [Gro12]. Poderá incluir avaliar o efeito devido a alterações na humidade relativa (Lub06) que originam a degradação superficial dos revestimentos.

A viabilidade de ações de manutenção, que permitam aumentar a durabilidade de revestimentos existentes quando sujeitos a variações na humidade relativa ou a humidade ascensional e sais

solúveis, deve ser estudada em cada caso como forma de aumentar a durabilidade dos revestimentos e assim adiar a necessidade da sua substituição.

As argamassas com base em cimento, cal hidráulica, cal aérea e cal aérea e ligante hidráulico – cimento ou cal hidráulica – e cal aérea e pozolanas apresentam diferentes intervalos de resultados relativamente às suas propriedades mecânicas e comportamento à água. Estes intervalos variam com o tipo de ligante, agregado e adições. As argamassas de cal aérea são compatíveis com os materiais pré-existentes, mas bastante próximas dos limites mínimos aceitáveis definidos nos requisitos de compatibilidade apresentados na tabela 2.9; por isso devem ser utilizadas em alvenarias pouco resistentes e em condições ambientais amenas [Vei08a, Vei10a].

Como se sabe a carbonatação é um processo moroso e as argamassas de cal aérea aumentam a sua resistência e compacidade ao longo do tempo. Por isso, é previsível que com o tempo estas argamassas se tornem adequadas mesmo em condições ambientais mais agressivas, tal como se verifica em algumas construções com argamassas antigas. No entanto, o tempo necessário é uma variável desconhecida pois o endurecimento das argamassas depende de vários fatores e a influência complexa de cada um não está completamente identificada [Mor05a, Mor05b]. A decisão terá que ter em consideração que, em condições ambientais mais severas, as argamassas podem ser destruídas antes de se tornarem suficientemente resistentes.

Em condições ambientais mais severas, algumas formulações com cal aérea e adições pozolânicas poderão oferecer uma boa possibilidade. Argamassas com cal aérea e pozolana natural de Cabo Verde, cal aérea e argila expandida e cal aérea e sílica de fumo parecem apresentar boas caraterísticas, especialmente quando as soluções são otimizadas. Não são conhecidas desvantagens na incorporação destes materiais em argamassas, para além de algumas dificuldades na aplicação e alguma fissuração, essencialmente devida à falta de conhecimento sobre as condições de cura e proporção de água a utilizar nestes materiais [Vei09c]. As argamassas com cal aérea e resíduos de vidro com uma cura apropriada poderão ser uma possibilidade. A utilização de argamassas de cal e pó de tijolo poderá também apresentar-se como uma possibilidade dada a elevada resistência obtida principalmente em situações de ação severa da água, podendo ser utilizada em alvenarias resistentes e em ações climáticas muito severas (por exemplo em ambiente marítimo, humidade ascensional e sais solúveis, etc.) [Fra13a].

As argamassas com cal hidráulica apresentam uma elevada heterogeneidade nas suas caraterísticas. Os produtos designados por cal hidráulica são mais diversificados do que os designados por cal aérea ou cimento, pois existe uma elevada gama de produtos com origem na calcinação de diferentes proporções de calcários e argilas, diferentes temperaturas de calcinação e diferentes tratamentos.

As argamassas de cal aérea e cimento poderão ser utilizadas em alvenarias antigas muito resistentes e em condições ambientais agressivas, especialmente se não existir humidade ascensional; no entanto existem riscos da introdução de sais na alvenaria.

A análise dos intervalos de valores obtidos e a sua comparação com os valores definidos em termos de requisitos de compatibilidade para edifícios antigos, juntamente com exigências específicas para os diferentes tipos de alvenarias e as condições físicas, climáticas e ambientais, permitem a seleção informada da melhor solução a utilizar em cada caso. A compatibilidade com os materiais pré-existentes, a durabilidade do edifício e num plano secundário, a durabilidade da argamassa, deve ser sempre a base para a escolha. Para além das caraterísticas intrínsecas do material, o cuidado na execução é crucial no desempenho final do revestimento e na sua durabilidade.

Para uma alvenaria pouco resistente, como por exemplo uma alvenaria calcária irregular com argamassas de cal aérea, em condições climáticas amenas a pouco agressivas, é possível recomendar a utilização de argamassa de cal, com ou sem adições hidráulicas. Se estivermos perante uma alvenaria muito resistente, com pedra regular, com exposição a ambiente marítimo (nevoeiro salino) e condições climáticas caraterizadas por elevadas variações higro-térmicas e ventos fortes, será necessária a utilização de uma argamassa mais forte, composta por cal e cimento ou cal e pozolanas com resistência mecânica mais elevada [Vei10a]. As argamassas de cimento ou cal aérea e elevadas proporções de cimento são incompatíveis e portanto não são recomendadas para utilização mesmo nos casos de ação severa da água (humidade ascensional e sais solúveis).

Caso não seja possível eliminar a origem da humidade, em ambientes marítimos ou quando existe humidade ascensional associada a sais solúveis, podem surgir problemas de cristalização no interior das paredes e poderá ser necessário recorrer a revestimentos de transporte ou acumulação de sais, considerados mais adequados a cada caso [Hee07a, Fra13]. É neste ponto que se foca o trabalho elaborado nesta tese, na qual se pretende- o desenvolvimento de um sistema de revestimento, compatível, durável e eficaz para alvenarias antigas sujeitas à ação severa da água, denominado “emboço ventilado”. Pretende-se que este sistema de revestimento que evite a acumulação de sais no suporte assim como na superfície exterior, e permita a sua acumulação no interior do revestimento sem que este se degrade, tendo uma porosidade adequada para permitir que os sais cristalizem sem originar degradação.

No projeto Europeu Compass [Hee07a] concluiu-se que a composição do ligante tem uma influência decisiva no transporte da solução salina, podendo o revestimento permitir o transporte da solução, a acumulação no revestimento, ou o bloqueio da solução salina, podendo a cristalização ocorrer atrás do revestimento.

Finalmente, cada tipo revestimento não poderá ser considerado uma solução única para problemas de humidade e sais solúveis. Cada revestimento deve ser estudado adequadamente por forma a determinar se será a melhor solução. Para além disso terá que se ter em conta que a eficácia e durabilidade de um revestimento de substituição para uma alvenaria antiga depende tanto da sua formulação como das suas condições de execução e aplicação.

3. DAMAGE DUE TO THE SEVERE ACTION OF SALT LADEN WATER: RESULTS OF CASE STUDIES

3.1 Introduction

In Portugal, interventions on monuments and historical centers, have obtained assuming increasing relevance. Most of these buildings have renders based on lime, usually with good cohesion and adhesion to the substrate.

In old buildings needing interventions the most current anomalies affecting masonry are usually due to humidity that penetrates in the walls from external sources such as: rising ground water, sea-salt spray, sea-flooding, etc. On one side, lime renders should be preserved and repaired; when there is a high degree of degradation and their substitution is needed, the application of new compatible renders is required; on the other side, the present requirements of habitability and aesthetic appearance, without de-characterization, in conservation interventions, should guarantee the maintenance of buildings integrity and durability. In order to achieve both goals, it is necessary to implement compatible renders, durable and in balance with surrounding conditions.

In a conservation action, the priority is to achieve compatibility and optimize the durability and adequate protection to water of the whole building [Mag06a, Vei09c] and some solutions do not match this goal. For example, an impermeable mortar keeps the water inside masonry or forces its transport through the more permeable old mortar and masonry. Besides, it should not have high contents of salts, to avoid the increase of salt contamination into the walls. Some studies [Cha00a, Gon07] refer to a synergetic effect of chlorides and sulphates that imply an aggravation of salt attack when both are present; so the contamination with sulphates (present in cement) may be particularly harmful in buildings close to the sea.

In the present work a compilation of five Portuguese case studies of buildings from the XV century to the XVII century, is made. These case studies have renders and plasters with several types of anomalies due to the exposition to humidity from different sources, especially rising capillary water and infiltrations due to damaged roofs [Fra11a, Fra11b]. The case studies are located in Portugal: two in the North - Santa Joana Museum (SJM) and Santo António Convent (SAC) - in Aveiro; two in the centre of Portugal - Inglesinhos Convent (IC) and Santíssimo Sacramento Church (SSC) - in Lisbon; and one in the South of Portugal - Nossa Senhora da Graça Convent (NSGC) - in Tavira.

A diagnosis methodology to define the possible causes of the anomalies is described, as well as the main anomalies; further the measures adopted for their repair are defined, for an adequate intervention, in each case. The diagnosis methodology adopted to evaluate the conservation state, allowed to identify the distribution and localization of the humidity in the renders and plasters, as

well as to evaluate the origin of the humidity and to establish if the source is still active or not. The quantification of the effects was also made, leading to an adjusted definition of a set of repair recommendations based on control of causes and on the minimization of their effects.

3.2 Case studies description

3.2.1 "Inglesinhos" Convent (IC) [Vei09b, Vei09f, Fra11a, Fra11b]

The English College, or "Inglesinhos Convent", as it is called by the people of Lisbon, is located in the middle of Bairro Alto, in the historical centre of Lisbon. The beginning of the construction dates back to the XVII century, in 1622. It was erected for the education of the English secular priests, named "St. Peter's and St. Paul's College" and known as Inglesinhos Convent [Vei09b]. Later, in 1644, a church adjacent to the main building was built, with interior walls covered with plaster simulating stones of different colors, creating a space full of beauty and technical and aesthetic singularity (Fig. 3.1).

Fig. 3.1 Inglesinhos Convent before and after intervention

In 1755, when the great Lisbon earthquake took place, the building suffered several damages and was submitted to various interventions. In the eighteenth century the English College had built a high reputation in the Iberian Peninsula and many foreigners, especially Spanish people, came to study in this institution. Only in the late nineteenth century, in 1898, the decorative program of the church was finished [Vei09b, Vei09f].

Although transformed, the old convent and English College maintained its nobility, constituting a milestone in the urban net of one of the most ancient Lisbon quarters. The building plant is composed by rectangles and organized in large circulation and distribution corridors; the ground floor roof is executed in groined vaults. The old renders and plasters were based on lime mortars,

with a pink coloration, as it was possible to observe in a lacuna existent in the entrance hall wall cover, constituted by ancient glazed tiles (“azulejos”) of great beauty and value.

In 2004, the building was sold and a project approved to convert the monument into a luxurious housing complex. The causes of the anomalies were identified and the repair measures were proposed in 2009, during the rehabilitation works.

Decay patterns

Before the beginning of the works, the roof remained in poor conditions for a long period of time, allowing water infiltrations to reach the vaults that form the ceilings of the ground floor. During the refurbishment works, the old renders and plasters based on air lime were removed and substituted by new ones, composed by lime and cement, in the interior and exterior of the building. The new renders showed shrinkage craks after application and were treated with a synthetic product designed to reduce shrinkage. Before the end of the works, several anomalies occurred such as: dark moisture stains, salt efflorescences, loss of cohesion of the paint, blistering and detachment of the paint both in external and internal façades (Figs. 3.2 to 3.5).

Fig. 3.2 Detachment of the paint: internal facades (left), external facades (middle) of walls and vaults composing the ceilings (right).

Fig. 3.3 Blistering of the paints in external (left and middle) and internal (right) facades of the walls.

Fig. 3.4 Dark moisture stains: in the base of the walls (left), floor-footers (middle) and built-in cupboards (right).

Fig. 3.5 Salts efflorescence in rendering cracks (left and middle) and detachment of the paint layer (right).

3.2.2 "Nossa Senhora da Graça" Convent (NSGC) [Vei10b, Fra11a, Fra11b]

The Convent of "Nossa Senhora da Graça" is located in the historic centre of Tavira. After the process of expulsion of the Jews and the evacuation of the space in that area due to the demolition of the synagogue and other buildings, by King Manuel I, the convent of the Order of Hermits of St. Augustine was founded in 1542, by Frei Pedro de Vila Viçosa. The construction of the Convent began in 1569 and continued for the next century. From this phase of the construction essentially the cloister remains, although several interventions were performed, the most extensive of which was in 1749. Only in this period the church was built, dated from the second half of XVI century, and several interventions were also performed later. In the XVIII century, between 1758 and 1778, the building was submitted to a renovation and expansion campaign, of which the main facade of the convent and the rectangular towers are the most visible evidences. The decay of the convent started since the extinction of the religious orders in 1834. Later, in 1839, it was allocated to the War Ministry where the Graça Quartel was located [Vei10b].

In 2003 it was bought by the city of Tavira and later converted into a Charming Hotel open since 2006. The old zones were conserved and new spaces were also constructed; the cloister remained and the rooms were allocated in the upper zones increasing the comfort and privacy.

The old renders and plasters were based on lime, especially visible in the renders in the cloister area. In Figure 3.6 the building before and after intervention is presented.

Fig. 3.6 Tavira Charm Hotel before and after intervention

In 2010 the causes of the anomalies, which appeared few months after intervention in 2006, were identified and the repair measures were proposed.

Decay patterns

Before rehabilitation works, the roof was in a poor conditions for a long period allowing rain water infiltration through the thick walls and, at that time, the renders were very damaged with generalized detachments, loss of cohesion and humidity spots (Fig. 3.7). These very damaged renders of old masonries constituting the exterior walls, with thickness of more than 1 m, were integrally removed.

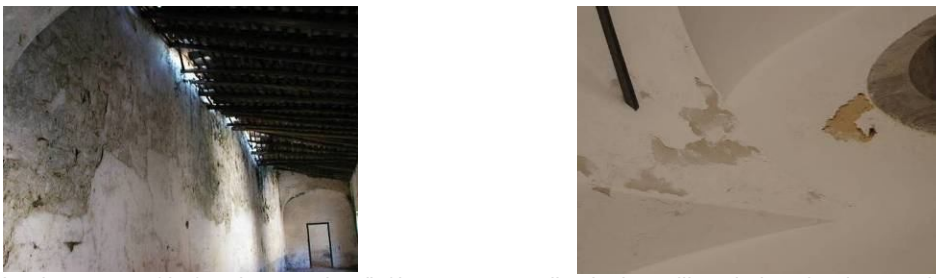

Fig. 3.7 The damage roof before intervention (left); some anomalies in the ceilings below the damaged roof after intervention (right).

According to in situ information: i) during removal of old renders some sea shells were observed, confirming the idea of the use of some non washed sea sand and so there may have occurred contamination with salts; ii) during the refurbishment works, these old renders based on air lime were removed and substituted by new ones, composed by lime and cement, in 2004-2005; iii) one year later the exterior paint was applied; it was described as a silicate paint although it was observed to form a film and according to the product datasheet is had also some water repellent properties; iv) projected gypsum plasters were executed in the internal facades; and v) during works execution, several anomalies were observed such as: dark moisture stains and blistering of

the paint both in external and internal façades; vi) during the humid season some superficial condensation was observed on calcareous stone surfaces of the floor-footers.

In 2010, several anomalies were observed such as: dark moisture stains, salt efflorescences, loss of cohesion of the paint, blistering and detachments of the paint both in external and internal façades (Figs. 3.8 to 3.11).

Fig. 3.8 Detachments of paint in the exterior facade (left), in the vaults (middle) and in the interior plaster (right) near the floor-footers

Fig. 3.9 Detachment, loss of cohesion and salts efflorescence in the renders (left) and in the vaults (right).

Fig. 3.10 Moisture stains in the exterior facades renders (left and middle) and interior plasters in the vaults (right)

Fig. 3.11 Moisture stains and salts efflorescence in the interior calcareous stone surfaces (left and middle) and blistering of the paint (right) in the interior plaster.

3.2.3 "Santissimo Sacramento" Convent (SSC) [San10, Fra11a, Fra11b]

The Santissimo Sacramento Convent, in Alcântara quarter, in Lisbon, was an innovative architectural project in the XVII century and one of the most important ecclesiastic structures at that period in Lisbon. An intervention aiming at the restoration of the monument's interior plasters was planned in 2009.

The Santissimo Sacramento Church of Lisbon (Fig. 3.12), placed in the ancient homonym Convent, is an excellent example of the architectural richness of Lisbon in the XVII century and one of the most important constructions built during the Spanish dynasty (1580-1640). The Convent was established in 1605 and the construction works ended in 1620, but the Church was rebuilt in 1635, due to its darkness and also reduced internal spaces. Survived at the terrible earthquake of Lisbon in 1755, the convent however became poorer and its decline started on 1834, with the suppression of the religious orders in Portugal [San10].

Fig. 3.12 Main facade of the church of "Santíssimo Sacramento".

At the beginning of the XX century the convent passed under the control of the Army and suffered several alterations; finally at the end of the 90's the convent was acquired by the Foreign Affairs Office, which decided to refurbish the entire complex.

The Church presents a greek cross plant with a dome widely decorated with lime plasters and mural paintings of great quality. The plasters are well conserved, although several phases of interventions during time are visible, and present interesting mural paintings simulating pink marble.

The causes of the anomalies were identified and the repair measures were proposed in 2009, during the rehabilitation works, to justify and support the conservation works.

Decay patterns

In general, the mortars were well conserved and presented interesting mural paintings simulating pink marble, although some detachments, loss of cohesion and salt efflorescence were observed (Figs. 3.13 to 3.15).

Fig. 3.13 Detachment of the stucco in pillar (left), detachments and cohesion loss in the walls (middle and right).

Fig. 3.14 Loss of cohesion in the arch (left); salts efflorescences and detachments of the plasters (middle and right).

Fig. 3.15 Detachment and loss of cohesion of the stuccos in the dome (left and middle), detachment of the plaster in the dome (right)

3.2.4 "Santa Joana" Museum (SJM) [Fra11a, Fra11b]

The Museum of Aveiro, old Convent of Jesus, is located in the historic centre of Aveiro and is part of the built heritage of the city. Over its six centuries of existence, the Convent was submitted to several interventions through the use of new materials and techniques distinct from the original (Fig. 3.16).

Fig. 3.16 Main facade of the Museum before (left) and after intervention (middle and right).

The actual museum of Aveiro had its origin in a Dominican Convent founded in 1458. In the context of liberal reform, in 1874, the date of death of the last religious orders, the Dominican convent was extinguished and, in 1882, the building was handed over to the Third Dominican Order who turns it into the College of Saint Joan. With the advent of the Republic in 1910, the college was

extinguished and the whole of Church of Jesus and contiguous area was decreed monument of national interest. In 1912, the Museum of Aveiro was installed in the Convent of Jesus.

The monumental area dates from the XV century, the Church of Jesus and the cloister from the XVI century. In 1715, a church was built, with interior walls covered with plaster simulating stones of different colours and “azulejos” (glazed ceramic tiles) creating a space full of beauty and technical and aesthetic singularity that remained until now. The main facade dates from the XVIII century.

During the XX century the Museum has underwent several interventions and in 2006 the new project of magnifying the Museum was characterized by a modern architectural building, endowed with audience, destined room for temporary expositions, educative services, library and laboratory of conservation.

The works for the renovation and extension of the Museum started in 2007and finished at the end of 2009. The plasters were cement based and an impermeable paint was applied. Before the end of the works several anomalies on the plasters and paints were observed.

Decay patterns

The new plasters presented moisture stains, salts efflorescence and blistering and detachments of the paint. The main decay patterns observed are described in Figures 3.17 to 3.20.

Fig. 3.17 Dark moisture stains in the paint and marble finishing surfaces on interior walls (left and middle), stains of humidity in the floor and detachments of the paint in interior facade of exterior walls (right).

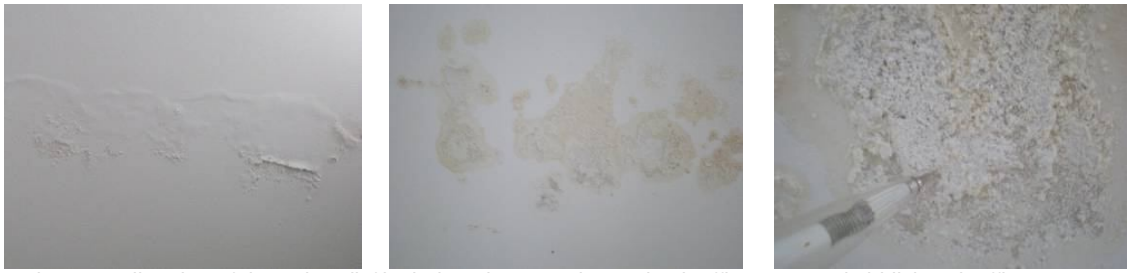

Fig. 3.18 Blistering of the paints (left), dark moisture stains and salt efflorescence (middle), salt efflorescence and detachment of the paint (right).

Fig. 3.19 Moisture stains in the ground floor (left and middle) and salts efflorescence in the old floor (right)

Fig. 3.20 Facades: Dark moisture stains along the plasters, efflorescences, detachments of the paint.

3.2.5 "Santo António" Convent and Church (SAC) [Fra11a, Fra11b]

The Church of the Convent of Santo Antonio, the Chapel of the "Ordem Terceira de S. Francisco" and the Convent (in which is the House of the Order) underwent several interventions (aesthetical and functional) since the XVI century (Fig. 3.21). It is located in Aveiro City.

Fig. 3.21 Main facade of the Church of the Convent of Santo António (left) and cloister of the convent (right).

The interior has decorative elements, "azulejos" and painting from the end of the XVII century. The oldest part of the building is Santo António Convent, dated of 1524, and later, in 1564 the convent was almost completely rebuilt. One century later the church was submitted to an intervention campaign and in the XVIII the church was submitted to a new decorative campaign.

The chapel of "Ordem Terceira de São Francisco" was built in 1670. The house of the Order (Casa do Despacho), the last building to be constructed in the XVII, with palace-like appearance, is developed in two floors. The old masonries show a thickness between 0.6 (interior walls) and 1.0 m (exterior walls). Several punctual interventions have been done since then with cement based plasters and severe and general damage of the plasters and renders were observed in 2010.

Decay patterns

The renders and plasters were very damaged with generally salts efflorescence, detachments, loss of cohesion and humidity spots. The main decay patterns observed are described in Figures 3.22 to 3.28.

Fig. 3.22 Exterior facade: dark moisture stains, detachments of plasters and paints (very damaged), presence of cement renders due to local substitutions along time.

Fig. 3.23 Interior facades: salts efflorescence and detachment of plaster (left), dark moisture stains (middle and right) - ground floor.

Fig. 3.24 Moisture in the vaults (left) and ceilings of the church (middle), detachment of plasters in the base of the walls (right).

Fig. 3.25 Dark moisture stains and biological colonization since the base of the exterior wall (left), moisture in the base and stairs (middle), moisture in the vase of the vaults and ceilings (right) – ground floor.

Fig. 3.26 Detachment of plasters Interior wall (left), moisture stains and biological colonization in the floor (middle); damage in the wood ceiling due to moisture (right) – ground floor.

Fig. 3.27 Biological colonization, moisture stains and detachment of plasters (left); moisture stains in the ceiling (middle); moisture and biological colonization and presence of cement plasters (right) – upper floor.

Fig. 3.28 Detachment of the plaster (left); detachment of the paint, loss of cohesion and salts efflorescence (middle) and biological colonization (right) – upper floor.

The lime renders and stuccos were very damaged both on the ground floor and 1st floor. In the 1st floor the wood pavements were in good state of conservation, with exception of areas near the walls which had a high moisture content.

According to in situ information: i) the roof was in poor condition for a long period (the last intervention in the roof was about 12 years before the visit) and actually several infiltrations through the roof were observed; ii) last intervention in stuccos was carried out before the intervention in the roof; iii) since then several local interventions were made with cement mortars, iv) about 20 years ago there was a stable with animals in the ground floor.

3.3 Diagnosis methodology and results

3.3.1 General

Non-destructive diagnosis was performed in situ using a methodology [Mag08b] based on visual observation of the anomalies, determination of the superficial moisture content and resistance and semi-quantitative identification of salts using simple equipment: a portable humidimeter, durometer,

impact hammer and strip tests (Fig. 3.29). This methodology was used in the several case studies, except in case studies SJM and SAC in which only superficial moisture and salt strip tests were performed, due to some difficulties in transporting the impact hammer and durometer equipment.

Fig. 3.29 In situ test with portable humidimeter, strip tests, impact hammer and durometer (from left to right).

The tests were performed in the most representative walls/areas in each case study, according to a preliminary visual evaluation of the anomalies.

A portable humidimeter – Tramex CRH - was used to evaluate the superficial moisture content in the walls [Vei09c, Mas93, Hen01]. This test was performed in several internal and external walls, at different heights - between 0.10 m and 1.80 m from the pavement following one vertical profile per wall/area. In some case studies they were performed at two different periods – dry weather and after a rainy week – in order to determine the possible origin of the water. This equipment presents a range of values from 0 to 6.9, corresponding to a dry and very wet render, respectively, based on electric resistance, function of the water content of the material in which the equipment is in contact. Values between 0 and 2 correspond to dry zones; 2 to 4 correspond to slightly humid zones, 4 to 6 humid zones and from 6 to 6.9 to very humid zones [Mag08b, Mag09a, Vei09b, Fra11b]. The superficial moisture content values in each case are related to the walls/areas where higher moisture content was observed. Hygroscopic salts may influence these values in isolated points, so the measurements should be done in several points and related with salt content evaluation, in order to identify this influence. On the other hand, a relevant general influence of salt contamination on the electric resistance values obtained was not detected. Reference values are also presented and the values are comparative and not absolute.

The testes with Karsten tubes were used especially to evaluate the renders permeability to water which is also related with the possible reduction of the normal evaporation of the moisture from the walls. This test is based on LNEC test data sheet LNEC FE Pa 39 based on the methodology adopted by RILEM test, for water absorption under low pressure [RILEM 1980]. This test consists in measuring the amount of water absorbed by a given plaster surface or finish after a set period of time by using small graded tubes, fixed to the test wall. The results are based on the decrease of the level of water observed in the water pipes at 5, 10, 15, extended up to 30 minutes or even 60 minutes, since the water level in the tubes permits reading of the values [Mag08b].

The strip tests were used for the semi-quantitative identification of salts in wall areas where salts efflorescence/damage were observed. They give information on the type of salts present as well as on the degree of contamination, based on semi-quantitative determination of ions associated with the type of salts [Bor99]. In renders of old buildings the most used strip tests are the ones corresponding to chlorides, sulphates and nitrates. The presence of sulphates can be associated to the presence of cement, some kinds of hydraulic limes in the mortars or some ceramic materials if not fired adequately, as well as to the atmospheric pollution [Arn89]; in spite of the lower dissolution rate of sulphates, when compared with the other salts present, the circulation of water in the walls can promote their dissolution and dissemination [Oto08a]. The chlorides can be associated to marine environment (contact of the building material with sea spray or marine fog), ground water and contaminated soils or to their presence in wall materials (stones, bricks, mortars or sand) (see chapter 2). The presence of nitrates can be due to contamination with organic products, mainly from animals or due to the treatment of the soil with organic fertilizers [Arn89]. The presence of nitrites points out that the moisture source from the ground may remain active or was active until recent times, because these salts are very unstable. [Hen01, Mag08b]. Salts can be transported in a porous material only if dissolved in water, thus their presence indicates water transport through the walls [Lub06a].

The tests with pendular Schmidt impact hammer – Schmidt type PM, produced by Proceq – based on ISO 7619:1997 and ASTM C 805 (adapted by TNO Delft for assessing quality of pointing tester, with impact energy of 0.883 N.m for low resistant mortars, with mechanical resistance around 5 N/mm2) and those with Durometer Shore A, based on ASTM D22240 (with a scale between 0 and 100 shore A) with impact energy between 550 and 8065 N.m., were performed to indirectly assess the strength of the superficial layers of renders, in order to verify how the moisture content affected the mortars' cohesion. The tests evaluate the mechanical strength and cohesion of the damaged and non damaged renders, by comparison with measurements performed on experimental panels made in-situ and with determinations carried out in previous case studies on sound mortars [Tav08a, Tav08b, Vei09e, San10, Vei09b, Vei08a, Vei10a, Vei09f, Fra11a, Fra11b and Tav09a]. The tests with pendular Schmidt hammer are more expressive of mechanical strength, as they assess the resistance of the last layers, than the Durometer measurements, which affect more superficial layers (stucco or paint). However, the Durometer measurements show a good correlation with cohesion.

The scale and evaluation of the results obtained with each of the instruments are described in Table 3.1.

Table 3.1 In situ tests: portable humidimeter, colorimetric strip tests, durometer and impact hammer – scale and evaluation

Test	Scale and evaluation					
Superficial moisture content (portable humidimeter)						
Portable humidimeter	0-2 Dry	2-4 Slightly humid	4-6 Humid	6-8 Very humid		
Soluble salts concentration (colorimetric strip tests)						
Chlorides (mg/l Cl^-)	500 Very low	1000 Low	1500 Moderate	2000 High	≥3000 Very high	
Sulphates (mg/l SO_4^{2-})	200 Very low	400 Low	800 Moderate	1200 High	1600 Very high	
Nitrates (mg/l NO^{3-})	10 Very low	25 Low	50 Moderate	100 Normal	250 High	500 Very high
Superficial resistance on plasters, renders and paints						
Durometer (Shore A)	< 30 Very low	30-50 Low	50-70 Moderate	70-87 Normal	>88 High	
	(1)Durometer reference values for new lime based renders: not damaged – 85-95; damaged - < 70					
Impact hammer (HV)	<20 Very low	20-30 Low	30-40 Moderate	40-55 Normal	55-75 High	>75 Very high
	(1) Impact hammer reference values for new lime based renders: not damaged – 25-35					

(1) Reference values for new lime renders [Vei09e]

In the following sections, the results obtained for the most representative walls/areas of each case-study are presented and interpreted. However, it should be stressed that several walls per case study were tested and all of them corroborate the present diagnosis. For each case study, the materials found are presented.

3.3.2 "Inglesinhos" Convent (IC) [Vei09b, Vei09f, Fra11a, Fra11b]

In this case study, the diagnosis methodology was performed using: portable humidimeter, salt strip tests, durometer and esclerometer. The superficial moisture content was determined in the more representative internal and external walls, using a portable humidimeter, both in internal and external facades (Fig. 3.30), at different heights – from 0.30 m to 1.80 m from the pavement – and in two different periods – dry weather and after a rainy week – in order to determine the possible origin of the water. The most representative in situ results are presented (Tables 3.2 to 3.4).

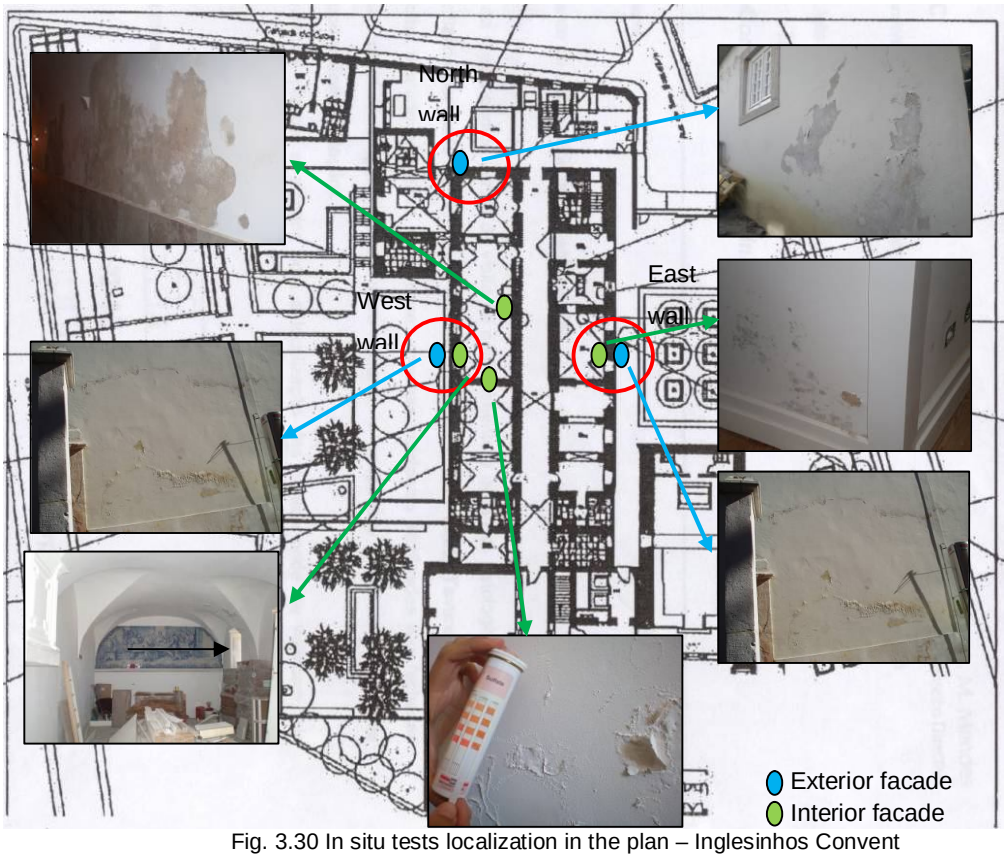

Fig. 3.30 In situ tests localization in the plan – Inglesinhos Convent

The comparative analyses of the results showed that the walls of the ground floor had a higher humidity content than the superior floors' walls (Table 3.2). The interior walls were found to have high moisture contents, almost as high as external walls'. This moisture increased after rainy periods. In the interior walls and some exterior walls, the humidity content was higher at the base, reducing towards the top of the walls. High moisture contents concentrated at the base of the vaults and in other particular places, especially near the windows and under the cornice.

Table 3.2 - Average results with portable humidimeter in the outer surface of the most representative walls (ground floor).

Local identification		Exterior wall (West)				Interior wall (West)		Interior wall (South)		Exterior wall (East)				Exterior wall (North)
		Exterior facade		Interior facade						Exterior facade		Interior facade		Exterior facade
Height from pavement (m)		0.30	1.80	0.30	1.80	0.30	1.80	0.30	1.80	0.30	1.80	0.30	1.80	0.30
Measure water rate (%)	After dry period	3.5	5.5	4.4	3.4	6.3	6.3	6.1	5.3	ND	ND	ND	ND	3.6
	After humid period	4.6	6.9	4.8	4.5	6.3	6.9	5.3	5.7	4.6	4.2	6.9	3.9	ND

ND – Not determined

These results showed that the main water source is not infiltration by exterior walls and that there is capillary rising water from foundations, as well as moisture from the roof vaults. In fact, moisture was detected on interior walls, as much as on exterior walls, values were higher near the ground

and also near the base of the vaults They also show the effect of some particular constructive issues that favour water retention.

Table 3.3 - Average results with strip tests in the outer surface of the most representative walls (ground floor).

Local identification	Exterior wall (West) Exterior facade	Interior wall (South)	Exterior wall (North) Exterior facade
Salts present	Sulphates (<200 mg/l)	Nitrates (≈250 mg/l) Sulphates (>1600 mg/l)	Chlorides (500-1000mg/l) Nitrates (5-10 mg/l) Sulphates (200-400mg/l)

The salts present (Table 3.3) were found to be mainly sulphates (large content in one of the interior walls) and chlorides, but also some nitrates were detected. Their presence was probably due to the interaction of contaminated water from the ground, to the presence of cement in the mortars and to the existence of salts in other wall materials or in the ground.

Table 3.4 - Average results with impact hammer and durometer in the outer surface of the most representative walls (ground floor).

Local identification	Exterior facade	Comparison render[3]
	Cement and air lime based render with acrylic paint[4]	Cement and lime based render
HV[1]	33	40
Shore A[2]	92	94

[1] Vickers HV = Hardness in Vickers degrees
[2] Unit measurement scale SHORE A from 0 to 100
[3] Comparison render 3 months after application, in good conservation state
[4] Presenting detachments and salt efflorescences

The most representative results of the tests with pendular Schmidt impact hammer and Durometer are shown in Table 3.4. The tests showed the reduction of mechanical resistance and cohesion of the degraded renders, in comparison with measurements performed in previous case studies [Fra11b].

This old convent of the seventeenth century, submitted to a refurbishment intervention to be adapted to a housing building, showed anomalies after replacing the old renders and plasters by new cement and lime mortars finished with acrylic paint. After observation of the wall coverings, the analysis of their state of conservation and the discussion of the in-situ test results, it was possible to identify the most probable causes of anomalies. The conclusion was that the anomalies were a consequence of the high accumulation of moisture in the walls and ceilings.

The presence of water inside the walls was extended in time due to difficulty of its removal through the new coverings. In fact, these coverings reduced the evaporation ability, when compared with the old renders, based on air lime, more porous and permeable. The reduced ventilation in the interior of building worsened the situation [Vei02b].

3.3.3 "Nossa Senhora da Graça" Convent (NSGC) [Vei10b, Fra11a, Fra11b]

In this case study the anomalies were particularly severe in SW and NW external facades. The diagnosis methodology was performed with the use of: portable humidimeter, salt strip tests, durometer, esclerometer and Karsten tubes. The superficial moisture content was determined in the more representative internal and external walls, both in internal and external facades (Fig. 3.31), at different heights – from 0.30 m to 3.00 m from the pavement – in order to determine the possible origin of the water. The most representative in situ results are presented (Tables 3.5 to 3.8).

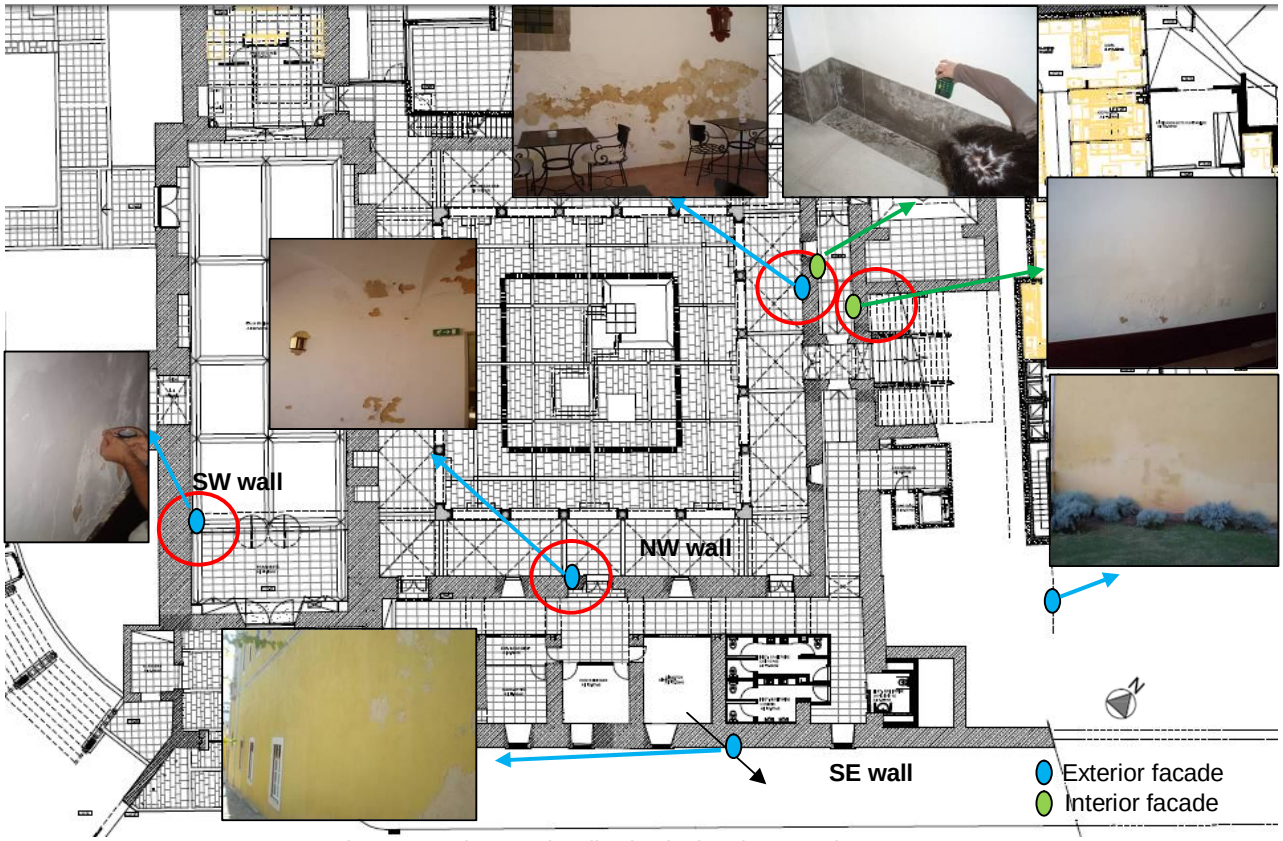

Fig. 3.31 In situ tests localization in the plan – Tavira Convent

The comparative analyses of the results from portable humidimeter reported high moisture content in the base of the walls of the ground floor (especially up to 1.2 m where severe damage of the renders was observed), in both interior and exterior facades, even during the dry period (Table 3.5). According to in situ information, some re-paints were done during time after the occurrence of the anomalies leading to their re-appearance. This behaviour is typical for capillary rising water through the foundations, indicating also that it still remains active.

Table 3.5 - Average results with portable humidimeter in the outer surface of the most representative walls (ground floor) – dry period.

Local identification	Exterior Wall (NW)				Exterior Wall (SE)				Exterior Wall (NE)		Exterior wall (SW)	
	Exterior facade				Exterior facade				Exterior facade		Interior facade	
	Damaged		Not damaged		Damaged		Not damaged		Damaged	Not damaged	Damaged	Not damaged
Height from pavement (m)	0.30	1.80	0.30	1.80	0.30	1.80	0.30	1.80	0.30	1.80	0.30	1.80
Measured water content (%)	6.9	6.9	6.9	3.3	6.9	4.8	3.5	3.8	6.9	4.4	6.9	4.4

Also in the vaults of the cloister some damage and high moisture content were observed [Vei10b] due to the damaged roof that allowed infiltrations before intervention. The high thickness of these vaults associated to limited surface drying (low permeable paint) makes the evaporation difficult and induces the humidity flow to the superior parts of the wall where high moisture content was also observed [Vei10b]. Some other particular infiltrations were observed under the cornice and near the windows.

Table 3.6 - Average results with strip tests in the outer surface of the most representative walls (ground floor).

Local identification	Exterior wall (NW) Exterior façade	Exterior wall (SE) Exterior facade	Exterior wall (NE) Exterior facade	Exterior wall (SW) Interior facade
Salts present	Chlorides (2000 mg/l)	Chlorides (500 mg/l)	ND	ND

ND – not determined

In the damaged wall of the cloister (NW wall) chlorides were found in large content and in lower content in the main facade (SE wall). These salts are typically present in coastal areas, and may be present both in the masonry and render materials, due to the use of non-washed sand and the interaction of contaminated water from the ground that flows to the walls by capillary rise (Table 3.6). Other salts (especially sulphates) may be present due to the presence of cement in the renders composed by cement and air lime.

Table 3.7 - Average results with using impact hammer and durometer in the outer surface of the most representative walls (ground floor).

Local identification	Exterior Wall (NW) Exterior facade		Exterior Wall (SE) Exterior facade		Exterior Wall (NE) Exterior facade	Exterior wall (SW) Interior facade	
	Damaged[3]	Not damaged	Damaged[3]	Not damaged	Not damaged	Damaged[3]	Not damaged
HV[1]	44	84	59	68	77	69	96
Shore A[2]	20	34	30	33	60	34	44

[1] Vickers HV = Hardness in Vickers degrees
[2] Unit measurement scale SHORE A from 0 to 100
[3] Presenting detachments and salt efflorescences

The more representative results of the tests with pendular Schmidt impact hammer and Durometer are shown in Table 3.7. The tests showed the reduction of mechanical resistance and cohesion in damaged renders (especially in NW and SE walls) and where high superficial moisture content was observed, in comparison with measurements performed in previous case studies [Tav09a]. Very low and low resistance was found on more damaged zones with durometer while with impact

hammer low to moderate resistance was observed. In non damaged zones the renders were observed to be resistant and cohesive showing a normal range of values for old masonries (Table+ 3.1).

Table 3.8 - Average results using Karsten tubes in the outer surface of the most representative walls (ground floor)

Local identification Time (min)	Exterior Wall (SE) (cm^3) Exterior facade (damaged)	Exterior facade (not damaged)	Exterior Wall (NE) (cm^3) Exterior facade (not damaged)
0	0	0	0
5	0.8	0.1	0
10	1.6	0.1	0.1
15	2.7	0.1	0.2
30	>4.0	0.1	0.3
60	-	0.2	-

The Karsten tubes were used especially to evaluate the paints permeability to water, which is related to the reduction of the normal evaporation of the moisture from the walls through the painted renders. From table 3.8 it is possible to compare the results obtained in not-damaged zones (painted lime and cement renders) and damaged zone (unpainted lime and cement renders). There was almost no absorption in the not-damaged zones (with paint) when compared with the damaged zones (without paint), showing that the paint used is rather impermeable and so not compatible with old renders especially in cases with high moisture content, reducing the evaporation through the painted render when compared with the unpainted render (Table 3.8). A film formation in the paint is observed that corroborates the results, as it shows it is not hardening mainly due to silicates formation in reaction with the substrate.

The interior walls were found to have high moisture contents, almost as high as external walls'. This moisture increased after rainy periods. In the interior walls and some exterior walls, the humidity content was higher at the base, reducing towards the top of the walls. High moisture contents concentrated at the base of the vaults and in other particular places, especially near the windows and under the cornice. These results showed that the main water source is not infiltration by exterior walls and that there is capillary rising water from foundations as well as moisture from the roof vaults. They also show the effect of some particular constructive issues that project from the wall, favouring water retention.

The renders used, although composed by cement and air lime (according to in situ information not a very strong dosage of cement was used) can be considered compatible with the old masonry, showing moderate values for resistance and capillarity [Vei10a]. Although there is a possible contamination of soluble salts by cement mortars, in this case it's not considered the main factor contributing for the severe damage observed in some walls.

Based on the whole testing and observation campaign, the severe damage observed in some walls especially in NW and SE tested walls (showing severe loss of cohesion, detachments and salt efflorescences), can be mainly attributed to the presence of high moisture content due to the active

capillary rise through the foundations associated to the presence of soluble salts and the impermeable painting.

3.3.4 "Santissimo Sacramento" Church (SSC) [San10, Fra11a, Fra11b]

In this case study the anomalies were particularly severe in the North wall and in the arches where the tests were performed (Figs. 3.32 to 3.37). The diagnosis methodology was performed with the use of: portable humidimeter, salt strip tests, durometer and impact hammer. The most representative in situ results are presented (Tables 3.9 to 3.11).

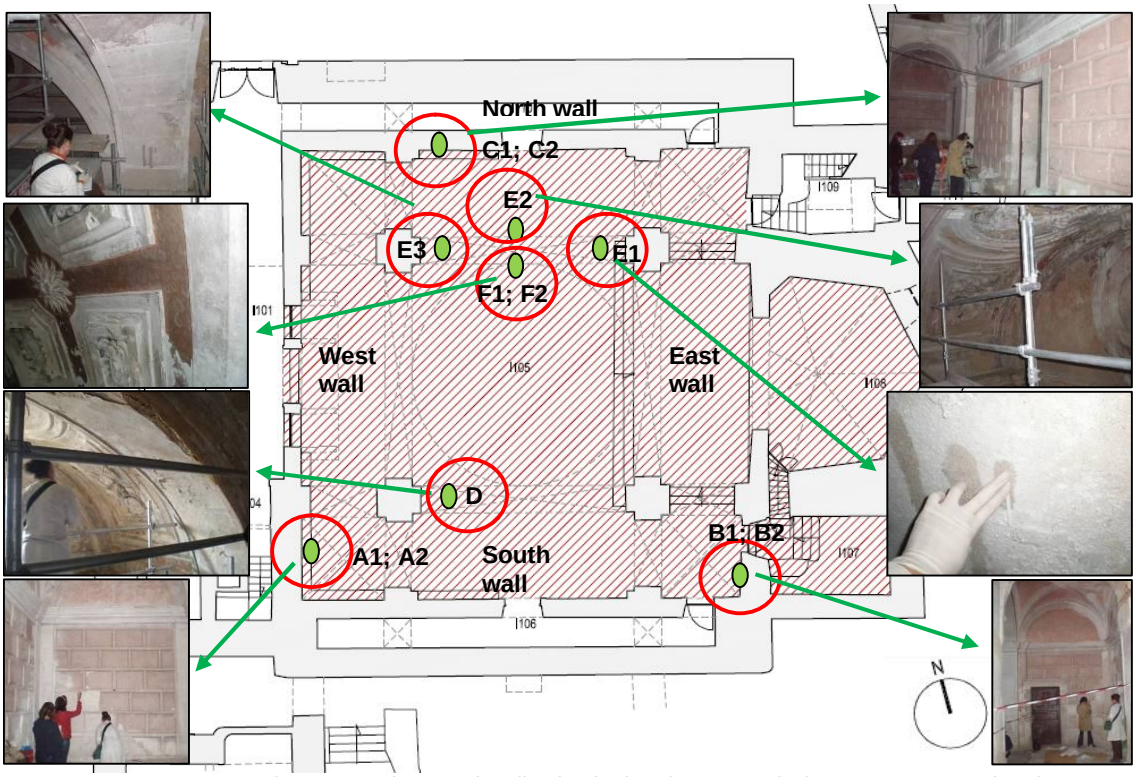

Fig. 3.32 In situ tests localization in the plan – Santissimo Sacramento Church

Fig. 3.33 West facade

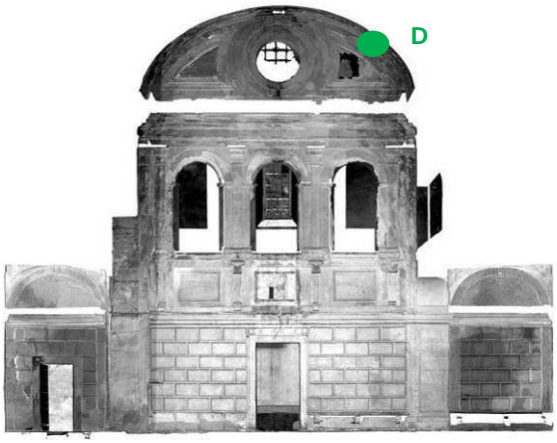

Fig. 3.34 South facade

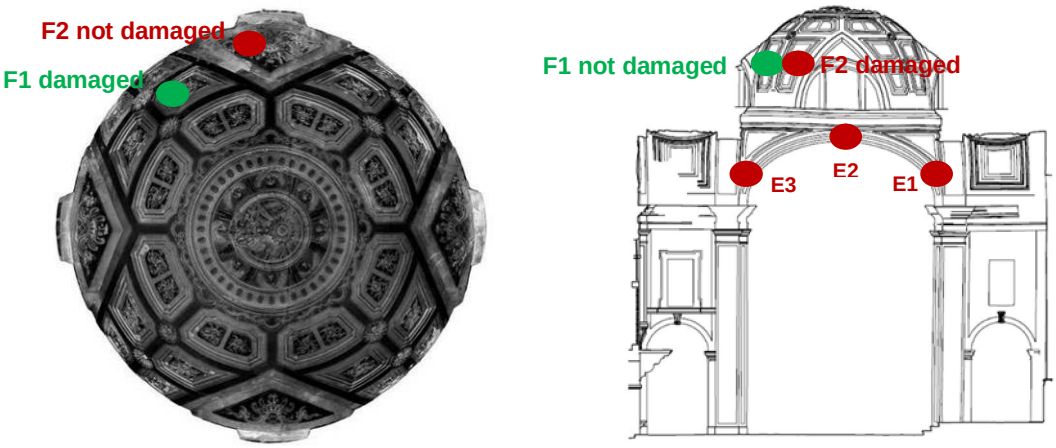

Fig. 3.35 North and dome of the church and arches

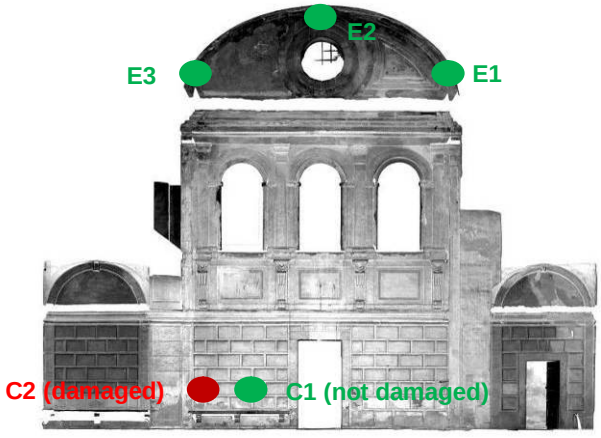

Fig. 3.36 North façade

Fig. 3.37 East façade

In the base of the East wall high superficial moisture content and soluble salts, especially nitrates, were observed. The high moisture can be associated to the presence of hygroscopic salts. In the North and South walls lower moisture content was observed, although in some damaged zones higher moisture was observed (table 3.9). No moisture was detected on the renders of the West wall.

Table 3.9 Average results with portable humidimeter in the outer surface of the most representative elements

Local identification	West wall (W)	East wall (E)	North wall (N)	South arch (S)	North arch (N)	North dome (N)
	A	B	C	D	E	F
	Damaged /not damaged	Damaged /not damaged	Damaged /not damaged	Damaged /not damaged	Damaged /not damaged	Damaged /not damaged
Measure water rate (%)	4 / 2	6.9 / 6.9	7 / 4	ND / 3	7 / 6	ND / 3

ND – Not determined

North arch shows high moisture content (especially near the pillars) and high quantity of sulphates and nitrates and lower of chlorides. The South arch, although considered not humid, shows high quantity of sulphates and nitrates and lower of chlorides, denoting the presence of previous infiltrations. The renders of the dome were considered dry although some located loss of cohesion was observed.

The presence of hygroscopic salts in renders, namely nitrates, sulphates and chlorides, may be influencing the results obtained with a portable humidimeter (Table 3.10). The more or less generalized contamination with chlorides can be due to the use of unwashed marine aggregates in old renders execution [San10]. The presence of fragments of shells is observed in those renders.

Table 3.10 Average results with strip tests in the outer surface of the most representative elements

Local	West wall (W)	East wall (E)	North wall (N)	South arch (S)	South arch (S)	North arch (N)	North arch (N)
	A	B	C	D	D	E	E
	Damaged	Damaged	Damaged	Damaged	Not damaged	Damaged	Not damaged
Salts	Sulphates (200-400 mg/l)	Sulphates (200-400 mg/l) Chlorides (500 mg/l) Nitrates (250 mg/l)	Chlorides (0-500 mg/l) Nitrates (250 mg/l)	Sulphates (1600 mg/l) Chlorides (0-500 mg/l) Nitrates (250 mg/l)	Chlorides (0-500 mg/l)	Sulphates (1600 mg/l) Chlorides (500 mg/l) Nitrates (50 mg/l)	Sulphates (1200 mg/l)

Table 3.11 Average results with using Pendular Schmidt impact hammer and durometer in the outer surface of the most representative elements

Local identification	West wall (W)	East wall (E)	North wall (N)	South arch (S)	North arch (N)	North dome (N)
	A	B	C	D	E	F
	Damaged /not damaged	Damaged /not damaged	Damaged /not damaged	Damaged* /not damaged	Damaged /not damaged	Damaged /not damaged
HV(1)	16 / 30	24 / 32	25 / 29	63 / ND	ND / ND	70 / ND
Shore A(2)	80 / 93	79 / 93	72 / 87	81 / 80	ND / ND	64 / 93

ND – Not determined
(1) Vickers HV = Hardness in Vickers degrees
(2) Unit measurement scale SHORE A from 0 to 100
(3) Presenting detachments and salt efflorescences

Considering the walls, durometer values are normal to high showing the cohesion and resistance of the finishing; impact hammer values are low to moderate in undamaged zones and very low to low in damaged zones. (table 3.11). The results obtained both with durometer and esclerometer in the dome and arches are higher than the reference ones and are considered “high and very high” showing the cohesion and superficial resistance of these renders. In general the renders show good resistance although loss of cohesion and adherence are observed in some damaged zones, maybe due to the presence of some salts in the renders.

The results show that higher moisture contents were observed in the base of the arches (near the pillars) and in more damaged zones of the East and North walls and in general moisture was not observed in the base of the walls; the dome is considered dry. These results indicate that currently no active source of water appears to be present, that may contaminate the walls by capillary rise, and also that currently there are no infiltrations through the dome.

The moisture presents results from old infiltrations through the roof that according to the applicant company was repaired before the start of the works. The moisture was retained in some areas where its evaporation was more difficult, due to the location and thickness of the elements, especially in the base of the arches near the pillars and in the base of some walls where hygroscopic salts are present and may retain the humidity.

It is expected slow drying of the arches and a reduction of moisture concentration especially in the base of arches where moisture was observed and from where the superficial hygroscopic salts

were removed, achieved by an interior environment stable in terms of humidity without allowing quick drying.

Medium to high resistance was observed in the renders although in some damaged zones there is loss of resistance, with loss of cohesion and adhesion.

As conclusion, from the results analysis and considering the historical and artistic value of the building and plasters, they should be preserved, whenever possible, and only in severe cases should they be removed and substituted by new ones. Substitution renders can be used in cases where loss of cohesion and severe damage is observed.

3.3.5 "Santa Joana" Museum (SJM) [Fra11a, Fra11b]

In this case study the anomalies were particularly severe in interior facades both on exterior and interior walls where the tests were performed (Fig. 3.38). The diagnosis was performed using: portable humidimeter and salt strip tests. The most representative in situ results are presented (Tables 3.12 and 3.13).

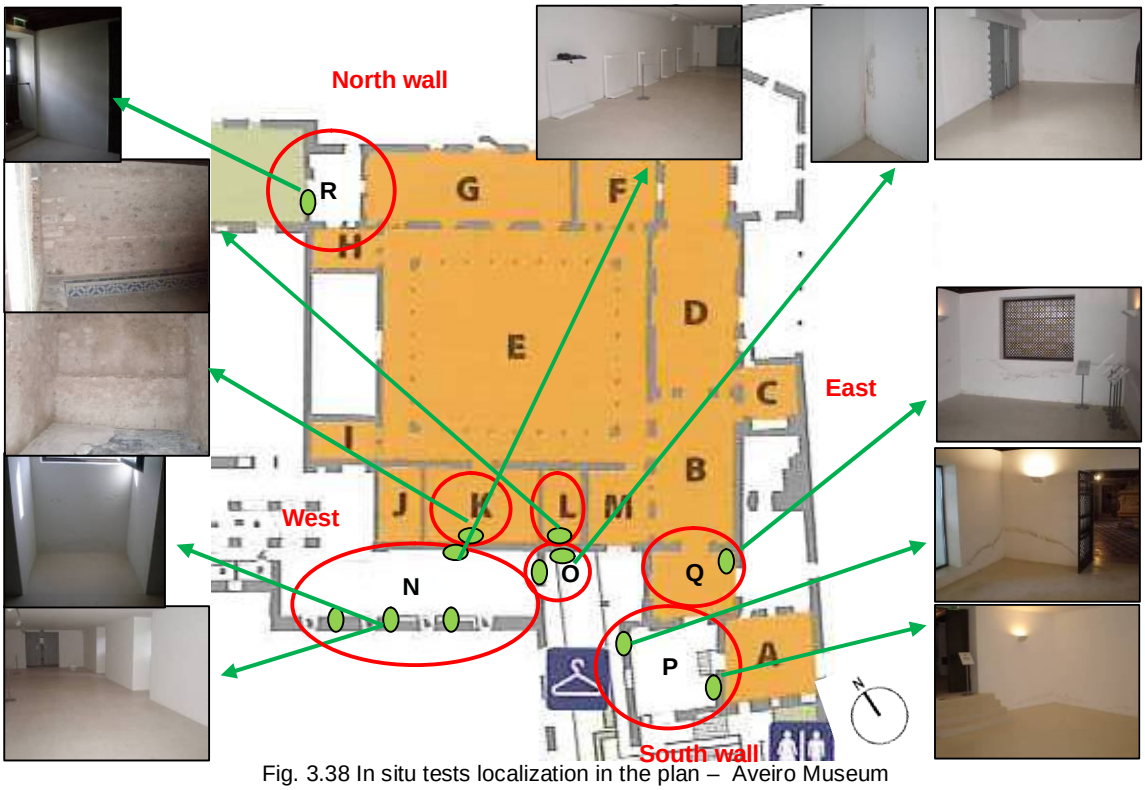

Fig. 3.38 In situ tests localization in the plan – Aveiro Museum

The interior walls were found to have high moisture contents, almost as high as internal facades of external walls. The moisture content was higher at the base, reducing towards the top of the walls also in the vaults was found high moisture content (Table 3.12).

Table 3.12 - Average results with portable humidimeter in the outer surface of the most representative walls, after dry period (ground floor).

Local	**Interior Wall** [(1)]																**Exterior Wall** [(2)]		**Middle of the arch**	**Interior wall** [(1)]	
	(W-P)		(E-P)		(W-Q)		(E-O)		(S-O)		(N-L)		(N-K)		(N-N)		(S-N)		(N)	(S-R)	
Height (m)	0.30	1.80	0.30	1.80	0.30	1.80	0.30	1.80	0.30	1.80	0.30	1.80	0.30	1.80	0.30	1.80	0.30	1.80	2.00	1.80	2.00
Moist. (%)	4.5	4.9	4.7	2.4	5.4	4.2	4.8	1.7	5.2	0	2.4	2.9	3.7	3.2	5.0	1.7	6.9	0.9	6.9	5.0	5.7

[(1)]**Interior wall**: W-P: West facade of room P; E-P: East facade of room P; W-Q: West facade of room Q; E-Q: East facade of room Q; S-O: South facade of room O; N-L: North facade of room L; N-K: North facade of room K; N-N: North facade of room N; S-R: South facade of room R.
[(2)]**Exterior wall**: S-N: South facade of room N.

High moisture content was found in the base of the walls, generally decreasing with height in interior walls. The highest moisture contents were found in the base of interior surfaces of exterior walls and in the middle of the arch of the ground floor. The main water sources could be infiltrations by exterior walls and capillary rising water from foundations as well as moisture from the roof vaults. They also show the effect of some particular constructive issues that favour water retention.

Table 3.13 - Average results with strip tests on the outer surface of the most representative elements

Local	Interior wall (S-O)	Interior wall (N-N)	Interior wall (S-R)
	Damaged	Damaged	Damaged
Salts	Sulphates (1600 mg/l) Chlorides (0-500 mg/l)	Sulphates (1600 mg/l) Chlorides (1000 mg/l)	Sulphates (1600 mg/l) Chlorides (1000 mg/l)

ND – Not determined

The salts present (Table 3.13) were found to be mainly sulphates in large content and chlorides. The presence of chlorides was probably due to the interaction of contaminated water from the ground as the building is located near a marine environment and the presence of sulphates to the presence of cement in the mortars.

3.3.6 "Santo António" Convent and Church (SAC) [Fra11a, Fra11b]

In this case study the anomalies were particularly severe in interior facades both on exterior and interior walls and in ground floor and 1st floor, where the tests were performed (Fig. 3.39). The diagnosis methodology was developed using: portable humidimeter and salt strip tests. The most representative in situ results are presented (Tables 3.14 and 3.15).

Fig. 3.39 In situ tests localization in the plan – Saint Francis Convent

The comparative analyses of the results reported that both in walls of the ground floor and 1st floor high moisture content was found. The interior walls were found to have high moisture contents, almost as high as external wall (Table 3.14). In ground floor the high moisture may be due to the capillary rising water from foundations and superficial water accumulation near the external walls; in 1st floor may be due to infiltrations from the roof and through the outer damaged renders.

Table 3.14 - Average results with portable humidimeter in the outer surface of the most representative walls, after dry period (ground floor).

Local	Interior Wall[(1)] (South-C)		Interior Wall[(1)] (North-C)		Exterior wall[(2)] Interior facade (East-C)		Exterior Facade[(2)] (West-C)		Interior Wall[(1)] (North-D)		Interior Wall[(1)] (West D)	
Height (m)	0.3	1.8	0.3	1.8	0.3	1.8	0.3	1.8	0.3	1.8	0.3	1.8
Moisture content (%) After humid period	6.9	4.9	6.9	4.7	6.9	6.9	5.1	ND	6.9	6.9	6.0	6.9

[(1)]**Interior wall**: South-C: South façade of room C; North-C: North façade of room C; North-D: North façade of room D; West-D: west façade of room D.
[(2)]**Exterior wall**: East-C: East façade of room C; West-C: West façade of room C.
ND – Not determined

In the damaged plasters and renders sulphates, chlorides and nitrates were found (Table 3.15). Sulphates and chlorides were found in larger content in ground floor and lower content in the 1st floor, while nitrates were found in larger content in the 1st floor.

Table 3.15 - Average results with strip tests in the outer surface of the most representative elements

Local	Interior wall (South-C)	(North-C)	Exterior wall Interior facade (East-C)	Exterior facade (West-C)	Interior wall (North-D)	(West D)
Salts After period	humid	ND	Sulphates (1200-1600 mg/l) Chlorides (500-1000 mg/l) Nitrates (25-50 mg/l)	Sulphates (<200 mg/l) Chlorides (1000-1500 mg/l) Nitrates (25-50 mg/l)	ND	Sulphates (200-400 mg/l) Chlorides (0-500 mg/l) Nitrates (50 mg/l)	Sulphates (200-400 mg/l) Chlorides (0-500 mg/l) Nitrates (50 mg/l)

ND – Not determined

Chlorides are typically present in coastal areas, and may be present both in the masonry and render materials, due to the use of non-washed sand and the interaction of contaminated water from the ground that flows to the walls by capillary rise. Sulphates may be present due to the presence of cement in the renders and plasters. Nitrates may be due to the contact with contaminated water with organic products mainly from animals, and maybe due to infiltrations.

3.4 Repair measures

3.4.1 General

The repair of anomalies should be preceded, if possible, by the elimination of their causes. If that approach is not possible, it is necessary to minimize the effects of those causes and control the related symptoms [Fre02a, Vei09b, Vei09f, Vei10b, Fra11a, Fra11b].

3.4.2 “Inglesinhos” Convent (IC) [Vei09b, Vei09f, Fra11a, Fra11b]

Elimination of the Causes

The repair of the roof, of the drainage systems and of the collectors of rainwater was performed. Drainage ditches along the exterior walls were constructed to prevent the accumulation of rain water and ventilation ditches were also made in order to facilitate the evaporation at the base of exterior walls of water rising from the ground (Fig. 3.40).

Fig. 3.40 Rainwater collectors and execution of drainage and ventilation ditches along the exterior walls.

Inside the apartments, ventilation tunnels were made under the floor of the ground-floor, where perforated tubes were introduced and connected to the exterior (Fig. 3.41) with the purpose of

avoiding capillary water rise. In order to promote air circulation, electric fans were installed in the exterior ventilation ditches.

Fig. 3.41 Ventilation tunnels in the interior spaces and gaps between floor footers and the wall.

A gap between the floor footers and the walls was left for ventilation of the interior walls, to allow for continuous drying of masonry over time. To promote drying of the wall bases and mitigate the effects of capillary water rise, ventilation ditches were executed close to the exterior walls and ventilation tunnels with perforated tubes and electric fans were placed along the walls of interior spaces. Forced mechanical ventilation was included, to turn on when very moisty exterior conditions prevent the natural extraction of humidity.

Minimization of the effects

The impermeable external coverings were removed – synthetic finishing, polymeric paints and other polymeric products – and replaced by a lime based finishing coat for the regulation of the walls and a silicate based paint application (Figs. 3.42 to 3.45). The lime based finishing coat, consisting of a thin air lime mortar, executed with siliceous sand and calcium carbonate, with volumetric dosage 1 : 3 (lime: aggregate) was carefully applied, with a soft squeeze with a mason trowel and periodic sprinkling of water. It was let dry for one month before the application of the final paint.

Fig. 3.42 Damage in the external walls due to the use of impermeable renders and paint.

Fig. 3.43 Removal of impermeable external coverings.

Fig. 3.44 Detachment of the external paint, before intervention (left) and final appearance of the exterior facades (middle and right).

Fig. 3.45 Final appearance of the exterior facades, executed with lime based finishing coat for the regulation of the walls and a silicate based paint.

In the internal space, ventilation during the works was promoted by opening the windows and installing portable fans.

The walls' and ceilings' cement and lime plasters were removed, and replaced by air lime and sand mortars, with a volumetric dosage 1:3 (lime: aggregate), covered with a traditional plaster composed by gypsum and air lime (Figs. 3.46 to 3.48). This traditional gypsum plaster is expected not to be painted for at least two years to improve the evaporation of the water retained inside the vaults and walls.

Fig. 3.46 Removal of ceilings' cement and lime plasters and replacement by air lime and sand mortars covered with a traditional plaster.

Fig. 3.47 Removal of cement and lime plasters of interior walls and vaults and replacement by air lime and sand mortars covered with a traditional plaster.

Fig. 3.48 Removal of cement and lime plasters of interior walls and ceilings and replacement by air lime and sand mortars covered with a traditional plaster.

3.4.3 "Nossa Senhora da Graça" Convent (NSGC) [Vei10b, Fra11a, Fra11b]

Elimination of the Causes

Repair of the roof, of the drainage systems and of the collectors of rainwater should be done; also the execution of drainage ditches along the exterior walls to prevent the accumulation of rain water is prescribed.

If the minimization of the effects referred in the next chapter are not enough, there should also be executed ventilation ditches along the base of the exterior facades of exterior walls (specially the most damaged ones) in order to facilitate the evaporation at the base of exterior walls of water rising from the ground.

Minimization of the effects

Considering the impossibility of completely eliminating the capillary water rise through the foundations, the renders should be as permeable as possible to allow drying, preventing the moisture concentration inside the walls. The use of repair, consolidation and substitution lime based renders should be improved and heterogeneities due to the use of renders with different mechanical and water behaviour characteristics should be avoided.

The low permeability paints from the ceiling, vaults and walls should be removed to allow moisture evaporation. It is especially important to remove the water repellent paints in the exterior and low permeability paints in the interior of the building. Between the removal of less permeable paints and execution of the more permeable paints there should be a period of time to allow drying.

The execution of an evaporation gap in the base of the walls can also be considered, and when necessary also near the ceilings, by renders removal. This can be executed both in external and internal facades, but it is especially advised in the most damaged walls of the cloister.

The most damaged external renders should be removed and substituted by permeable renders without salt content that don't create heterogeneities with the pre-existing renders and masonry. The use of a air lime and hydraulic lime based render without soluble salts content, using washed sand, can be considered. In zones where only the partial removal of the render is considered, a lime and cement based render (with low dosage of cement) may be used, with washed sand as aggregate [Vei10a]. It is always important to consider the use of materials of controlled quality. It is important to allow the drying of the walls before renders execution. After at least 28 days curing of the render, a silicate paint, with low organic content (< 5%), should be used.

3.4.4 “Santissimo Sacramento” Church (SSC) [San10, Fra11a, Fra11b]

Minimization of the effects

In zones where damaged plasters with loss of cohesion and adhesion are observed, and where the conservation and/or restitution of the adherence and cohesion is not possible, the old plasters should be removed and substituted by new ones. The use of compatible materials showing similar composition and porous structure as old plasters, lower or similar mechanical resistance, and capillary coefficients and similar or higher permeability is required.

The low drying rate of the walls and arches showing high moisture content should remain in order to allow salt crystallization in the surface of the plaster, as efflorescence. As there is no significant active source of water, if the drying is accelerated the salt crystallization can happen within the render and may induce even higher damage on the valuable plasters.

As observed, there doesn’t seem to be active capillary water rise through the foundations and walls or infiltrations through the roofing, although there is still moisture inside some elements. Based on that, it is possible to recommend the replacement of damaged plasters by new air lime plasters that may have the addition of hydraulic lime with low content of salts, covered with a traditional plaster composed by gypsum and air lime.

The paints should be compatible, based on lime and mineral pigments, as similar as possible to the original ones and durable.

3.4.5 “Santa Joana” Museum (SJM) [Fra11a, Fra11b]

Elimination of the Causes

Repair of the drainage systems and of the collectors of rainwater should be done as well as their application in case they don’t exist; also the execution of drainage ditches along the exterior walls to prevent the accumulation of rain and superficial water is advised (especially in the South facade).

If the minimization of the effects is not enough, also ventilation ditches should be made along the base of the exterior facades of exterior walls (specially the most damaged ones) in order to facilitate the evaporation at the base of exterior walls of water rising from the ground.

Minimization of the effects

The polymeric paints and other polymeric products should be removed. In the exterior facades, the present paint should be substituted by silicate paint and in the interior facades, the plaster should

be substituted by a plaster composed by gypsum and air lime; before their execution the wall should be let dry as long as possible.

Some days after the diagnosis of the anomalies and the application of the repair measures, according the journal "Diário de Aveiro" (http://www.aveiro.co.pt/noticia.aspx?id=79310 &notic=Aveiro:%20Claustros%20do%20Museu%20sofreram%20inunda%C3%A7%C3%A3o) in 7th December 2010, the cloisters of Aveiro Museum were flooded. According to this journal "The rain was too intense for the flow capacity of the drainage systems... getting half a meter" and a responsible from the museum said that some works concerning the repair of the drainage system were done just sometime before but this was clearly not enough, referring the urgency of restoring the efficiency of the drainage systems to inhibit the occurrence of similar situations.

3.4.6 "Santo António" Convent and Church (SAC) [Fra11a, Fra11b]

Elimination of the Causes

Repair of the roof, of the drainage systems and of the collectors of rainwater must be done.

The execution of drainage ditches along the exterior walls, especially along the west facade is strongly recommended, to prevent the accumulation of rain and superficial water. The interior space C is at lower quota than the outer ground surface, so the measures to inhibit the superficial water to attain the west wall are recommended.

Minimization of the effects

The building renders present severe damage due to the lack of maintenance during the last decades.

The zones where damaged plasters with loss of cohesion and adhesion are observed, and where the conservation and/or restitution of the adherence and cohesion is not possible, the old plasters should be removed and substituted by new ones. The punctual substitution of renders on the base of cement mortars should be removed as well as water repellent paints; these should be substituted by lime based renders and more permeable paints.

3.5 Discussion

The state of conservation and the diagnosis of the causes of anomalies in six case studies were established through the analysis of the constructive history of the buildings and with resource to in-situ tests. Then, repair recommendations were defined. The adopted diagnosis methodology allowed the identification of the causes and the location and quantification of effects, leading to an adjusted definition of a set of repair recommendations.

Based on visual observations it could be seen that the main anomalies could be due to humidity and salts, because the main observed anomalies were mainly dark stains of moisture, loss of adhesion and cohesion of the renders and plasters, associated with the presence of salts in most of the cases.

Based on the results of the case studies, the main anomalies are due to the high moisture content, in general with soluble salts, in the interior of the thick and porous walls constituted by stone and lime mortar. The damage is mainly observed in the base of the walls (until 1.50 m from the base) and in the elements of the ceilings as arches and vaults. The determination of the type of salts present helps on the definition of their origin: interaction with contaminated water from the ground, presence of cement mortars, sea salt water and spray or salts existing in other materials and the use of non-washed sand.

The prolonged presence of water significantly reduces the superficial resistance of the plasters and renders. An ineffective rehabilitation and/or conservation interventions using inadequate render solutions, due to the lack of knowledge about the materials, conservation techniques, maintenance principles and particular surrounding conditions (humidity conditions, presence of soluble salts, ventilation conditions), are factors that promoted the premature degradation.

3.5.1 Causes of the anomalies – case studies

Both visual observations and in-situ tests helped in the evaluation of the origin, localization and distribution of the moisture in the walls. With the analysis of the results obtained with the adopted in situ methodology it was possible to identify the causes of the anomalies. In most of the cases they were mainly a consequence of the high accumulation of water in the walls and ceilings. The evaluation of the distribution and localization of the humidity allowed the identification of the origin of the water.

Depending on the values obtained and the distribution of the humidity it was possible to establish the origin of humidity. When wet or very wet zones were concentrated on the lower parts of the walls the probability is that the causes are rising damp or infiltration of superficial water due to the lack or inefficient drainage. When moisture symptoms were localized on the upper parts of the walls, the probable origin of the water could be damaged roofs or damaged or ineffective roof drainage systems. If there is humidity in the vaults and roofs the moisture is probably inside the walls due to infiltrations by a damaged roof.

After observation of the wall coverings, the analysis of their state of conservation and the discussion of the in-situ test results, it was possible to identify the most probable causes of anomalies. The conclusion was that the anomalies were a consequence of the high accumulation of water in the walls and ceilings. From the distribution of moisture on the walls, the water

appeared to have different origins [Hen01, Mass93, Mag02a, , Vei09b, Vei09f, Vei10b, Fra11a, Fra11b] (Table 3.16): (i) capillary rising water from underground through foundations and walls, (ii) capillary rising water from the soil surface, due to the accumulation of rain water near the external walls, and to the absence or disability of drainage systems, (iii) water infiltrations from the exterior with saturation of the roof during a long period before the intervention, (iv) localized infiltrations in some areas of the exterior walls, (v) localised problems in interior walls due to rupture or defects of canalisation, and (vi) condensation moisture in the interior walls.

Table 3.16 Summary of source of humidity in each case study

Case studies	Source of the water/humidity
IC, NSGC, SJM, SAC	Capillary rising water from the underground through foundations and walls
IC, NSGC, SJM, SAC	Capillary rising water from the surface, due to the accumulation of the rain water near the base of external walls and/or due to the absence or disability of rain drainage systems
IC, NSGC, SSC, SJM, SAC	Water infiltrations from the exterior with saturation of the walls and ceilings due to the absence or inability of the roof during a long period and in some cases before the intervention
IC, NSGC, SAC	Localized infiltrations in some areas of the exterior walls
IC, NSGC	Condensation moisture in the interior walls

3.5.2 Elimination of the causes of the anomalies – case studies

The major objectives of these measures were the increase of the water drying rate to the exterior, turning it as close as possible to the capillary rising rate, and the limitation of the water volume that reaches the walls above the floor. The causes of the anomalies should be eliminated whenever possible. The water by capillary rise through foundations, due to high ground water level, is difficult to completely eliminate. In several cases the elimination of the causes is directly related to the source of moisture and if it remains active or not.

The elimination of the causes of the anomalies should be implemented whenever possible (Table 3.17).

Table 3.17 Summary of elimination of the causes of the anomalies in each case study

Case studies	Elimination of the causes of the anomalies
NSGC, SAC	Repair of the roof, of the drainage systems and of the rainwater collectors
IC, NSGC, SJM, SAC	Construction of drainage ditches along the exterior walls to prevent the accumulation of rain water (in case of absence)
IC, NSGC, SJM, SAC	Construction of ventilation ditches at the base of exterior walls, in order to facilitate the evaporation of water rising from the ground through the masonry, avoiding superficial water infiltration.
IC, SJM, SAC	Promotion of ventilation during the works by opening the windows, whenever possible.
IC, NSGC	Execution of a gap between the floor footers and the floor to allow the ventilation of the interior walls and the continuous drying of masonry over time.
IC	Ventilation tunnels under the floor of the ground-floor, with perforated tubes connected to the exterior to avoid capillary rise.

The repair of the roof, of the drainage systems and of the collectors of rainwater should be performed. Drainage ditches along the exterior walls to prevent the accumulation of rain water and

ventilation ditches to facilitate the evaporation at the base of exterior walls of water rising from the ground, should be executed whenever necessary.

If the previous elimination of the causes is not enough to reduce the symptoms after intervention, ventilation tunnels can be constructed under the floor of the ground-floor, where perforated tubes are introduced and connected to the exterior, to avoid capillary rise through the floor inside the buildings, complemented with electric fans installed in the exterior ventilation ditches. Ventilation of the interior spaces should be promoted.

3.5.3 Minimization of the effects of the anomalies – case studies

The presence of water inside the walls may be extended in time due to difficulty of evaporation through the new finishings. In fact, these less permeable finishes reduce the evaporation ability, when compared with the old renders, based on air lime. Reduced ventilation in the interior of the buildings may worsen the situation [Vei02b]. The impermeable renders and paintings should be replaced by materials more compatible with wet walls, such as air lime mortars and silicate paints. In the interior the plasters should be replaced by lime and gypsum plasters. The use of sands with low soluble salts content is of main importance to reduce the risks of damage due to salt crystallization.

The minimization of the effects of the anomalies must also be implemented to reduce the symptoms of the anomalies (Table 3.18).

Table 3.18 Summary of minimization of the effects in each case study

Case studies	Minimization of the effects of the anomalies
IC, NSGC, SAC	Removals of impermeable external paint and replace them by permeable renders and plasters.
IC, NSGC, SJM	Allow the drying of the renders and plasters before the application of the final paint.
IC, NSGC, SJM	Removals of the impermeable plaster and paint from the walls, ceilings and vaults and substitute them by traditional plasters to improve the evaporation of the water retained inside.
NSGC, SSC, SJM	Partial removal of damage renders and plasters and of those with different behaviour/ composition than the original and their substitution by similar ones to the original.
IC, SAC	Full removal of damage renders and plasters and substitution by lime based new ones, compatible with the support and with adequate resistance, considering each specific case.

3.5.4 Substitution renders – case studies

Mortars to be used in old buildings must be compatible with the substrate and the existing mortars. Compatibility is a concept dependent on the characteristics of the old masonry and on the specific conditions of the building. In each case, an evaluation must be carried out concerning the strength, deformability and water permeability of masonry and of the old mortars in contact. In parallel, an assessment of the main physical conditions must be performed, considering specifically: the water transport situation (capillary rising water and exposure to rain), the climatic conditions (humidity

and temperature ranges, wind and rain intensity) and the environmental issues, such as air pollution and salt environment [Fre02a, Vei09b, Vei10a, Gro,12].

Case studies with cement, lime and cement, and hydraulic lime renders, could present severe anomalies after interventions (see Chapter 4), especially in cases with continuous rising damp and/or moisture from damaged roof. If an intervention is needed, the choice of compatible renders (lime based renders specially designed for each case) for old buildings becomes crucial for the success of the intervention.

When the anomalies due to water are local and not severe, they can be solved by cleaning and/or substituting the damaged zones by new compatible renders or paintings. When the anomalies are more severe, the choice of the renders should be done case by case. In those cases when the presence of water inside the walls is extended in time due to difficulty of evaporation because of the use of less permeable renders than the old ones, they should be removed and substituted by lime based ones (pure or with small contents of hydraulic additions), more porous and permeable [Ott08a, Vei10a].

The impermeable renders and paintings (synthetic finishings, polymeric paints and other polymeric products) should be replaced by materials more compatible with walls with humidity problems, such as lime based mortars and silicate based paints [Vei02b]. A lime based finishing coat, consisting of a thin air lime mortar, can consist of siliceous sand and calcium carbonate and carefully applied, with a soft squeeze with a mason trowel and periodic sprinkling of water. It should be left to dry for one month before the application of the final paint.

In the interior the plasters should be replaced by lime or lime and gypsum plasters and ventilation should be promoted in the interior spaces, by opening the windows and installing portable fans if necessary. The use of sands free of salts is always required, to reduce risks due to salt crystallization [Vei09b]. If there is lime and cement in the walls and ceilings, it should be also removed and replaced by air lime and sand mortars, covered with a traditional plaster composed by gypsum and air lime, whenever that kind of finishings existed originally. This traditional gypsum plaster is expected not to be painted for at least two years to enhance the evaporation of the water retained inside the vaults and walls. A gap between the floor footers and the walls can be placed for ventilation of the interior walls, allowing continuous drying of masonry walls over time.

It is particularly important to check if there is still capillary water rise. If this is the case and the solutions mentioned are not enough to minimize the anomalies, mainly for those cases with severe damage due to salt crystallization and when the moisture sources remain active, solutions able to conceal the anomalies can be a possibility. A possible substitution salt accumulation render system, called “ventilated render” has been developed in the scope of this thesis (see Chapters 4

and 6). This render system is able to accumulate salts in its interior significantly reducing damage on the render system [Fra10e, Fra12a, Fra13a].

When it is not possible to eliminate the water source, problems with salt crystallization inside the wall are likely to appear and it is usually safer for the durability of old masonry to adopt, for renders and plasters, water permeable mortars, classified as salt transport solutions [Hee07a]. A lime based render with brick powder as an addition, developed in the scope of this Thesis, could be also a possible solution (see chapter 6) for these cases presenting good durability, resistance and efficiency on the transport of the salts to the surface, even in cases of severe action of salt laden water.

3.5.5 Substitution renders - buildings in maritime environment

Other case studies located in coastal areas (fortresses) [Vei09c, Tav08b, Vei05a] submitted to sea salt water and/or sea salt spray, are subjected to particularly severe actions. They require the use of substitution renders with special properties to assure durability to the referred actions [Vei10a]. The mortars must have high mechanical strength to resist erosion of sea wind and salt crystallization pressure, moderate elasticity modulus to accommodate deformations due to sudden thermal variations, moderate capillary coefficient and high water vapour permeability to retard the entrance of water and allow for quick drying [Vei10a]. Samples collected from several constructions located in Lisbon and coastal surroundings show clearly that very resistant and durable materials were used [San02a], usually based on air lime and additions or aggregates that promoted pozzolanic reactions.

The studied Fortresses had been submitted to previous intervention and premature anomalies were observed on their renders. In the intervention the original mortars of the Fortress of the XVII century had been substituted by lime based renders with water repellent, which showed severe damage, with generaly loss of cohesion; the original mortars of the Fortress of the XVIII century had been substituted by cement mortars showing several anomalies. In both cases the original mortars were composed by air lime.

Fig. 3.49 Fortress on the coast of Lisbon (from the XVII century) before intervention (left) and approximately 1.5 years after intervention, after total substitution of renders by air lime and metakaolin mortars (right) [Vei05a, Vei09c]

Fig. 3.50 Fortress on the coast of Lisbon (from the XVIII century) before intervention (left) and approximately 6 months after intervention, after total substitution of renders with air lime and cement mortar and silicate paint (right) [Tav08b]

The renders of both Fortresses were replaced. Mortars composed of lime and metakaolin were used in the XVII Fortress and based on lime and low content of cement in the case of the XVIII Fortress. The use of mortars composed by air lime and low content in cement can be adequate, although there are some risks of introducing salts into masonry. Mortars formulated with air lime and pozzolans can be adequate to those buildings depending on the type and proportion of pozzolan and curing conditions of the mortar [Vei10a].

3.6 Conclusions

The state of conservation and the diagnosis allowed the assessment of the causes of anomalies. The main repair recommendations were defined: increase water drying rate to the exterior, turning it as close as possible to the capillary rising rate, and limiting the water volume that reaches the walls. The choice of repair or substitution solutions for renders, plasters and paintings are of high relevance to improve the functionality and durability of the masonry walls, especially when they are affected by high water content due to capillary rising or to previous infiltrations through the roof.

This chapter intends to be a practical contribution to the definition of renders conservation state, based on an adopted diagnosis methodology to determine the causes of the anomalies. The definition of the repair solution was done case by case, considering the moisture source and quantity, as well as its distribution and localization, the conservation state and the compatibility with the substrate, and were defined in order to allow moisture drying to the exterior of the walls, avoiding as much as possible its evaporation to the interior and the water absorption by capillary rise through the foundations and walls, limiting the soluble salts.

In cases where soluble salts and active moisture sources are present, although the renders still showing good condition, the removal of salts could be an interesting action to increase renders durability, as a way to delay the occurrence of damage related to salt crystallization (chapter 4). From the investigation of these five case studies, the main anomalies and causes of the anomalies were determined, as base point for laboratory experiments development and validation (chapters 5, 6 and 7); the laboratory testing conditions that efficiently test the renders, under severe action of water, can be defined and the anomalies obtained after laboratory experiments can be compared with the ones observed in the case studies (chapters 5, 6 and 7).

4. ELECTRIC DC FIELD FOR REMOVAL OF NACL FROM RENDERED BRICKS

4.1 Introduction

The definition of a maintenance action to improve renders durability served as basis for the development of this part of the research; the application of electrokinetic desalination method for salt removal from renders and masonry was tested.

Electromigration and electroosmosis are movements of ions and movements of water under the influence of an electrical potential gradient. Electromigration transport mechanism in moist porous materials is used in civil engineering for desalination of concrete, realkalisation of carbonated concrete, crack closure in concrete, injection of organic corrosion inhibitors into concrete, re-impregnation of wood in structures and in the scope of this study, for removal of salts from brick masonry [Ott09b].

The removal of salts sounds easy, but in practice it could be very difficult especially in big monuments. The use of poultice materials to remove salt content from monuments is a well known conservation technique but due to the complex structure and nature of soluble salts the results of such interventions are variable [Ott12a, Hee13, Lub09]. When using poultice materials it is important to know at least the drying conditions and salt distribution of the element to treat. With application of electric DC field a more controlled transport of salt aiming at its removal may be obtained [Ott08a, Ott09b, Ott12a].

According to previous work, electrokinetic desalination of bricks has proved successful at laboratory scale [Ott08b, Rör09a, Ott09b] and encouraging results have been obtained in pilot scale with desalination of brick masonry [Ott08a].

Test the efficiency of electrokinetic desalination, as a maintenance action, as a way to improve the renders durability delaying its replacement can be an interesting possibility; compared with other desalination treatments, a more controlled transport of salt ions towards its removal can be obtained and well as the possibility of its efficient use when active sources of salty solution, such as rising damp, are present.

The present work is focused on the electrokinetic removal of chlorides as a step towards developing a desalination method for brick masonry, taking into consideration the interface between brick and mortar. This work reports results from laboratory experiments conducted with single bricks and rendered bricks. Although there are studies concerning the sodium chloride removal with the application of an electric field DC on bricks and tiles [Ott08a, Ott09a, Ott09b], the influence of the whole system (brick + render) still needs to be deeply studied.

The experimental study described in this chapter was carried out at the Technical University of Denmark (DTU) – Civil Engineering Department, within the group work and supervised by Prof. Lisbeth Ottosen from DTU.

4.2 Electrokinetic desalination

When an electric field is applied to a wet porous medium, the electric field is carried by ions in the pore solution (electromigration) and at the metallic electrodes, from where the current is applied, by electrons [Ott09b, Ott12a]. The processes that transform the current by electrons to current carried by ions and vice versa are called “electrode processes”. The type of ongoing electrode processes depends on the availability of the various chemical species in the vicinity of the electrode surface and on the electrode potential. During the electrokinetic treatment, ions and ionic species are transported towards the electrodes thus the concentration of Na+ and Cl- will decrease in the contaminated specimen (with NaCl solution) as results of these ions concentration around the electrode of opposite polarity. The principle of electrokinetic treatment is shown in Fig.4.1.

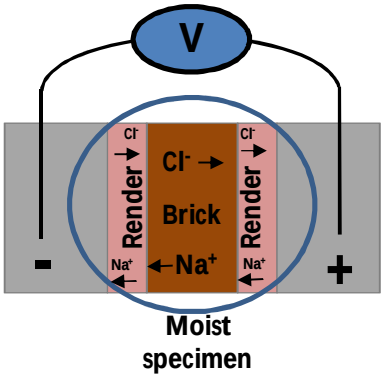

Fig. 4.1 Principle of electrokinetic desalination of specimens. Ions move in moist pores towards the electrode of opposite polarity in the applied DC field and concentrate in the poultice in the electrode compartments.

In this electrode process, using inert electrodes, there is the electrolysis of water: $H_2O \rightarrow 2H^+ + ½O_2$ (g) + $2e^-$ (at the anode) and $2H_2O + 2e^- \rightarrow 2OH^- + H_2$ (g) (at the cathode). When the removed Cl^- reaches the surface of the anode its oxidation to Cl_2 is likely to occur from the electrode process: $2Cl^- \rightarrow Cl_2$ (g) + $2e^-$ [Ott09b, Ott12a].

Electrolysis influences pH around the electrodes. Because the acid is harmful to the masonry it is necessary to prevent acidification of the experimental specimens from the anode [Ott09b]. Around the anode the material is acidified and around the cathode the material becomes alkaline and due to this the metallic electrodes should not be placed directly in the brick; the masonry (support) must be protected from the products from the electrode processes, thus, when choosing the composition of clay for the electrode units for the salt removal process from masonry, it is important that H^+ produced at the anode is hindered in being transported into the masonry [Ott09b]. This is important because the acid could destroy the binder in the mortar and the brick or stone also could be affected [Ott07b].

Electromigration of OH^- from the cathodic reaction of water electrolysis into the brick may be unwanted too, because increase in OH^- concentration results in a decreased transference number of other anions (the part of the current carried by a specific ion) to be removed [Ott08a]. Ottosen [Ott08a] referrs that Castellote et all. observed that in concrete the transference number of chloride ions decreases during chloride extraction because OH^- is taking over the transport due to faster charge transfer than with all other anions.

From previous electrokinetic experiments [Ott12a], it is known that an acidic front develops very slowly in calcareous soils and due to this a choice was made to place the metallic anode in clay with high carbonate content. The clay at the anode was placed on the surface of the specimen. The acid is hindered from entering the specimens since it is neutralized in the clay. The cathode was placed in the same type of clay, but the main purpose of the clay was to serve as place for the ions to concentrate; it is expected that the alkaline front is slowed down during the process due to precipitation of various hydroxides, e.g. Ca(OH)2 [Ott09b]. When placing the metallic electrodes in clay (Fig. 4.2), it is also possible to remove the salts from the specimens after the treatment by removing the clay as the salts concentrate in it during the process.

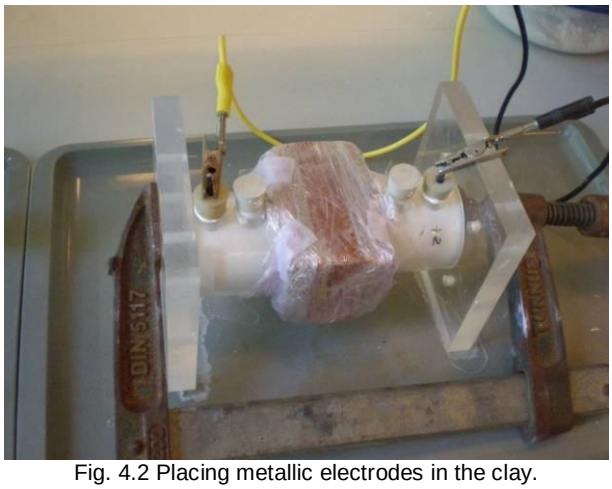

Fig. 4.2 Placing metallic electrodes in the clay.

Transport of water (electroosmosis) is expected to occur in brick, mortar and clay as a result of the applied electric field. The net-flux of ions towards one of the electrodes pushes water molecules in the same direction and electroosmosis occurs. Electroosmosis is expected to happen in the clay at the electrodes during the application of current. The inner surfaces of bricks and mortars are negatively charged [Ott07b] and electroosmosis can also occur in bricks and mortars. Since the inner surfaces of both clay and bricks are negatively charged, the electroosmotic transport of water will be in the direction of the cathode in both cases. However, at high salt solution concentrations the electroosmotic effect can be expected to be almost absent because of the high conductivity in the pore water outside the electric double layer which means that the current preferentially passes here. It is only at low salt concentrations that electroosmosis is expected to play a major role [Ott07b, Ott09b, Ott12a].

4.3 Experimental work

4.3.1 Specimens for experiments

Six different renders were used: four permeable lime mortars: L, LMet, F1 and F7 and two high hydraulic, low permeability mortars: C and Cres. The render mixes were selected from a previous study [Vei10a] (see chapter 2), with exception of mortar mixes F1 and F7 that are formulations from Fradical developed in the present work (see chapter 5). All mortars were prepared according to standard procedures, following EN1015-2 and specimens were cured in conditioned environment (20ºC and 65%HR). Two specimens with each composition were executed. Render's composition is described in Table 4.1.

The specimens were composed by red solid traditional Portuguese bricks (red solid 80×60×34 mm) rendered on both sides with the same render formulation (Fig. 4.3). Seven different specimens were used. A brick without render was used for comparison.

Table 4.1 Mortars formulation to be used as render in the specimens for the experimental work

Specimen	Days of electrokinetic	Render used in both larger sides	Volumetric dosage	Curing time
L	5 days	Slaked lime putty and siliceous river sand	1:3	3 months
LMet		Slaked lime putty, metakaolin and siliceous river sand	1:0.2:3.5	
C	5 and 15 days	Cement and siliceous river sand	1:4	1 month
CRes		Ready-to-use cement mortar with acrylic addition	Ready-to-use	
Brick		-	-	-
F1	15 days	Lime putty; pozzolanic addition; fine and medium size calcareous sand	1:0.2:(1+3)	3 months
F7		Lime putty; pozzolanic addition and other admixtures; brick powder and medium size calcareous sand	1:0.5:(1+3)	

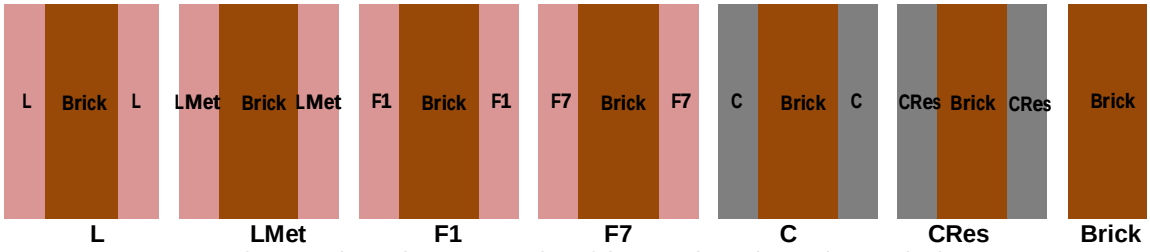

Fig. 4.3 Schematic representation of the tested specimens (upper view)

The specimens were contaminated with NaCl in the laboratory by submersion in NaCl solution (concentration 79.6 g/l) for 2 days in an uncovered container. The 2 days submersion was considered long enough to reach equilibrium between concentration in the pore solution and the soaking solution (Fig. 4.4). The NaCl concentration was chosen based on the literature [Ott12a], which was the concentration measured in salt damaged sandstones in laboratory.

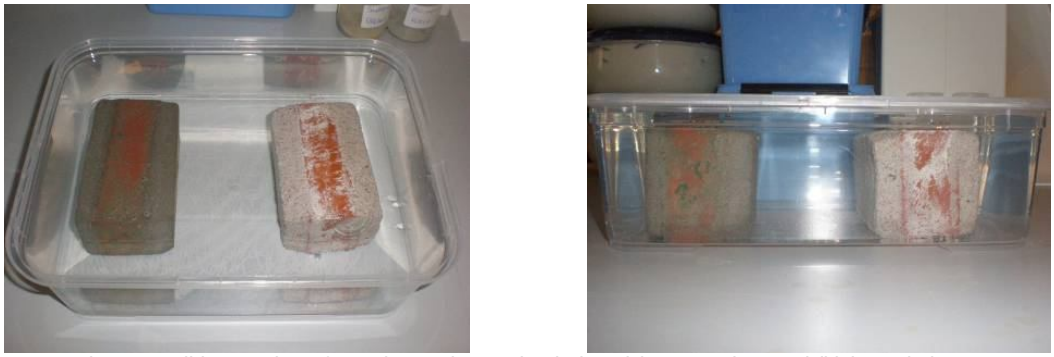

Fig. 4.4 Full immersion of specimens in NaCl solution: (a) upper view and (b) lateral view.

At the end of the experimental work the seven different types of specimens [Fra10b, Fra10f] were tested. Because the specimens used (rendered bricks) are non-homogeneous materials, differences must be expected between the specimens, even though the same materials are used.

4.3.2 Bricks and renders characterization

For chemical analyses, extractions were made with 5 g of dry clay or 5 g dry powdered brick or render and 12.5 ml distilled water. The suspensions were placed on a shaking table and agitated for 24h. The pH and conductivity were measured in the suspension with a Radiometer pH electrode and a conductivity cell, respectively.

The suspensions were filtered through 0.45 µm filter paper and the chloride concentrations determined with potentiometric $AgNO_3$ titration (Metrohm 716 DMS Titrino). The chloride value obtained from the analysis was the acid soluble chloride content. The water content was measured as weight loss at 105°C for 24 h (calculated as weight of water/dry weight).

4.3.3 Experimental setup for electrokinetic desalination

The specimens were placed between two cylindrical electrode compartments made from polymethyl methacrylate. The internal diameter of the electrode was 4.0 cm and the length was 5.0 cm. The electrode compartments were filled with clay poultice (Fig. 4.5). The clay matrix was defined and mixed in laboratory from kaolin and $CaCO_3$ after a recipet developed for desalination of brick masonry [Rör08a]. The laboratory setup for the electrokinetic desalination experiments is shown in Fig. 4.6.

Fig. 4.5 Filling of the plastic electrodes compartments with clay

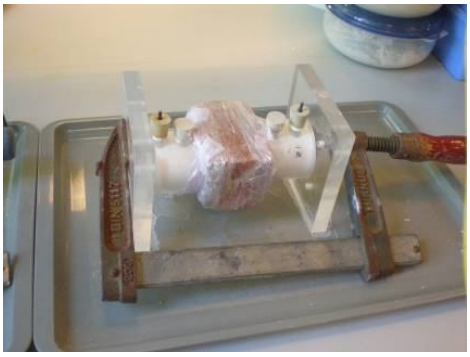

Fig. 4.6 Wrapping of the samples with plastic to avoid evaporation

The specimens were wrapped with plastic film during experiments to limit evaporation and subsequent drying of specimen and poultice. The ends of the tubes away from the specimens were closed. On the upper side of the electrode compartments were two holes (1.0 cm diameter). The holes closest to the specimens were closed during the experiments and were not used in this setup. In the outer holes the electrodes were placed. They were bar-electrodes (platinum coated) with a diameter of 2.9 mm. The electrodes reached approximately 3.5 cm vertically into the electrode compartments. The electrodes were constructed based on previous work [Ott07a1]. At the top the electrodes were placed in a stopper to close the hole around the electrode. The electrode compartments were filled with clay. A constant current of 10 mA was supplied by Hewlett Packard E3612A power supply (Fig. 4.7).

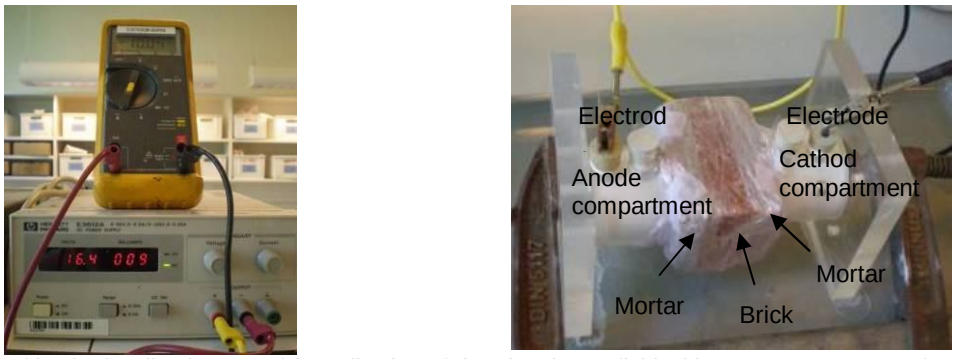

Fig. 4.7 Electrokinetic desalination test: (a) application of the electric DC field with a constant current of 10 mA and (b) specimen for the experiment.

4.3.4 Experiments and procedure

Twenty experiments were made, see Tables 4.2 and 4.3 for overview: ten with reference specimens (Brick1, Brick2, L1, LMet1, F11, F71, C1, C2, CRes1 and CRes2), that were submerged in NaCl solution for 2 days and wrapped in plastic and left at room temperature as long as the duration of the desalination test in the same specimen type (during 5 or 15 days) and ten electrokinetic desalination experiments were made differing in type of specimen and/or duration (Brick3, Brick4, L2, LMet2, F12, F72, C3, C4, CRes3 and CRes4).

All electrokinetic experiments were conducted with constant current of 10 mA and the voltage was monitored. It was not possible to maintain a good contact between anode and clay poultice for longer than 5 days without manual interference and during experiments the clay was pushed back to surround the anode. In experiments Brick4, F12, F72, C4 and CRes4 (experiments with longest duration) distilled water was added into cracks in the poultice at the anode as the clay was too dry to obtain sufficient contact. In those experiments, the clay poultice from both electrodes was replaced by a new one, 3 times, during the experiment.

At the end, both reference and electrokinetic specimens were segmented into 9 slices. The render in both larger sides of the specimens was separated in three parts: one slice from each end far from the electrodes (designated as A and C) and one in between (designated as B) (Fig. 4.8). The slices had approximately the same dimension. The segmentation was done by hand with a hammer and chisel. The bricks were segmented into 3 slices (slice from each end far from the electrodes and one in between) and from each one a powder sample from the brick was obtained with a mechanical drill.

Fig. 4.8 Segmentation of the specimens at the end of the experiments: (a) segmentation of the render in each of the larger sides into three slices and brick into three slices, (b) chisel used for segmentation of the render and (c) mechanical drill for powder brick sample in each brick slice.

The render slices and brick powder were weighed and dried at 105°C. The render slices were pulverized. At least two samples (for double determination) were taken from the powder for measurements of pH, conductivity and Cl concentration. Water content and pH of the poultice were measured (including the poultice removed in the experiments with replacement).

4.4 Results and discussion

4.4.1 Characterization of the materials

The reference (not submitted to electrokinetic treatment) and electrokinetic experiments in specimens are presented in Table 4.2, by parameters such as current intensity and current duration. Also the dry weight, water content just after submersion and weight loss during experiments, are given in this table, for each tested specimen.

The initial water content of specimens, after submersion in NaCl solution varies among specimens (10.8-19.3%) (Table 4.2). The initial water content for brick specimens was between 11.2 and

19.3%; for L specimens between 11.3 and 15.7%, for LMet specimens between 11.2 and 14%, for F1 specimens 12.8%, for F7 specimens between 13.5 and 15.5%, for C specimens between 11.4 and 14.7% and for CRes specimens between 10.8 and 14.1%.

Table 4.2 Current and initial water content in experimental specimens. Dry weight of specimens and initial water content just after submersion.

Specimen	Immersion (days)	Current (mA)	Duration (days)	Dry weight (g)	Initial water content (%)
Brick1	2	0	5	320.75	15.7
L1	2	0	5	592.80	11.3
LMet1	2	0	5	594.35	11.2
C1	2	0	5	532.62	13.3
CRes1	2	0	5	530.52	13.2
Brick3	2	10	5	371.37	11.2
L2	2	10	5	538.16	15.7
LMet2	2	10	5	538.45	14.0
C3	2	10	5	590.32	11.4
CRes3	2	10	5	599.54	10.8
Brick2	2	0	15	319.63	12.0
F11	2	0	15	534.17	12.8
F71	2	0	15	500.48	15.5
C2	2	0	15	567.34	11.8
CRes2	2	0	15	488.99	14.1
Brick4	2	10	15	294.24	19.3
F12	2	10	15	574.56	12.8
F72	2	10	15	556.90	13.5
C4	2	10	15	523.49	14.7
CRes4	2	10	15	516.32	13.5

As can be seen in Figure 4.9, after 5 or 15 days wrapped with plastic film a tendency for water content to be lower in the middle slice of bricks than in end section slices was observed for specimens with lime based renders and the opposite for cement based specimens; similar water content for renders was observed for all slices in each specimen, in most of the specimens.

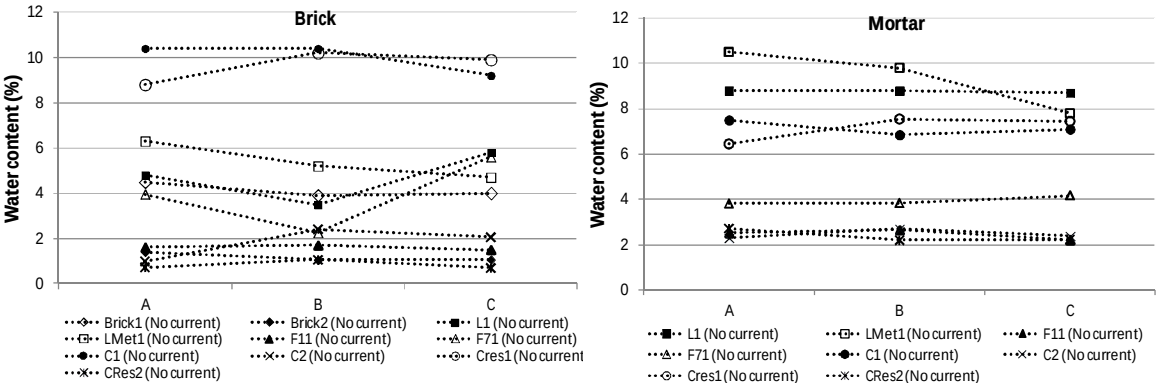

Fig. 4.9 Mean values of water content profiles in each end section slices (A and C) and in the middle slice (B) on reference specimens (after submersion and 5 or 15 days wrapped in plastic film): (a) brick and (b) mortar.

4.4.2 Overall results from the desalination experiments

To evaluate the chloride removal by the application of the electric field DC it is necessary to know the variation in concentration in the same specimen with and without application of the electric field (blank specimens).

To evaluate the salt concentration in specimens in relation to hygroscopic moisture content the Austrian ÖNORM B 3355-1 “Trockenlegung von Feuchtem Mauerwerk – Bauwerksdiagnostik und Planungsgrundlagen” (Deshumidification of masonry – Building diagnosis and planning principles) is used in the present work. According to this Norm, the salt concentrations are separated into three categories for Cl^-: < 0.03% weight (< 300 mg/kg) – no risk; 0.03 - 0.10% weight (300 – 1000 mg/kg) – individual evaluation necessary and > 0.10% weight (> 1000 mg/kg) – active salt removal advised.

An overview of experimental results on reference specimens is provided in Table 4.3. Mean values and standard deviations, for water content, pH, conductivity and chloride concentration, are given for the analyses made on each blank specimen. The reference specimens were submersed in NaCl solution during 2 days and wrapped in plastic film as long as the duration of the application of the electric field, 5 and/or 15 days, in the same type of specimen. The weight loss after 5 and 15 days wrapped in plastic film is shown in Table 4.3. The mean chloride concentration and the standard deviation, the pH and conductivity for reference specimens are shown in Table 4.3.

Table 4.3 Mean values and standard deviation of different measurements made on reference specimens at the end of tests. The Cl concentration, pH and conductivity of the reference specimens (based on measurements of 6 segments in mortars and 3 segments in brick).

Specimen	Current (mA)	Duration (days)	Water cont. (%)	Cl conc. (mg/kg)	pH	Conductivity (mS/cm)
Brick1	0	5	4.13±0.2	7457 ±104	7.3±0.3	7.51±0.19
L1 (m)	0	5	8.8±0.1	5151 ±602	12.6±0.0	13.55±0.52
L1 (b)	0	5	4.7±1.2	5664 ±788	9.6±0.2	6.27±0.87
LMet1 (m)	0	5	9.4±1.7	5107 ±266	12.6±0.0	12.98±0.55
LMet1 (b)	0	5	6.0±0.8	5311 ±230	9.6±0.1	6.69±0.24
C1 (m)	0	5	7.2±0.4	3585 ±313	11.9±0.1	10.29±0.61
C1 (b)	0	5	9.2±0.7	6606 ±340	8.5±0.9	7.85±0.88
CRes1 (m)	0	5	7.2±1.3	3734 ±213	12.7±0.0	13.26±0.40
CRes1 (b)	0	5	9.6±0.7	6471 ±376	9.3±1.1	7.51±0.53
Brick-2	0	15	1.2±0.2	8449 ±686	9.0±0.1	8.18±0.75
F11 (m)	0	15	2.5±0.2	3058 ±428	11.4±1.2	7.44±1.14
F11 (b)	0	15	3.0±1.9	4690±361	8.2±1.0	4.51±0.59
F71 (m)	0	15	3.9±0.1	3558±298	11.3±1.1	8.08±2.05
F71 (b)	0	15	3.9±1.1	4953±539	8.1±1.0	4.71±0.57
C2 (m)	0	15	2.5±0.2	2141±227	11.2±1.1	5.95±0.77
C2 (b)	0	15	1.8±0.5	5643±294	7.1±0.7	5.43±0.57
CRes2 (m)	0	15	2.3±0.3	2752±293	11.6±1.2	11.00 ±0.78
CRes2 (b)	0	15	0.8±0.2	6446±143	9.3±1.1	5.97±0.64

From Table 4.3 it can be seen that the Cl content in blank specimens (both brick and mortar) by far exceeds the highest value of the ÖNORM B 3355-1, being the initial concentrations considered damaging for the masonry.

Table 4.4 Mean values and standard deviation of different measurements made on specimens at the end of electrokinetic experiments. The Cl concentration, pH and conductivity of the reference specimens (based on measurements of 6 segments in mortars and 3 segments in brick).

Specimen	Current (mA)	Duration (days)	Water cont. (%)	Cl conc. (mg/kg)	pH	Conductivity (mS/cm)
Brick3	10	5	3.2±0.2	2472±921	10.9±0.2	3.83±0.66
L2 (mc)	10	5	8.7±0.1	1361±487	12.5±0.1	11.17±0.83
L2 (b)	10	5	12.6±0.6	5345±586	10.6±0.9	6.60±0.65
L2 (ma)	10	5	10.6±0.4	4235±260	12.4±0.2	11.32±0.39
LMet2 (mc)	10	5	7.4±0.2	1049±526	12.6±0.0	10.34±0.87
LMet2 (b)	10	5	4.1±0.2	3747±1005	10.7±1.1	5.24±0.99
LMet2 (ma)	10	5	7.7±0.3	3213±712	12.5±0.1	9.63±0.50
C3 (mc)	10	5	5.6±0.3	836±476	12.5±0.0	8.14±0.12
C3 (b)	10	5	2.6±0.1	3518±727	11.0±2.5	4.59±0.87
C3 (mc)	10	5	5.0±0.3	1508±390	12.4±0.3	6.11±0.75
CRes3 (mc)	10	5	5.4±0.9	1686±946	12.5±0.2	12.07±0.55
CRes3 (b)	10	5	6.4±0.2	2847±704	11.4±2.1	4.47±0.47
CRes3 (m)	10	5	5.1±0.0	2884±197	12.4±0.3	11.04±0.37
Brick4 (c)	10	15	5.3±0.1	6022±869	10.5±0.1	6.37±0.87
Brick4 (a)	10	15	5.3±0.5	5480±872	10.3 ±0.0	6.50±0.81
F12 (mc)	10	15	2.4±0.1	154±73	12.2±0.0	4.10±0.53
F12 (b)	10	15	3.9±0.5	0±0	10.9±0.0	0.84±0.07
F12 (ma)	10	15	2.3±0.2	55±73	9.9±0.1	0.09±0.01
F72 (mc)	10	15	2.5±0.3	188±65	12.2±0.0	7.43±0.82
F72 (b)	10	15	4.4±0.1	0±0	10.9±0.1	0.72±0.06
F72 (ma)	10	15	2.5±0.2	96±15	11.7±0.1	1.64±0.40
C4 (mc)	10	15	1.9±0.8	28±38	11.9±0.1	6.43±1.16
C4 (b)	10	15	4.0±0.4	387±189	11.5±0.0	2.00±0.12
C4 (ma)	10	15	1.7±0.2	285±39	11.9±0.1	4.00±0.89
CRes4 (mc)	10	15	1.2±0.1	466±255	11.5±0.1	10.66±0.47
CRes4 (b)	10	15	2.1±0.2	178±32	11.2±0.1	1.70±0.05
CRes4 (ma)	10	15	1.0±0.1	189±63	11.7±0.0	0.19±0.12

At the end of the desalination, in specimens Brick3, L2, LMet2, C3 and CRes3 the mean Cl concentration was higher than 0.10 wt%, i.e. damaging concentrations were found and active salt removal is still advised after 5 days of current; on specimens LF12, LF72, C4 and CRes4 the mean Cl concentration was lower than 0.03 wt%, i.e. no risk after 15 days current, although for Brick4 specimen salt removal is still advised (Table 4.4).

4.4.3 Changes in water content due to desalination treatment

During experiments the water content of the clay poultices in both compartments decreased compared to initial values. Further, in every experiment the water content in the clay poultice at the anode was lower than the water content in clay poultice at the cathode (Fig.4.10). The water content in the specimens decreased during all experiments so there was an overall loss of water

from the cell. Evaporation from the clay occurred through the holes in the electrode compartments and the plastic film may not have completely avoided evaporation from the specimens.

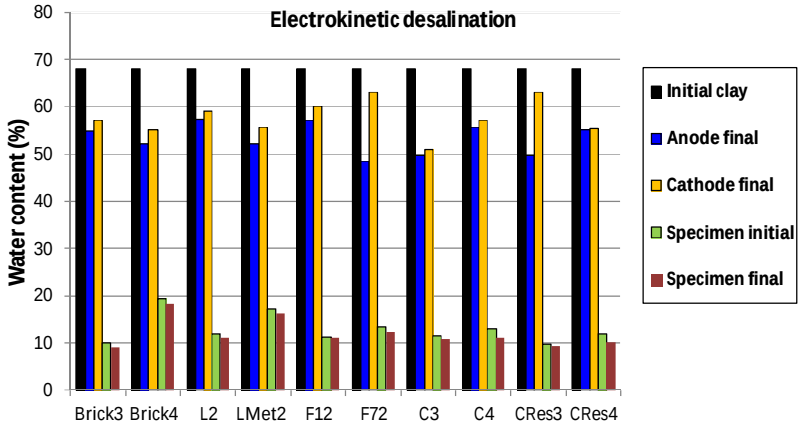

Fig. 4.10 Water content in clay poultice and specimens before and after experiments.

The difference in water content in anode and cathode clay poultices is due to electroosmosis [Ott12a, Ott09b, Rör09a]. All specimens have a porous structure (composed by bricks and mortars) and a high salt content and the electroosmotic transport of water is regarded as limited compared to electroosmosis in the clays [Ott12a].

The electroosmosis occurs under the application of the electric potential gradient. The electroosmotic coefficient is different in the different materials. Specimens (composed by brick and different mortars) and clay were water saturated at the beginning of the experiment, but as the electrode compartments were open to the air through the holes, drying possibly happened. According to Esrig as referred by Ottosen [Ott12a] the pore pressure can build up in the electrode compartments and may uncompress both clays during electroosmosis. It is also important to refer that the electroosmotic flow in the clay changes over time, due to the drying of the clay and to the conductivity changes in the pore water due to electrolysis at the electrodes [Ott12a] and ions arriving from the brick, mortars and clay. Electroosmosis is more significant at low ionic concentration than at high concentration and so more significant electroosmosis is expected at the beginning of the experiments in the clay and almost no electroosmosis in the specimens due to their high salt concentration in the beginning of the experiments.

The profiles of water content in blank experiments (where the specimens were wrapped in plastic and left at room temperature during 5 or 15 days, as long as the duration of the electrokinetic experiments) for bricks and renders are shown in Fig. 4.11.

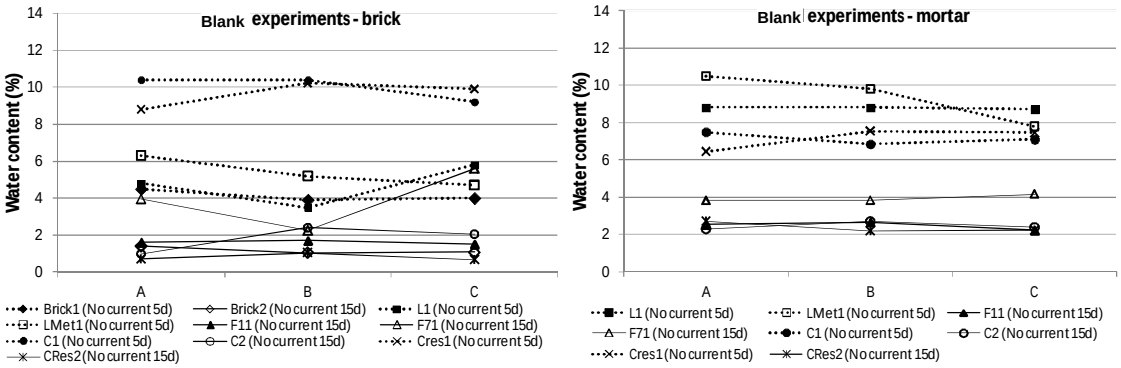

Fig. 4.11 Mean values of water content at the end of blank experiments on specimens at the end far (A and C) and middle (B) slices: (a) on bricks and (b) on renders.

Generally the water content at the end of 5 days of blank experiments is observed to be lower on brick than mortar on specimens with lime based renders (L1, LMet1, F11 and F71) and the opposite happens on cement based specimens (C1 and CRes1). After 15 days the water content was similar on the brick and mortars of the same specimens. The water content decreases with longer duration of the blank experiments. In blank experiments lost water and evaporation from specimens is expected to be similar to the one at the end of electrokinetic experiments.

The composition of those cement based renders may be influencing the water content as they can be considered less permeable than lime based renders reducing the water absorption through the render during immersion, although after 15 days wrapped in plastic film a homogeneous diffusion of the water through the whole specimen could have been reached.

The profiles of water content at the end of the electrokinetic experiments during 5 and 15 days are shown in Fig. 4.12 (a) and (b) for bricks, in Fig. 4.13(a) and (b) for mortars near anode and in Fig. 4.14(a) and (b) for mortars near cathode.

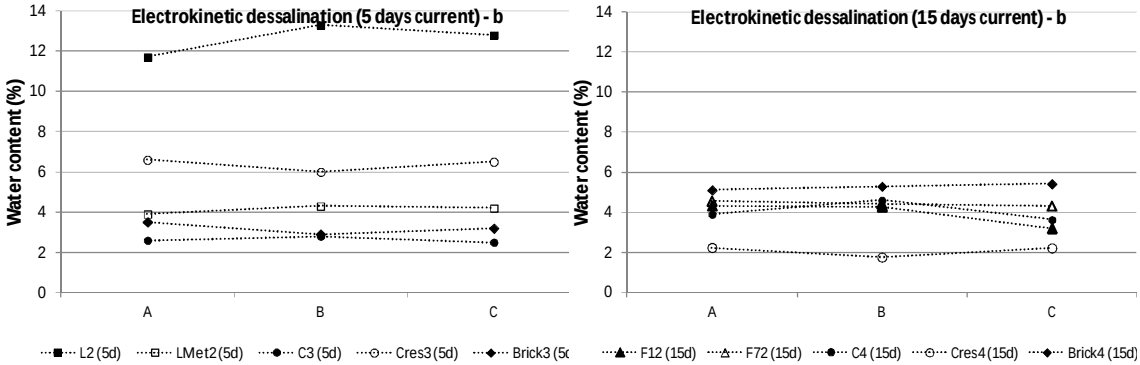

Fig. 4.12 Mean values of water content at the end of the electrokinetic experiments at the end far (A and C) and middle (B) slices on bricks - b: (a) 5 days and (b) 15 days.

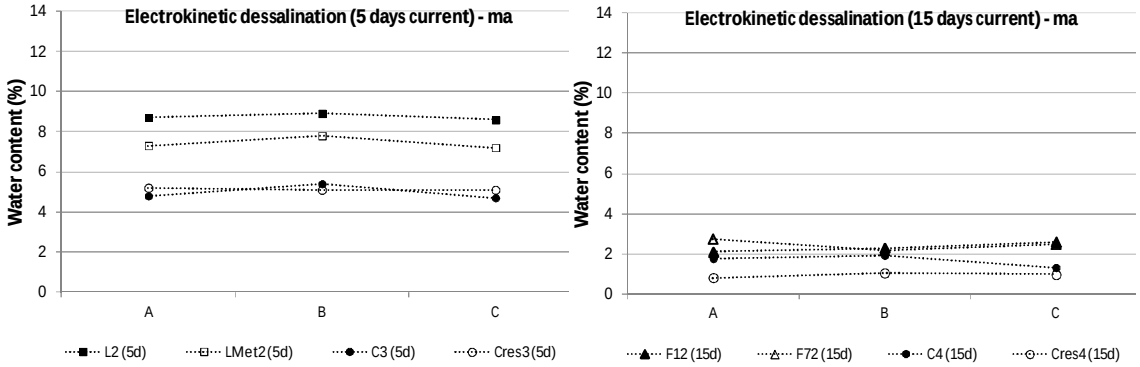

Fig. 4.13 Mean values of water content at the end of the electrokinetic experiments at the end far (A and C) and middle (B) slices on mortars near anode - ma: (a) 5 days and (b) 15 days.

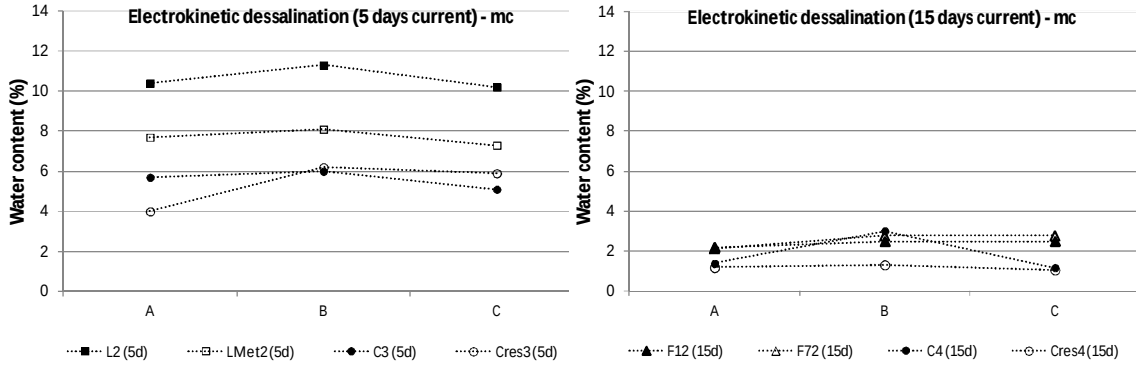

Fig. 4.14 Mean values of water content at the end of the electrokinetic experiments at the end far (A and C) and middle (B) slices on mortars near cathode - mc: (a) 5 days and (b) 15 days.

The water content decreased with longer duration of electrokinetic experiments. From table 4.4 it can be seen that lower conductivity was found on two experiments C4 and CRes4 when compared with C3 and CRes3. After 15 days of electrokinetic all experiments were dewatered to a low level of less than 3.0 wt% in mortar-cathode and mortar-anode and lower than 5.5 wt% in brick. This, together with the fact that water profiles show the lowest water content closest to the anode (Fig. 4.13) and the highest closest to the cathode (Fig. 4.14) can be an indication of electroosmosis in specimens when the conductivity of the pore water is low. The very low water contents were obtained only on renders after 15 days of electrokinetic desalination and electroosmosis could be considered almost inexistent.

The loss of contact between electrodes and clay was solved by moving the electrode in the clay in the 5 days of electrokinetic experiments, although for 15 days of electrokinetic experiments addition of water in the clay was necessary and its removal and substitution by a new one.

From the results described above some partial conclusions concerning the water content can be drawn:

- The variation in water content does not seem to be different due to the use of lime based renders or cement based renders in specimens; the difference in water content found in bricks after

desalination treatment seems to be mainly due to some differences on the bricks production (as they were traditionally made some heterogeneities may be found) than to the different renders used;

- The water content is lower in the clay in the anode (+) than in the clay in the cathode (-) in every experiment indicating electro-osmotic transport of water;

- Neither the average water content in the clay nor in the specimens seems to have decreased to a level where it is considered problematic to the electrical conductivity of the system, at the end of 5 days while at the end of 15 days current the water content decreased to an extent considered problematic to the efficiency of the electric desalination treatment in all specimens.

4.4.4 Changes in pH due to desalination treatment

At Tables 4.3 and 4.4 and Fig.4.15 it can be observed that the pH changes from the electrode processes have influenced the pH in specimens, both on mortar and brick.

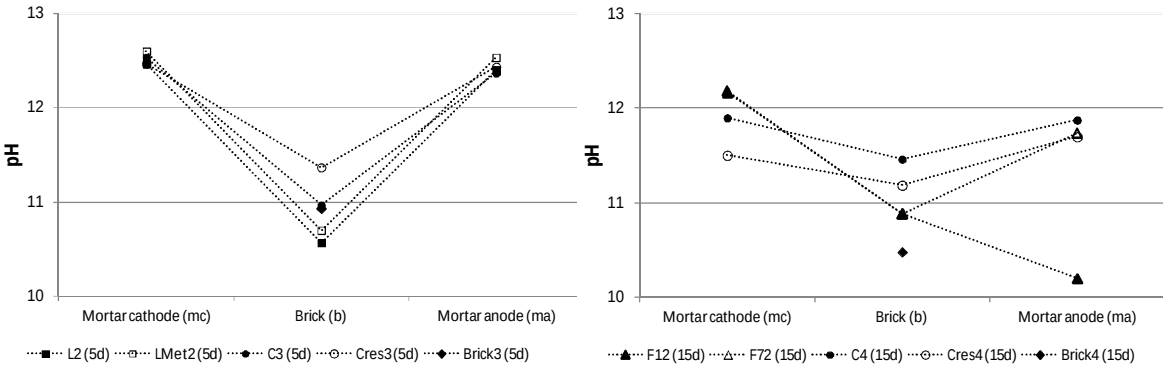

Fig. 4.15 pH at the end of the electrokinetic experiments: (a) 5 days and (b) 15 days .

Due to the electromigration an increase in pH in the clay next to the cathode is expected, as well as a decrease in the clay next to the anode [Ott12a, Ott09b]. At the end of the experiments the pH was between 11.3 and 11.6 in the clay next to the cathode and in the clay next to the anode pH was between 8.8 and 9.8. Initially the pH in the clay was around 8.9. The clay neutralizes the acid produced at the anode, since pH of the clay still nearly neutral through a pH decrease was seen in some experiments.

The pH profiles in specimens (Fig.4.15) show that the pH changes from the electrode processes have influenced the pH in specimens, both mortar and brick. The pH in blank specimens (both mortar and brick) was between11.2 and 12.7 in mortars and between 7.1 and 9.6 in bricks (Table 4.3). The pH after electrokinetic experiments is shown in table 4.4. All slices made at the end of the electrokinetic experiments time showed a similar or higher pH than after submersion. This shows that the development of acidic front from the anode was successfully prevented by the neutralizing effect of the carbonates in the clay poultice. After 5 days of desalination there was observed higher increase in pH than after 15 days.

From the results described above some partial conclusions concerning the pH can be drawn:

- Due to electrode process there was an increase in pH at the clay cathode and a decrease at the clay anode;

- After electrokinetic experiments an increase of pH was observed in both renders and bricks composing the specimens; after 15 days of desalination the neutralizing effect of the clay on the acid from the anode is reduced compared with 5 days of treatment.

4.4.5 NaCl removal

For the determination of Cl content profiles in mortar-anode, mortar-cathode and brick mean values of the contents were determined in the middle slice of each material, considering 2 determinations per piece.

Reference experiments

The standard deviation of Cl concentration in the six slices of renders and three slices of brick in each blank specimen is quite large (Table 4.3) and varies between 1.4 – 14% of the mean value. The mean chloride concentration is higher for brick than render in each specimen. Higher Cl concentration was found on brick of Brick specimen when compared with the brick of the other specimens. Bigger difference on Cl concentration between brick and render was found on specimens with cement based renders (C and CRes).

The Cl profiles for blank specimen's bricks and renders are shown in Fig. 4.16 (a) and (b), respectively. The Cl profiles are mean values of the far end sections slices A and C and middle section slice B in each specimen, both for renders and bricks. The Cl concentration in each slice is very high and above the limit of no risk from the ÖNORM of 300 mg Cl/kg.

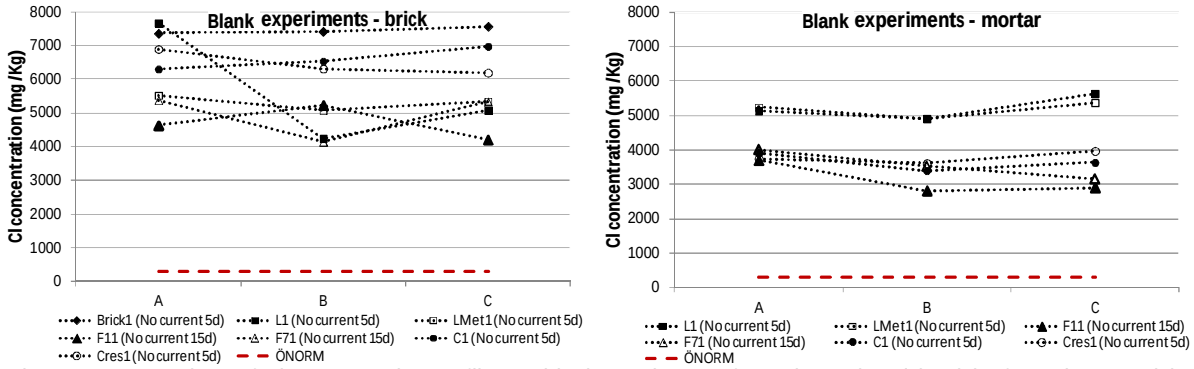

Fig. 4.16 Mean values of Cl concentration profiles on blank specimens after submersion. (a) Brick of specimens Brick, L, F1, F7, LMet, C and CRes and (b) Mortars of L, F, F7, LMet, C and CRes.

There is a general tendency of the most tested specimens for Cl concentration to be lower in the middle slice (B) than in the far end slices (A and C), (data not shown) both for mortars and bricks. The reason may be that chloride diffusion has not levelled out the concentration differences

[Ott09b] after 2 days of submersion followed by 5 or 15 days wrapped in plastic film. Also the water content was lower in the middle slice of bricks in blank specimens. These lower concentrations in the middle slices could be justified by Pel et al. observations made on bricks, as referred by Ottosen [Ott12a], where during water absorption in a calcium-silicate brick a sharp wetting front developed, but the Na profile was clearly lagging behind the moisture profile and hardly any Na was present near the wetting front. This means that if constant water content in the materials had been reached during submersion, the lagging behind of Na (and Cl since electroneutrality remains) would mean lower concentrations in the middle of the material [Ott12a].

Electrokinetic experiments

The profiles of chlorides concentration in clay and specimens at the end of the electrokinetic experiments in Figs. 4.17-4.20 show that in every specimen segment the chloride concentration decreased compared with the same type of specimen without treatment. Chloride is expected to electromigrate towards the anode in the applied electric field and a concentration profile significantly lower in the mortar near the cathode than in the mortar near the anode, is expected at the end of electrokinetic experiments as a result of electromigration.

The chloride concentration after electrokinetic experiments in the clay next to the anode and next to the cathode is shown on Fig. 4.17. This clearly shows that chloride was transported by electromigration towards the anode. The chloride was transported out from the specimen and into the clay which enables removal of chlorides when the clay is removed from the specimen.

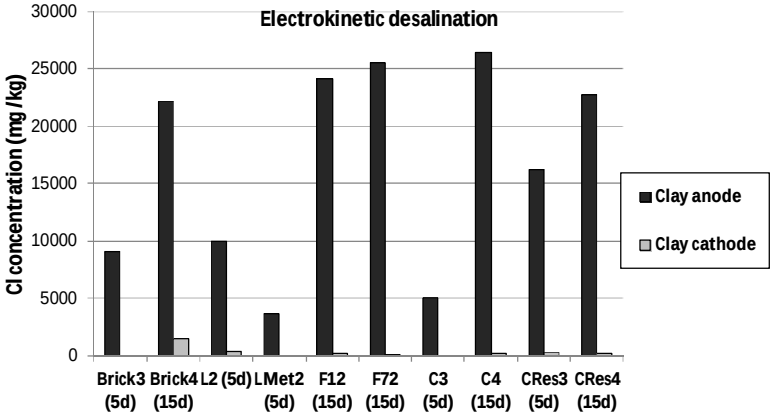

Fig. 4.17 Mean values of Cl concentration in the clay next to the anode and in the clay next to the cathode at the end of electrokinetic experiments.

The chlorides concentration at the clay anode after 15 days treatment was much more than the double at the clay anode after 5 days treatment (exception for CRes specimens). The chlorides content removed from specimens after 5 days or 15 days treatment were similar among all specimens, proving once more the efficacy of the treatment.

The chloride was not sufficiently removed from the specimens after 5 days with current (Fig. 4.18a). Thus 5 experiments (Brick4, F12, F72, C4 and CRes4) were conducted with similar

experimental conditions except for the duration of the desalination treatment, which was prolonged during 15 days. To see if there is a pattern in Cl concentration the resulting Cl profiles obtained from these electrokinetic experiments are shown in Figs. 4.18-4.20.

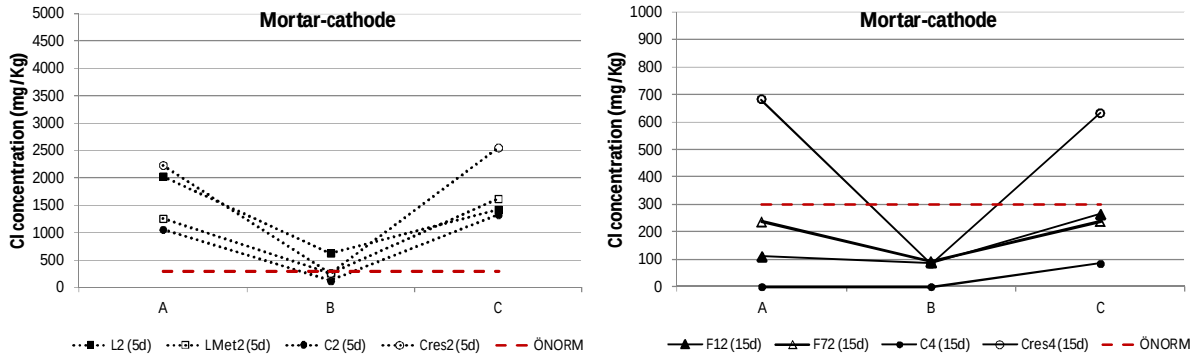

Fig. 4.18 Mean values of chloride concentration in mortar segments near the cathode for each specimen at the end of electrokinetic experiments: (a) after 5 days and (b) after 15 days.

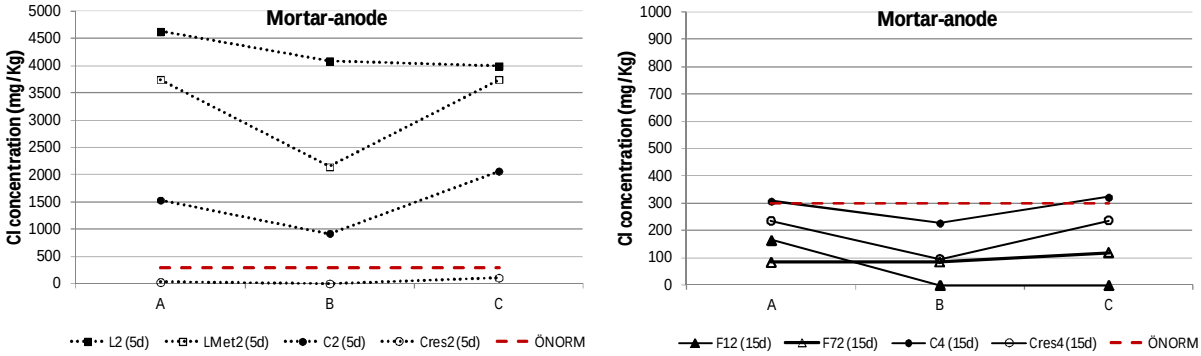

Fig. 4.19 Mean values of chloride concentration in mortar segments near the anode for each specimen at the end of experiments. (a) After 5 days current and (b) after 15 days current.

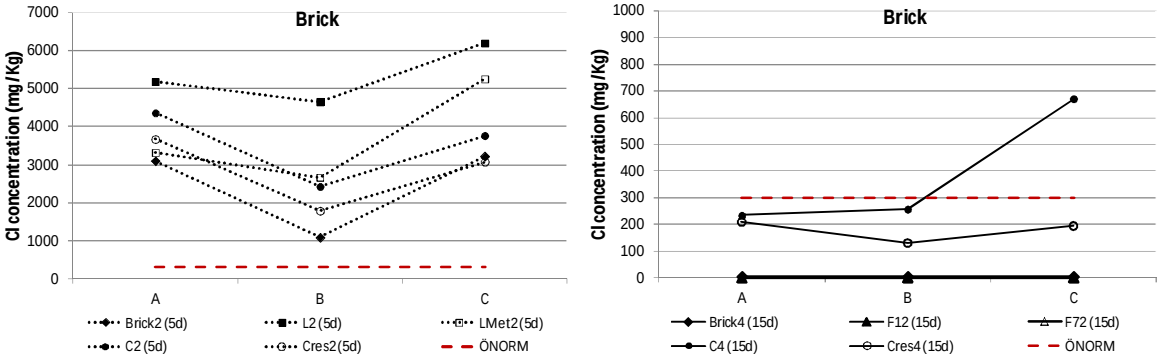

Fig. 4.20 Mean values of chloride concentration in brick segments for each specimen at the end of experiments. (a) After 5 days current and (b) after 15 days current.

The standard deviation of Cl^- concentration in the six segments of render of each specimen is quite large (Table 4.4), being lower on brick segments. As the chlorides move towards the anode when the electric field is applied the Cl concentration is significantly higher in mortar anode than in the mortar cathode.

The concentration decreased in every slice of each type of specimen after 5 days of current. The limit of risk from the ONORM of 300 mg Cl/kg is shown in Figures 4.18 – 4.20, and only after 15 days of current all measured concentrations in bricks and mortars slices were below this value (except the far end mortar cathode slices of CRes4 and the far end brick slice of C), meaning no risk.

From the results described above some partial conclusions concerning the Cl removal can be drawn:

- The chlorides were not sufficiently removed from specimens after 5 days of desalination (only in the middle of the slice of mortar cathode (B) the desalination was effective, below 300 mg Cl/kg);

- After 15 days of treatment the chlorides were efficiently removed from the wet specimens, both in the support (brick) and renders in the applied electric field; only CRes specimen was observed to be an exception, as in this case some slices of mortar anode and brick showed higher chlorides than the limit of risk from the ONORM (300 mg Cl/kg);

- In specimens with lime based renders (L, LMet, F1 and F7), 15 days of treatment seem to be too much for their complete desalination; specimens with cement mortars (C), 15 days of treatment seems to be the necessary for chlorides removal; in specimens with ready to used cement mortars with acrylic addition (CRes) some more days of treatment seem to be necessary to the efficient removal of the chlorides (below 300 mg Cl/kg).

4.5 Discussion and conclusions

Electrokinetic experiments were conducted for NaCl desalination of specimens. The chloride concentrations after treatment, in the mortar cathode, brick and mortar anode, clearly show the effect of electromigration. After treatment the negatively charged ions (Cl^-) were transported towards the anode (positive electrode). The results obtained show that electrokinetic desalination is efficiently used for desalination of the rendered bricks and reduces or even eliminates the risk of decay: by applying 10 mA during 15 days it was possible to obtain an efficient reduction in chloride concentration in brick and mortar in almost all specimens (below 300 mg Cl/kg).

The chloride concentration in mortar-anode, brick and mortar cathode decreased for all specimens, when compared to reference specimens (not submitted to electrokinetic treatment). The higher reduction in chloride concentrations was found in mortar cathode for all specimens. Higher chlorides removal was found on specimens with lime based renders ((L, LMet, F1 and F7) considering the same duration of treatment. The Cl concentration strongly depends on render formulation as was confirmed by the different results obtained for the several specimens. The highest Cl^- concentration was in the anode revealing that the method works. The lowest

concentration was in the cathode and it was almost zero, for all specimens after 15 days of treatment.

Comparing to the limiting concentrations from ÖNORM B 3355-1 “Dehumidification of masonry – Building diagnostics and planning principles” it is seen that before electrokinetic desalination treatment, chloride concentration exceeds the upper limit of the Norm, where desalination is advised. After 5 days of treatment active salt removal is still advised in all specimens and 15 days of treatment were considered enough for salt removal both from brick and render; the exception seems to be specimens with pre-dosed cement mortars with acrylic addition (CRes) where in mortar cathode and in the support (brick) the chlorides content were observed to be higher than 300 mg Cl/kg, so the duration of the treatment was not sufficient in this case.

The results found in the laboratory are encouraging for the efficiency of electrokinetic desalination on rendered bricks, in presence of salty water, although further experimental work should be carried out to establish a possible correlation between the efficiency of this method in laboratory and in-situ scale. This method shows to be an interesting possibility in cases of active moisture sources; however, results points out to the inexistence of electrokinetic desalination at very low water contents.

In the future after attesting the efficacy of the method in situ, it could be used for increasing the durability of NaCl contaminated renders and masonries using electrokinetic desalination as maintenance procedure.

5. INFLUENCE OF SUBSTITUTION RENDERS

5.1 Introduction

In Portugal, rehabilitation and conservation interventions are considered of increasing relevance. Renders are used as decorative and protective coats, acting as sacrificial layers that are particularly exposed to climatic actions and mechanical and environmental impact, becoming the most vulnerable constituents of historical buildings. In such buildings conservation renders that are incompatible with the substrate and the pre-existing materials, and are inappropriate for the existing conditions, are often adopted, producing new pathologies [Vei09b, Vei10a, Vei08a].

Rising damp, amongst the sources of moisture present in old masonry, is the most dangerous. Systems based on physical cuts or on the injection of chemical products to prevent moisture in a structure, are often ineffective due to the heterogeneity of the masonry [Lub06a]. The high moisture content introduced in the masonry combined with its salt content, can promote the crystallization of such salts [Lub06b].

Salt crystallization, is considered one of the major causes of render decay. The extension of this phenomenon is dependent on the salt transport behaviour of the substrate/render, as well as on the surrounding temperature and relative humidity. Unfavourable surrounding conditions may cause repeated cycles of dissolution/crystallization, leading to the rapid damage of building materials [Lub08a].

Salt damage may occur at the surface or within the render layer. In the first case salt accumulates on the surface as a result of salt moisture transport from inside the wall (rising damp, etc.) or from outside (salt-spray, etc.) and consequent dissolution/crystallization cycles may lead to superficial damage. Salt accumulation inside the render (crypto-florescence) usually causes more serious damage, and may be due to a drying front within the render, changes in porosity due to the co-existence of different materials and the use of water repellents, etc. [Gro09a].

In materials contaminated with hygroscopic salts, changes in temperature and relative humidity (RH) may produce dissolution/crystallization cycles of the salt which enhance the damage. In the specific case of sodium chloride (NaCl), cycles of temperature are not harmful, since the solubility of this salt does not significantly vary with temperature; however, a change in RH may lead to dissolution/crystallization cycles which can therefore cause increased damage. Salt damage is rarely a result of a single crystallization event, but rather the consequence of repeated crystallization cycles creating gradients in the salt and in the stress distribution which gradually weaken the material [Lub08a].

Recently crystallization damage mechanisms in mortars and plasters have been studied by several authors [Lub06b, Gro09a, Gon07]; however a deeper knowledge concerning the influence of the whole system (brick masonry + render) is often lacking.

The experimental work in present chapter was performed to: i) develop laboratory experiments able to simulate the severe action of water in specimens, ii) develop render systems considering both the renders and the support, to be tested in laboratory and ii) define ability of the performed laboratory experiments, on the developed specimens, in simulating the main renders anomalies observed in situ. Two less permeable lime based render mixes and two high permeable cement based render mixes were considered, selected from a previous study [Vei10a] (see chapter 2).

In this study the entire system (brick + render) is taken into consideration and tested in the laboratory. This preliminary experimental research has been undertaken to study the location and type of sodium chloride crystallization in rendered brick masonry when submitted to dissolution/crystallization cycles.

Chapter layout

In this chapter the selection and characterization of materials composing the render systems and render systems execution is presented in section 5.2. In section 5.3 the effect of the simulation of the severe action of salt laden water is analysed by visual observation, weight variation and quantification of crystallization, at the end of the 4^{th}, 6^{th} and 8^{th} dissolution crystallization cycles, as well as the damage evolution 6 months after the end of the tests. The render systems are classified in terms of working principle and performance in section 5.4. An overall discussion focusing on the objectives of the research and the main conclusions, in this phase, is presented in section 5.5.

5.2 Materials

In the experimental research in this chapter the render solutions were chosen taking into account the entire system, render+brick+plaster, simulating both render and plaster in brick masonries. The renders were selected based on their behaviour in terms of water and water vapour permeability: i) permeable renders/plasters – based on lime or lime and metakaolin L and LMet; ii) less permeable renders/plasters – based on cement or ready-to-use cement mortars with acrylic addition, C and CRes. Lime and metakaolin based render is a render developed by Fradical Company.

The objective is to study the behaviour of the specimens when submitted to dissolution/crystallization cycles, performed with all possible combinations of these renders. Perforated bricks were used as support because they are lighter than solid bricks and their performance is analogous

The final analysis intends to understand the behaviour of the specimens when the following layers occur: i) permeable render/ brick/permeable plaster; ii) permeable render/brick/less permeable plaster; iii) less permeable render/brick/less permeable plaster.

Specimen's composition and preparation

Four different renders were used: two permeable lime mortars (L and LMet) and two hydraulic, low permeability mortars (C and Cres), selected from a previous study where their main properties are presented [Vei10a]. All renders were prepared according to standard procedures – EN1015-2. Two specimens with the same composition were executed and all combination were done in twofold. Specimens' composition is described in Table 5.1. Table 5.2 describes the specimens' compositions and curing conditions.

Table 5.1 Mortars formulations to be used as render in the specimens

Render	Composition	Volumetric dosage*
L	Slaked lime putty and siliceous river sand	1:3
LMet	Slaked lime putty, metakaolin and silicious river sand	1:0.2:3.5
C	Cement and silicious river sand	1:4
CRes	Ready-to-use cement mortar with acrylic addition	Ready-to-use

* Mortars formulation to be used as render in the specimens

Table 5.2 Specimens preparation and curing

Specimen	Side A		Side B		Curing time
	Render	Curing conditions	Plaster	Curing conditions	
L	L	23ºC/ 50% RH	-	-	4 months
L-L	L		L	23ºC/ 50% RH	
L-LMet	L	20ºC/ 65% RH	LMet	20ºC/ 65% RH + Sprayed with water twice a day during the first 7 days	
L-C	L		C		
L-CRes	L		CRes		
LMet-LMet	LMet	20ºC/ 65% RH + Sprayed with water twice a day during the first 7 days	LMet		
LMet-C	LMet		C		
LMet-CRes	LMet		CRes		
C-C	C		C		1 month
C-CRes	C		CRes		
CRes-CRes	CRes		CRes		
CRes	CRes		-	-	

Specimens were cured in conditioned environment characterized by 20ºC and 65% relative humidity RH until testing and sprayed twice a day during the first 7 days, with the exception of specimens of lime putty, which were cured in dry conditions (23ºC and 50% RH).

The specimens, specially designed for the purpose of the work, were composed of red perforated bricks (300 mm × 195 mm × 40 mm) with a 1.5 cm mortar layer on either both sides or one side (in

the case of L and CRes specimens), to simulate internal plaster and external render on brick masonry (Fig. 5.1).

The specimens were carefully executed in order to reduce problems during testing which could be related to inadequate workmanship (Fig. 5.2).

Fig. 5.1 Specimens execution.

Fig. 5.2 Render execution on perforated brick.

Specimens were not sealed, so the evaporation was able to occur on all sides. Before testing (after curing) they were dried in a ventilated oven at 40 °C until constant mass and afterwards they were left to equilibrate in a conditioned room (20 °C and 65% RH).

5.3 Effect of the severe action of salt laden water on specimens

Salt crystallization test procedure

Fig. 5.3 Partially immersion of specimens for dissolution/crystallization cycles reproduction.

Fig. 5.4 Specimens drying in a ventilated oven at 40ºC.

After curing, the specimens were subjected to crystallization tests by dissolution/crystallization cycles. They were partially immersed in NaCl solution (27g/L – similar to sea content [Aug90]) (Fig. 5.3) to allow capillary rise through the specimens, reproducing rising damp close to sea, in laboratory conditions (under the same temperature and relative humidity of the air). After each wetting cycle the samples were then dried at 40ºC in a ventilated oven, to speed up the drying (Fig. 5.4). The wetting and drying phases of each cycle were prolonged until constant mass of the specimens. The samples were not brushed between cycles. The test stopped when damage in the plaster was found or after 8 dissolution/crystallization cycles.

Study of the influence of different renders for the location and type of sodium chloride crystallization in rendered brick masonry and their crystallization quantification, when submitted to dissolution/crystallization cycles.

The specimens were subjected to dissolution/crystallization cycles without brushing between cycles, to check the evaluation of the salt distribution and study the crystallization and damage patterns in the material's structure at different time intervals during the test.

5.3.1 Visual observations on salt crystallization

The salt crystallization was evaluated by visual monitoring and by weighing the specimens daily. The damage was evaluated by visually monitoring of salt crystallization and decay and by weighing the specimens. Visual observations of sodium chloride crystallization in the 4th and 6th cycles are shown in Table 5.3. These observations were performed to qualify the crystallization patterns due to different render compositions, simulating internal plastering and external rendering in brick masonry when submitted to the same temperature, relative humidity and salt concentration solution. The different specimens show different crystallization patterns. Until the 4th cycle almost no material loss was found, while at the end of 6th cycle there was damage and material loss (exception to CRes, C, C-C and CRes-CRes in which cycles were prolonged until the 8th cycle). The salt crystallization was confirmed both by visual observation during absorption and drying and material loss by the prompt detachment of particles during rising damp and that were accumulated in the solution. Some differences were observed in the crystallization between the different specimens at the end of the 4th and 6th dissolution/crystallization cycles.

Table 5.3 Visual evaluation of specimens' crystallization on the top of the brick and at the outer surface of the render

Cycles	**4th cycle**	**6th cycle**
Specimen L		
		
Mortar	++(L)	+++(L)
Brick	++	++
Specimen L-L		
		
Mortar	++(L)	++++(L)
Brick	+	+++

Table 5.3 (Cont.)Visual evaluation of specimens' crystallization on the top of the brick and at the outer surface of the render

Cycles	4th cycle	6th cycle
Specimen L-LMet		
	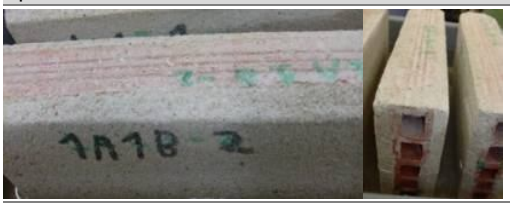	
Mortar	++(L); ++(LMet)	++++(L); +++(LMet)
Brick	++	+++
Specimen L-C		
		
Mortar	++(L); +(C)	++++(L); ++(C)
Brick	+	++++
Specimen L-CRes		
	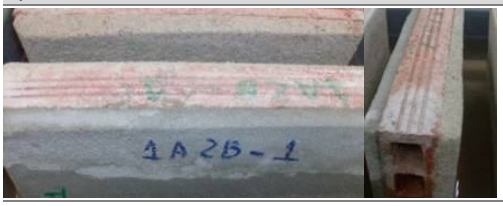	
Mortar	+++(L); -(Cres)	+++++(L); +(Cres)
Brick	++	++++
Specimen LMet-LMet		
		
Mortar	++(LMet)	+++(LMet)
Brick	+	+++
Specimen LMet-C		
	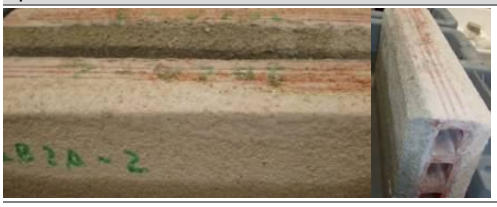	
Mortar	++(LMet); +(C)	++++(LMet); ++(C)
Brick	+	++++

Table 5.3 (Cont.)Visual evaluation of specimens' crystallization on the top of the brick and at the outer surface of the render

Cycles	4th cycle	6th cycle
Specimen LMet-CRes		
	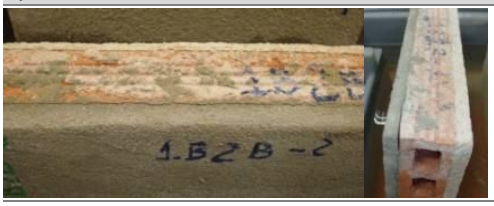	
Mortar	+(LMet); -(CRes)	++++(LMet); +(Cres)
Brick	+++	++++
Specimen C-C		
		
Mortar	++(C)	++(C)
Brick	++	++++
Specimen C-CRes		
	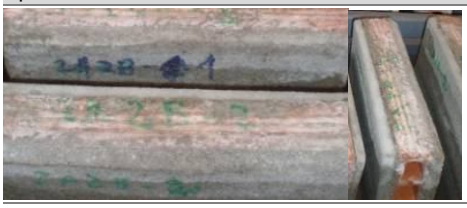	
Mortar	+(C); -(CRes)	++(C); +(CRes)
Brick	++	++++
Specimen CRes-CRes		
		
Mortar	-(CRes)	+(CRes)
Brick	++	++++
Specimen CRes		
		
Mortar	-(CRes)	+(CRes)
Brick	++	+++

**The damage evaluation range: (-) no crystallization; (+) some crystallization located as "hair crystals"/whitening of the surface; (++) crystallization generalized as "hair crystals" (fluffy efflorescence); (+++) dense crust crystallization (powdery efflorescence); (++++) dense crust crystallization associated with sanding; (+++++) dense crust crystallization associated with scaling/crumbling; (++++++) detachment of the render.

On C-C, L-CRes, LMet-CRes, C-CRes, Cres-CRes and CRes, where at least one render coat was based on cement, the salts formed a dense crust on the top of the brick, although salt crystallization variations between the samples did occur, at the end of 6th cycle. In CRes-CRes and CRes specimens almost no salt crystallization can be seen on the surface of the render, while on C-C there was some salt accumulation on the surface. CRes render prevented the salt transport to the surface and caused high crystallization on the top of the brick, at the end of 6th cycle.

On C, L and LMet renders´ surface there was salt accumulation. On samples with CRes render on one or both sides higher crystallization on the top of the brick and/or on the surface of the more permeable renders of the same specimen (C, L and LMet) was observed, probably because the transport through the CRes render was reduced.

On L, L-L, L-Met, L-C, LMet-LMet and LMet-C, salts appear as “hair crystals” at the end of 4th cycle and evolving to dense crust at the end of 6th cycle, on the top of the brick and on the surface of the renders, but some differences can be observed. On the surface of the renders, salt crystallization appears as generalized “hair crystals” at the end of 4th cycle and dense crust crystallization at the end of 6th cycle although for L, L-L, LMet-LMet these crystals were less generalized. On the surface of L-LMet, L-C and LMet-C samples, the salts appear as generalized “hair crystals” at the end of 4th cycle and dense crust at the end of 6th cycle on the upper part of the render, appearing higher than those with the same render formulation on both sides, as L, L-L or LMet-LMet.

5.3.2 Weight variation of specimens during cycles

The weight variation for specimens with at least one render based on lime is reported in Figure 5.5. Some cycles were longer, as in some cases the weekend measures were not made, and the cyles were longer. The constant mass was achieved when constant mass in three consecutive days was found. Until the end of the tests in these specimens (6th cycle) a tendency for weight increase during absorption of NaCl aqueous solution and drying in each cycle, in relation to the previous one, is observed. The absorption/drying tests stopped at the end of the 6th cycle due to the damage observation (detachment of render from the support in some specimens and to the high quantity of material loss in all specimens at this stage).

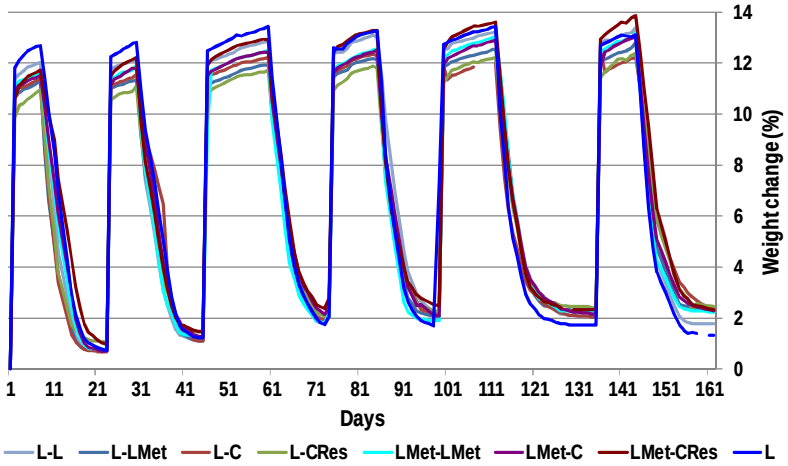

Fig. 5.5 Weight variation (%) of specimens L-L, L-LMet, L-C, L-CRes, LMet-LMet, LMet-C, LMet-CRes, L, during the 6 cycles.

The weight variation for specimens with both renders based on cement is reported in Figure 5.6. Until the end of the tests in these specimens (8th cycle) a tendency for weight increase during absorption and drying in each cycle, in relation to the previous one is observed. This observation can be attibutted to the higher presence of soluble salts on specimens, along each cycle, which retrains the moisture and increases the time needed for complete drying. The absorption/drying tests stopped at the end of the 8th cycle due to the damage observation (high damage degree on the top of the brick was observed, inducing high quantity of this material loss in all specimens at this stage).

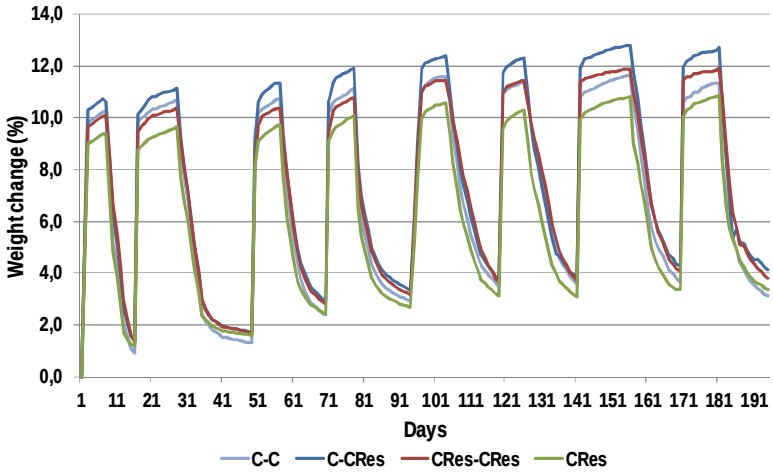

Fig. 5.6 Weight variation (%) of specimens C-C, C-CRes, CRes-CRes, CRes, during the 8 cycles.

Some differences were observed in weight variation (%) in relation to the initial weight among tested specimens:

CRes specimen showed the least weight change; this specimen was rendered only on one side and the properties of the render (extremely impermeable) reduced its salt solution uptake during absorption and evaporation during drying. Considering the whole specimen, the influence of CRes render is not a big influence during drying as one side is not rendered.

The presence of CRes in both sides reduced the absorption and evaporation of the specimen.

L-CRes and LMet-CRes followed the same tendency as CRes-CRes but in lower percentage; when compared with the other specimens, with at least one render based on lime, these specimens show lower weight change at the end of absorption stages and higher at the end of drying stages. Again the presence of CRes render in both specimens influenced the absorption and drying behaviour.

L specimen shows the highest weight change until the 3rd cycle both in absorption and drying; since the 4th cycle the weight variation reduces maybe due to some material loss when compared with the other specimens.

Specimens with cement based render on both sides show lower weight change (%) when compared with specimens with at least one render based on lime.

Quantification of salt crystallization

The increase in salt load (g/kg) in each specimen is presented in Figure 5.7. This quantification was obtained by the weight difference of each specimen between the beginning of the crystallization/dissolution test cycles and the end of each cycle. The crystallization at the end of each cycle is the crystallization in the referred cycle added to the crystallization of the previous cycles. The quantification of crystallization (%) in each specimen until the end of 6th cycle is presented. In specimens C, CREs, C-C and CRes-CRes the salt crystallization quantification was evaluated until the 8th cycle.

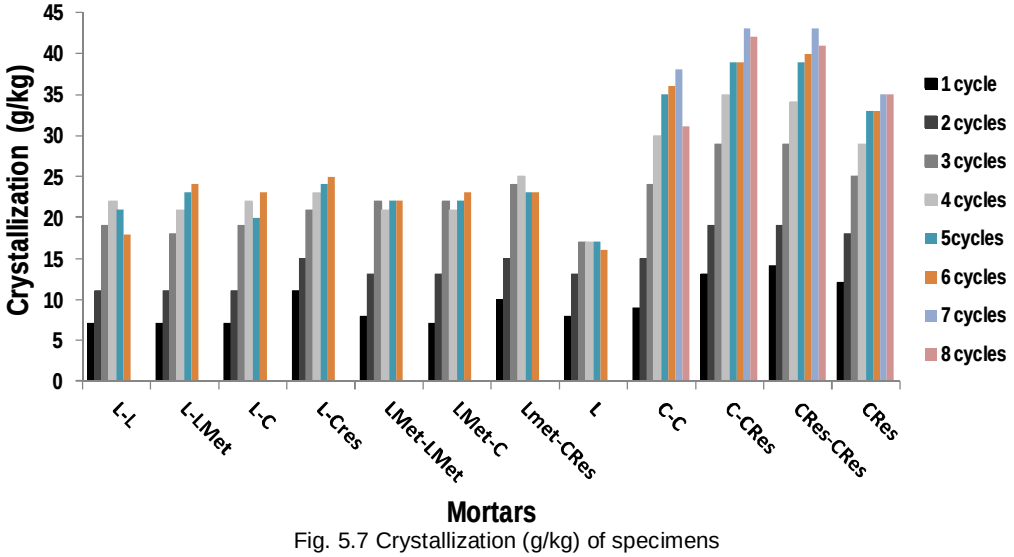

Fig. 5.7 Crystallization (g/kg) of specimens

Some differences were observed in the crystallization % between the different specimens.

An increase in crystallization amount after each cycle was found for all specimens. This increase is higher for specimens with cement based renders in all cycles. The highest difference in crystallization is found from the 2nd to 3rd cycles in all specimens. Specimens with lime based renders on both sides (L-L, LMet-LMet) showed less crystallization in each cycle, than samples with cement based renders on both sides (C-C, CRes-CRes). L-L and LMet-LMet showed a small difference between them at the end of 4th cycle although at the end of 6th cycle the difference is higher maybe due to higher damage in L-L specimens compared with LMet-LMet specimen; for the cement based samples C-C and CRes-CRes, a higher difference between them was found.

At the end of the 6th cycle, specimen L had the lowest crystallization amount followed by L-L specimen; the highest crystallization amount corresponds to CRes-CRes and C-CRes. Among specimens with at least one render based on lime, the highest crystallizations at the end of 6th cycle were found on L-Cres. LMet-LMet, LMet-C and LMet-CRes showed a lower weight gain (even a small weight loss), which is being interpreted as lower crystallization in 6th cycle when compared to the 5th cycle. However, this weight loss was maybe due to some material loss. L and L-L specimens present a decrease in weight, interpreted as some material loss from 5th to 6th cycle. C-C, C-CRes, CRes-CRes and CRes specimens show an increase in weight until the 7th cycle, although in C-C, C-CRes and CRes-CRes specimens a decrease was observed from 7th to 8th cycle. This may be due to some material loss from 7th to 8th cycle.

The results show that lime based rendered specimens show less crystallization amount than cement based rendered specimens. For L-L and LMet-LMet specimens a small difference was found between them, as well as for CRes and CRes-CRes specimens. The highest crystallization amount corresponds to CRes-CRes specimens and the lowest to LMet-LMet specimens.

The higher salt accumulation in specimens with cement based on both sides can be attributed to lower damage of these renders (reducing the detachment of renders particles between cycles); also the higher salt crystallization accumulation at the interface between the support and the render and on the support can be considered (lower salt accumulation on the outer surface was observed – due to salt solution transport reduction - and higher in the support) in these specimens.

According to the Austrian ÖNORM B 3355-1, the salt concentrations are separated into three categories for Cl^-: < 0.03% weight (< 300 mg/kg) – no risk; 0.03 - 0.10% weight (300 – 1000 mg/kg) – individual evaluation necessary and > 0.10% weight (> 1000 mg/kg) – active salt removal advised. All renders in specimens show higher concentrations than the limit of risk from the ONORM (300 mg Cl/kg) and active salt removal is advised since the 2nd cycle. The application of eletrokinetic treatment for Cl removal could be a possible option, in order to remove its content as well as inherent damage.

5.3.3 Damage evaluation six months after the end of the cycles - specimens

After experiments, the specimens were left in a non conditioned room, since May until September. Although specimens were not submitted to salt crystallization tests anymore, there was evolution on salt crystallization observed after this period (Table 5.4). The presence of relative humidity and temperature cycles may be the origin of the increase in salt crystallization observed, both in render and brick. The ambience relative humidity (RH) varies around 40% and 80% (see chapter 7).The RH of equilibrium of NaCl at 20ºC is 75.5% [Arn87]; although the presence of two or more salts and their simultaneous presence affects their individual solubility, as referred by Charolla [Cha00]: i) if the salts do not have any ions in common (as can be the case of sodium chloride and calcium sulphate dehydrate–gypsum) the solubility of both salts increase, ii) if the salts have an ion in common, such as sodium sulphate and sodium sulphate, solubility of both will decrease.

Table 5.4 Visual evaluation of specimen's damage six months after the end of the cycles

Damage evaluation			**Detail of salt crystallization in the most permeable render of each specimen**
Specimen L			
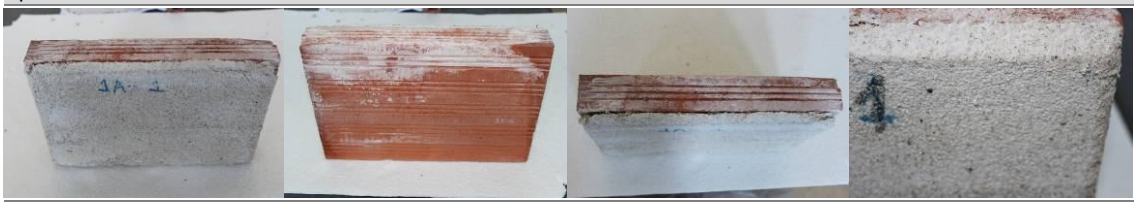			
(L) ++++/+++++++ (detachment of the render in one specimen)	(Brick) +++	(Top brick) +++	
Specimen L-L			
			
(L) +++++/++++++ (detachment of the render in one side of both specimens)		(Top brick) ++++	
Specimen L-LMet			
			
(L) +++++	(LMet) ++++	(Top brick) +++	

Table 5.4 (Cont.) Visual evaluation of specimen's damage six months after the end of the cycles

Damage evaluation			**Detail of salt crystallization in the most permeable render of each specimen**
Specimen L-C			
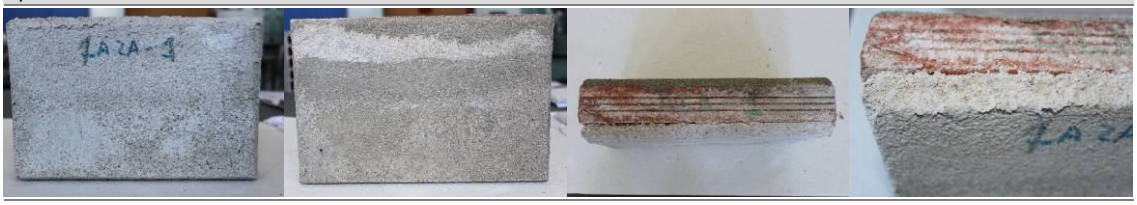			
(L) +++++/++++++ (L render was detached in one of the specimens)	(C) +++	(Top brick) +++++	
Specimen L-CRes			
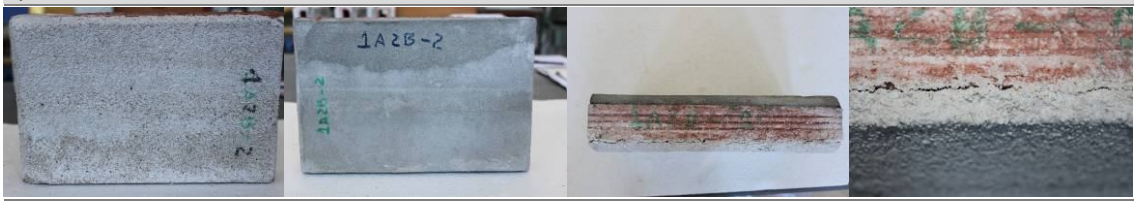			
(L) +++++	(CRes) +	(Top brick) +++++	
Specimen LMet-LMet			
	-		
(LMet) ++++		(Top brick) +++	
Specimen LMet-C			
			
(LMet) ++++	(C) +++	(Top brick) +++++	
Specimen LMet-CRes			
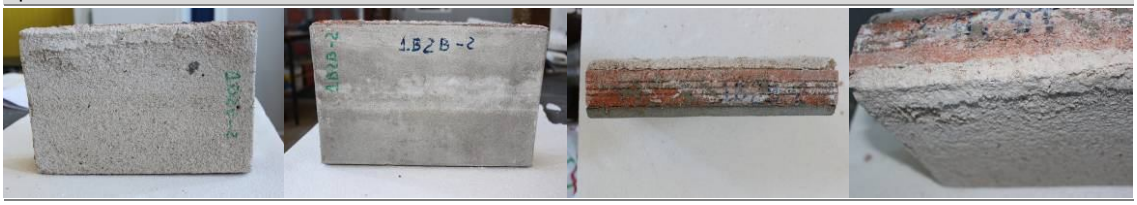			
(LMet) +++++/++++++ (L+(CRes) render was detached in one of the specimens)		(Top brick) +++++	

Table 5.4 (Cont.) Visual evaluation of specimen's damage six months after the end of the cycles

Damage evaluation			**Detail of salt crystallization in the most permeable render of each specimen**
Specimen C-C			
		 	
(C) +++		(Top brick) ++++++	
Specimen C-CRes			
		 	
(C) +++	(CRes) +	(Top brick) +++++	
Specimen CRes-CRes			
		 	
(CRes) +		(Top brick) ++++++	
Specimen CRes			
		 	
(CRes) +	++++	(Top brick) ++++	

* All specimens were tested until the 6th cycle, due to their damage, with detachment of the lime based render from the support, exception to C-C, C-CRes, Cres-CRes, CRes (until 8th cycle)
**The damage evaluation range: (-) no crystallization; (+) some crystallization located as "hair crystals"/whitening of the surface; (++) crystallization generalized as "hair crystals" (fluffy efflorescence); (+++) dense crust crystallization (powdery efflorescence); (++++) dense crust crystallization associated with sanding; (+++++) dense crust crystallization associated with crumbling; (++++++) detachment of the render.

An increase in salt crystallization was observed at the outer surface of the specimens, when compared with the evaluation at the end of the 6th cycle, especially in the most permeable render and top of the brick in each specimen (table 5.4).

In specimens L, L-L, L-C, LMet-CRes the lime based render was completely detached and fell from the support at least in one of the specimens; in specimens L-CRes, LMet-LMet, LMet-C, LMet-CRes the detachment of lime based render from the support was observed, although absence of render was not observed in any of these specimens (Table 5.5).

Table 5.5 Visual observation of render detachment of lime based renders six months after the end of the cycles

Specimen L	Specimen L-L	Specimen L-C	Specimen LMet-CRes
			
Detachment in one specimen	Detachment in both specimens	Detachment in one specimen	Detachment in one specimen
Specimen L-LMet	Specimen L-Cres	Specimen LMet-LMet	Specimen LMet-C
			
Detachment observed in both specimens			

Another interesting observation was the presence of high quantity of salt efflorescences as “fluffy efflorescence” in L-L specimen. In this specimen the detachment of the outer layer occurred at the end of the tests. The presence of NaCl salts in the support as well as on renders surface due to salt solution absorption and the relative humidity flotation in the non-conditioned room contributed to this (Figure 5.8).

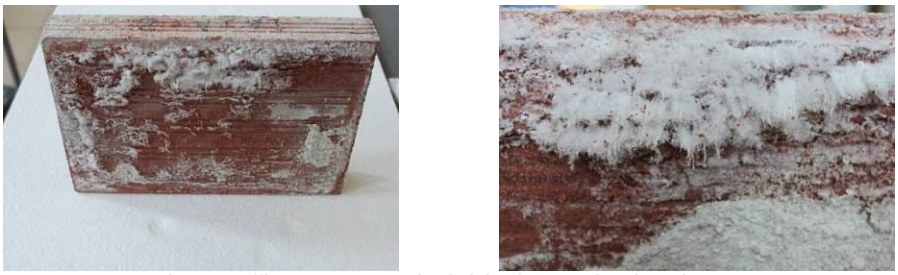

Fig. 5.8 Efflorescence on the brick after render detachment

In NaCl contaminated specimens the relative humidity changes, even in the absence of any other moisture source, and it was observed to cause an increase on salt accumulation in the outer surface. This phenomenon was investigated by Lubelli [Lub07],who observed that if salts having a RH of crystallization in a range easily crossed by the air RH, induces salts accumulation just beneath the surface of the material: i) RH changes through the RH of crystallization, may dissolve and re-crystallize the salts in the pores of the material causing damage and ii) the hygroscopic effect due to RH changes is clearly increased by the presence of salt near the surface.

5.4 Classification of render systems – working principle and performance

Taking into consideration the analyses of the results obtained in this chapter on tested specimens, a classification of the render systems in terms of durability classes based on the occurrence of the first signs of damage (such as cohesion loss or detachment on render and on support) as a classification parameter referred by Rodrigues [Rod07], was implemented and adapted to this work.

In table 5.6 the classification of each tested specimen is described, taking into consideration the working principle (transporting, accumulating, blocking and sealing) and performance (no decay, slow decay, moderate decay and fast decay) and considering the influence of the whole system (render+ perforated brick). The support was also visually evaluated to understand the influence of different render mixes on salt accumulation on the support (brick).

Table 5.6 Classification of tested specimens under the severe action of salt laden water (NaCl absorption and drying)

Render solution	Render (side A)	Support	Render (side B)
L	L - Transporting (moderate)	Transporting (slow)	-
L-L	L - Transporting (moderate)	Transporting (slow)	L - Transporting (moderate)
L-LMet	L - Transporting (moderate)	Transporting (slow)	LMet - Transporting (slow)
L-C	L - Transporting (moderate)	Transporting (moderate)	C – Transporting (no decay)
L-CRes	L - Transporting (fast)	Transporting (fast)	CRes – Sealing
LMet-LMet	LMet - Transporting (slow)	Transporting (slow)	LMet - Transporting (slow)
LMet-C	LMet – Transporting (moderate)	Transporting (moderate)	C - Transporting (no decay)
LMet-CRes	LMet - Transporting (fast)	Transporting (fast)	CRes - Sealing
C-C	C - Transporting (slow)	Transporting (fast)	C - Transporting (slow)
C-CRes	C - Transporting (slow)	Transporting (fast)	CRes – Sealing
CRes-CRes	CRes – Sealing	Transporting (fast)	CRes - Sealing
CRes	CRes - Sealing	Transporting (moderate)	-

The use of renders with different permeability properties, especially in the cases where one side is lime based (L-C, L-CRes, LMet-C, LMet-CRes), increases solution transport through the highly permeable materials - lime based renders (L and LMet) and the support; in this case reduced transport is observed in the less permeable renders (C and CRes) and even less in CRes.

Although less permeable than lime renders, the render C (cement based) allows some transport of salt solution, but increases the decay of the highly permeable materials. This may be enhanced by the introduction of new soluble salts in the system (namely sulphates) that, when mixed with sodium chloride, may increase the decay [Cha00] of the more permeable renders; the less permeable render CRes, besides introducing also soluble salts, works like moisture sealing preventing the solution transport and induces the faster decay of the more permeable materials (lime based renders and the support).

5.5 Discussion and conclusions

The present experimental work demonstrates that accelerated dissolution/crystallization cycles with sodium chloride, favour the accumulation of NaCl salt efflorescence on the render and/or on the top of the brick representing the masonry. The observations allowed the assessment of crystallization and damage patterns, under the same conditions, on specimens when different render compositions are present, simulating internal plaster and external render. The work presented demonstrates that dissolution/crystallization cycles of NaCl produce different damage patterns due to salt crystallization, depending on specimen composition and renders permeability.

The render mixes were seleted from a previous study [Vei10a], where several renders (including these ones) were compared concerning their viability to be used as substitution renders in historic buildings masonry, taking into consideration the general quantified requirements (concerning some characteristics for rendering substitution mortars for ancient buildings).

The visual evaluation of specimen's surface crystallization and the crystallizations quantification give coherent results. The highest crystallization was observed on the brick for CRes-CRes and C-CRes specimens. Apparently Cres render acts as a barrier for NaCl aqueous solution transport, restricting the evaporation of the water through render and inducing higher crystallization on the top of the brick, where the evaporation occurs. This behaviour indicates a tendency of cement renders of lower permeability, especially when additive with a resin (CRes) render, to favour crystallization in the support (brick) and as result, in real cases, increasing damage inside the wall (see chapter 2). On medium permeable specimens C-C, cement based but more permeable than CRes-CRes, a high tendency for salt crystallization in the support (brick) was observed as well as in the render, so NaCl solution was allowed to be transported through the render. The coexistence of soluble sodium chlorides from solution and soluble alkali-carbonate salts from the cement based renders may even have intensified the effects, increasing the damage especially on the brick due to salt crystallization. This was also present in L-C and LMet-C specimens, increasing the damage due to salt crystallization on the support (brick) and on more permeable renders of those systems, L and LMet. The specimens with highly permeable renders L, L-L and LMet-LMet, concentrated crystallization on the render, preventing damage in the support (brick).

From these investigations, the following conclusions can be drawn:

- Relevant differences were found in final salt distributions between specimens with cement based render (less permeable) and lime based (permeable) render. Generally, for more permeable specimens there is a similar distribution of salts on the surface of renders and on top of the brick; for less permeable specimens there is a higher salt concentration on the top of the brick when compared to the render's surface. The specimens with high heterogeneity (more or less permeable renders) between the internal plaster and external render, simulating a old masonry with

replacement cement renders and lime based plasters and/or partial replacements of lime based renders by cement renders, show the highest damage, namely those rendered on one single side, and those with a lime render (L or LMet) on one side and CRes on the other.

- These results point to the conclusion that highly permeable renders are to be preferred in the conservation of old walls, considering that the objective is to increase the durability of the masonry, to the detriment of the render if necessary. These renders should therefore be more favourable in protecting old masonry from NCl salt damage where rising damp is prevalent. Based on the concluded above and from the results obtained it seems that in field (considering that 27 g/l is the NaCl content of the Atlantic ocean, see chapter 2): i) using less permeable renders (cement based) as partial substitutions can increase the solution transport in the pre-existant highly permeable renders (lime based) resulting in their higher damage due to salt crystallization (Fig. 5.9); ii) in case of using of less permeable substitution renders and highly permeable substitution plaster could result in higher solution transport through the highly permeable plaster as well as its accumulation in the very thick old masonry, since the solution transport through the less permeable renders could be inhibited, increasing the damage in the masonry as well as in the plasters; iii) if the render adopted shows high permeability and the plaster less permeable properties, the opposite happens and highest damage is supposed to be observed in the render. It is important to refer that: iv) in the interior spaces it is easier to control the temperature and relative humidity conditions that may control the evaporation through the internal plaster and inherent damage on it; v) in the exterior it is difficult to control the evaporation rate as the wall could be exposed to sun radiation and high changes in relative humidity and may result in high damage, in the highly permeable exterior renders due to salt crystallization within the render; in case of using less permeable renders damage can happen mainly at the interface between the render and the masonry, where the drying front occurs, induced by salt crystallization.

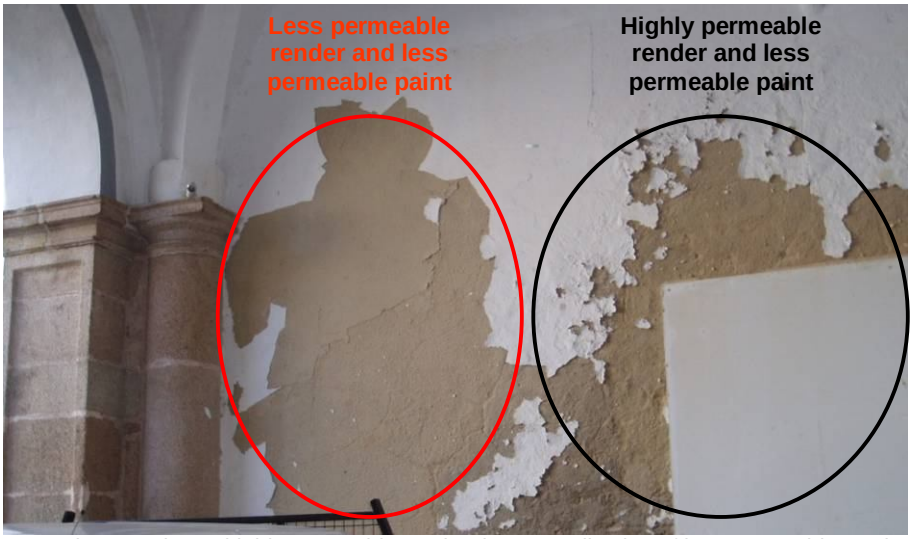

Fig. 5.9 Damage in pre-existent highly permeable render due to application of less permeable render and paint (a panel was used for hiding the anomalies above the pre-existent render)

- The specimens specially designed for this experimental work were able to simulate masonry with internal plaster and external render; although the specimens were not sealed in the lateral and upper sides, due to the difficulty on doing that when using perforated bricks. This prelimary study concerning the crystallization and damage patterns and its evolution is crucial for their understanding in rendered masonry. With the adopted testing methodology, the main differences in crystallization, considering a whole system (brick masonry + render more or less permeable), could be understood and could be implemented in the following chapters (Chapter 6 and 7) when developing a substitution render system, “ventilated render”, for old buildings masonries when submitted to the severe action of salt laden water.

With this preliminary work, it was possible to define small scale specimens able to simulate a rendered brick masonry; however, improved small scale specimens, where evaporation from the upper and lateral sides is prevented, are considered necessary, and used in the next chapter. It was also possible to develop dissolution/crystallization cycles able simulating the effects of the severe action of water in the specimens, that are used in chapter 6 for the design and development of ventilated render system from Fradical,

6. DEFINITION OF A SUBSTITUTION RENDER SYSTEM: "EMBOÇO VENTILADO"- LABORATORIAL WORK

6.1 Introduction

There are several factors that can contribute to crystallization damage in porous building materials: environmental conditions, type of salt, substrate nature, moisture conditions or the presence of paint layers, or water repellent mixed in mortars used for rendering.

Several studies are being performed concerning the development of replacement accumulating renders, especially for salt loaded masonries [Gon07, Pet10a, Pet10b, Hui07]; the basic principles of these kind of renders are: i) preventing water and salt accumulation at the surface and ii) alowing salt accumulation in the base layer with bigger porosity, in order to allow salt crystallization without damage (see chapter 2).

The present research is undertaken with the aim of investigating the behaviour of renders of a wall exposed to salt crystallization. The main objective is to design and develop a durable, efficient and compatible render, "ventilated render" ("emboço ventilado" in Portuguese) from Fradical, for historic constructions when submitted to the severe action of salt laden water which is defined by the presence of high moisture supply (namely rising damp) and high salt content (namely NaCl) [Fra13a].

To avoid damage in the substrate when moisture and soluble salts are present, the substrate should dry faster than the render [Hui07]. In an accumulating system based on a two layer render system applied on a substrate, the base layer should have smaller pores than the substrate and the outer layer wider pores than the substrate due to the drying behaviour in the absence of salts [Hui07]. The problem is that in the presence of salts the drying capacity changes and the accumulating performance of the render system becomes lower, so that the system acts as a transporting system allowing salt crystallization in the outer layer and preventing this outer layer to dry fully.

Some studies [Gon07, Pet10a, Pet10b, Hui07] show that salt accumulating renders could be achieved by applying a water repellent agent in the outer layer, thus preventing water and salt transport to the surface and so favouring salt accumulation in the base layer with bigger porosity; although it may show as main disadvantage the reduction of support moisture evaporation (see chapter 2).

Environmental Portuguese conditions can show an average of values between 40% of RH until 90% of RH, or more, along the year (see chapter 7) and also have high variation during day/night. Based on these observations, when rising damp and soluble salts (severe action of water) are

present, the execution of grooves in base layer may allow "dry" air to circulate inside them and allows moisture evaporation from support and base layer, inducing salt crystallization in the grooves. This is the main principle that served as base for ventilated render system design.

The render layer with water repellent mixed in the mortar was selected from previous studies from Fradical [Mag08a, Mag06a] (see chapter 2).

The experimental work, concerning the design and development of "ventilated render" was developped on six different small scale specimens executed using traditional solid bricks covered on both sides, with different renders. Four renders, intended to work as accumulation renders, where salts are wanted to be able to accumulate in the grooves of base layer. The render/plaster systems were tested in combined plaster-brick-render specimens in order to enable a reproduction of real situations and to verify degradation on the interfaces.

In this chapter, an experimental program based on dissolution/crystallization cycles with NaCl solution is described (see chapter 5), which was performed in order to investigate: i) the performance of the six different render systems executed in traditional brick in relation to NaCl crystallization, evaluating the damage patterns and salt accumulation; ii) the influence of the vertical grooves in the base layer and water repellent mixed in the mortar of the outer layer, on the damage patterns and location of salt accumulation; iii) the adequacy of the render systems with different working principles to different practical situations.

The reliability of the dissolution crystallization cycles (environmental tests) used in the experimental program has been assessed comparing the damage patterns obtained with situations observed in case studies (chapter 3). This research has been focused on the effects of absorption and drying tests on the salt distribution in the several layers of the render/plaster systems and in the location of NaCl crystallization.

Chapter layout

In this chapter the research on the small scale render solutions is presented. The selection and characterization of materials composing the render systems and render systems execution are presented in section 6.2. The salt crystallization test procedure is described in section 6.3. The results obtained on decay patterns are presented and discussed in section 6.4: pull off tests on render systems after testing in section 6.4.1 and decay patterns on outer surface by visual observation and optical microscope (M.O.) investigation in section 6.4.2; the location of salt crystallization is discussed on section 6.4.3 and the results of chlorides quantification is discussed in section 6.4.4. In section 6.5 are deeply studied the selected render systems from section 6.4: in section 6.5.1 the chlorides content are quantified; in section 6.5.2 the location of salt crystallization is deeply investigated by ESEM investigations; the influence of pore characteristics on salt uptake and distribution is discussed on section 6.5.3. In section 6.6 the render systems classification,

based on working principle and performance, is presented. An overall discussion focusing on the conclusions related to the objectives of the research, in this phase, is presented in section 6.7.

6.2 Materials

The experimental study described in the following sections was carried out at the Wall Covering Laboratory of the National Laboratory of Civil Engineering (LNEC) in Lisbon. The render systems (composed by one or more layers with different mortars compositions) developed in this chapter were developed to resist salt loaded substrates in high humidity conditions; they have been developed in cooperation with Fradical Lda company [Fra10e].

Selection and characterization of mortars materials

The composition of the improved studied mortars from Fradical is described in Table 6.1.

Table 6.1 Mortars composition

Mortars	Composition	Volumetric dosage*
F1	Lime putty; pozzolanic addition; mixture of medium and fine size calcareous sand	1:0.2:(3+1)
F2	Lime putty; pozzolanic addition and other admixtures; mixture of medium and fine size calcareous sand	1:0.4:(3+1)
F6	Lime putty; pozzolanic addition and other admixtures; mixture of medium and fine size calcareous sand	1:0.5:(3+1)
F7	Lime putty; pozzolanic addition and other admixtures; brick powder and medium size calcareous sand	1:0.5:(1+3)
F8	Lime putty; pozzolanic addition and other admixtures; brick powder and mixture of medium and fine size calcareous sand	1:0.5:(1+2+1)

* Volumetric dosage in relation to the binder.

In this study two calibrated calcareous sands were used (medium and fine), mixed in order to obtain a particle size distribution similar to siliceous river sand commonly used in renders in Lisbon region (Tagus river sand). The granulometric curves of the sands studied (medium sand, fine sand, two different mixtures of medium and fine sands - in volumetric proportions 2:1 and 3:1 respectively - and the Tagus river sand, for comparison) are presented in Fig. 6.1.

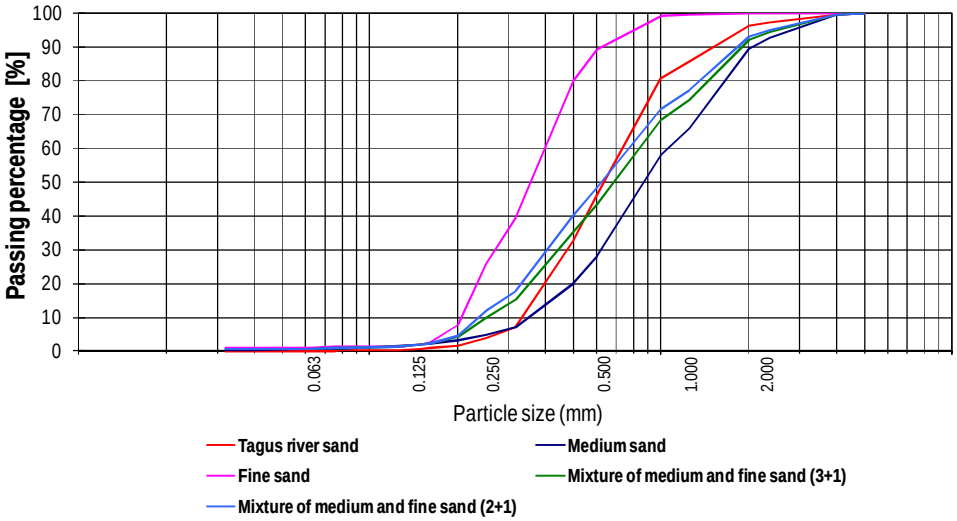

Fig. 6.1 Granulometric curves of sands used on mortars

As described in table 6.1 different mixtures of calcareous sands were selected and different volumetric dosages were used: in F1, F2 and F6 mortars formulations the sand mixture of 3+1 (medium: fine) was used, showing the most similar particle size distribution to siliceous river sand; in F7 and F8 mortars formulations, as brick powder was added and may act as a filler rather than as a pozzolan, sand 3 (medium) and the sand mixture 2+1 (medium+fine) respectively were used.

The restriction of the extraction of sand from rivers, due to environmental reasons, and the great availability of aggregate, proceeding from limestones quarries, makes from calcareous sand a serious alternative [Fra10e]. The substitution of siliceous aggregates by calcareous aggregates in air lime mortars generally tends to improve mortar mixes mechanical characteristics [Fra10e], thus it is a potential good solution. In addition some works reports that calcareous aggregate shows chemical affinity with lime binder and it has been found in durable ancient mortars [Ste05c].

The studied mortars were prepared and mixed according to standard procedures (EN 1015-2), and cured according to the conditions specified by EN 1015-11. The laboratory characterization performed to evaluate the main mechanical and physical characteristics of the studied mortars included: 1) compressive strength (Rc) and flexural strength (Rt), based on EN 1015–11 methods; 2) elastic modulus (E), determined by resonance frequency method following French standard NF B10-511 (1975); 3) water absorption coefficient due to capillary action (C), based on EN 1015-18 method; and 4) water vapour permeability based on EN 1015–19 method and expressed by the thickness of the air coat of equivalent diffusion (Sd). The water absorption curve following EN 1015-18 method was also determined for each mortar material, as well as the drying curve. These tests are illustrated in Figures 6.2-6.6.

In the graphics results the maximum and minimum limits according the general requirements defined by LNEC, concerning some characteristics for rendering and repointing substitution mortars for ancient buildings, aged 90 days, are shown [Vei04a].

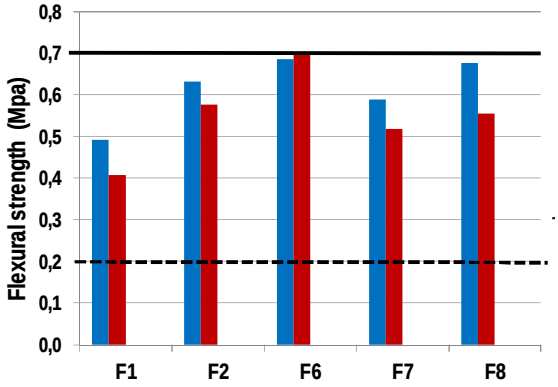

Fig. 6.2 Flexural strength of render mortars (MPa).

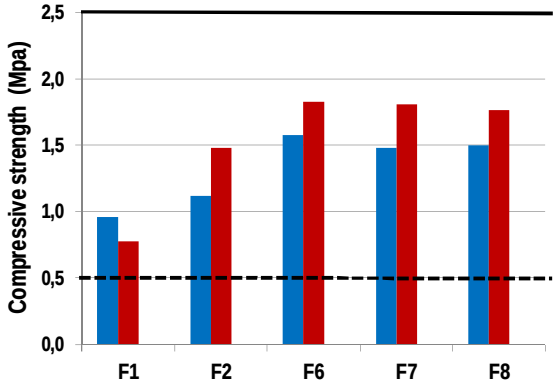

Fig. 6.3 Compressive strength of render mortars (MPa).

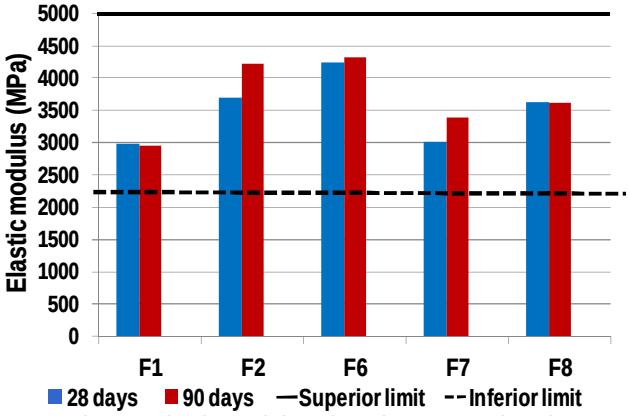

Fig. 6.4 Elastic modulus of render mortars (MPa).

All formulations show similar flexural and compressive strength, although mortars with higher percentage of pozzolanic addition (F6, F7 and F8), corresponding to 0.5 in volume in relation to binder, show somewhat higher flexural and compressive strength, compared with the other formulations. The addition of brick powder does seem to improve mechanical characteristics of mortars until the 90 days. However the addition of brick powder may contribute to high water retention [Hees12] that could be favourable for the pozzolanic reaction and increase the resistance of the renders, mainly at later ages.

Lower flexural and compressive strength was found on mortars with lower percentage of pozzolanic addition corresponding to 0.2 in relation to the binder and without brick powder (F1 and F2), although the addition of other admixtures in F2 mortar contributed to a slight increase of mechanical resistance.

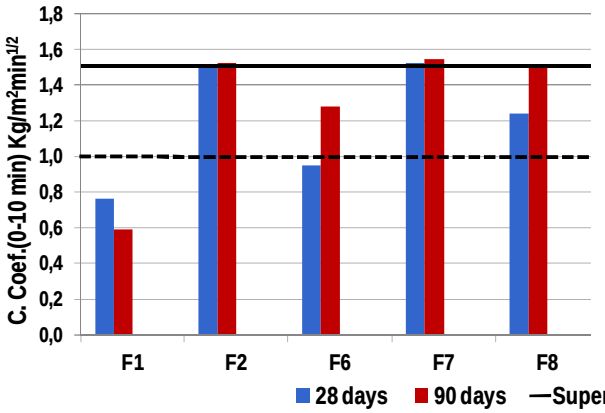

Fig. 6.5 Water capillary coefficient of render mortars (0-10 min).

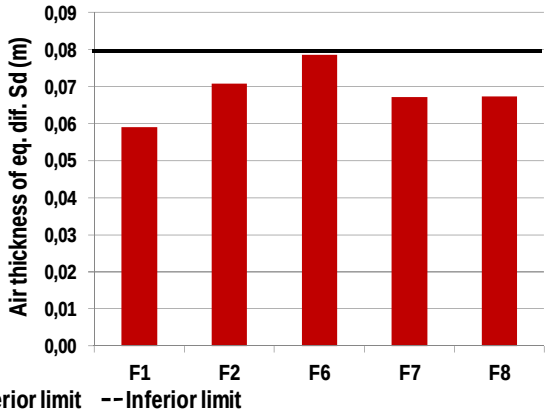

Fig. 6.6 Water vapour permeability.

The highest capillary coefficient was observed in F2, F7 and F8 mortars (Figs.6.5 and 6.6).

All mortars show flexural and compressive strength and water behaviour comprised in the interval of limits according the general requirements defined by LNEC, concerning some characteristics for rendering and repointing substitution mortars for ancient buildings, at 90 days.

The water absorption and drying at 28 and 90 days is represented in Figures 6.7 and 6.8. F7 mortar attains the highest absorption both at 28 and 90 days of curing, and F1 the lowest. The intitial water absorption at 5 minutes was not measured.

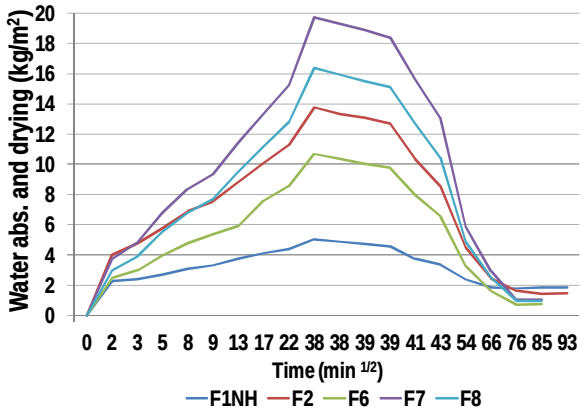

Fig. 6.7 Capillary water absorption and drying after 28 days curing.

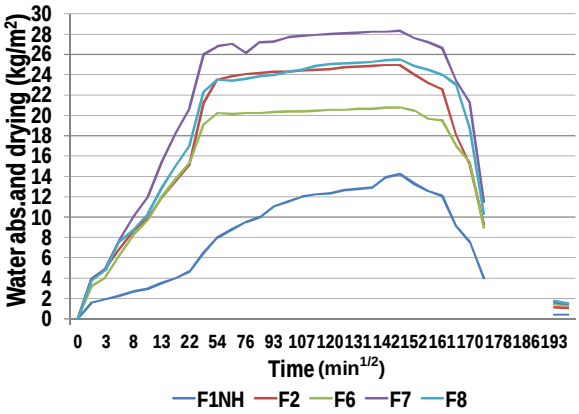

Fig. 6.8 Capillary water absorption and drying after 90 days curing.

Considering these results all mortars are according to the general requirements defined by LNEC. F6 and F8 are too close the upper limit for flexural strength and F6 is very near the limit defined for water vapour permeability. From the studied mortars F1, F2 and F7 were the ones selected to be used in render systems execution.

Render systems

The composition of the render systems was based on the results of the experimental program on Fradical Lda. new mortars formulations (F1, F2, F6, F7 and F8) in this chapter, as well as on

results obtained from small specimens with extreme render characteristics (L, LMet, C and CRes) (see chapter 5).

Six different render systems were defined to be used: four with vertical grooves in the base layer (FH7, FNH7, FNH2 and FNH1) and two without vertical grooves in the base layer (NH7 and NH1) (Fig. 6.9). After executing the grooves a glassfibre mesh (2 mm x 2 mm) was applied to avoid filling the grooves and enable the adherence between base and outer layer. The composition of the different render systems studied is summarized in Table 6.2.

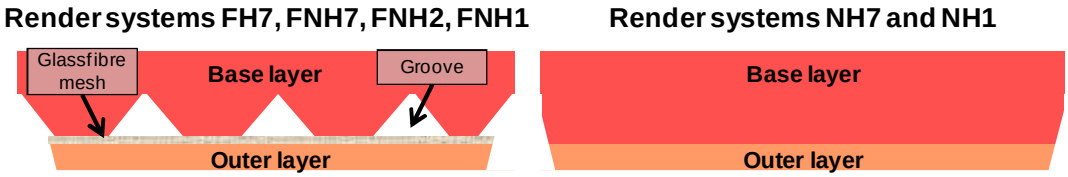

Fig. 6.9 Schematic representation of the render systems (upper view)

Table 6.2 Composition of the render systems

Render system*	Base layer (mortar)	Existence of grooves	Layer between internal and external layer (mortar)	External layer (mortar)
FH7	F7	yes	Lime putty and fine sand	F1h
FNH7	F7	yes		F1
FNH2	F2	Yes		F1
FNH1	F1	Yes		F1
NH7	F7	No	-	F7
NH1	F1	No	-	F1

*Render system codes: F – with grooves; H – water repellent additive in outer layer; NH – without water repellent additive in outer layer; 7 – F7 mortar mix in base layer; 2 – F2 mortar mix in base layer; 1 – F1 mortar mix in base layer.

F1h is a pre-dosed lime based mortar with water repellent from Fradical Lda. [Mag08b, Mag06b, Oli06a].

The six render systems, described in Table 6.2, were designed mainly to understand the influence of grooves in base layer and water repellent additive in outer layer. Three different mortar mixes (F1, F2 and F7) were considered in base layer (with grooves) in order to understand which one is more efficient on salt solution transport until the grooves where evaporation is expected to happen, resulting in salt crystallization within the grooves. F7 mortar mix was especially design for this work: brick powder addition is referred in the literaterature to favour mortars water retention [Hees12] and the mortars resistence can be improved, as it also has a pozzolanic effect [Fra13a, Vel06a] (see chapter 2).

Specimen's composition and preparation

The tested specimens were improved in relation with those used in the preliminary testing campaign and consisted of red solid bricks (traditional bricks) covered on both larger sides with

different render systems, to simulate internal plaster and external render on brick masonry; they were sealed on upper and lateral sides with a commercial waterproofing paint, to prevent evaporation and improve unidirectional migration of moisture. A specimen without render systems was also used. Three specimens of each type were tested.

In Table 6.3 the composition of the studied specimens is presented, and in Fig. 6.10 is presented a schematic representation of these specimens that were submitted to accelerated salt crystallization tests in laboratory. The render systems in specimens were carefully executed (see render systems application and execution in see chapter 7) in order to reduce problems during testing, which could be related to inadequate workmanship (Figs. 6.11 and 6.12).

Table 6.3 Composition of the tested specimens

Specimen	Render system (Side A)	Render system (side B)
T	-	-
FH7	FH7	NH1
FNH7	FNH7	NH1
FNH2	FNH2	NH1
FNH1	FNH1	NH1
NH7	NH7	NH1
NH1	NH1	NH1

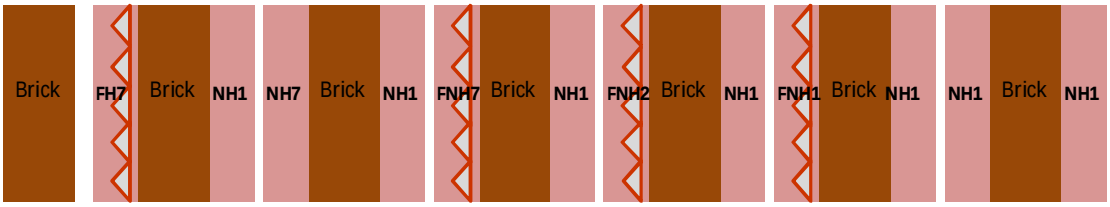

Fig. 6.10 Schematic representation of the tested specimens (upper view)


Fig. 6.11 Execution of the render system with vertical grooves (left); Final appearance of render system with vertical grooves (right)

Fig. 6.12 Execution of render system without vertical grooves (left); Final appearance of render system without vertical grooves (right)

The ventilated render systems (executed with vertical grooves in base layer, namely FNH7, FH7, FNH1 and FNH2) are two-layer render systems (base and outer layer) and were designed to act as transporting systems in which the salts were supposed to crystallize in the vertical grooves of the base layer and not in the substrate or in the external layer. The other render systems without vertical grooves (NH7, NH1) were designed to allow comparison in terms of crystallization location habits and damage patterns evolution.

The specimens were cured under conditions of 20°C and 65% relative humidity and were sprayed with water twice a day during the first 5 days of curing. After 3 months curing the specimens were dried in a ventilated oven at 60 °C until constant mass and then they were left to equilibrate in a conditioned room (20 °C and 65% RH).

Specimen's absorption and drying behaviour

Before testing the specimens were characterized in terms of absorption and drying behaviour. In the first stage specimens were submitted to one cycle of capillary rise with tap water, by partial immersion in 1 cm of water and afterwards they were let to dry in the same conditions (20°C and 65% RH) (Figs. 6.13 and 6.14).

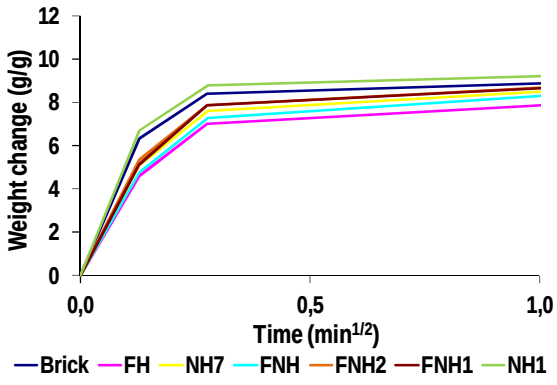

Fig. 6.13 Partial immersion of specimens on tap water

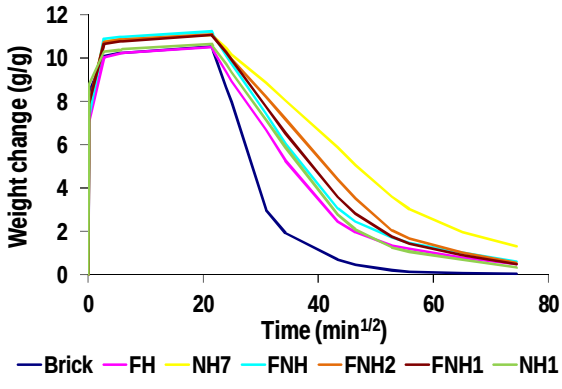

Fig. 6.14 Drying of specimens

The highest initial absorption was found for brick and NH1 specimens and the lowest for FH specimen. At the end of the absorption stage (when the weight of the specimen remained constant)

the highest absorption was found for NH7, FNH and FNH1 and the lowest for brick and FH specimens.

The fastest drying was found on brick specimen and the lowest on NH7 specimen. The NH7 specimen behaviour may be attributed to the presence of brick powder that easily absorbs water but slowly releases this water.

6.3 Simulating the severe action of salt laden water on the systems

Salt crystallization test procedure

In the second stage, the specimens were contaminated with NaCl solution (concentration 27g/l – similar to sea water content [Aug90]) in the same temperature and relative humidity conditions – by partial immersion to allow capillary rise through the specimens, reproducing in the laboratory, typical rising damp conditions, during several cycles (Fig. 6.15). Once they got constant weight, in each cycle, the specimens were dried. To speed up the drying they were left in a ventilated oven at 60°C during a week (Fig. 6.16) and then they were subjected again to partial immersion cycles in NaCl solution). In each cycle the wetting and drying phases were prolonged until constant mass of the specimens was attained. The test stopped when damage in the plaster was found or after 8 dissolution/crystallization cycles. The samples were not brushed between cycles.

Fig. 6.15 Partial immersion of specimens on NaCl solution


Fig. 6.16 Drying of specimens on the ventilated oven

6.4 Effect of the severe action of salt laden water on the systems - damage evaluation due to salt crystallization

The observation of the damage evolution in practice is crucial for the understanding of the damage mechanism in renders. The damage was evaluated by visually monitoring of the salt crystallization and decay of the tested render systems.

The salt crystallization was evaluated by means of optical microscope observations, SEM observations, and chlorides quantification. The specimens were subjected to

dissolution/crystallization cycles without brushing between cycles, to check the damage and evaluation of the salt distribution and study the crystallization and damage patterns in the material's structure of the renders at different time intervals during the test.

The survey of render systems, in this chapter, is divided in two stages. In the 1st stage, render systems decay patterns were evaluated by visual observations and the location of the salt crystallization was evaluated by optical microscope observations, both at the end of 4th, 6th and 8th dissolution/crystallization cycles. The chlorides quantification was also made for all render systems on the 4th cycle. Based on the results obtained, the best render systems to be used as substitution render on salt loaded substrates were defined at the end of this stage.

In a 2nd stage of the investigation a deeper study was made on selected render systems by means of SEM investigations and chlorides quantification. The ESEM investigation was only made after the 4th cycle of dissolution/crystallization due to the damage of the samples removed after the 4th cycle and the difficulty associated to the observation (after the 4th cycle the samples were too much damaged to be investigated by means of SEM).

6.4.1 Pull off test on specimens

At the end of the 4th dissolution crystallization cycle, pull off tests were performed following EN – 1015-12:2000, to evaluate the type of rupture and if it happened between the outer layer of render systems and the base layer (FH7, FNH, FNH2 and FNH1 specimens) or between the render and the support (NH7 and NH1 specimens). Pull off tests were performed at the end of the 4th dissolution/crystallization cycle due to loss of cohesion of outer layer in almost all specimens observed since this stage, that made the execution of the test in a later stage more difficult. The tests were carefully executed and specimens had to be adapted; a wood base for their support (a especially developed structure) was designed to perform the tests on these singular specimens in order to allow the pull off tests without damaging the render system on the opposite side of the tested render (Fig. 6.17).

Fig. 6.17 Pull off tests on render systems: a)preparation of specimens (left) b) application of specimens in the wood structure for pull off tests (middle) and c) pull off test (right)

In Table 6.4 the type of rupture in the render system of each specimen is described.

Table 6.4 Visual observations of the rupture in each of the render systems after 4 dissolution/crystallization cycles

Specimen FH7	
Render system FH7	
Evaluation: Adhesive rupture (rupture occurred between outer and base layer)	
Specimen NH7	
Render system NH7	
Evaluation: Adhesive rupture (rupture occurred between render system and the support)	
Specimen FNH7	
Render system FNH7	
Evaluation: Cohesive rupture (rupture occurred in the outer layer)	
Specimen FNH2	
Render system FNH2	
Evaluation: Adhesive rupture (rupture occurred between outer and base layer)	
Specimen FNH1	
Render system FNH1	
Evaluation: Adhesive rupture (rupture occurred between outer and base layer)	

Table 6.4 (Cont.) Visual observations of the rupture in each render system after 4 dissolution/crystallization cycles

Specimen NH1			
Render system NH1			
Evaluation: Adhesive rupture (rupture occurred between render system and the support)			

In render systems FH7, FNH2 and FNH1 (render systems with grooves) adhesive rupture is observed at interface between outer and base layers and, as result, the adherence to the support is higher than the adherence between outer and base layer. In render system FNH7 (render system with grooves) cohesive rupture is observed in the outer layer meaning that the adherence between outer and base layer is higher than outer layer's cohesion. Render systems NH7 and NH1 (render system without grooves) show adhesive rupture between the render and the support and, as result, the adherence between render and the support is lower than the adherence between outer and base layer.

The pull-off tests were performed to understand if the tested renders systems change their adherence between layers or between render and the support after tests. In fact the pull-off tests were performed on render systems only after the 4th cycle, but there seems to be similar adherence between render systems with grooves and render systems without grooves.

6.4.2 Decay patterns of the render systems outer layer surface due to salt crystallization

The visual observations of sodium chloride crystallization at the outer surface in contact with the exterior atmosphere, at the end of 4th, 6th and 8th cycle are shown in table 6.5. These observations were performed to: i) evaluate the crystallization and, ii) qualify decay patterns, related with different render compositions, simulating external render and internal plaster on brick masonry when submitted to the same temperature, relative humidity and salt concentration solution.

The salts accumulate on the support surface (T render system) as a dense crust since the 6th cycle and in the 8th cycle they are generalized. When the support is rendered, with the render systems allowing the salt aqueous solution transport through them the salts tend to crystallize: i) on the surface of the outer layer of the render solution; ii) at the interface of the substrate/render solution; iii) at the interface between the different layers of render systems; iv) in the vertical grooves.

The crystallization and damage patterns related with the render systems used will be described next.

Until the 4th cycle almost no material loss was found; since the 6th cycle some material loss, as sanding and crumbling, was found on the surface of the top layer, in some of the studied render systems. The different render systems show different crystallization patterns in the surface of the external layer (Tables 6.5. and 6.6) .

Visual and optical microscope observations on deterioration patterns

The damage patterns due to salt crystallization were described and evaluated, for each render system in each specimen. The damage pattern of traditional brick without render was also considered (named specimen T).

Some differences in crystallization and decay patterns were observed on the surface of the studied render systems at the end of the 4th, 6th and 8th dissolution/crystallization cycles (Tables 6.5 and 6.6).

Table 6.5 Visual observations (V.O.) (×1) and optical microscope observations at the surface (M.O.) (×7) of specimens after 4, 6 and 8 cycles of dissolution/crystallization

Cycles	**4th cycle**		**6th cycle**		**8th cycle***	
Type obs.	V.O. (×1)	M.O. (×7)	V.O. (×1)	M.O. (×7)	V.O. (×1)	M.O. (×7)
Specimen T						
T (support)						
Descript.	Efflorescence/ whitening of the surface		Salt crust		Generalized salt crust	
Evaluat.	+		++		+++	
Specimen FH7						
Render system FH7						
Descript.	No damage		No damage		Detachment of the outer render layer (crumbling)/efflorescence	
Evaluation	-		-		+++++	
Render system NH1						
Descript.	Efflorescence/ Whitening of the surface		Generalized efflorescence has “hair crystals”/some sanding		Generalized efflorescence has “hair crystals”/some sanding	
Evaluat.	+		+		+++	

Table 6.5 (Cont.) Visual observations (V.O.) (×1) and optical microscope observations (M.O.) (×7) of specimens after 4, 6 and 8 cycles of dissolution/crystallization

Cycles	**4th cycle**		**6th cycle**		**8th cycle***	
Type obs.	V.O. (×1)	M.O. (×7)	V.O. (×1)	M.O. (×7)	V.O. (×1)	M.O. (×7)
Specimen NH7						
Render system NH7						
Descript.	Generalized efflorescence has “hair crystals”		Efflorescence/salt crust		Salt crust/efflorescence, superficial sanding	
Evaluat.	++		+++		+++	
Render system NH1						
Descript.	Localized efflorescence as “hair crystals” on the bottom		Generalized efflorescence has “hair crystals”/sanding		Generalized efflorescence has “hair crystals”/some sanding	
Evaluat.	+		++		++	
Specimen FNH7						
Render system FNH7						
Descript.	Localized efflorescence as “hair crystals”/ some sanding		Generalized efflorescence has “hair crystals”/powdering		Salt crust, powdering	
Evaluat.	++		+++		++++	
Render system NH1						
Descript.	Localized efflorescence as “hair crystals”/ some sanding		Generalized efflorescence has “hair crystals”/sanding		Generalized efflorescence has “hair crystals”/sanding	
Evaluat.	++		+++		++++	
Specimen FNH2						
Render system FNH2						
Descript.	Localized efflorescence as “salt crust”, sanding		Localized efflorescence as “salt crust”/some sanding, peeling		Detachment of the outer render layer (crumbling)/ localized efflorescence	
Evaluat.	+		++		+++++	
Render system NH1						
Descript.	Localized efflorescence as “hair crystals”/ some sanding		Generalized efflorescence has “hair crystals”/sanding		Dense crust crystallization/crumbling	
Evaluation	++		+++		+++++	

Table 6.5 (Cont.) Visual observations (V.O.) (×1) and optical microscope observations (M.O.) (×7) of specimens after 4, 6 and 8 cycles of dissolution/crystallization

Cycles	**4th cycle**		**6th cycle**		**8th cycle***	
Type obs.	V.O. (×1)	M.O. (×7)	V.O. (×1)	M.O. (×7)	V.O. (×1)	M.O. (×7)
Specimen FNH1						
Render system FNH1						
Descript.	Localized efflorescence as “hair crystals”, some sanding/powdering		Salt crust, some sanding		Generalized dense crust, peeling, scaling, sanding/powdering	
Evaluat.	++		+++		+++++	
Render system NH1						
Descript.	Efflorescence/ Whitening of the surface		Generalized efflorescence has “hair crystals”/sanding		Dense crust crystallization/sanding	
Evaluat.	+		++		+++	
Specimen NH1						
Render system NH1						
Descript.	Efflorescence, sanding		Generalized efflorescence has “hair crystals”, powdering		Detachment of the outer render layer (crumbling)/whitening of the support	
Evaluat.	+		+++		+++++	

The crystallization evaluation range: (-) no crystallization; (+) some crystallization located as “hair crystals”/whitening of the surface; (++) crystallization generalized as “hair crystals” (fluffy efflorescence); (+++) dense crust crystallization (powdery efflorescence); (++++) dense crystallization associated with render sanding; (+++++) dense crystallization associated with render crumbling.
* All specimens were tested until the 8th cycle with exception to FH7 (until 7th cycle), FNH2 (until 7th cycle) and NH1 (until 6th cycle) due to their damage (detachment of the outer layer from the base layer or of the layer and the support.

On specimen T (brick without render - support) the crystallization, on lateral sides of the brick, varies from whitening of the surface on 4th cycle until generalized efflorescence and dense crust at the end of 8th cycle.

In specimen FH7, in render system FH7 no efflorescence was observed on the surface of the outer layer, until the end of 6th cycle (the render system FH7 prevented the salt transport to the surface), while at the end of the 7th cycle the outer layer was detached and efflorescences could be observed on the interface between the top and base layer; in render system NH1 the crystallization pattern varied from whitening of the surface on the 4th cycle, until generalized hair crystals associated to some sanding.

In specimen NH7, in render system NH7 generalized hair crystals were observed since the 4th cycle until a dense crust formation at the end of the 8th cycle; in render system NH1 some sanding could be observed since 6th cycle with generalized hair crystals.

In specimen FNH7, in render system FNH7 localized hair crystals associated to some sanding could be observed since the 4th cycle, while at the end of 8th cycle a dense crust of crystallization was formed and crumbling was observed; in render system NH1, generalized crystallization with sanding was observed at the end of 8th cycle.

In specimen FNH2, in render system FNH2 until the end of 6th cycle, localized dense crust was observed, associated to some sanding, while at the end of 7th cycle the top layer was detached and some sanding was observed in the base layer; in render system NH1, since the 6th cycle, generalized crystallization was observed with crumbling.

In specimen FNH1, in render system FNH1 some sanding was observed since the 4th cycle, until crumbling occurred and generalized efflorescence appeared as hair crystals and a localized dense crust was formed in the 8th cycle; in render system NH1 in 4th cycle the whitening of the surface was observed while at the end of 8th cycle generalized crystallization with dense crust and sanding was observed.

In specimen NH1, render system NH1 in both larger sides, at the end of 4th cycle whitening of the surface was observed; on the 6th cycle generalized efflorescence with sanding was observed while on the 8th cycle, one of the sides detached from the support, and the whitening of the support was observed.

These observations are in line with the ones from Chapter 5. Salt transporting renders (L-L, L-LMet, LMet-LMet) from Chapter 5 show similar salt damage on the outer surface as NH1, NH7, FNH1, FNH2 and FNH7 developped in the present Chapter. Although FNH1, FNH2 and FNH7 were executed with grooves in base layer they still act as salt transporting renders, allowing salt crystallization on the outer surface.

In laboratory work, during dissolution/crystallization cycles, the detachment of renders from the support was observed in chapter 5 (when using perforated bricks). It is attributed to execution problems that results in lack of adherence between renders and brick. In the present chapter the detachment was only observed at later stages of cycles, for some render systems, so the use of traditional bricks, that were very well wet for prior renders application, reduced the problems related with the lack of adherence between brick and render in laboratory specimens.

The crystallization patterns were deeply investigated, in the support and render solutions outer surface, by means of optical microscopy (O.M.) (Table 6.6).

Table 6.6 Optical microscope observation of render systems' surface after 4, 6 and 8 cycles of dissolution/crystallization (magnification x70)

Cycles	4th cycle	6th cycle	8th cycle*
Specimen T			
T (support)			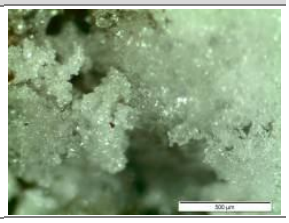
Description	Agglomeration of crystals	Dense crust	Dense crust
Specimen FH7			
Render system FH7			-
Description	Efflorescence has "hair crystals"	Efflorescence has "hair crystals"	
Specimen NH7			
Render system NH7	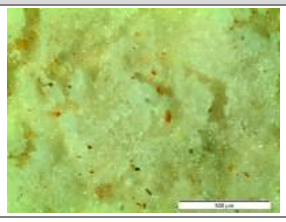	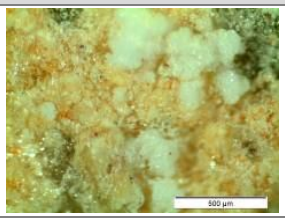	
Description	Agglomeration of crystals	Agglomeration of crystals as efflorescence and dense crust	Dense crust
Specimen FNH7			
Render system FNH7			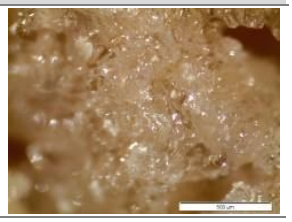
Description	Efflorescence has "hair crystals"	Dense crust	Dense crust
Specimen FNH2			
Render system FNH2	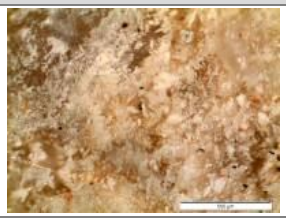		-
Description	Efflorescence has "hair crystals"	Dense crust	

Table 6.6 (Cont.) Optical microscope observation of render systems' surface after 4, 6 and 8 cycles of dissolution/crystallization (magnification x70)

Cycles	4th cycle	6th cycle	8th cycle*
Specimen FNH1			
Render system FNH1			
Description	Efflorescence has "hair crystals"	Dense crust	Dense crust
Specimen NH1			
Render system NH1		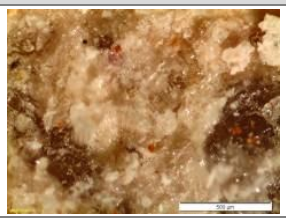	-
Description	Efflorescence has "hair crystals"	Dense crust	

* All specimens were tested until the 8th cycle with exception to FH7 (until 7th cycle), FNH2 (until 7th cycle) and NH1 (until 6th cycle) due to their damage (detachment of the outer layer from the base layer or of the layer and the support.

The O.M. observations in table 6.6 show that at the end of the tests there was salt crystallization as dense crust in the surface of all render systems, except in FH7 render system where salt efflorescences having "hair crystals" were observed.

On specimen T (support) the salt crystallization at the end of the 4th cycle was observed as an agglomeration of crystals, while since the end of the 6th cycle the salt accumulated in the surface as a dense crust. In specimen FH7, in render system FH7 only some localized "hair crystals" were observed until the end of the 6th cycle; on the other renders dense crust was observed since the 6th cycle. On specimen NH7, in render system NH7 an agglomeration of crystals until the end of the 6th cycle was observed; at the end of the 8th cycle dense crust was observed. On specimen FNH7, in render system FNH7, efflorescence was observed at the end of the 4th cycle, while dense crust was observed since the 6th cycle. On specimen FNH2, in render system FNH2 dense crust was observed since the 6th cycle. On specimen FNH1, in render system FNH1 dense crust was observed at the end of the 6th cycle. On specimen NH1, in render system NH1 dense crust is observed since the 6th cycle.

From the observed above, where the damage patterns on the systems varied from no crystallization or some localised crystallization as "hair crystals"/whitening of the surface to dense crystallization associated with render sanding or crumbling, some partial conclusions can be drawn:

- The 8th cycle can be considered very aggressive due to damage observed in all specimens' render systems, at this stage. The outer layer render systems FH7 and FNH2 detached at the end

of the 7th cycle and NH1 in NH1 specimen detached at the end of 6th cycle; this is in accordance with the results from pull-off tests in section 6.4.1 where was observed that in FH7 and FNH2 the rupture occurs through the interface between outer and base layer.

- In specimen FH7 the existence of water repellent in the outer layer of FH7 render system prevents the occurrence of damage in the surface of this render, although at the end of the tests there was the detachment of this outer layer; there was not observed an increase of the damage in the render system of the opposite side (NH1) compared with the other systems. This observation reflects that render system FH7 (with water repellent additive in outer layer and brick powder and grooves in base layer) seems to allow salt solution transport through the base layer until the grooves, where evaporation and salt crystallization is expected to happens; salt damage was not observed in NH1 render system in the opposite side, and as result no preferential salt solution transport through this render seems to happens.

- The existence of F7 formulation (with brick powder) in render system of specimens FH7, FNH7, and NH7, seems to slightly reduce the occurrence of damage in the render system NH1 of the same specimen, when compared with specimens without this formulation (FNH1, FNH2 and NH1). In NH7 render system composed only by F7 formulation high efflorescences were observed and at the end salt crust in its surface (higher than in other formulations) although no big surface damage was found; maybe there is a preferential salt solution transport through this layer until the surface where evaporation occurs.

- At the end of the cycles, the higher superficial damage was found in specimens FNH1, FNH2 and NH1, in both render systems, and similar to FNH7 (although in NH1 render system of FNH7 specimen it seems to be a bit lower).

- The vertical grooves in render systems FNH1, FNH2, FNH7 does not seem to increase the durability of the render system, as similar superficial damage to NH1 render system was found; the water repellent in the outer layer associated with the presence of these vertical grooves seems to increase the efficiency and durability of the render system.

- None of the renders appears to induce salt accumulation in the support as always salt transport to the surface and to the vertical grooves was observed; the transport to the surface was observed after the detachment of the outer layer of FH7 and FNH2 render systems at the end of the 7th cycle.

These observations will be deeply investigated in the following sections of the present chapter.

6.4.3 Location of NaCl crystallization in and on the renders due to salt crystallization test

The crystallization was deeply observed by means of optical microscope (O.M) visualization at the end of 4th, 6th and 7th or 8th cycle (these two last ones depending on the damage of the render system) (Tables 6.7 to 6.10). The observations were made in one of the larger sides in all specimens: a) at the interface between base and outer layers in the case of two layer render systems (FH7, FNH7, FNH2 and FNH1), b) inside the vertical grooves of the base layer in the case of two layer render systems (FH7, FNH7, FNH2 and FNH1) and c) at the interface between render layer and support in the case of one layer render system (NH1 and NH7 render systems in specimens NH1 and NH7 respectively). Three different specimens of each type were considered; at the end of the 4th, 6th and 7th or 8th cycles the tests stops for one specimen and samples were removed for the analyses.

Crystallization observation at the interface between base and outer layers

Some differences were observed in crystallization patterns of FH7, FNH7 FNH2 and FNH1 render solutions at the interface between outer and base layers at the end of the 4th, 6th and 7th or 8th dissolution/crystallization cycles (Table 6.7).

Table 6.7 Optical microscope observation of render between base and outer layers after the 4th, 6th and 8th cycle of dissolution/crystallization (magnification x70)

Cycles	4th cycle	6th cycle	8th cycle*
Specimen FH7			
Render system FH7			
Description	Crystallization as agglomeration of crystals	Generalized crystallization as layer of crystals	Layer of NaCl crystals
Specimen FNH7			
Render system FNH7			
Description	Agglomeration of NaCl crystals	Generalized crystallization as layer of crystals	A layer of crystals/ agglomeration of crystals

Table 6.6 (Cont.) Optical microscope observation of render between base and outer layer after the 4th, 6th and 8th cycle of dissolution/crystallization (magnification x70)

Specimen FNH2			
Render system FNH2			
Description	no crystallization	localized crystallization	agglomeration of crystals as a layer
Specimen FNH1			
Render system FNH1		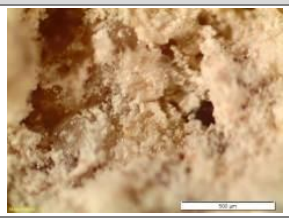	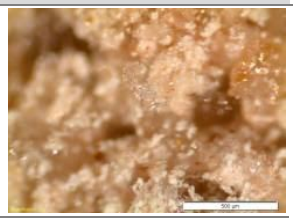
Description	no crystallization observed	no crystallization observed	localized crystals

* All specimens were tested until the 8th cycle with exception to FH7 (until 7th cycle), FNH2 (until 7th cycle) and NH1 (until 6th cycle) due to their damage (detachment of the outer layer from the base layer or of the layer and the support.

In FH7 render system crystallization agglomeration was observed since 4th cycle and at the end of the 7th cycle it became more evident as a layer of crystals. In FNH7 render system some disperse crystallization was observed until the 6th cycle and at the end of the 8th cycle there was some crystals agglomeration, but not so evident as in FH7 render system. In FNH2 render system no crystallization was observed at the end of 4th cycle while at the end of 6th cycle there was some crystallization; at the 8th cycle the outer layer was detached and crystallization as “well defined crystals” was observed at the interface near the grooves. In FNH1 render system no crystallization was observed at the interface until the end of the 6th cycle, while at the end of the 8th cycle localized crystals were observed.

Crystallization observation in the vertical grooves

Some differences were observed in crystallization pattern between inside the vertical grooves of FH7, FNH7, FNH2 and FNH1 renders, at the end of the 4th, 6th and 8th dissolution/ crystallization cycles (Table 6.8).

Table 6.8 Optical microscope observations of renders inside the vertical grooves after 4, 6 and 8 cycles of dissolution/crystallization (magnification x70)

Cycles	**4th cycle**	**6th cycle**	**8th cycle***
Specimen FH7			
Render system FH7			
Description	Localized “hair crystals”	“Hair crystals”	Agglomeration of crystals
Specimen FNH7			
Render system FNH7			
Description	Crystallization has “hair crystals”	Well defined “hair crystals”	Dense crust adherent
Specimen FNH2			
Render system FNH2		-	-
Description	No crystallization observed		
Render system FNH1		-	
Description	No crystallization observed		Some crystallization

* All specimens were tested until the 8th cycle with exception to FH7 (until 7th cycle), FNH2 (until 7th cycle) and due to their damage (detachment of the outer layer from the base layer).

Some differences were observed in crystallization pattern between inside the vertical grooves of FH7, FNH7, FNH2 and FNH1 renders, at the end of the 4th, 6th and 8th dissolution/crystallization cycles.

On FH7 render system localized air crystals were observed at the end of 4th cycle and at the end of the 8th cycle there was agglomeration of crystals. On FNH7 render system hair crystals were observed at the end of 4th and 6th cycle, although more generalized at the end of 6th cycle, and dense crust at the end of the 8th cycle. On FNH7 render system no crystallization was observed at the end of the 4th cycle. On FNH1 render solution no crystallization was observed at the end of the 4th cycle and at the end of the 8th cycle some agglomeration of crystals was observed.

Crystallization observation in the interface between render layer and the support

Some differences were observed in crystallization pattern between render layer and the support of FH7, NH7, FNH2, FNH1 and NH1 render solutions at the end of the 4th, 6th and 7th or 8th dissolution/crystallization cycles (Table 6.9).

Table 6.9 Optical microscope observations of renders between base layer and the support (brick) after 4, 6 and 8 cycles of dissolution/crystallization (magnification x70)

Cycle	4th cycle	6th cycle	8th cycle*
Specimen FH7			
Render system FH7			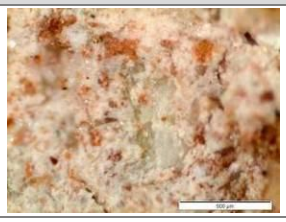
Description	Some localized crystallization	Some crystallization	Crystallization
Table **Specimen NH7**			
Render system NH7		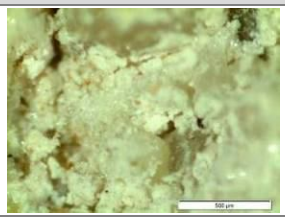	
Description	No crystallization observed	Some localized crystallization	Some crystallization
Specimen FNH7			
Render system FNH7			
Description	No crystallization observed	No crystallization observed	Some crystallization
Specimen FNH2			
Render system FNH2			
Description	No crystallization observed	No crystallization observed	Localized crystallization
Specimen FNH1			
Render system FNH1			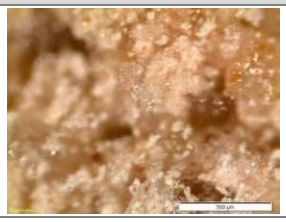
Description	No crystallization observed	No crystallization observed	Localized crystallization

Table 6.9 (Cont.) Optical microscope observations of render solutions between base layer and the support (brick) after 4, 6 and 8 cycles of dissolution/crystallization (magnification x70)

Cycle	4th cycle	6th cycle	8th cycle*
Specimen NH1			
Render system NH1	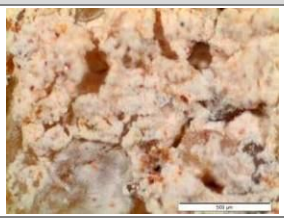	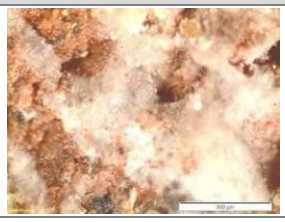	-
Description	No crystallization observed	Some localized crystallization	

* All specimens were tested until the 8th cycle with exception ofFH7 (until 7th cycle), FNH2 (until 7th cycle) and NH1 (until 6th cycle) due to their damage (detachment of the outer layer from the base layer or of the layer and the support).

On FH7 render system some localized crystallization was observed since the 4th cycle while at the end of the 8th cycle generalized crystallization was observed. On NH7 render system no crystallization was observed at the end of the 4th cycle and since the 6th cycle some localized agglomeration of crystals at the interface was observed. On FNH7 render system some localized crystallization was observed at the 8th cycle. On FNH2 and FNH1 render systems some localized crystallization at the 8th cycle was observed. On NH1 render system some localized efflorescence since the 6th cycle was observed at the interface.

Crystallization observation in the support

Almost no differences were observed in crystallization patterns in the support (brick) near the interface between the support and FH7, NH7, FNH2, FNH1 and NH1 renders at the end of the 4th, 6th and 7th or 8th dissolution/crystallization cycles (Table 6.10).

Table 6.10 Optical microscope observations of renders in the support (brick) after 4, 6 and 8 cycles of dissolution/crystallization with NaCl solution (magnification x70)

Cycle	4th cycle	6th cycle	8th cycle*
Specimen FH7			
Render system FH7			
Description	No crystallization observed	No crystallization observed	Some localized crystallization
Specimen NH7			
Render system NH7			
Description	No crystallization observed	No crystallization observed	Some crystallization

Table 6.10 (Cont.) Optical microscope observations of render solutions in the support (brick) after 4, 6 and 8 cycles of dissolution/crystallization with NaCl solution (magnification x70)

Cycle	4th cycle	6th cycle	8th cycle*
Specimen FNH7			
Render system FNH7			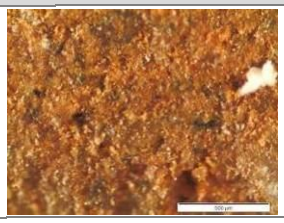
Description	No crystallization observed	No crystallization observed	Some crystallization
Specimen FNH2			
Render system FNH2			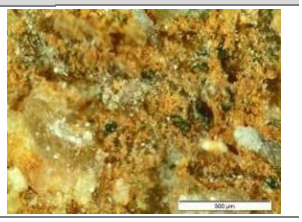
Description	No crystallization observed	No crystallization observed	Some crystallization
Specimen FNH1			
Render system FNH1			
Description	No crystallization observed	No crystallization observed	Some crystallization
Specimen NH1			
Render system NH1			-
Description	No crystallization observed	Crystallization observed	

* All specimens were tested until the 8th cycle with exception to FH7 (until 7th cycle), FNH2 (until 7th cycle) and NH1 (until 6th cycle) due to their damage (detachment of the outer layer from the base layer or of the layer and the support.

For all studied render systems no crystallization was observed on the support at the end of the 6th cycle, with exception of NH1 render solution (with some localized crystallization at the end of the 6th cycle); since the end of 8th cycle all systems show some crystallization on the support.

- At the interface between base and outer layer salt accumulation as a layer seems to be found in render systems FH7, FNH7 and FNH2, although in FNH1 render system (with the same composition in base and outer layer) there seems to be only localized crystallization. The salt accumulation at this interface could be mainly attributed to the different render formulations of base and outer layer (FNH2, FNH7 and FH7). The existence of water repellent in the outer layer of FH7 does not seem to lead to substantial increase of the crystallization at the interface.

Some partial conclusions can be drawn:

- There seems to be higher salt accumulation in the vertical grooves in render systems FNH7 and FH7 (although less than in FNH7). Again the existence of formulation F7 (with brick powder) in those render systems seems to increase the preferential transport salt solution through those systems, allowing the salt crystallization in the vertical grooves. The difference observed in salt crystallization in the vertical grooves between FH7 and FNH7 render system, may be due to water repellent in the outer layer of FH7 render system.

- None render system seems to induce salt crystallization in the support (brick). Some crystallization was observed in the support (brick) for all specimens, as a result of the salt solution transport from the support.

These partial conclusions will be deeply investigated in the following sections of this chapter.

6.4.4 Quantification of chlorides content in render systems at the end of the 4th cycle

Samples were removed from the specimens for chlorides quantification at the end of the 4th cycle, on all render systems, and were reduced to powder (Φ 100 μm). The method used to determine the total chloride % percentage consists of extraction with diluted nitric acid and determination of chlorides by potentiometric titration, performed in NMM at LNEC.

According to Lubelli [Lub06] at the evaporation surface salt content of about 1% by mass Cl^- (1.6% NaCl) and in some cases Cl^- contents up to 2% by mass (3.2% NaCl) have been measured. As salts tend to accumulate at the evaporation surface, according to the same author, the measured percentage of salt will strongly depend on the thickness of the sampled layer: sampling either the outer 1 cm or 2 cm layer will give two different percentages of salt content (lower when 2 cm is used). This made it difficult to compare the results of samplings performed using different procedures. In the present work for each layer all thickness was considered (1 cm – outer layer; 1.5 cm – base layer).

Higher damage due to salt crystallization was observed around 15 cm from the base of the brick (evaporation zone), when compared with other heights. Besides the thickness of the sample also the height from where the samples are removed could give different percentages of salt content. Samples were removed at 15 cm from the base considering that this zone could be the most representative of a fast response of NaCl concentration differences among render systems. This procedure will be adopted for chlorides quantification, in all sections.

In this case the chlorides concentration just beneath the outer layer in two different places (named Ext or Ext_groove), at the base layer just beneath the vertical grooves (named Int) in order to

achieve a fast response of the NaCl concentration to the RH changes (dissolution/crystallization cycles). In Figure 6.18 the location where the samples were removed from on each render system is represented.

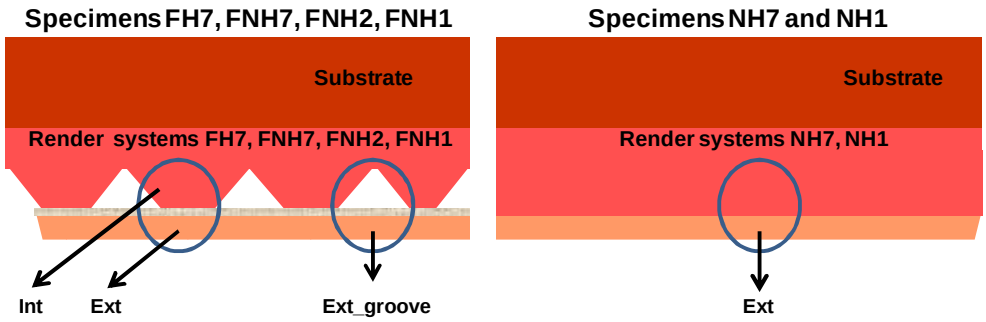

Fig. 6.18 Schematic representation of the location of the samples removed from render systems FH7, NH7, FNH7, FNH2, FNH1 and NH1.

The chloride quantification at the end of the 4th cycle, in each render system is presented in Figure 6.19.

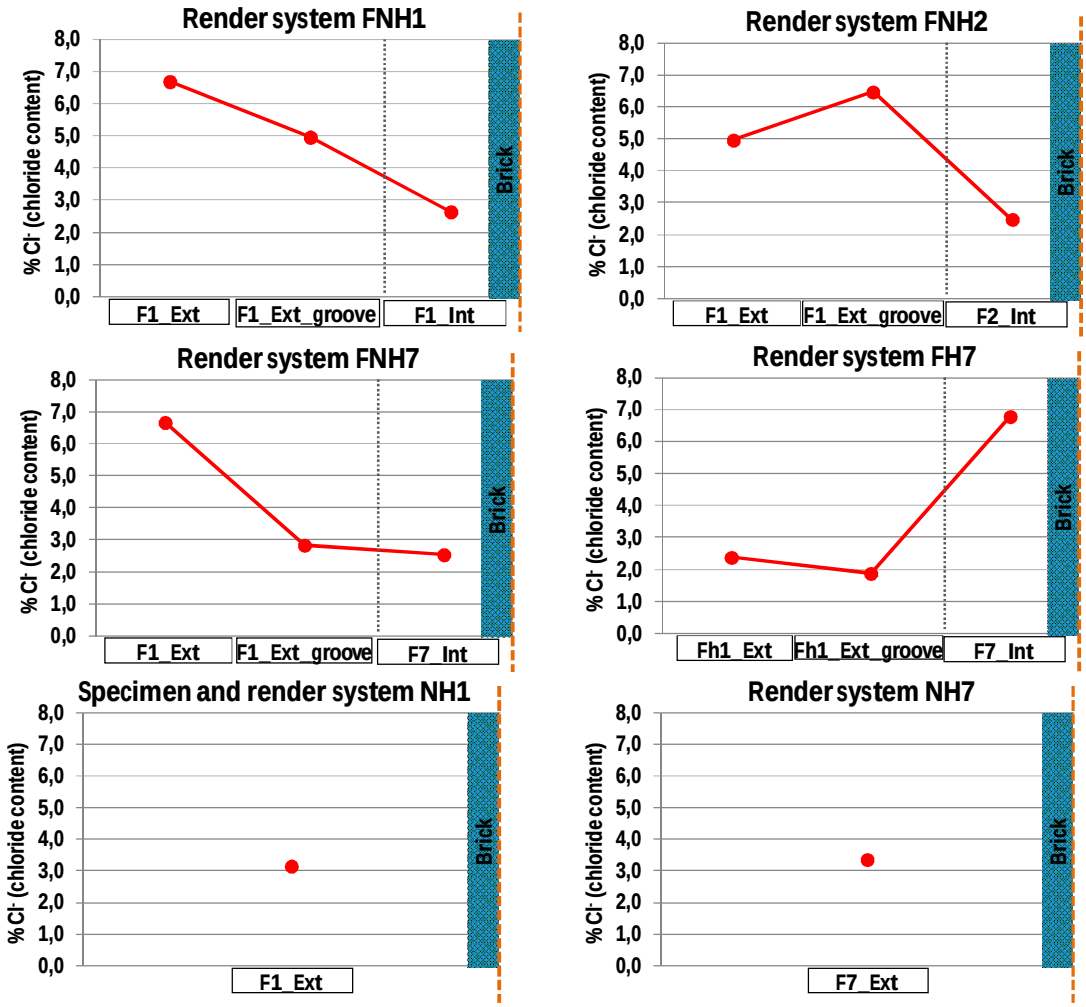

Fig. 6.19 Chlorides quantification of render systems in each specimen at the end of the 4th cycle.

The chlorides content was determined in all tested specimens, in render systems FH7, NH7, FNH7, FNH2, FNH1 and NH1, both in outer (ext) and base layers (int).

In render systems FH7, NH7 and FNH7 (with F7 formulation in the base layer) some differences were observed: i) in FH7 render system the existence of water repellent in the outer layer induces the highest chlorides content in base layer and the lowest in outer layer, ii) FNH7 render system (without water repellent in the outer layer) shows the opposite behaviour; iii) NH7 in render system without vertical grooves induces higher chlorides content in the outer layer than FH7 and lower than in FNH7.

In render systems with vertical grooves and without water repellent in the outer layer FNH1 (F1 formulation in base and outer layer), FNH2 (F2 in base layer and F1 in outer layer) and FNH7 (F7 in base layer and F1 in outer layer), similar chlorides content were found in base layer; the highest chlorides content were observed in the outer layer of FNH7 and FNH1, while in FNH2 was lower.

In the outer layer of NH1 and NH7 (without vertical grooves) similar chlorides content were found.

Sampling the outer layer in the grooves zone (Ext_groove) was not considered very representative due to lower salt concentration compared with the samples from outer layer (Ext), except in FNH2 render systems that was a bit higher.

From the results in Fig. 5.19 the following partial conclusions can be drawn:

- Considering specimens with vertical grooves in the base layer (“ventilated render”) it can be pointed out: i) the existence of water repellent in the outer layer (FH7 render system) results in the lowest chlorides content in the outer layer and the highest chlorides content in the base layer; ii) when there is not water repellent the opposite happens and similar chloride content is found on the base layer and the outer layer of the render systems FNH1, FNH2 and FNH7.

- The water repellent has a big influence on chlorides content of base and outer layer in render systems with vertical grooves (FH7 compared with FNH1, FNH2 and FNH7).

- The presence of F7 formulation, with brick powder additive, in the base layer of render systems FNH7 and NH7 does not seem to affect significantly the chlorides content, when compared with render systems FNH1 and NH1 without F7 formulation.

-

6.4.5 Discussion on damage evaluation due to salt crystallization

Some differences were observed in the crystallization between the different render systems at the end of the 4th, 6th and 8th dissolution/crystallization cycles:

From the 4th to the 6th cycle, on T specimen, the crystallization varied from whitening of the surface to dense crust crystallization and then to generalized efflorescence with dense crust on the 8th cycle.

On specimen FH7, in render system FH7: i) in the outer surface no damage was observed until the 7th cycle and efflorescence with hair crystals was only observed by means of Optical Microscopy (O.M.); ii) at the end of the 7th cycle the detachment of the outer layer occurred; iii) crystallization was observed by O.M.. at the interface between the top and base layer and inside the vertical grooves since the 4th cycle; iv) crystallization quantification shows the lowest Cl content in the outer layer and highest in the base layer, among all render systems. On specimen FH7, in render system NH1: i) no crystallization at the interface with the support was observed until 8th cycle by means of O.M.

On specimen NH7, in render system NH7: i) some crystallization was observed at the interface between the support and the render layer and since 6th cycle by means of O.M. and agglomeration of crystals are observed at the interface; ii) generalized efflorescence as hair crystals is observed in the outer surface since the 4th cycle and at the end of the 6th cycle there was salt crust; iii) no big damage was observed on the render. In render system NH1 crystallization at the interface with the support was not observed along the 8 cycles.

On specimen FNH7, in render system FNH7, some crystallization was observed both at the interface between the top and base layer and inside the grooves until the 6th cycle; on the 8th cycle crystallization was observed at the interface between the outer and base layer and dense crust crystallization inside the grooves; in NH1 render system there was no crystallization until the 6th cycle, although on the 8th cycle there was some crystallization at the interface between the render layer and the support.

On specimen FNH2, in render system FNH2, no crystallization was observed at the interface and in the grooves until the 4th cycle, while since 6th cycle some crystallization was observed at the interface and grooves and on 7th cycle the outer layer was detached and crystallization was observed in the grooves; in NH1 render system no crystallization was observed at the interface until 6th cycle and in 8th cycle some crystallization was observed at the interface.

On specimen FNH1, in render system FNH1 no crystallization was observed at the interface and in the grooves until the 4th cycle, on the 6th cycle no crystallization was observed at the interface but some was observed in the grooves and on 8th cycle crystallization was observed both at the

interface and in the grooves; in render system NH1 no crystallization was observed at the interface until 4th cycle and since 6th cycle some was observed at the interface.

On specimen NH1 in render system NH1, no crystallization was observed at the interface until 4th cycle, on 6th cycle some crystallization was observed at the interface and on the 8th cycle the render layer was detached.

As a result the lowest superficial damage can be found in FH7 render system with water repellent in the outer layer and F7 formulation in the base layer. This render system seems to allow higher salt solution transport from the support through the base layer (F7 formulation), as well as salt accumulation in the vertical grooves. Higher salt accumulation at the interface between the base and outer layer was not observed compared with the other systems. This render system "emboço ventilado" seems to accumulate salts in the vertical grooves, preventing the salt accumulation in the support, without damage of the surface.

The efficient salt solution transport of the base layer and its resistance to salts attack can be proved by the observations on NH7 render system (mix with brick powder additive). Although high salt accumulation as efflorescence and salt crust was observed in NH7 surface, this render showed less superficial damage when compared with the other render systems and can be considered a durable render.

"Emboço ventilado" render systems FNH1, FNH2 and FNH7 with vertical grooves show similar salt damage and chlorides concentration

Although the studied render systems could be considered compatible with old masonry walls, render system FH7 (with vertical grooves and water repellent in the outer layer) seems to be the most durable and efficient considering the severe action of salt laden water. Render system FH7 will be deeply investigated in the following sections and also FNH7 will be considered for comparison (same base formulation as FH7 render system but without water repellent in the outer layer), to test the durability and efficiency of the render system when submitted to the severe action of salt laden water (rising damp and soluble salts).

6.5 Study on selected render systems for salt load substrates - results

From the results obtained from first stage of specimen's survey, in section 5.4, the render system FH7 that show the highest resistance to salt crystallization was selected to be further investigated in the second stage (section 6.5). From the 1st stage also render system FNH7, for comparison with FH7, was selected to be further investigated.

6.5.1 Quantification of chlorides content in selected render systems

The chlorides quantification was made on the two selected specimens FNH7 and FH7 on the 2nd stage of the investigation, after the 4th and 6th dissolution/crystallization cycles to deeply study the salt distribution due to repeated dissolution/crystallization cycles. The concentration of chlorides just beneath the outer layer (named Ext), at the base layer just beneath the vertical grooves (named Int), in the support just beneath the surface of the brick (named brick). The method used to determine the total chloride % percentage consists of extraction with diluted nitric acid and determination of chlorides by potentiometric titration, performed in NMM at LNEC. In Figure 6.20 the location where samples were removed from FH7 and FNH7 specimens is represented.

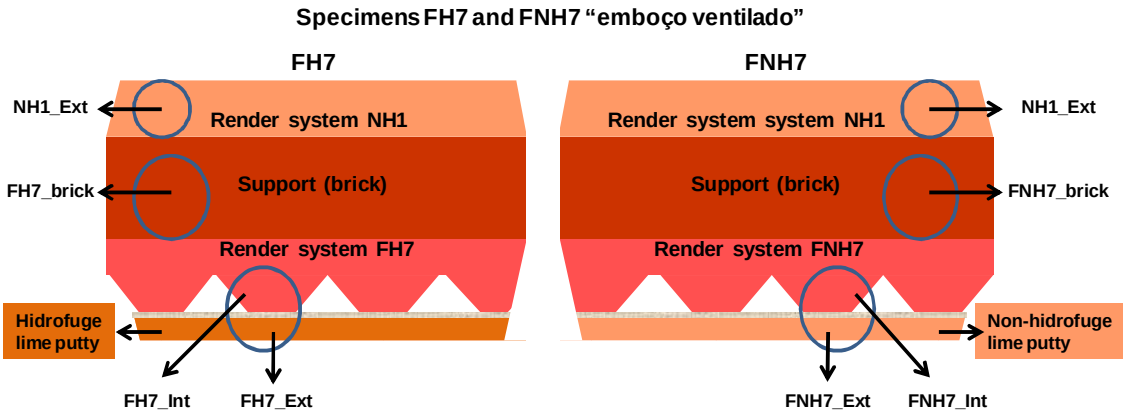

Fig. 6.20 Schematic representation of the location of the samples removed from the render solutions FH7 and FNH7 as well as from the support.

The chloride quantification at the end of the 4th and 6th dissolution/crystallization cycles in the render systems and the substrate of FH7 and FNH7 specimens and in T specimen are presented in Fig. 6.21.

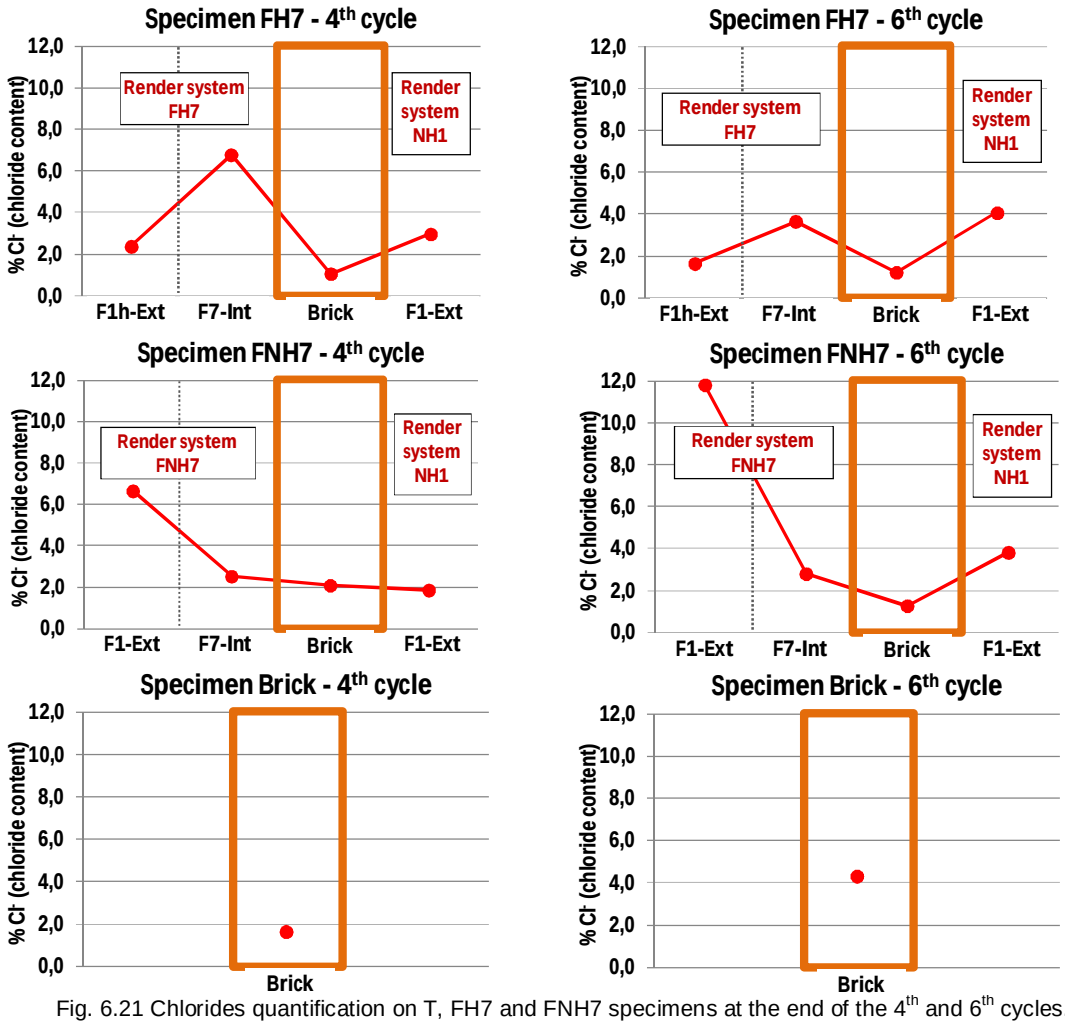

Fig. 6.21 Chlorides quantification on T, FH7 and FNH7 specimens at the end of the 4th and 6th cycles.

No significant difference on salt content on the substrate was observed from 4th to 6th cycle on both FH7 and FNH7 specimens. They seem to prevent salt accumulation in the substrate.

The water repellent in the outer layer clearly reduces the superficial salt accumulation. The salt content in the outer layer without water repellent of FNH7, at the end of the 6th cycle was considerably higher (11.8%) than on the same layer of FH7 render system with water repellent (1.6%).

The base layer of both render systems, composed with F7 formulation (with brick powder), seems to be able to accumulate some salts, which indicates that could be able to transport the salt solution until the vertical grooves where salts could crystallize. There is a tendency for higher salt content on the base layer of FH7 render when compared with FNH7 render system. On FH7 render system, from the 4th to the 6th cycles there was a reduction of salt content in base layer, that may be associated to some problem during sampling.

In specimen FH7 the existence of water repellent in the outer layer of render system FH7 does not seems to induce the salt accumulation in the render system NH1. On render system NH1 of both

specimens FH7 and FNH7 there is similar chlorides content at the end of the 6th cycle (4.1% and 3.8% respectively), although at the end of the 4th cycle the chloride content on the render system NH1 of specimen FNH7 was lower (1.9%) when compared with FH7 render system (3%).

6.5.2 Location of NaCl crystallization in the selected renders due to salt crystallization test

Environmental Scanning Electron Microscopy (ESEM) studies have been performed on FNH7 and FH7 specimens subjected to four dissolution/crystallization cycles, after their complete drying.

The cross sections (about 5 mm thick) of the outer layer, of the interface between the outer and base layer, of the interior of the grooves and at the interface between the support and the base layer of the mortars were observed. The composition of the salt crystals was checked with Energy Dispersive Spectroscopy X-ray Microanalyses (EDX).

The investigation aimed to study the location and habits/type of salt crystallization for the selected renders (FH7 and FNH7) due to repeated dissolution/crystallization cycles. The preferential location of sodium chloride in pores and the effects of the crystallization on the structure of the substrate is also studied.

Crystallization observation in the outer layer

External layer – surface	
Render system FH7	Render system FNH7

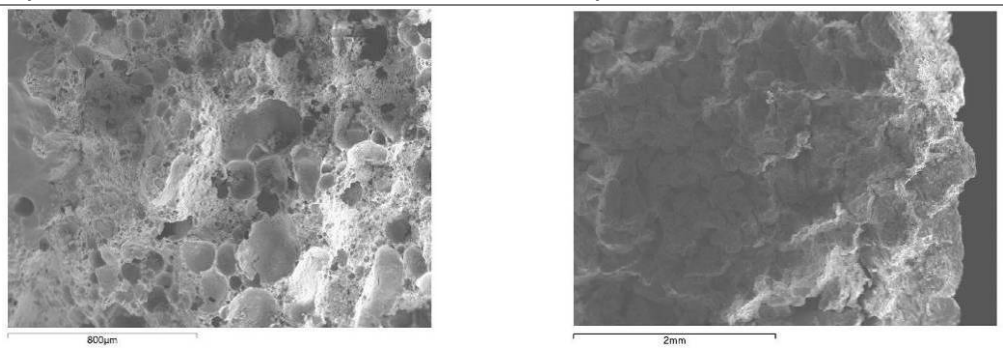

Fig. 6.22 SEM photograph on the material structure: a) porous structure of outer surface of FH7 render system, mag. x70 (left); b) not so porous structure of outer surface of FNH7 render system, mag. x30 (right).

External layer – surface	
Render system FH7	Render system FNH7

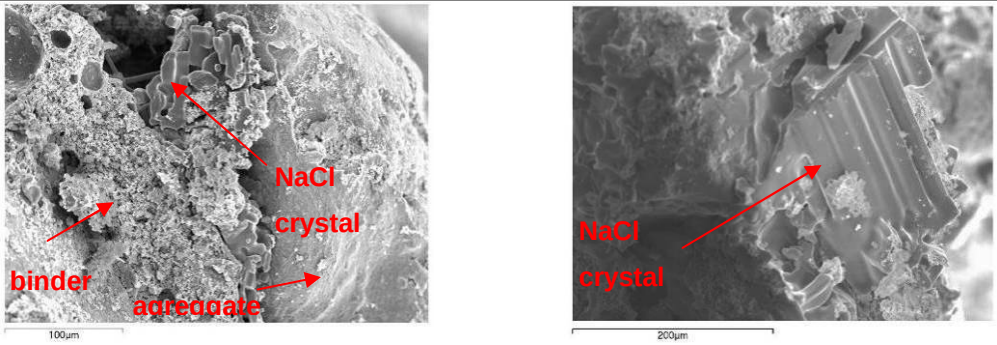

Fig. 6.23 SEM photograph of NaCl crystals: a) outer surface of FH7 render system, magnification x350 (left); b) Big NaCl crystals disperse in the surface of FNH7 render system, magnification x300 (right).

Differences were observed in the surface structure of the outer layer of the renders systems: a very porous structure and with large pores was found on FH7 outer layer when compared with FNH7 outer layer (Fig. 6.22).

In the outer layer of FNH7 salts are visible in larger pores, creating a layer over the pore walls; it looks as if a strong interaction exists between the material and the salt crystals (Figure 5.22). On FH7 the salt crystallizes in the pores but doesn't show a strong affinity with the substrate: it does not cover the pore walls in the form of layer, but crystallizes mainly as agglomerations of crystals, not strongly attached to the material (Fig. 6.23).

External layer – 3/5 mm from the surface	
Render system FH7	Render system FNH7

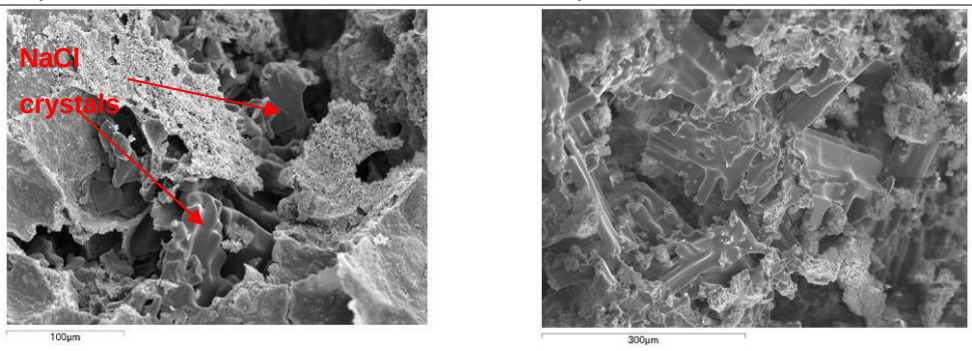

Fig. 6.24 SEM photograph at 3/5 mm from the outer surface: a) In FH7 render system a lot of small NaCl crystals in the middle of the binder and very well carbonated mortar, more than in other zones, magnification ×300 (left); b) In FNH7 Several crystals in the middle of the binder, magnification x200 (right).

Deeper in FH7 (around 3 mm from the surface) smaller NaCl crystals were observed (Figure 6.24) than the ones observed on the surface; small NaCl crystals localized in the middle of the binder and around the aggregate were found and no relevant damage to the mortar structure was detected after the 4 dissolution/crystallization cycles (see section 6.4.2.).

In the surface of FNH7, the crystals were bigger (Fig. 6.24) than on FH7 and generalized through the surface; in FNH7 the crystals are preferentially in the middle of the binder. This preferential location of the crystallization may explain the sanding observed on the surface of FNH7 outer layer at the end of the 4th cycle (see section 5.4.1.). A strong interaction between the material and the salt crystals in FNH7 is noticed again (Figure 6.24).

Crystallization observation in the interface between base and outer layers

Internal layer – interface base and outer layers	
Render system FH7	Render system FNH7

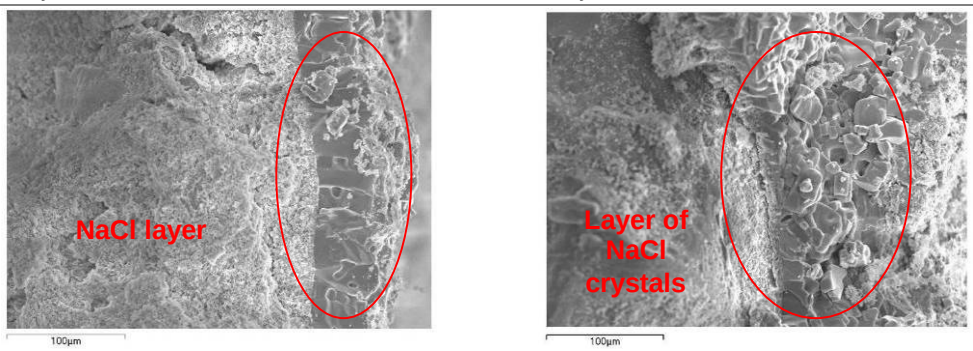

Fig. 6.25 SEM photograph at the interface between base and outer layers: a) In FH chlorides layer at the interface growing from the binder, magnification ×400 (left); b) In FNH chlorides at the interface in the middle of the binder accumulate as a “layer”, magnification x350 (right).

In both render systems, at the interface between base and outer layer, there is a salt layer that covers the binder. In FH7 the salt layer is denser and more defined than the one observed in FNH7 (Fig. 6.25), where the layer seems to be an agglomeration of crystals growing from the binder and mixed in it. These observations confirm the ones observed in section 6.4.1. at the interface: a layer

of NaCl crystals is observed at the interface with FH7 and an agglomeration of crystals is observed at the interface with FNH7 render system at the end of the 4th cycle (see section 6.4.1.). The crystallization habits obtained by ESEM investigation at the end of the 4th cycle may explain the detachment of the outer layer (with water repellent) observed at the end of the 7th cycle in FH7 (see section 6.4.1).

Crystallization observation in the interior of the grooves

Base layer - Interior of the groove	
Render system FH7	Render system FNH7

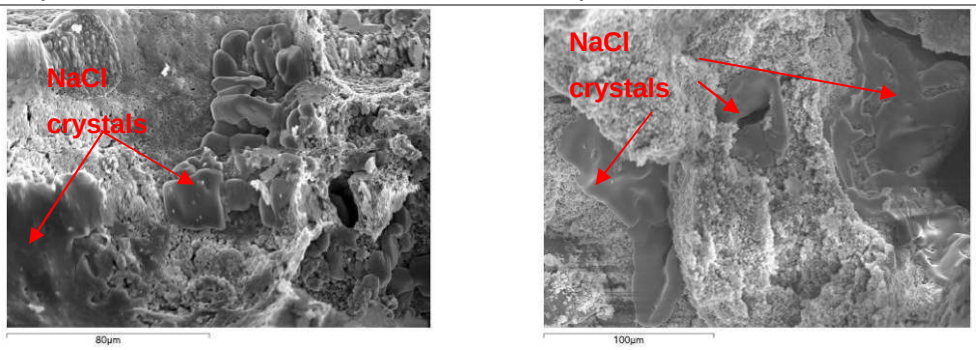

Fig. 6.26 SEM photograph at the groove: a) In FH7 a lot of NaCl crystals in the porous system, in the middle of the binder, magnification ×750 (left); b) In FNH7 NaCl crystals in the porous system; but much lesser than in the surface of the external layer, magnification x500 (right).

On both render systems (FH7 and FNH7) a tendency for chlorides crystallization inside the vertical grooves was observed, although with different shape: in FH7 they seem to grow as salt accumulation in the surface and mixed in the matrix and in FNH7 render system they grow adherent to the material in the surface of the porous system (Figure 6.26). With these observations the vertical grooves seem to be able to accumulate salts where evaporation is induced.

Crystallization observation in the base layer

Base layer	
Render system FH7	Render system FNH7

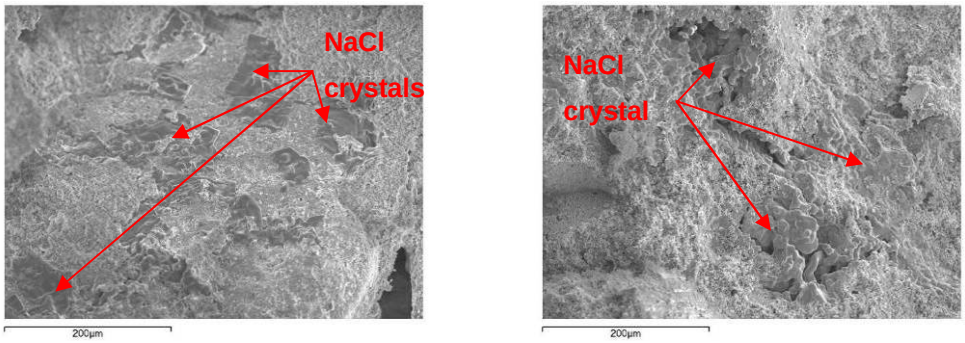

Fig. 6.27 SEM photograph in base layer: a) In FH7 disperse big crystals of NaCl in the middle of the binder, magnification ×250 (left); b) In FNH7 NaCl crystals in the concavities of the porous system, magnification x250 (right).

Base layer	
Render system FH7	Render system FNH7

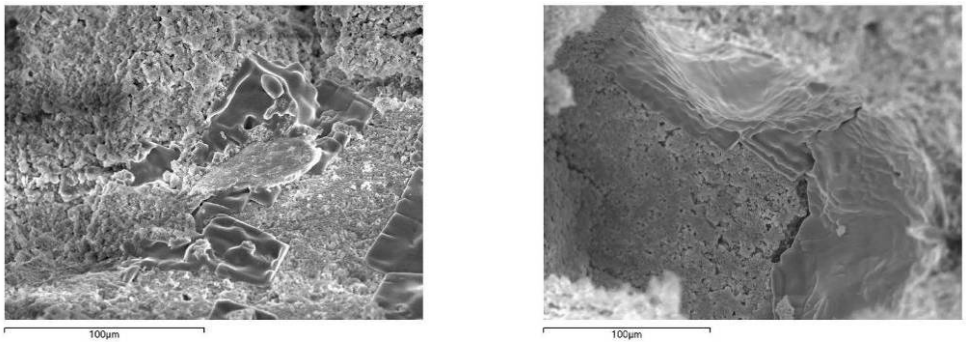

Fig. 6.28 SEM photograph in base layer: a) in FH7, magnification ×300 (left); b) In FNH, magnification x500 (right).

In both render systems (FH7 and FNH7) there are big crystals adhering to the material and mixed in the binder in the base layer, although there seems to be higher salt concentration in FH7 render (Figs. 6.27 and 6.28) which seems to be in accordance with the chlorides quantification in section 6.5.1. The salt crystals seem to be able to accommodate in the pore system of base layer (F7 formulation with brick powder) without damaging it.

Crystallization observation at the interface between support and base layer

Internal layer – interface between support and base layer	
Render system FH7	Render system FNH7

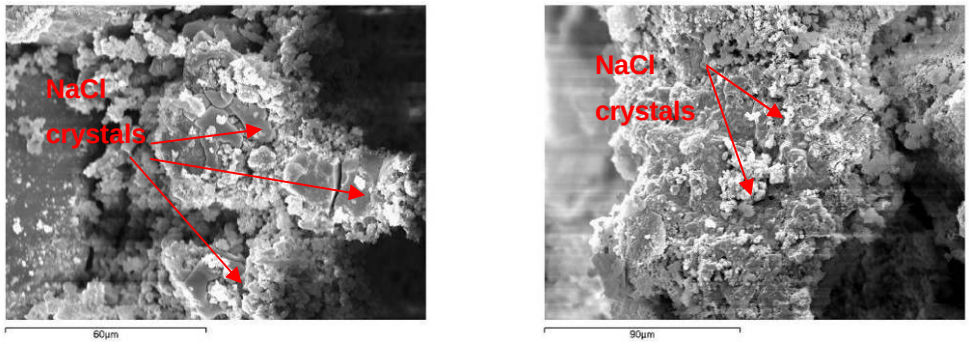

Fig. 6.29 SEM photograph of interface: a) in FH7 a lot of small crystals are observed, magnification ×1000 (left); b) In FNH7, small crystals are observed, magnification x500 (right).

A tendency for salt accumulation, as small crystals distributed over the binder at the interface between base layer and support is observed in both FH7 and FNH7 renders (Fig. 6.29). This finding is in agreement with what was observed in section 6.4.3. for FH7 render system; similar tendency to FNH7 for salt accumulation was observed at the interface between support and base layer

To understand the tendency for salt accumulation in the base layer, render system NH7 was investigated as it is composed by F7 formulation identical to base layer of FNH7 and FH7 (Figures 6.30 and 6.31).

Surface
Render system NH7

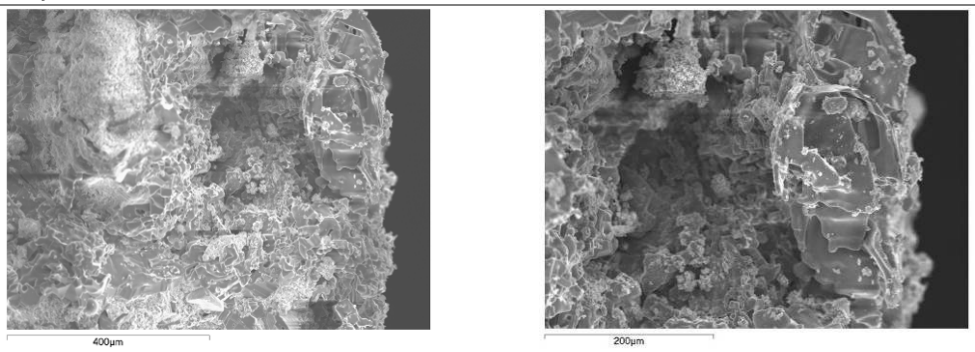

Fig. 6.30 SEM photograph of the outer surface: a) in NH7 a lot of small crystals is observed, magnification ×150 (left); b) NaCl crystals at the surface, magnification x250 (right).

A dense crust, as agglomeration of NaCl crystals, well adhering to the material is observed on the outer surface of NH7 (Fig. 6.30).

Interface between the support and the render layer
Render system NH7

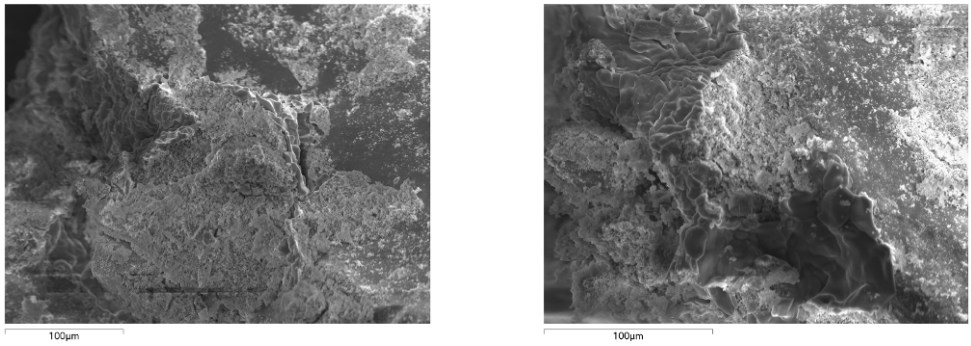

Fig. 6.31 SEM photograph at the interface with the support: a) in NH7 few crystals, magnification ×350 (left); b) NaCl crystal at the interface with the aggregate, magnification x450 (right).

At the interface, between support and NH7 render system, few crystals are visible growing at the binder/aggregate interface but well adhering to the material; there is no evidence of de-cohesion of the binder (Fig. 6.31).Based on this observation, base layer with F7 formulation (with brick powder) used in render systems FH7 and FNH7 does not seem to induce salt accumulation at the interface between the support and this layer.

As a result of SEM observations, in the outer surface of FH7 with water repellent there is observed high quantity of large pores and lower affinity of the NaCl crystals (small crystals dispersed through the body and no damage is observed) when compared with the outer layer of FNH7 where smaller pores are observed (a lot of crystals dispersed through the body and loss of cohesion of the binder). At the interface between outer and base layer in both render systems some salt accumulation is observed, although in FH7 (with water repellent in the outer layer) a layer seems to form and in FNH7 there seems to be an agglomeration not so well defined. In render systems FH7, FNH7 and NH7 no significant salt crystallization was observed at the interface between support (brick) and render system.

6.5.3 Influence of pore characteristics on salt uptake and distribution

The total connected porosity (P_c) and pore size distribution of renders FNH7, FH7 and NH7 were determined by Mercury Intrusion Porosimetry (MIP) (Figs. 6.32 and Table 6.11). Pore size distribution was performed using Quantachro AutoScan 60 Mercury Porosimeter with a total range of pressure between 0.17 and 344 MPa. Pressure, pore diameter and intrusion volume were automatically registered.

The samples were removed from the specimens at superior zone (around 15 cm from the base of the specimen) from the outer surface of the render systems FNH7, FH7 and NH7, pre-experiment and post-experiment at the end of 4th and 6th cycles (Fig. 6.32).

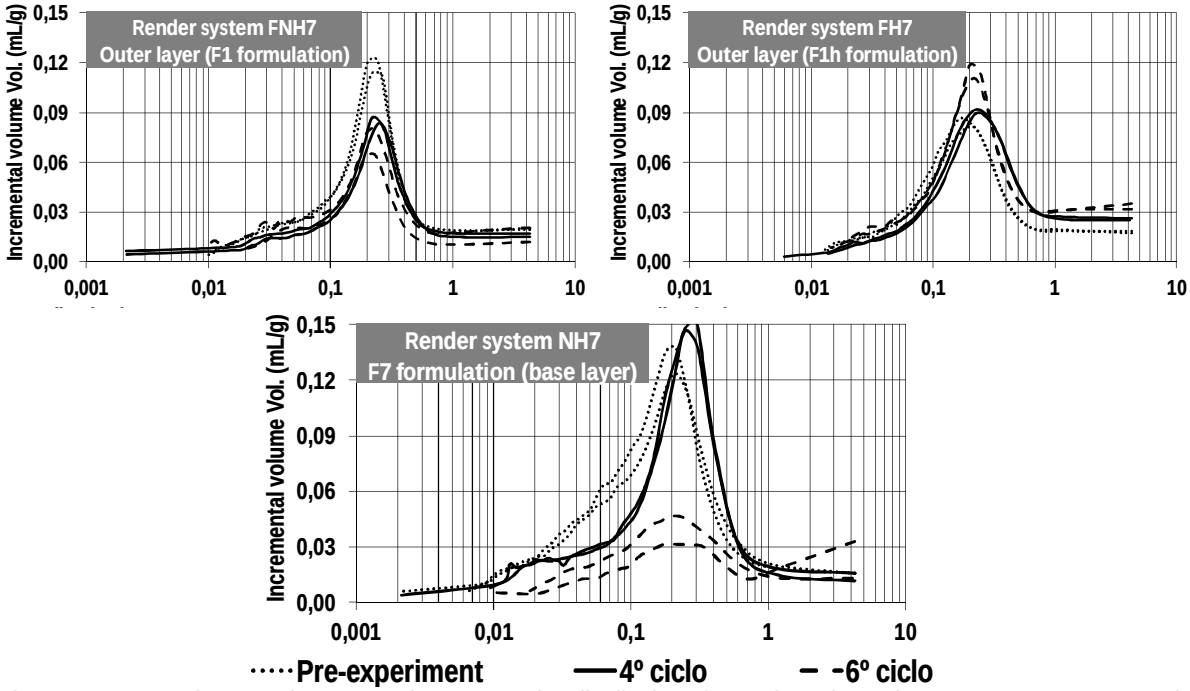

Fig. 6.32 Pre-experiment and post-experiment pore size distribution of outer layer in render systems FNH7, FH7 and NH7

The samples show total connected porosity (Pc) ranging from 13.6 until 24.7%. Five microporosities were determined, to evaluate the pore size relative influence on salt crystallization damage, by setting five upper limits of micropore size, attributed by Yu and Oguchi [Yu10] to salt damage. The microporosities (P<5 μm to P<0.01 μm) in Table 5.11 represent the volume percentages of pores smaller than respectively 5, 1, 0.1, 0.05 and 0.01 μm radius. The pore range between 5 μm and 100 μm were not determined.

Table 6.11 Total porosity and pore size distribution on the render layers of render systems NH7, FNH7 and FH7 – pre-experiment and post-experiment (at the end of 4th and 6th cycles).

Render layer properties	Sample								
Render system	NH7			FNH7			FH7		
Render layer	F7			F1			F1h		
Pore size distribution (μm)	Pre-exp.	4th cycle	6th cycle	Pre-exp.	4th cycle	6th cycle	Pre-exp.	4th cycle	6th cycle
5-1	8.26	22.57	7.57	13.23	15.34	13.69	12.73	18.24	16.66
1-0.1	58,39	48.37	67.95	63.01	57.48	64.87	60.14	62.01	65.08
0.1-0.05	15,49	11,00	10.87	10.22	13.05	9.88	15.23	11.01	9.03
0.05-0.01	15,39	8.47	12.43	11.97	13.18	9.25	10.06	8.01	6.95
Connected porosity P_c (%)	24,7	13.72	22.04	19.1	13.61	14.57	17.3	20.87	19.50
Microporosity, $P_{<5\mu m}$ (%)	24,57	12.56	21.96	18.83	13.53	14.37	17.07	20.82	19.16
Microporosity, $P_{<1\mu m}$ (%)	22,53	9.47	20.29	16.3	11.44	12.38	14.87	17.02	15.91
Microporosity, $P_{<0.1\mu m}$ (%)	8,11	2.83	5.31	4.27	3.62	2.92	4.46	4.07	3.22
Microporosity, $P_{<0.05\mu m}$ (%)	4,29	1.32	2.92	2.31	1.84	1.49	1.83	1.78	1.46
Microporosity, $P_{<0.01\mu m}$ (%)	0,49	0.16	0.18	0.04	0.05	0.14	0.13	0.10	0.11

Note: $P_{<5\mu m}$, $P_{<1\mu m}$, $P_{<0.1\mu m}$, $P_{<0.05\mu m}$, $P_{<0.01\mu m}$ are the microporosities of pores smaller than 5, 1, 0.1, 0,05 and 0.01 μm radius, respectively; Pre-exp. - Pre-experiment; 4th cycle – after 4 cycles of dissolution/crystallization; 6th cycle – after 6 cycles of dissolution/crystallization.

More than 55% of the total connected porosity was found in pore range between 0.1 and 1 um and more than 20% was found between 0.1 and 0.01 μm, for all specimens before experiment.

Before the experiment, the highest connected porosity was found in F7 (24.7%) and the lowest in F1h (17.3%) followed by F1 (19.1%). F7 presented the highest percentage of pore range between 0.1-0.01 μm radius and lowest in pore range 5-0.1 μm, while in F1 the opposite was observed. After experiment there was a tendency for total connected porosity to decrease (although the range between 5 μm and 100 μm was not evaluated in F7 and F1 and for an increase in F1h; the highest connected porosity was found in F7, followed by F1h. In the 4th cycle the pore size distribution seems to have become coarser in F1h and F7, while in F1 pores became smaller. In the 6th cycle, the render system showed the same tendency as in 4th cycle, although in F1 this tendency was very slight when compared with the others.

According to the bibliography, a pore range between 0.1 and 5 μm seems to be more effective in increasing solution/salt absorption [Yu10, Zeh89]. The presence of water repellent in FH7 may inhibit salt solution uptake in pores wider than 0.1 μm and thus inducing salt crystallization in smaller pore ranges; also some salt solution uptake may happen disrupting the layer formed by water repellent, contributing to the increase of the porosity in a pore range higher than 0.1 μm.

Comparing the results obtained in this section with the observed damage patterns in section 6.4.2 and the observations on the location and type of salt crystallization in sections 6.4.3 and 6.5.2, and salt distribution determination in sections 6.4.4 and 6.5.1, at the end of the 6th cycle, the following can be concluded:

i) on F7 render with brick powder (same formulation as base layer of FNH7 and FH7 render systems) there is a small decrease in total connected porosity and the tendency for pore range to move towards coarser pores (in pore range between 0.1 and 1 μm); this render allows the transport of salt solution to the vertical grooves where evaporation happens and consequently crystallization occurs and, at the same time, is able to accumulate some crystallization in its pore structure without causing much damage at the end (efflorescences and some superficial sanding).

ii) in F1 render (outer layer without water repellent from FNH7 render system) there is the highest decrease in total connected porosity and a tendency for pore range to move towards smaller pores; this reflects the high salt content determined inside it as a result of salt accumulation (see sections 6.4.4 and 6.5.1) and salt damage as salt crust and powdering was observed at the surface (see section 6.4.2).

iii) In F1h render (outer layer with water repellent from FH7 render system) there was an increase in total connected porosity and a tendency for pore range to move towards coarser pores; that may be explained by the salt solution uptake in some large pores (higher than 0.1 μm) that may disrupt the layer formed by the water repellent, increasing the porosity in this range, as well as the total connected porosity; in this layer salt damage was not observed at the surface (see section 6.4.2) and very low salt content was determined (see sections 6.4.4 and 6.5.1) resulting from the fact that salt accumulation in this layer is not significative.

6.5.4 Discussion on selected render systems for salt loaded substrates

From the experiments performed a different behaviour was observed, concerning the location of salt accumulation, on both specimens FH7 and FNH. On FH7 render system, salts tend to accumulate in the base layer, while on render system FNH, they accumulate in the outer layer. There is no significant difference on salt accumulation on render system NH1 of both specimens and according to the results they show lower total chlorides content when compared with the total amount of chlorides on both outer and base layers of FH7 and FNH7 render systems. There is not a tendency for salt accumulation on the support of both render systems, meaning that the render allow salt solution transport through them. According these experiments in the small specimens in laboratory the tested render systems FH7 and FNH7 can be possible solutions for salt loaded masonries.

ESEM investigation on the type and location of crystallization, on FH7 and FNH7 render systems, may explain some of the differences observed on damage pattern of those render systems. On the outer layer surface of the specimens, NaCl crystals show a strong affinity with the material, on render systems FNH7 and NH7, whereas they grow as a well adhering layer in the pore walls; in FH7 render system they grow as an agglomeration of small crystals not strongly attached to the material. Deeper in the outer layer high quantity of small crystals localized in the porous system

were observed in render system FH7, while in render system FNH7 there is the presence of bigger crystals and the de-cohesion of the binder. The porous structure of the outer layer seems to: i) in FH7 render system allow some small crystals to grow in the porous structure preventing their transport to the surface (the high porosity induced in the render due to the presence of water repellent has already been noticed by some authors [Lux07a, Wij07a]); ii) in FNH7 render system allow the migration of salt solution to the outer surface where the salts grow and accumulate. This may explain the damage observed on the surface of the render system FNH7 where salts accumulate as efflorescences at the end of the 4th cycle and salt crust at the end of the 8th cycle, while no damage is observed on render system FH7 due to salt crystallization (see section 6.4.2). At the interface NaCl crystallizes as a layer in both FH7 and FNH7 render systems, although in FH7 render system it appears as a denser and compact crystallization barrier explained by the presence of water repellent mixed in the mortar of the outer layer that prevents the salt solution transport through it, and therefore inducing the salt accumulation below it (at the interface). This preferential crystallization habits may explain the detachment of the outer layer observed at the end of the 8th cycle in FH7 render system. The accumulation of crystals at the interface between different porous materials has also been noticed by some authors [Arn91, Lub06a].

6.6 Classification of render systems – working principle and performance

In table 6.12 the classification of each tested specimen is described (adapted from the one defined by Rodrigues et al. [Rod07a]), taking into consideration the working principle (transporting, accumulating, blocking and sealing) and performance (no decay, slow decay, moderate decay and fast decay) and considering the influence of the whole system (render+ solid traditional brick).

Table 6.12 Classification of tested specimens under the severe action of salt laden water

Specimen	Render system (side A)	Render system (side B)
FH7	FH7 – Accumulating (slow)	NH1 – Transporting (slow)
NH7	NH7 – Transporting (slow)	NH1 - Transporting (slow)
FNH7	FNH7 - Transporting (moderate)	NH1 - Transporting (slow)
FNH2	FNH2 – Transporting (moderate)	NH1 – Transporting (moderate)
FNH1	FNH1 – Transporting (moderate)	NH1– Transporting (moderate)
NH1	NH1 – Transporting (moderate)	NH1 – Transporting (moderate)

It is observed that in each specimen both render systems have influence in terms of working principle. In NH7 render system salt crystallization was observed on the outer layer at the 4th cycle but occurrence of sand disintegration or mass loss were not observed, being the system classified as transporting (slow). The other renders systems (except FH7) were also considered transporting but moderate in terms of performance, i.e. moderately deveping damage.

The render systems were classified based on their behaviour until the 6th cycle, as since this cycle the tests could be considered too much aggressive for renders resulting in high superficial damage and/or detachment of the render systems (between base and outer layer or from the support).

Specimen FH7: FH7 render system with F7 formulation in base layer and F1h formulation (with water repellent) in the outer layer is classified as an accumulating render; salt accumulation is observed in the vertical grooves of the base layer and no damage due to salt accumulation occurs in the outer surface. The render system NH1 works as a transporting render while no significant damage was observed.

Specimen NH7: NH7 render system with F7 formulation and without vertical grooves is classified as a transporting slow render; the salts accumulate in the surface, mainly as efflorescences, and no significant salt damage is observed. The render system NH1 works as transporting render; no significant damage was observed.

Specimen FNH7: FNH7 render system with F7 formulation in base layer and F1 formulation (without water repellent) in the outer layer is classified as transporting (moderate); salt accumulation is observed in the vertical grooves of base layer and some damage due to salt accumulation in the outer surface. The render system NH1 works as transporting render; no significantly damage was observed.

From these observations, it seems that the existence of F7 formulation in the base layer of FH7, NH7 and FNH7 seems to induce higher salts solution transport through these render systems and lower in the NH1 render system.

Specimens FNH1, FNH2 and NH1: both render systems are classified as transporting with a moderate damage development. The different compositions of the several layers of the render systems and the existence or not of vertical grooves produce the same behaviour in terms of salt damage. From these observations it seems that: the vertical grooves do not have influence on damage due to salt crystallization and the different formulation seems to have no influence on salt solution transport.

6.7 Conclusions

The analysis of the results from the present experimental work demonstrates that accelerated dissolution/crystallization cycles with sodium chloride favor the accumulation of NaCl salt efflorescence on the outer render layer surface (exception in FH7 render system with water repellent in the outer layer – F1h formulation) and base layer, without provoking salt accumulation in the support. As a result render systems may act as transporting or accumulating renders with different performance in terms of outer surface damage and salt accumulation in the base layer and vertical grooves.

The main conclusions that can be drawn from this experimental work are:

- In ventilated render systems (FNH7, FNH1 and FNH2) salts crystallize in vertical grooves and in the base layer although the transport of salt solution was also allowed to the outer surface. The increase of salt accumulation and dissolution and re-crystallization results in the de-cohesion of the binder and/or detachment of the render, although in FNH2 there was also the detachment of the outer layer at the end of the tests.

- The water repellent in the outer layer surface of FH7 render system prevents the salt transport through it; in this layer indeed the lowest salt content was observed, preventing salt efflorescence at surface; higher salt accumulation was observed in the base layer and vertical grooves (where evaporation occurs).

- Render systems without vertical grooves in the base layer, NH1 (without brick powder) and NH7 (F7 mortar with brick powder) show salt accumulation in the outer layer surface. In NH7 render (F7 mortar with brick powder) high crystallization as efflorescences was observed in the outer layer although it proved to be very resistant (as result from the combination of the pozzolanic addition and brick powder, in F7 mortar, and its hability in sprayed during the first days of curing initial curing conditions) when compared with the other render systems, showing less damage at the end. F7 mortar (with brick powder) seems to be better on salt solution uptake and transport to the evaporation surface (vertical grooves in case of FH7 and FNH7 render system and outer surface in NH7 render system). F7 render shows the highest connected porosity between 0.01 μm and 5 μm, compared with the other mortars, and this fact seems to have a determinant effect on its susceptibility for salt damage due to the increase of porosity in the crystallization range; this effect related to the presence of brick powder in mortars and the high moisture retention of those kind of mortars, which is essencial for pozzolanic reaction, is described in chapter 2.

- The render systems FNH1, FNH2 and NH1 in each specimen seems to induce the higher and similar damage patterns, crystallization habits and chlorides content of NH1 render system in the opposite larger side of each specimen; in render systems FNH7, NH7 and FH7 seems to induce lower and similar salt damage in NH1 render system on the opposite larger side of the specimens.

- Not any of the tested render systems showed a tendency for salt accumulation in the support (brick).

- In some cases (FH7, FNH2 and NH1 render systems) the outer layer was detached in the 7th cycle due to salt damage and the other render systems present severe superficial damage as dense crust crystallization associated with sanding and crumbling. It is

important to keep in mind that 7th cycles simulate a very aggressive stage with severe degradation for the render systems (detachment of the render from the support - NH1 - or detachment of the outer layer from the base layer – FH7 and FNH2) .

The study of crystallization location and damage patterns evolution, in these small scale specimens, was crucial for their understanding in brick masonry. The accumulation of the salt in the vertical grooves is crucial for the “emboço ventilado” render system development as it was designed with this as the main objective (working as an accumulation system) without damaging the outer surface. After testing, FH7 render system: i) does not induce salt damage in the support (as well as the other tested render systems) or base layer detachment, ii) base layer with brick powder shows an ability on salt accumulation in the pore structure without damage and salt crystallization was observed at the grooves, iii) water repellent in outer layer does not seem to lead to substantial increase of salt crystallization at the surface (compared with the other tested render systems) and iv) at the outer layer no salt damage was observed neither the presence of efflorescences. FH7 was the one classified as accumulating render system and was selected to be executed on a real-size masonry wall in chapter 7, as it seems to be the best option as no damage of the outer surface and the salt accumulation in the vertical grooves, without salt accumulation in the support, were observed.

From the investigation of the render system applied on the full scale masonry (Chapter 7), at the end of the tests, render system H (with water repellent in outer layer and without grooves and with brick powder in base layer) shows higher superficial damage than FH7 (with waster repellent in outer layer and brick powder and grooves in base layer). The grooves in base layer were found to induce the masonry as well as render evaporation and the reduction of support moisture evaporation referred in literature [Gon07, Pet10a, Pet10b, Hui07] when water repellent in used in outer layer, can not be considered a problem with render system FH7. From small scale specimens in Chapter 6 , it was found that F7 render mix (with brick powder) is more resistant to salt damage than the “more traditional render” F1 (without brick powder). Considering all studied salt transporting renders (both from Chapter 5 and 6) the use of F7 render mix (with brick powder) shows to be durable and efficient on salt transport and crystallization on the outer surface; as results it is the best studied solution for base layer render mix on ventilated render system FH7. Based on the referred above the render system FH7 may be classified as accumulating render system and could be the best option concerning the low damage of the outer surface and the salt accumulation in the vertical grooves. This render system and FH7 was named “emboço ventilado” and was chosen to be executed on a real-size masonry wall in chapter 7.

7. PERFORMANCE OF THE RENDER SYSTEM: "EMBOÇO VENTILADO"- LABORATORY WORK

7.1 Introduction

In historic buildings rising damp can be considered one of the major causes for materials decay [Fra10a]. Rising damp occurs due to the capillary suction in porous masonry materials such as brick, mortar and stone. The strong affinity of water with the capillary pores of those materials in the masonry and the lack of capillary cuts draw moisture up into the walls from the ground and make rising damp a very damaging mechanism [Fra10a, Gui10].

Indeed, the way water enters and moves through render and masonry mortars is related to moisture inside walls, salt crystallization problems, biological colonisation, etc [Vei09a]. When rising damp is associated with the presence of soluble salts, the result may be particularly severe with an extensive decay of the masonry materials and/or of the renders of the walls. In this case rising damp may carry dissolved soluble salts up into the walls where cyclic wetting and drying may take place due to temperature and relative humidity variations. Consequently crystallization, as efflorescence and crypto-florescence, within the pores of the masonry happens: when there is crypto-florescence, the detachment between the several layers of the render or between the render and the support, may occur; when there is efflorescence, lacunae or loss of cohesion, as sanding or crumbling, may occur in the evaporation zone [Vei09b].

To effectively deal with the problem there is the need of taking into consideration both rising damp and hygroscopic salts. On one side we know that in many cases even when we cut off rising damp the hygroscopic salts can still dissolve and recrystallize due to changes in the atmospheric humidity (the hygroscopic nature of salts attracts (liquid water or water vapour) moisture from humid atmospheres leading to their dissolution and an apparently dry wall becomes suddenly damp). On the other side, the techniques that have been used to minimize the effects of rising damp, such as: physical and chemical barriers [Mas93, Hen01, Fre02, Lub13, Hee95, Hee96] and electrosmotic barriers [Hen01, Fre02], have demonstrated to be in most cases of difficult application and considered ineffective due to the high thickness and heterogeneous composition of historic buildings' walls; the ventilation on the wall base, due to the difficulty of access or to the existence of render may be insufficient to eliminate the problems due to the presence of capillary rise [Vei09a,Tor07]; the electrocinetic removal of soluble salts [Fra10b, Ott07] has been demonstrating good laboratory results, but it is still necessary to test its efficacy considering the support, the render and in situ conditions; the development of transporting and accumulating systems [Gon07, Pet10a] are tested solutions, but they present practical difficulties as how to be materialized in each building.

In this study, an innovative accumulating render system was developed and its performance analyzed, to be used as replacement render in salt loaded historic masonries in the presence of moisture due to capillary rise.

This render system FH7, a “ventilated render” (“emboço ventilado” in Portuguese), is a two-layer render (base layer with brick powder and vertical grooves and outer layer with water repellent) and is expected to act as an accumulating render system in which the salt may crystallize in the base layer of the render system, avoiding contaminating the masonry or the outer layer (see chapter 6).

A full-scale stone masonry wall with lime bedding mortar and traditional lime render on one of the wall’s larger sides was used as substrate. The opposite large wall face was divided in four zones. One of the zones was rendered with FH7 render system and three more variation render systems were selected, for comparison. The masonry wall (350 cm x 279 cm x 50 cm), with traditional lime render in one of the larger faces, was first submitted to capillary rise with water and subsequent drying. After the render systems placement in the opposite larger face of the wall, an aqueous solution with NaCl was used for capillary absorption and drying.

The experiments described in this chapter were meant to test the compatibility, efficiency and durability of the “ventilated render” system in a full-scale masonry wall when submitted to the severe action of salt laden water (soluble salts and capillary water rise). It intended to verify if the render system: i) does not induce crystallization inside the masonry; ii) has higher durability compared with other render systems, due to allowing crystallization inside the vertical “grooves”; iii) does not produce damage on the outer layer contributing to good external appearance.

Chapter layout

The full-scale masonry wall execution and render systems materials and characteristics are presented in section 7.2. The testing procedure for the simulation of severe action of salt laden water on the masonry, during absorption and drying, before and after render systems application, is described in section 7.3. The effects of the severe action of salt laden water in the full-scale masonry wall before and after render systems application is analysed, based on the constant monitoring with probes of a humidity measuring device and hygrothermal probes connected to a data acquisition and recording system, in section 7.4. The damage evaluation is described in section 7.5 by means of: pull off tests in section 7.5.1; visual observation in section 7.5.2; optical microscopy analyses in section 7.5.3; Scanning electron microscopy analyses in section 7.5.4; Chlorides quantification in section 7.5.5; and pore size distribution and total connected porosity determination before and after experiments in section 7.5.6. In section 7.6 the render systems classification based on working principle and performance is presented. The concluding remarks of this chapter are presented in section 7.7.

7.2 Materials

The experimental work described in the following sections was carried out in LERevPa (Laboratory of Wall Covering) at the National Laboratory of Civil Engineering (LNEC) in Lisbon.

Full scale masonry wall with traditional lime render

A full-scale masonry wall from a previous study [Mat10a] was used, composed by calcareous stone and lime bedding mortar, rendered on one larger side (side A) with a traditional lime mortar 2 cm thick (1:3 binder:aggregate dosage by volume). The bedding mortars and traditional lime render (reference) present the same composition (AL). The main characteristics of stone (S) and bedding constituting the masonry wall are presented in Table 7.1. The wall (350 cm x 270 cm x 50 cm) was erected on a plastic tray, in order to make it possible to submit it to capillary rise with water and to subsequent drying.

Table 7.1 Characteristics of the substrate materials, stone (S) and bedding mortar (AL), and traditional lime (AL) render in one large side (standardized tests) – masonry wall [Mat08a]

	Density (kg/m^3)	Porosity (V/V%)	C[1] ($Kg/m^2.min^{1/2}$)	Sd[2] (m)	(Wmax)[3] (% m/m)
S (Stone)	2460	8.2	1.7*	n.d.	3.4
AL (reference lime render and bedding mortar)	1720	15.9	6.5*	0.06	18.0

[1] Water absorption coefficient between 0-30 min at 90 days; [2] Thickness of air layer with equivalent diffusion of water vapour; [3] Maximum water absorption determined by total immersion
* Matias et al. 2010 [Mat10]

Tested render systems

The mortar compositions that were tested in the lab test specimens were developped to resist the severe action of salt laden water, allowing a better behaviour in render systems in terms of capillary rise and drying capacity when water with NaCl is present (see chapter 5 and 6), before testing in the wall.

The aim of this full scale research is testing the efficiency and durability of the render system FH7. This render system compatible with historic constructions masonries, called “emboço ventilado”, was specially designed to allow the accumulation of salts in the base layer (with brick powder and grooves), without creating damage in the external surface of the outer layer (with water repellent) (see chapter 6).

Besides FH7 render system three more render systems (composed with base and outer layer) were selected to be tested in the full-scale masonry wall, for comparison: FNH7 similar to FH7 but without water repellent within the outer layer, and NH and H similar to FNH7 and FH7, respectively, although without grooves in the base layer. FH7 and FNH7 were selected from chapter 5. H and NH were not tested before and were used for comparison purposes. These four different render systems were applied on what can be considered the external face of the wall. With these render

systems the influence of “continuous vertical grooves” in the renders base layer and water repellent in outer layer on the efficacy and durability of the render system, was evaluated, considering the damage due to moisture and to salt crystallization along testing time.

The render system with traditional lime render (reference - AL) already existent on the opposite side of the masonry wall was used for comparison purposes with the new renders systems (FH7, H, NH and FNH7).

The composition of the render systems tested on the wall is described in Table 7.2 and of each single layer in Table 7.3.

Table 7.2 Composition of renders systems applied to the full-scale wall

Render system	Base layer	Existence of grooves	Layer between internal and external layer	External layer
AL (reference)	Al	-	-	Al
FH7	F7	Yes	Lime putty and fine sand	F1h
H	F7	-	-	F1h
NH	F7	-	-	F1
FNH7	F7	Yes	Lime putty and fine sand	F1

Table 7.3 Materials constituents of each render layer

Render layer	Composition
Al	Traditional air lime mortar
F1	Lime putty; pozzolanic addition; mixture of fine and medium size sand (1+3)
F1h	Lime putty with water repellent additive in the putty; pozzolanic addition; mixture of fine and medium size sand (1+3)
F7	Lime putty; pozzolanic addition and other admixtures; brick powder; medium size sand

The vertical grooves in the base layer should create an evaporation surface due to contact with the temperature and humidity of the surrounding ambience, inducing the accumulation of the salts in their interior, increasing the durability of the render system and allowing in the future the removal of the salts from the interior of the grooves (not tested in this work). Water repellent was used in the outer layer to inhibit salt solution transport to the surface of the render and avoid in this way the appearance of surface damage. According to Lubelli [Lub09], depending on the effectiveness of the water repellent and on where the water repellent is present (in the whole render system or only in the outer layer), salt will accumulate either at the substrate/render interface or in the inner part of the render system. The water repellent in the outer layer of the tested render systems should not allow the salts to come to the exterior (not resulting invisual de-characterization), when compared with the system without water repellent exterior layer.

FH7 render system is expected to increase the durability and efficiency of the system and allow salt accumulation within the grooves, reduce the superficial damage, as well as be compatible with the pre-existent materials.

The properties of the render mortars were determined on specimens prepared in the laboratory using the same materials as the ones of the several layers of the real-size masonry wall render (Table 7.4).

Table 7.4 Characteristics of the render layers (standardized tests) – full-scale wall

	Density (kg/m^3)	Porosity MIP (V/V%)	C[1] ($Kg/m^2.min^{1/2}$)	Sd[2] (m)	(Wmax)[3] (% m/m)
Side B					
Bedding mortar (traditional lime AL)	1720*	15.9	6.50*	0.06*	18*
Side A					
Outer layer (F1 formulation)	1590	19.1	1.26	0.07	15
Outer layer(F1h formulation)	n.d.	17.3	n.d.	n.d.	n.d.
Base layer (F7 formulation)	1580	24.7	1.41	0.07	43

[1] Capillary coefficient between 0-30 min at 90 days; [2] Air thickness of equivalent diffusion to 0,10 m of mortar; [3] Maximum water absorption determined by total immersion (90 days)
* Matias et al. 2010 [Mat10]

One of the secrets of lime renders' good performance is surely their ability to dry. Capillarity tests and water vapour permeability tests, which are meant to evaluate this property, do not permit to simulate the reality of applications, namely thickness, different coats and finishing. The values obtained lack sometimes the accuracy needed to distinguish between different renders with diverse performance in practice [Vei09a]. The drying capacity is particularly important when there is water on the foundations rising by capillarity.

In Figure 7.1 is a schematic representation of render systems applied in full-scale wall. In table 7.5 are defined the main objectives when comparing the new render systems (FH7, H, NH and FNH7).

Table 7.5 Main objectives comparing the tested render systems

Render systems	Objectives
FH7 and H	Compare the influence of the grooves on the moisture transport and moisture transport with the presence of NaCl and salt crystallization, with water repellent in the outer layer mortar.
NH and FNH7	Compare the influence of the grooves on the moisture transport and moisture transport with the presence of NaCl and the salt crystallization, without water repellent in the outer layer mortar.
FH7 and FNH7	Compare the influence of the water repellent in the outer layer on the moisture transport and moisture with NaCl transport and salt crystallization, with grooves in the base layer mortar.
N and NH	Compare the influence of the water repellent in the outer layer on the moisture transport and moisture with NaCl transport and salt crystallization, without grooves in the base layer.

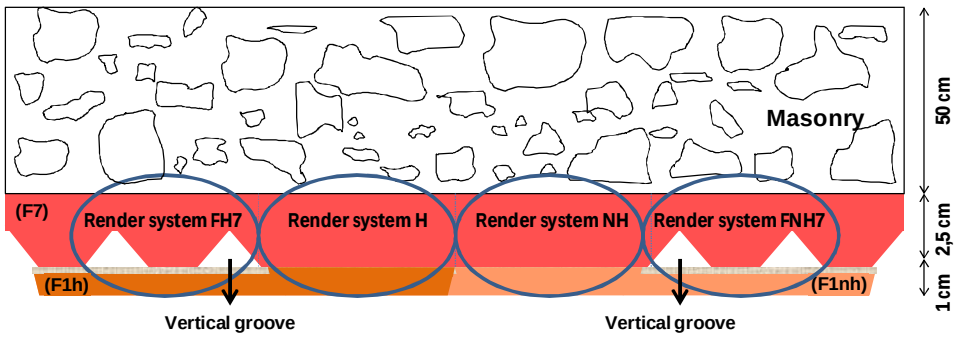

Fig. 7.1 Schematic representation of the render systems (FH7, H, NH and FNH7) in the full-scale masonry wall - upper view

Render systems application

The four render systems were applied on the real masonry wall with 3.5 cm of total thickness. The render systems have different formulations; two of them were executed with vertical “grooves” and so called “ventilated renders”. The lateral (right & left) sides of the wall was also rendered but with water repellent within the render to avoid preferential moisture transport in this direction.

The full-scale wall before the four render systems were applied (side B) and with traditional lime render on the other side (side A) is presented in Fig. 7.2.

Fig. 7.2 Full-scale masonry wall – larger side A without render (before the tested render systems placement) (left); Full-scale masonry wall – larger side B with traditional lime render (right).

First the masonry was brushed to remove loose material, after which the masonry was strongly wetted by spraying it with clean water. The water was allowed to soak in and then sprayed again; this procedure was repeated until the surface of the masonry (stone and bedding mortar) was thoroughly damp.

The regularization mortar (pre-dosed F7 formulation) was carefully applied on the wall to regularize the masonry surface. A render gun using air pressure was used to apply the render material on to the wall providing a consistent distribution of the material (Fig. 7.3). The thickness of this regularization layer was the necessary to provide a regular surface.

Fig. 7.3 Application of regularization mortar with render gun (left); Regularization of the support (middle); Final appearance of the masonry before base layer placement (right)

After this first phase, the base layer (pre-dosed F7 render) was executed with about 2 cm thickness (Fig. 7.4). This base layer was divided into four panels with the same width, in which the four render systems were applied. The render systems named FH7, H, NH, FNH7 were applied, respectively, from left to right (Figure 7.7). Grooves were executed in the base layer in the panels corresponding to render systems FH7 and FNH7. In the two panels of the middle, H and NH render systems, no grooves were executed. The bottom and top of the grooves were exposed to outside air allowing circulation of air within the grooves.

Fig. 7.4 Execution of base layer - F7 render (left); Final appearance of base layer of render systems H and NH (middle); Execution of vertical grooves in base layer of render systems FH7 and FNH7 (left).

After executing the grooves in panels FH7 and FNH7 a glassfibre mesh (2 mm x 2 mm) was applied to avoid filling the grooves and enable the adherence between base and outer layer. A mortar composed by lime putty and fine sand was used to close the glassfibre mesh. In Fig. 7.5 is the final aspect of the base layer of all render systems.

Fig. 7.5 Grid applied above the vertical grooves in base layer of render systems FH7 and FNH7 (left); Mortar used to close the grid (middle); Final appearance of base layer in al render systems (right).

The base layer was left to carbonate and in the next day the outer layer was executed. Water was sprayed on the base layer before the outer layer execution.

The outer layer of the two panels of the left was executed with F1h formulation (with water repellent additive in the putty) and the two of the right with F1 (without water repellent additive in the putty) render (Fig. 7.6). This layer was executed with 1 cm thickness. The excess of material was removed using a wood float, which results in an open texture on the render surface.

Fig. 7.6 Execution of outer layer with water repellent in render systems FH7 and H (left); Use of render gun for render systems execution of the outer layer (middle); Execution of outer layer without water repellent in render systems NH and FNH7 (right).

On the next day, a plastic trowel was used through the outer layer surface with a strong circular movement to consolidate and create a smooth polished finish (Fig. 7.7). Some shrinkage that was present on the outer layer surface was removed using this process. The render systems were sprayed twice a day with water during five days after the execution of the outer layer.

Fig. 7.7 Plastic trowel used to consolidate the outer layer (left); Spraying of the outer layer with water (middle); Final appearance of the render systems FH7, H, NH and FNH7 (right).

The render systems placed in the real masonry wall, with 3.5 cm of total thickness, were left to cure during 3 months before starting the cycles on it. In Figure 7.7 is the final appearance of the four render systems to be tested on the full-scale masonry wall. Schematic representations of the four render systems (FH7, H, NH and FNH7) can be found in Figure 7.8.

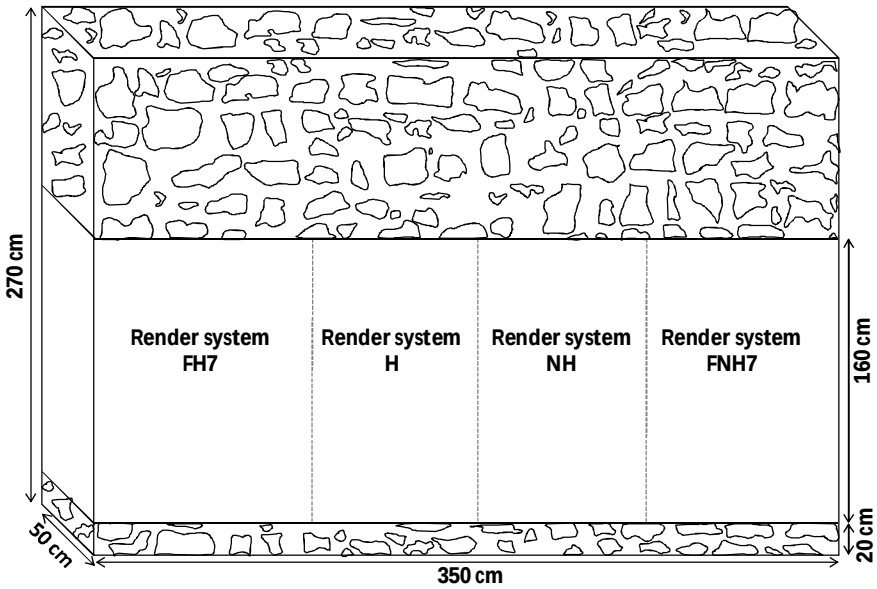

Fig. 7.8 Schematic representation of the render systems (FH7, H, NH and FNH7) in the full-scale masonry wall - frontal view

7.3 Simulating the severe action of salt laden water

In this chapter the experimental research program was performed in the laboratory, concerning the simulation of severe action of salt laden water, on the rendered full-scale masonry wall.

In real walls, salt solutions typically migrate from the interior of the masonry towards the outer surface of the plaster/render. Salt crystallization tests are absorption and drying tests performed on the full-scale masonry wall, by submitting the wall to rising damp with salt solution. They are in fact artificial ageing tests that simulate the severe action, as they evaluate salt damage and not only moisture transport. For these tests high concentration of salt solution and repeated contaminations, and changeable environmental conditions were used in order to achieve damage.

The existing salt crystallization tests are usually not effective to evaluate the renders resistance to salt crystallization [Wij07]. Most of these renders that contain water repellent additive show slow absorption and drying. Previous experiments showed that, in crystallization tests, damage appears only after several months of testing in laboratory and only in case of specimens contaminated with the most aggressive salts, like sodium sulphate [Wij02]. However, the same renders , when applied in practice, may show considerable damage a few years after application [Hee03].

To test the render systems, an experimental program was developed in the laboratory in non conditioned environment, simulating real conditions of sea water in a masonry wall. This wall was continuously monitored through the use of a humidimeter and after the render systems placement, also hygrothermal probes were used to allow the control of the test conditions.

The full-scale masonry wall was partially immersed with a 10 cm level that remained constant during the 2 months of rising. Before the render systems placement, during the 1st cycle the tap water was allowed to rise in the structure during 2 months until drying during 6 months; after the render systems placement during 2nd and 3rd cycles, NaCl aqueous solution with concentration 21g/L was used following the same procedure as in 1st cycle (Table 7.6).

Table 7.6 Description and duration of the cycles

Cycle	Render systems	Solution	Capillary rise	Drying
1st cycle	Before execution	Tap water		
2nd cycle	After execution	NaCl solution (21g/L)	2 months	6 months
3rd cycle	After execution	NaCl solution (21g/L)		

Rising damp with tap water

The wall was first submitted to capillary rise with tap water (during 2 months) and was subsequently left to dry (during 6 months) in order to allow a better understanding of the moisture transport by capillary rise through the masonry when rendered on one side with traditional lime render (reference render) in the presence of moisture due to capillary rise.

This 1st cycle was performed before the render systems placement and did not introduce any sodium chloride contamination in the masonry wall, so it did not produce any damage due to salt crystallization.

Rising damp with NaCl solution

After the render systems placement (FH7, H, NH and FNH7), the full-scale masonry wall was submitted to two cycles by artificial contamination with NaCl aqueous solution during 2 months followed by drying for 6 months after each cycle.

The concentration of 21g/l of NaCl aqueous solution was used to simulate real conditions of rising damp with sea water [Aug90]. The two cycles of capillary rise with NaCl aqueous solution and prior drying were performed to study the durability (salt damage) and efficiency (salt damage and moisture transport) of the studied render systems when moisture and salts are present, due to capillary rise, compared with the traditional lime render.

7.4 Effect of the severe action of salt laden water - Continuous monitoring

In order to investigate the influence of render systems on the absorption and drying behaviour of the substrate, when submitted to the severe action of salt laden, a full-scale masonry wall was continuously monitored through the use of Palma humidimeter and hygrothermal probes to allow the control of relative humidity and temperature (Figs. 7.9 and 7.10).

The continuous monitoring of the full-scale masonry wall during submission of the masonry to the severe action of salt laden was defined as an important part of the work based on the following considerations: i) drying behaviour strongly influences the salt accumulation and, in this case, render systems should allow substrate (full-scale masonry wall) to dry in order to avoid salts accumulation in it and ii) the presence of high moisture content after a long period of drying may reflect the presence of hygroscopic salts that are known to accumulate moisture inside it.

The probes were placed in the full-scale masonry wall and the temperature and relative humidity were recorded continuously over a period of 26 months. The humidimeter probes were used since the beginning of the tests (since the beginning of the 1st cycle of rising damp with H_2O before render systems placement). The hygrothermal probes to measure temperature and relative humidity were used since the drying in the 1st cycle.

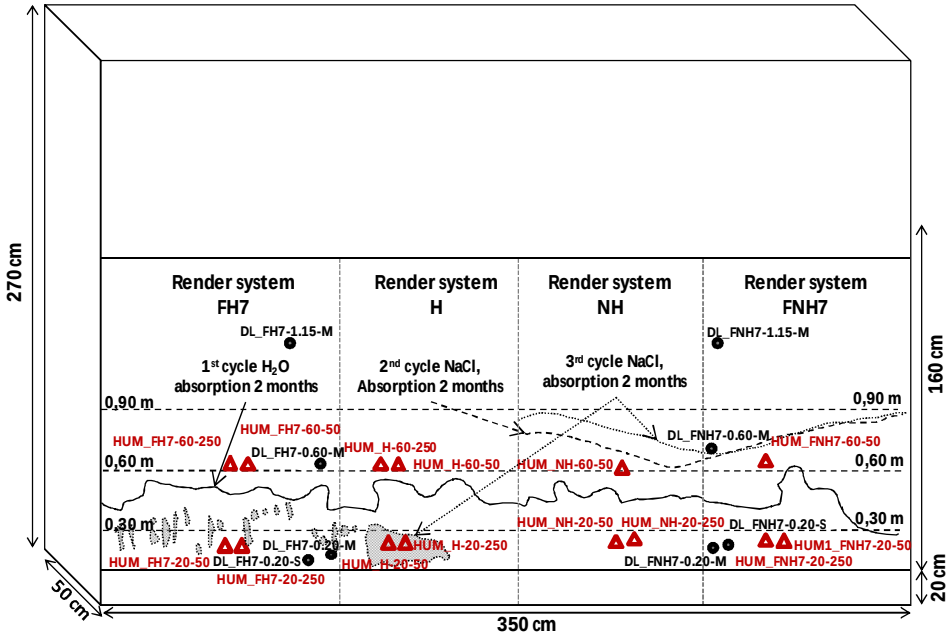

Fig. 7.9 Full-scale masonry wall: localization of FH7, H, NH and FNH7 render systems; total height obtained with capillary rise in all cycles before and after the placement of the render systems; location of hygrothermal and humidimeter probes

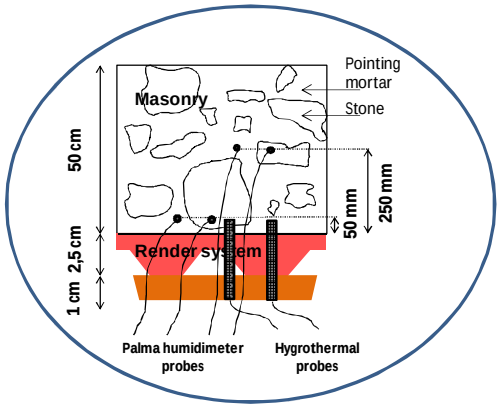

Fig. 7.10 Location of hygrothermal and Palma humidimeter probes in the masonry wall

The results obtained with humidimeter monitoring of the full-scale wall masonry are presented in section 7.4.1. The results obtained with hygrothermal probes are presented in section 7.4.2. Finally the discussion on continuous monitoring is presented in section 7.4.3.

7.4.1 Humidimeter monitoring

7.4.1.1 Probes

To evaluate the moisture content variation of the full-scale masonry wall's bedding mortar, Palma humidimeter probes (HUM), were inserted at different heights and depths in the masonry wall. The Palma humidimeter is an electric resistance based equipment designed by Palma, at LNEC, with simple components, for determination of the moisture content of mortars and concretes [Pal92, Pal05, Pal01]. The values are acquired by electrodes specially designed for it, which were connected to the Palma humidimeter data acquisition and recording equipment. The results were transferred to a computer equipped with specially designed software [Pal01]. The data obtained was then worked out through conventional commercial software. These probes were inserted at different heights (0.2 m and 0.6 m from the base of the masonry) and at 50 mm and 250 mm from the surface of the masonry wall (Table 7.7 and Figs. 7.11 and 7.12).

Table 7.7 Location of the humidimeter probes in the full-scale masonry wall

	Location	**Render system**			
		FH7	**H**	**NH**	**FNH7**
Palma humidimeter probes	0.2 m from the base (bedding mortar)	HUM_FH7-20-25, HUM_FH7-20-250	HUM_H-20-50, HUM_H-20-250	HUM_NH-20-50, HUM_NH-20-250	HUM_FNH7-20-250, HUM_FNH7-20-60
	0.6 m from the base (bedding mortar)	HUM_FH7-60-50, HUM_FH7-60-250	HUM_H-60-50, HUM_H-60-250	HUM_NH-60-50,	HUM_FNH7-60-50,
	50 mm from the surface of the render (bedding mortar)	HUM_FH7-60-50, HUM_FH7-20-50	HUM_H-60-50, HUM_H-20-50	HUM_NH-60-50, HUM_NH-20-50	HUM_FNH7-60-50, HUM_FNH7-20-50
	250 mm from the surface of the render (bedding mortar)	HUM_FH7-60-250, HUM_FH7-20-250	HUM_H-60-250, HUM_H-20-250	HUM_NH-20-250	HUM_FNH7-20-250

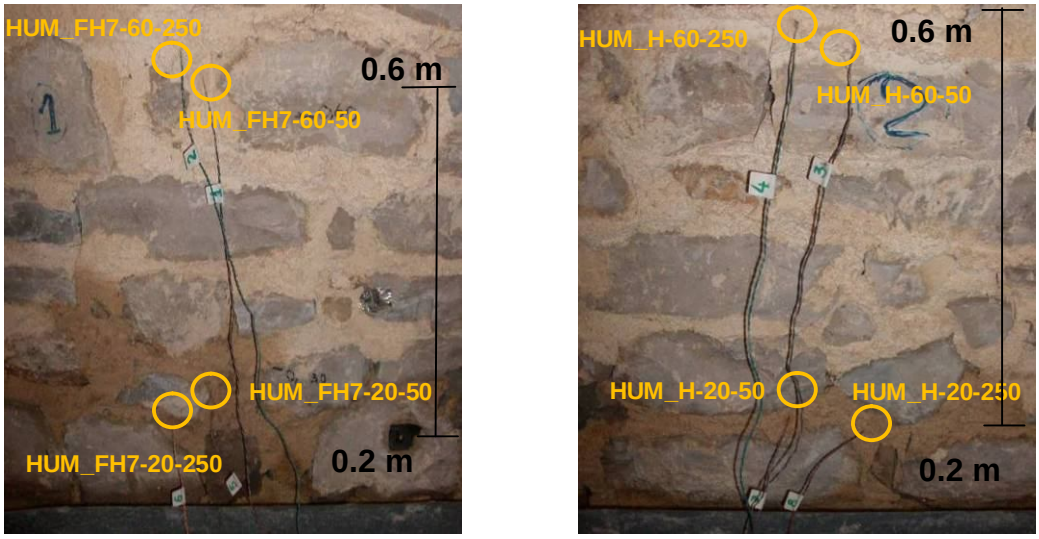

Fig. 7.11 Location of humidimeter probes in the full-scale masonry wall: a) zone where FH7 was executed (left), b) zone where H was executed (right).

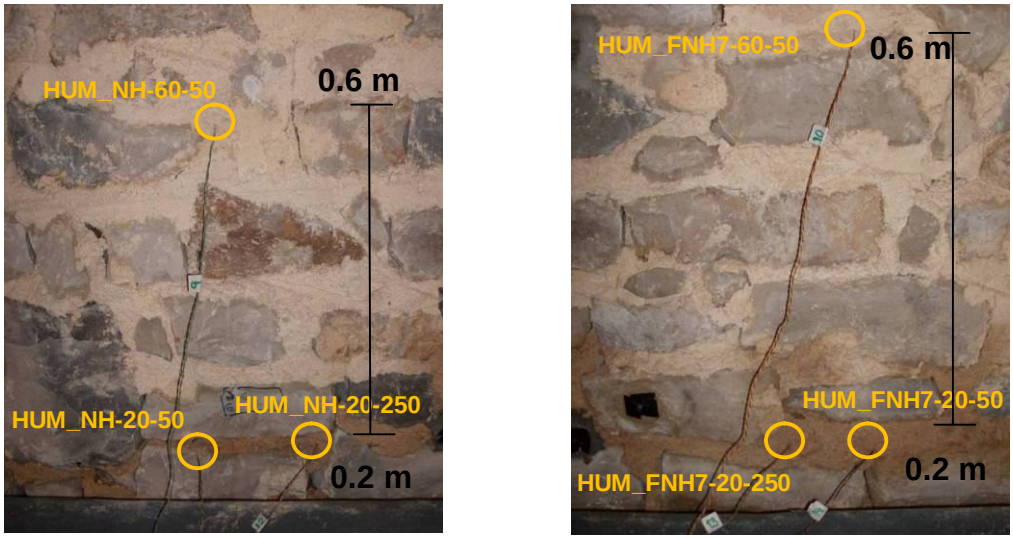

Fig. 7.12 Location of humidimeter probes in the full-scale masonry wall: a) zone where NH was executed (left), b) zone where FNH7 was executed (right).

7.4.1.2 Test method

The test method, developed for renders, consists on fixing the electrodes on a background, applying the render on it with the number and thickness of coats used in real work and, after curing, measuring and registering, with the humidimeter, the time needed for water with a determined pressure, to wet the background and then to dry out again, after taking out the source of water [Vei09a]. The method has been previously tried and improved in some studies developed at LNEC that permitted the definition and verification [Vei09a, Gon97, Vei98, Vei00] of some parameters to interpret the results obtained and to classify the material behaviour, such as W and D: W (wetting delay), measured in hours, is the time needed for the water to wet the background. It is defined as

the delay between the water pressure application on the specimen until the electric tension on the electrodes falls 5%; D (drying delay), measured in hours, is defined as the time during which the background stays wet, considering this happens while the electric tension is kept under 95% of the initial dry value. The test method is described in a Test Specification Sheet of LNEC [Vei09a].

In the present humidimeter tests the background used was the full-scale masonry. For correlation, capillarity tests and water vapour permeability tests for renders were used as defined by EN 1015-18 and EN 1015-19 tests, respectively.

The Palma humidimeter values are measured in unities related to electric tension (mV) based on the electric resistance of the water content of the mortar near the probe. If there is a high water content (at the end of capillary rise absorption) in the pores of the humid mortar, the electric resistance is low and the electric tension value read is 0 mV. During drying (the water content becomes lower) the electric resistance of the mortar increases and the electric tension is higher. The maximum electric tension read is around 1000 mV which means a "dry" mortar. In this stage it can be stated that the water content corresponds to the hygroscopic domain, in equilibrium with the surrounding ambient.

7.4.1.3 Results

The average values read by the humidimeter probes measured during the tests (1st, 2nd and 3rd cycles) are presented in Figures 7.13 to 7.17. The main results are compiled in Tables 7.8 to 7.10.

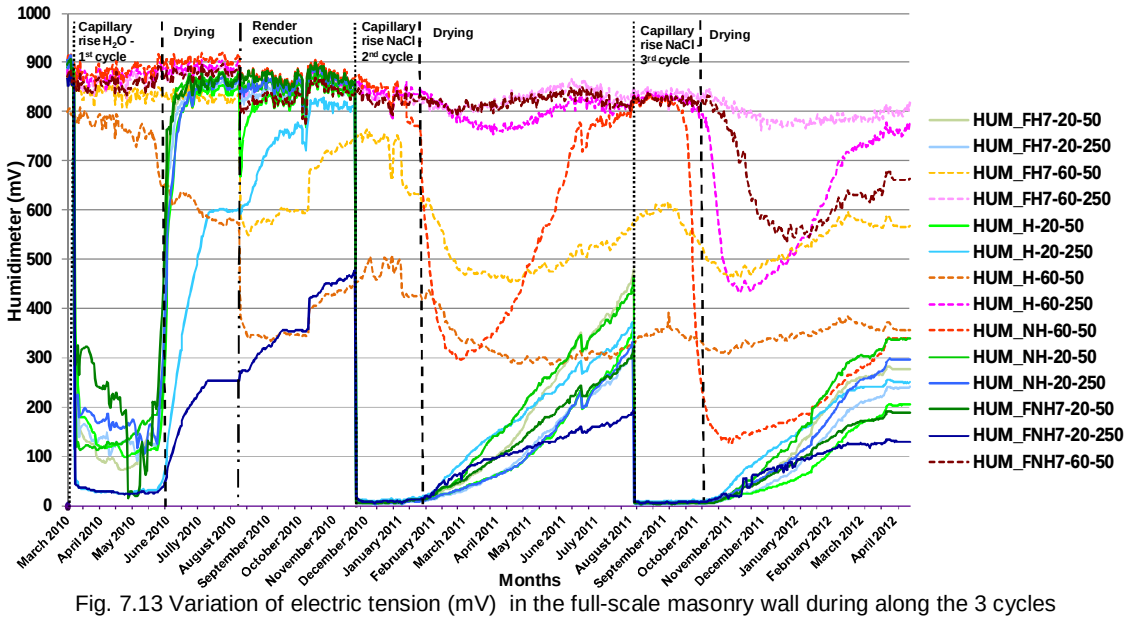

Fig. 7.13 Variation of electric tension (mV) in the full-scale masonry wall during along the 3 cycles

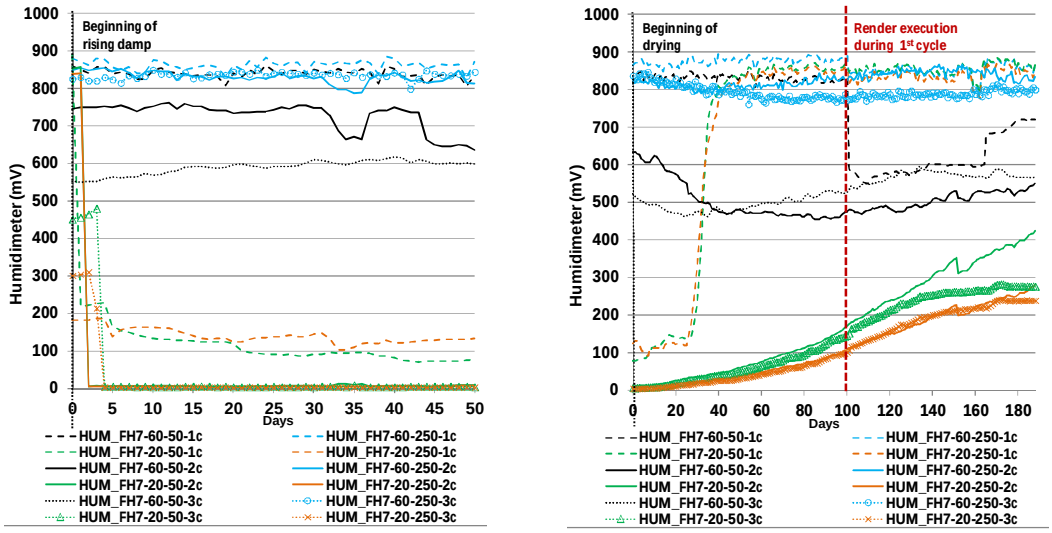

Fig. 7.14 Variation of electric tension (mV) in the full-scale masonry wall along the 3 cycles – FH7 location: a) capillary rise, b) drying.

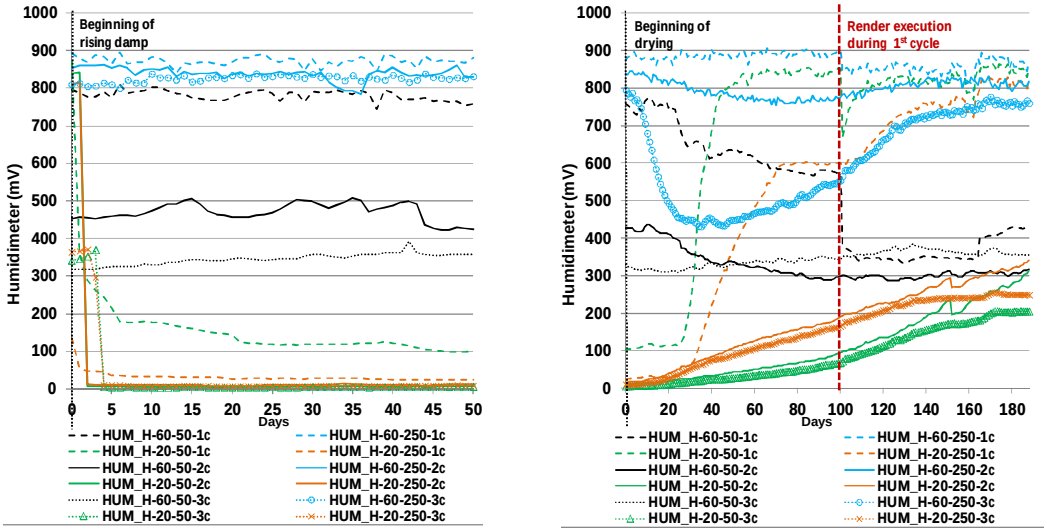

Fig. 7.15 Variation of electric tension (mV) in the full-scale wall along the 3 cycles – H location: a) capillary rise, b) drying.

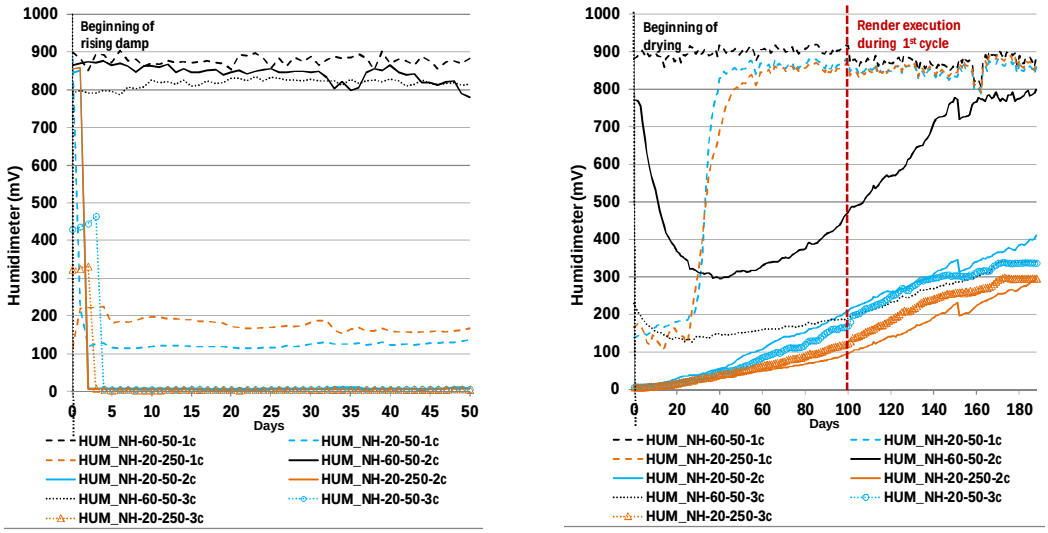

Fig. 7.16 Variation of electric tension (mV) in the full-scale wall along the 3 cycles – NH location: a) capillary rise, b) drying.

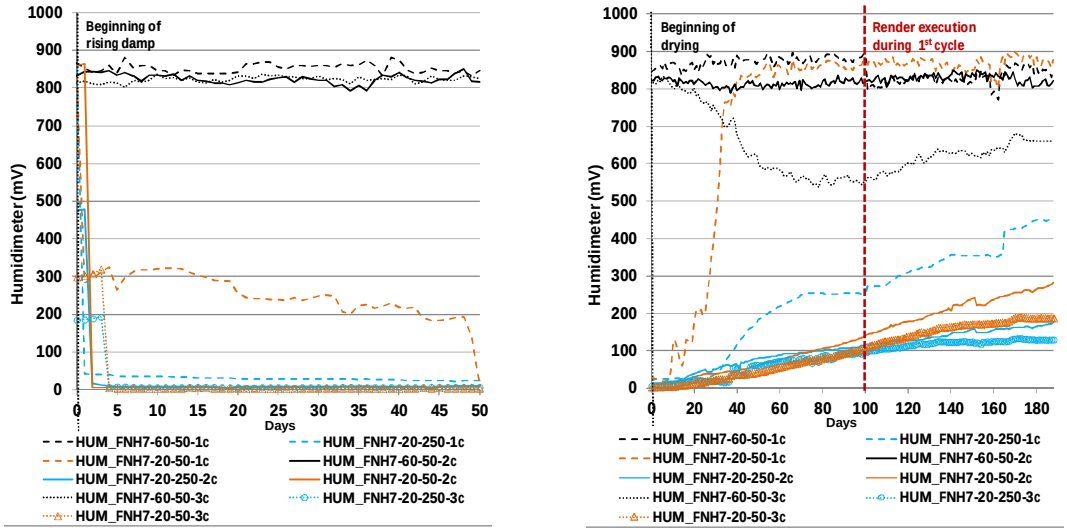

Fig. 7.17 Variation of electric tension (mV) in the full-scale wall along the 3 cycles – FNH7 location: a) capillary rise, b) drying.

Tables 7.8 to 7.10 present the wetting and drying delay in 1st, 2nd and 3rd cycles for each humidimeter probe.

Table 7.8 Results compilation - humidimeter probes in the masonry wall along 1st cycle (tap water; before render systems placement)

Probes	W (h)	D (days)	Obs.
HUM_FH7-60-50	>1440h (min 550 mV)	> 4320 h (max 750 mV)	not fully dry
HUM_FH7-60-250	(850 mV)	850 mV	dry
HUM_FH7-20-50	12h (min 100 mV)	960 h (40 days)	dry
HUM_FH7-20-250	6h (300 mV)(min 100 mV)	960 h (40 days)	dry
HUM_H_60-50	>1440h (min 350 mV)	> 4320 h (max 450 mV)	not dry
HUM_H-60-250	(850 mV)	850 mV	dry
HUM_H_20-50	24h (300 mV) (min 100 mV)	1200h (50 days)	dry
HUM_H-20-250	6h	160 days (3840h)	dry
HUM_NH-60-50	(900 mV)	900 mV	dry
HUM_NH-20-50	30h (100 mV)	40 days (960h)	dry
HUM_NH-20-250	24h (200 mV)	40 days (960h)	dry
HUM_FNH7-60-50	(850 mV)	850 mV	dry
HUM_FNH7-20-250	10h (50 mV) (min 0 mV)	> 4320h 180days (max 450 mV)	not dry
HUM_FNH7-20-50	6h (300mV) (min 0 mV)	30 days (720h)	dry

Table 7.9 Results compilation - humidimeter probes in the masonry wall along 2nd cycle (NaCl; after render systems placement

Probes	W (h)	D (days)	Obs.
HUM_FH7-60-50	>1440h (min 450 mV)	> 4320 h (max 550 mV)	not fully dry
HUM_FH7-60-250	(850 mV)	(850 mV)	dry
HUM_FH7-20-50	48h	> 4320 h (max 450 mV)	not dry
HUM_FH7-20-250	48h	> 4320 h (max 300 mV)	not dry
HUM_H_60-50	>1440h (min 400 mV)	> 4320 h (max 300 mV)	not dry
HUM_H-60-250	>1440h (min 750)	> 2880 h (max 800 mV)	dry
HUM_H_20-50	48h	> 4320 h (max 350 mV)	not dry
HUM_H-20-250	48h	> 4320 h (max 350 mV)	not dry
HUM_NH-60-50	>1440h (min 300 mV)	3840h	dry
HUM_NH-20-50	48h	> 4320 h (max 400 mV)	not dry
HUM_NH-20-250	48h	> 4320 h (max 300 mV)	not dry
HUM_FNH7-60-50	(850 mV)	(850 mV)	dry
HUM_FNH7-20-250	24h	> 4320 h (max 300 mV)	not dry
HUM_FNH7-20-50	48h	> 4320 h (max 200 mV)	not dry

Table 7.10 Results compilation - humidimeter probes in the masonry wall along 3rd cycle (NaCl; after render systems placement)

Probes	W (h)	D (days)	Obs.
HUM_FH7-60-50	>1440h (min 450 mV)	4320 h (máx 550 mV)	not fully dry
HUM_FH7-60-250	>1440h (min 800 mV)	> 4320 h (máx 800 mV)	dry
HUM_FH7-20-50	96h	> 4320 h (máx 250 mV)	not dry
HUM_FH7-20-250	72h	> 4320 h (máx 250 mV)	not dry
HUM_H_60-50	(300 mV)	> 4320 h (máx 350 mV)	not dry
HUM_H-60-250	>1440h (min 450)	> 4320 h (máx 800 mV)	dry
HUM_H_20-50	96h	> 4320 h (máx 200 mV)	not dry
HUM_H-20-250	96h	> 4320 h (máx 250 mV)	not dry
HUM_NH-60-50	>1440h (min 150 mV)	> 4320 h (máx 350 mV)	not dry
HUM_NH-20-50	96h	> 4320 h (máx 350 mV)	not dry
HUM_NH-20-250	72h	> 4320 h (máx 300 mV)	not dry
HUM_FNH7-60-50	>1440h (min 550)	> 4320 h (máx 650 mV)	not fully dry
HUM_FNH7-20-250	96h	> 4320 h (máx 150 mV)	not dry
HUM_FNH7-20-50	96h	> 4320 h (máx 200 mV)	not dry

Influence of the distance to the ground

In the capillary rise stage, the moisture introduced in the full-scale masonry wall easily reaches material around probes both at 50 mm and 250 mm from the surface of the masonry at a height of 0.2 m since 1st cycle. Only since the 2nd cycle does the water reach the height of 0.6 m. In 2nd and 3rd cycles the moisture took a bit longer to reach the material around the probes at 0.2 m, maybe due to the influence of the presence of render systems in these two cycles; also the read values were lower.

In 2nd and 3rd cycles, at 0.2 m the drying of the bedding mortars in the masonry was easier when compared with the height of 0.6 m, maybe due to the proximity to the base of the wall without render systems (the zone between 0 and 0.2 m in the wall was not rendered) allowing easier evaporation.

Influence of the presence of water repellent

The systems execution introduced some water in the masonry. This effect was mainly observed in the probes at 50 mm from the surface of the masonry (near the interface between the render systems and the masonry).

At 0.6 m from the base at 50 mm from the surface (HUM_FH7-60-50 and HUM_H-60-50) corresponding to render systems FH7 and H the read values were always below the drying limit; this drying difficulty may be due to the presence of water repellent in the outer layer of render systems FH7 and H, not allowing an easy evaporation of the moisture introduced in the masonry. The render systems FNH7 and NH allowed easier drying of the masonry.

At 0.2 m from the base in those render systems this behaviour was not observed (exception for HUM_H-20-50 in render system H that presented a drop but at the end of 1st cycle it was considered completely dry) may be due to the proximity of the wall base without render allowing an easier evaporation.

By visual observation, the moisture was around 0.4 m and 0.6 m from the base of the masonry after 2 months of capillary absorption in 1st cycle, along all length of the masonry; in 2nd cycle around 0.6 m and 0.8 m and in 3rd cycle around 0.7 m and 0.9 m in NH and FNH7 render systems; in 2nd and 3rd cycles no moisture was observed in the outer surface of FH7 and H render systems.

Influence of the presence of grooves

At 0.6 m from the base, the read values show that the water introduced in the masonry due to the render systems placement easily dried in the zone where render system FH7 was placed (HUM_FH7-60-50) when compared with the zone with H render system (HUM_H-60-50).

This behaviour was also observed on 2nd and 3rd cycles, during drying after capillary absorption of NaCl solution. At 0.6 m, at the end of 3rd cycle in the bedding mortar near the render system with water repellent (FH7), the moisture content near the render with grooves (HUM_FH7-60-50) is lower than in the material near the render system without grooves (H) (HUM_H-60-50); the same happens when comparing the material near the render systems without water repellent (FNH7 and NH).

The difference between them may be due to the presence of grooves in the base layer of FH7 and FNH7 render systems, allowing an easier evaporation of the moisture in the masonry, as well as in the render.

Influence of the cycles

In 1st cycle the water easily reached the masonry bedding mortar at 0.2 m from the base (read values between 0 and 100 mV) but did not get to 0.6 m height; it took around 30 and 50 days to dry completely. Some humidimeter probes located in the middle of the masonry wall (HUM_H-20-250 and HUM_FNH7-20-250) show different drying behaviour, taking longer to dry or even did not dry (HUM_H-20-250 dried after 160 days and HUM_FNH7-20-250 was not dry at the end of the cycle).

In 2nd cycle the masonry bedding mortar, at 0.2 m height, took longer to be affected by moisture and at the end of 6 months drying was not complete (read values between 200 and 450 mV); in the 3rd cycle it took even longer to get in touch with moisture and after 6 months drying the read values where even lower than in previous cycles (between 150 mV and 250 mV);

The fact that the material was not considered completely dry after 6 months drying after the 2nd and 3rd cycles may be due to the: presence of salts that may retain moisture and also to the influence of the render system with water repellent in the external layer (FH7 and FNH7).

As conclusion: i) In 1st cycle of capillary rise with water at 0.2 m, the moisture introduced in the real-size wall easily reaches the surface and the interior of the wall, but does not attain 0,60 m high; at the end of the test cycles, the bedding mortar of the masonry behind the render systems is not dry until 0.6 m (only at 0.6 m from the base and 250 mm deep the bedding mortar it was considered dry); ii) the existence of render systems with water repellent seems to reduce a bit the drying of the moisture/salt solution in the bedding mortar, in 1st cycle, although at the end of the tests similar drying behaviour was obtained in bedding mortar below all render systems; iii) the bedding mortar salt solution uptake seems to take longer (since 2nd cycle) than moisture uptake in 1st cycle with tap water.

7.4.2 Hygrothermal monitoring

7.4.2.1 Probes

To evaluate the temperature (T) and relative humidity (RH) in an air space confined inside the wall and in hygrothermal equilibrium with the masonry materials (bedding mortar or stone) that delimit the space, hygrothermal probes were introduced. These probes were inserted at different heights (0.2 m, 0.6 m and 1.2 m from the base of the masonry) and at 50 mm from the surface of FH7 and FNH7 render systems (Table 7.11 and Fig. 7.18). One of the probes was measuring the relative humidity and temperature in the laboratory during tests. The average values read by hygrothermal probes are presented in Figures 7.19 to 7.21. The values were measured every two hours.

Table 7.11 Location of hygrothermal probes

	Location	Identification
Hygrothermal probes	0.2 m from the base (in the stone)	DL_FH7-0.2-S DL_FNH7-0.2-S
	0.2 m from the base (in the bedding mortar)	DL_FH7-0.2-M DL_FNH7-0.2-M
	0.6 m from the base (in the bedding mortar)	DL_FH7-0.6-M DL_FNH7-0.6-M
	1.2 m from the base (in the bedding mortar)	DL_FH7-1.2-M DL_FNH7-1.2-M

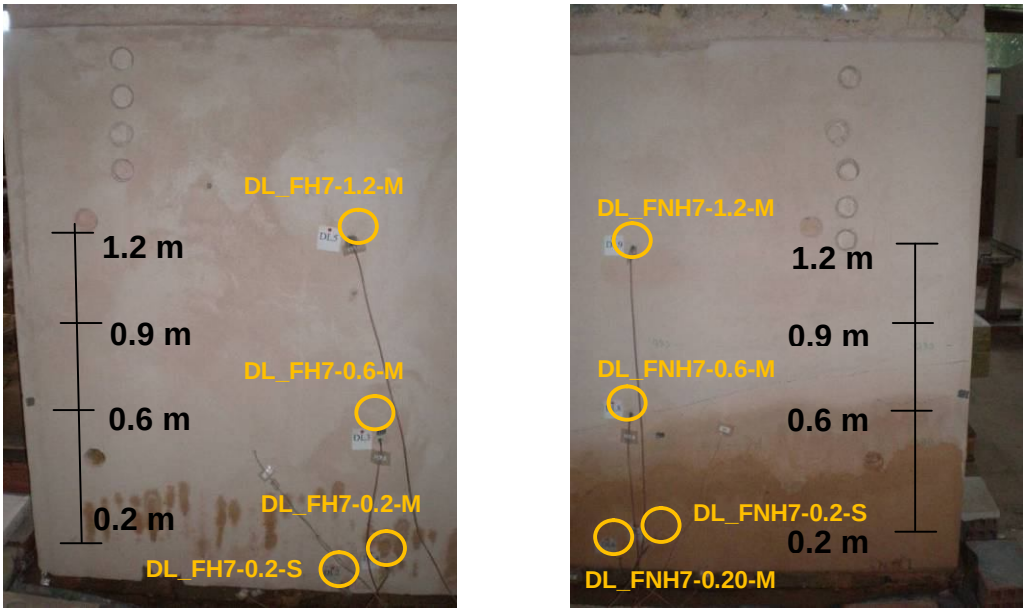

Fig. 7.18 Location of hygrothermal probes in the full-scale masonry wall after the render system execution: a)FH7 (left) and b) FNH7 (right).

7.4.2.2 Test method

Due to the reduced air volume inside the open spaces and to the low thermal and hydric capacity of the probes, it can be assumed that the temperature (T) and relative humidity (RH) read by the probes are the values of the air inside these spaces in equilibrium with the existent hygrothermal conditions of the surrounding material (bedding mortar or stone) .

When there is hygroscopic equilibrium of the water content in a saturated ambient (≈ 100% RH), the read values of relative humidity (RH) by the probes will be always 100%, independent of the quantity of absorbed water loss due to evaporation.

7.4.2.3 Results

The average values read by the hygrothermal probes during the tests (since drying stage in 1st cycle) are presented in Figs. 7.19 to 7.21. The values were measured every two hours. The main results obtained in 2nd and 3rd cycles with the hygrothermal probes are compiled in Tables 7.12 and 7.13.

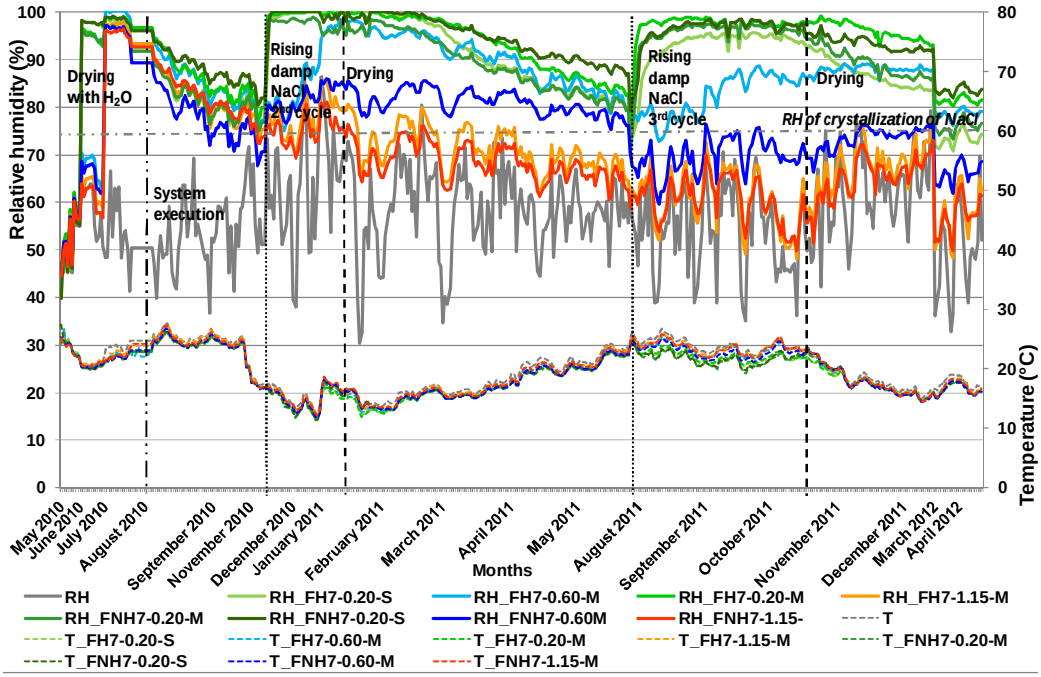

Fig. 7.19 Variation of relative humidity and temperature in the full-scale masonry wall along the 3 cycles

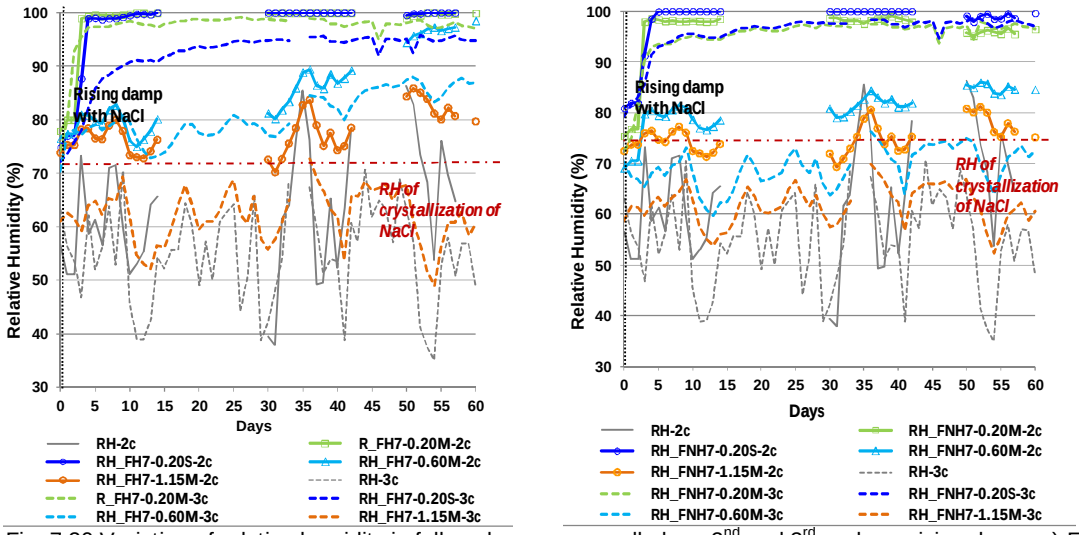

Fig. 7.20 Variation of relative humidity in full-scale masonry wall along 2nd and 3rd cycles – rising damp: a) FH7 location, b) FNH7 location

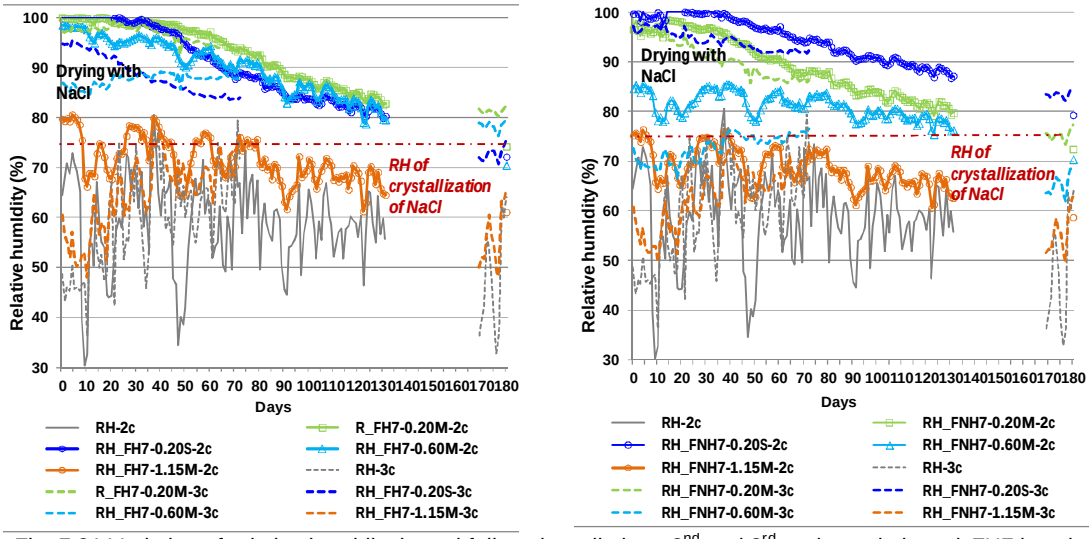

Fig. 7.21 Variation of relative humidity in real full-scale wall along 2nd and 3rd cycles – drying: a) FH7 location, b) FNH7 location

The results show that the temperature during absorption was a bit lower than in the drying stage, although it was also observed to be influenced by the external environment temperature.

In tables 7.12 and 7.13 the wetting and drying delay during 2nd and 3rd cycles are presented, described for each hygrothermal probe.

Table 7.12 Results compilation - hygrothermal probes in the masonry wall during 2nd cycle (NaCl; after render systems execution)

Probes	W (h) (> 95%)	D (days) (< 75%)	Observations
RH_FH7-1.20-M	(máx 80%)	80 days	Influenced by ambience RH both in absorption and drying
RH_FH7-0.6-M	50 days	> 130 days; < 180 days	Some influence of the ambience RH
RH_FH7-0.2-M	48h - 2days	180 days	No influence of the ambience RH
RH_FH7-0.2-S	72h - 3days	> 130 days; < 180 days	No influence of the ambience RH
RH_FNH7-1.2-M	(máx 80%)	10 days	Influenced by ambience RH both in absorption and drying
RH_FNH7-0.6-M	(máx 85%)	> 130 days; < 180 days	Some influence of the ambience RH
RH_FNH7-0.2-M	72h - 3days	> 130 days; < 180 days	No influence of the ambience RH
RH_FNH7-0.2-S	96h - 4days	> 180 days	No influence of the ambience RH

Table 7.13 Results compilation - hygrothermal probes in the masonry wall during 3rd cycle (NaCl; after render systems execution)

Probes	W (h) (> 95%)	D (days) (< 75%)	Observations
RH_FH7-1.2-M	(máx 75%)	-	Influenced by ambience RH both in absorption and drying
RH_FH7-0.6-M	(máx 88%)	> 180 days	Some influence of the ambience RH
RH_FH7-0.2-M	72h - 3days	> 180 days	No influence of the ambience RH
RH_FH7-0.2-S	960h - 40days	> 75 days; < 165 days	No influence of the ambience RH
RH_FNH7-1.2-M	(máx 70%)	-	Influenced by ambience RH both in absorption and drying
RH_FNH7-0.6-M	(máx 75%)	-	Some influence of the ambience RH
RH_FNH7-0.2-M	240h - 10days	170 days	No influence of the ambience RH
RH_FNH7-0.2-S	240h - 10days	> 180 days	No influence of the ambience RH

Influence of the distance to the ground

At 0.2 m and 0.6 m from the base of the masonry almost 100% of RH was read by higrothermal probes at the end of the absorption stage, in both 2nd and 3rd cycles. At 1.2 m the read RH was only influenced by the RH of the ambience; there is no influence of moisture due to salt solution absorption.

By visual evaluation, in the outer surface of the render system FH7 there was some localized moisture since 2nd cycle at the height around 0.3 m (corresponding to the massive part of the vertical grooves) and in the outer surface of render system H some localized moisture was observed in a large area between 0.2 m and 0.4 m. At the end of 3rd cycle visual degradation was observed in a large area of render system NH e FNH7 (drying front) between 0,50 m and 0,80 m; although in render systems FH7 and H the damage is reduced to a small area when compared with other render systems (Fig. 7.29).

This observation results are in accordance with the values read by the hygrothermal probes; at 0.6 m the RH varies up and down of the RH of equilibrium of NaCl (RH of NaCl crystallization is 75%), resulting in salt crystallization and dissolution of the salt at this height inducing higher degradation in this area of evaporation front; at 0,2 m the RH is always higher than 75%, so there is not so much salt crystallization in this area.

Influence of the water-repellent

A small difference was observed in relative humidity (RH) in the stone and bedding mortar of the masonry near render systems FH7 and FNH7 during 2nd and 3rd cycles; higher values at 0.6 m were read near FH7 render system when compared with FNH7; this may be due to the presence of water repellent in the outer layer of FH7 render system that reduces the evaporation.

Both at 0.2 and 0.6 m the results point out that the drying is a bit faster in FNH7 render system; again the existence of water repellent in the FH7 render system, reducing the evaporation rate, may be the explanation.

Influence of the cycles

At 0.2 m and 0.6 m, the RH at the masonry near the interface with the render systems FH7 and FNH7, at the end of the 3rd cycle is higher than the one at the end of the 2nd cycle; this may be due to the re-introduction of salts that may retain the moisture. The read values (RH_FH7-0.2-M and RH_FNH7-0.2-M) at 0.20 m near the interface with both systems show that the humidity takes almost the same time to get to this stage, although drying takes a bit longer in RH_FH7-0.2-M; the same happens when comparing RH_FH7-0.2-S and RH_FNH7-0.2-S. At 0.6 m, RH_FH7-0.6-M and RH_FNH7-0.6-M show that humidity takes longer to get to this stage when compared with

probes located at 0.2 m; RH_FH7-0.6-M gets higher humidity and takes longer to dry when compared with RH8. The different behaviour observed between RH_FH7-0.6-M and RH_FNH7-0.6-M, may be due to the presence of water repellent in the render system where the probe RH_FH7-0.6-M is located.

At 1.2 m the read values in RH_FH7-1.2-M and RH_FNH7-1.2-M show the influence of the ambience RH both in absorption and drying.

In the 2nd cycle absorption is faster to attain 95% RH than in the 3rd cycle at 0.2 m (RH_FH7-0.2-S, RH_FH7-0.2-M, RH_FH7-0.2-M and RH_FNH7-0.2-S); in the 3rd cycle the drying is slower and after 180 days the RH is higher than in the 2nd cycle.

7.4.3 Discussion on continuous monitoring

Although the tested render systems have compatible formulations with the full-scale masonry wall, the results from continuous monitoring during tests show that the render systems composition influences moisture/NaCl aqueous solution transport and drying behaviour of the masonry. The water repellent in the outer layer in contact with atmosphere and the grooves in the base layer of the render systems are the main factors influencing the masonry behaviour.

The execution of the render systems changed the absorption and drying behaviour of the masonry until 0.6 m of height; the time needed for water to reach the same height in the masonry increased and the evaporation rate reduced. The existence of water repellent in the outer layer somewhat increases the height attained by the moisture/NaCl aqueous solution in the masonry due to the evaporation reduction when compared with the system without water repellent, and reduces the moisture/solution transport through the outer layer. The grooves increase the evaporation rate when there is water repellent in the outer layer (render system FH7), although there is a small influence on drying rate of render systems without water repellent (render systems FNH7 and NH).

Another important variable that influences the probes read values is the presence of soluble salts (NaCl). These salts were introduced in the masonry and render systems in the 2nd and 3rd cycles and contribute to change their drying behaviour.

It is important to state that the 3rd cycle simulates a very aggressive stage with severe degradation for the render system, meaning that the results obtained at the end of this cycle may already represent the damage of the render system, affecting its behaviour.

The use of higrothermal probes enables the understanding of the absorption and drying capacity of bedding mortar and stone in the masonry near the interface with the render systems FH7 and FNH7; the use of humidimeter probes at the bedding mortar of the masonry (at 50 mm and 250

mm from the interface with the render systems FH7, H, NH and FNH7) enables the understanding of the influence of the four different render systems studied in the drying capacity of the masonry.

7.5 Effect of the severe action of salt laden water - damage evaluation

To study the influence of salt damage on the render systems, since the 2nd cycle, NaCl aqueous solution was used. The salt solution was absorbed through the masonry and render systems by capillary rise and salt crystallization was observed on the outer surface of the render systems during drying on the 2nd and 3rd cycles. The salt crystallization was confirmed both by visual observation during drying and by the prompt detachment of particles during rising damp and that were accumulated in the solution in the base of the wall.

Salt efflorescences became visible since the first month of drying on 2nd cycle both on the surface of the traditional render as well as on the surface of the render systems. Some generalized efflorescence started to be visible on the traditional lime render and on the FNH7 and NH render systems, while on FH7 and H render systems the presence of efflorescences was confined to a small region on the base of the render.

Fig. 7.22 Damage observation on the traditional lime render on the full-scale masonry wall: a) after 1 month drying on 2nd cycle (left); after 6 months drying on 3rd cycle (right).

In one of the larger sides of the full-scale masonry wall, traditional lime render was executed. Fig. 7.22 shows scaling and crumbling mainly between 0.5 and 0.7 m from the ground during drying in 2nd cycle: after the 1st month of drying, generalized hazy efflorescence was observed; after 6 months of drying, efflorescence and crumbling became more intense and generalized. In 3rd cycles, in the beginning of drying the damage due to salt crystallization was more evident and after 6 months of drying, efflorescence and crumbling were very intense and generalized.

Fig. 7.23 Damage observation on render systems FH7, H, NH and FNH7 on the full-scale masonry wall: a) after 1 month drying on 2nd cycle; b) after 6 months drying on 3rd cycle

On the other larger side of the full-scale masonry wall, the render systems FH7, H, NH and FNH7 were placed. In Fig. 7.23 it is observed that salt efflorescences increased with time during 2nd and 3rd cycles, and at the end became generalized through the surface of NH and FNH7 render systems (render systems without water repellent in the outer layer). Render systems NH and FNH7 after 1 month drying on 2nd cycle showed efflorescences and scaling (mainly between 0.5 and 0.7 m from the base) in the drying front; after 6 months of drying efflorescences and crumbling were observed. After 1 month drying on 3rd cycle crumbling became visible in higher degree; after 6 months drying crumbling was generalized, efflorescences as dense crust that could not be brushed were observed on the surface and sanding was observed on the surface below (up to0.70 m from the base of the wall).

The damage observed due to salt crystallization in the surface of all render systems, after drying on the 2nd cycle (0 and 15 days, 1 and 6 months) and after the 3rd cycle (0, 1 and 6 months) is presented in section 7.5.1.The influence on the damage of NaCl crystallization is discussed based on the distance to the ground, on the presence of water repellent, on the dissolution/crystallization cycles and on the presence of grooves.

The location of NaCl crystallization on the several layers of the studied render systems is described in section 7.5.2, based on optical microscopy analyses (OM) and scanning electron microscopy analyses (SEM/EDS).

In section 7.5.3 the chlorides quantification in each layer of each render system is determined by Potentiometric titration to analyse differences on the salt accumulation of each render system layer at the end of tests. In that section the influence of the distance to the ground, of the presence of water repellent, of the dissolution/crystallization cycles and of the presence of vertical grooves for the results obtained is discussed.

Pore characteristics of each render layer, determined by mercury porosimetry, are presented in section 7.5.4. The influence of total connected porosity and pore size distribution on the damage observed in each render system after experiments is discussed.

7.5.1 Pull-off tests

At the end of the 2nd cycle, pull-off tests were performed following EN – 1015-12:2000, to evaluate the type of rupture and if it happens between the outer layer of render systems and the base layer (FH7 and FNH7 render system) or between the render and the support (H and NH render systems). Pull-off tests were performed before the cycles, because since the 2nd cycle the loss of cohesion on the surface outer layer of FNH7 and NH render systems didn´t allow the execution of the test; also some difficulty associated to the samples execution for pull-off tests. The tests were carefully executed and the equipment for samples execution for pull off tests had to be adapted to be able to be used on the wall, specially without damaging FNH7 and FH render systems where grooves were executed (Fig. 7.24).

Fig. 7.24 Pull-off tests on render systems: a) equipment adaptation (left), b) careful execution of circular tears (middle) and, c) pull off test (right).

The tests were performed before absorption/drying tests. On AL, NH and FNH7 render systems some samples were broken during perforation. On Table 7.14 is described the type of rupture observations in samples after pull-off tests.

Table 7.14 Pull-off tests on render systems on the full scale masonry wall

Side A – reference	Side B - Render systems			
AL	FH7	H	NH	FNH7
				
				

Table 7.14 (Cont.) Pull-off tests on render systems on the full scale masonry wall

Side A – reference	Side B - Render systems			
AL	FH7	H	NH	FNH7
				
Evaluation				
AL	Adhesive rupture: between render and the support (values between 0 and 0,10 MPa)			
FH7	Adhesive rupture: between outer and base layer (in the glassfiber mesh) (values not determined)			
H	Adhesive rupture: between outer and base layer (values between 0 and 0.15 MPa)			
NH	Adhesive rupture: between outer and base layer (values between 0 and 0.10 MPa)			
FNH7	Adhesive rupture: between outer and base layer (in the glassfiber mesh) (values not determined)			

In FH7, H7, NH7 and FNH7 renders adhesive rupture was observed between outer and base layer, meaning that the adherence to the masonry is higher than the adherence between render layers. In FH7 and FNH7 (renders with grooves in the base layer) it was not possible to determine a pull-off test value due to low area connecting base and outer layer in the testing zone, while in H7 and NH7 the values were between 0 and 0.15 MPa and 0 and 0.10 MPa, respectively.

In AL render system the adhesive rupture was observed between the render and the masonry, and as result, the adherence to the support is lower than the adherence between render layers. The result obtained for pull-off test in AL render was found between 0 and 0.10 MPa and as result the adherence of this render to the masonry can be considered the lowest among the tested renders, as FH7, H7, NH7 and FNH7 have all the same base layer composition.

7.5.2 Visual observation of the damage due to salt crystallization

Salt damage was observed on the outer surface of the render systems and traditional lime render. Differences were observed on damage due to salt crystallization on the tested render systems, especially during drying on 2nd and 3rd cycles. The main differences observed in damage due to salt crystallization are described in Tables 7.15 and 7.16. The discussion on the damage patterns due to salt crystallization is performed based on the influence of: i) the distance to the ground, ii) the presence of water repellent on the outer surface of the render systems, iii) the existence of vertical grooves within the base layer and iv) the number of cycles.

Table 7.15 Overview of the damage due to salt crystallization after 0, 15, 30 and 120 days of drying on the outer layer surface of the render systems and traditional lime render in the masonry wall (2nd cycle)

Days	Side B - Reference	Side A - Render systems			
	AL	FH7	H	NH	FNH7
0	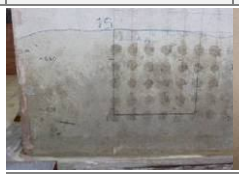				
	Efflorescence	Localized efflorescence	Localized efflorescence	Efflorescence	Efflorescence
15					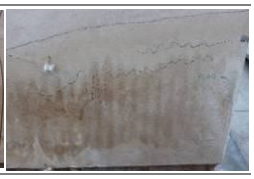
	Efflorescence and some scaling	Localized efflorescence	Efflorescence	Efflorescence	Fluffy efflorescence
30					
	Generalized efflorescence, scaling and crumbling	Localized scaling (grooves)	Efflorescence, localized scaling (bottom)	Delamination and scaling; efflorescence as air crystals	Delamination, scaling; efflorescence as air crystals
120			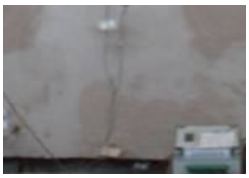		
	Efflorescence and crumbling ++	Localized scaling +	Localized scaling +	Scaling and delamination +; efflorescence +	Scaling and delamination +; efflorescence +

Table 7.16 Overview of the damage due to salt crystallization after 0, 30 and 120 days of drying on the outer layer surface of the render systems and traditional lime render in the masonry wall (3rd cycle)

Days	Side B - Reference	Side A - Render system			
	AL	FH7	H	NH	FNH7
0					
	Efflorescences and crumbling +++	Localized scaling ++ Localized efflorescence ++	Localized scaling and spalling ++ Localized efflorescence ++	Delamination and scaling +++; Crumbling +++ efflorescence ++	Delamination and scaling +++; Crumbling +++ efflorescence ++
30					
	Efflorescences and crumbling +++	Localized scaling ++ Localized efflorescence ++	Localized scaling and spalling ++ Localized efflorescence ++	Delamination and scaling +++; Crumbling +++ efflorescence ++	Delamination and scaling +++; Crumbling +++ efflorescence ++
120					
	Efflorescences ++++ and crumbling ++++ Sanding +++	Localized scaling +++ Localized efflorescence +++	Localized scaling and spalling ++ Localized efflorescence ++	Delamination and scaling ++++; Crumbling ++++ efflorescence ++++; sanding +++	Delamination and scaling ++++; Crumbling ++++ efflorescence ++++; sanding +++

After 6 months of drying on the 3rd cycle, severe damage due to salt crystallization was observed on render systems NH and FNH7 and on traditional lime render. The damage appears as generalized bulging of the surface and loss of cohesion (sanding) mainly between 0.3 m and 0.9 m from the base of the masonry wall.

Influence of the distance to the ground

Salt crystallization was noticed 15 days after the beginning of drying in the 2nd cycle. The surface damage in each render system corresponds to the zones where moisture stains were noticed during absorption stage in each cycle. The moist, due to salt solution absorption through the base of the wall, got different heights depending on the render system. The zone where damage was observed in the outer surface of each render system was similar in both 2nd and 3rd cycles.

At the end of the 3rd cycle it was observed that damage occurs mainly in a zone that is alternately wet and dry, between 0.3 m and 0.9 m from the ground on NH and FNH7 render systems and on AL, traditional render. This last render presented higher damage degree than the others. This

behaviour was already described by Wijffels at al. [Wij07a]. Some located damage was observed between 0.3 m and 0.6 m from the ground on FH7 and H render system.

Influence of the presence of water repellent

The presence of water repellent in render systems FH7 and H reduces evaporation and prevents an easy salt solution transport through the outer layer of the render systems to the surface. Thus, at the end of 3rd cycle, the damage at the outer surface of those render systems is reduced to located areas of the surface as can be observed in table 7.16. The damage in the outer surface of the other render systems without water repellent in the outer layer is observed to be in much more extent, as they can act as transporting systems where soluble salts can easily crystallize on the outer surface.

Influence of the cycles

The higher contribution to damage from the crystal growth was mainly observed during drying in 3rd cycle.

Influence of the presence of vertical grooves

The contribution of the grooves on the reduction of salt damage was observed in render system FH7 where some damage was observed just in small zones on the outer surface near the grooves, while in H render system a bigger damage zone on the outer surface was observed. In render system FNH7 and NH, the vertical grooves have no influence on surface damage and both render systems show high surface damage degree.

7.5.3 Location of salt crystallization - Optical microscopy analyses

The salt crystallization was deeply investigated by means of optical microscope visualization at the end of 2nd and 3rd cycles. At the end of the 2nd cycle the salt crystallization evaluation was only made at 0.30 m from the base of the masonry, because at the outer surface some crystallization was observed at this height (Table 7.17). At the end of the 3rd cycles the evaluation was made at 0.3, 0.6 and 1.2m from the base of the masonry (Table 7.18). At each height, the observations were made on: a) the outer layer surface, b) interface between outer and base layer and c) inside the vertical grooves within the base layer.

Table 7.17 Optical microscope observations: salt crystallization in the several layers of the render systems and traditional lime render in the masonry wall, at the end of the 2nd cycle of absorption/drying

	Side A - reference	Side B - Render system			
	AL	**FH7**	**H**	**NH**	**FNH7**
					
Description	Generalized efflorescence ("hair crystals") and sanding	Localized efflorescence associated to sanding in the grooves zone	Localized efflorescence associated to sanding	Generalized efflorescence associated to sanding in the evaporation zone	Localized efflorescence associated to sanding in the grooves zone
Crystallization evaluation	(+++)	(+)	(+)	(++)	(++)
Optical microscope observation		**at 0.3 m from the base**			
External layer (x7)	n.o.				
External layer (x70)	n.o.				
Description		No crystallization	No crystallization	Efflorescence as "air crystals and dense crust"	Generalized efflorescence as "air crystals" and localized "dense crust"
Crystallization evaluation		(-)	(-)	(+++)	(+++)
Interface between external and internal layer (x70)	n.o.			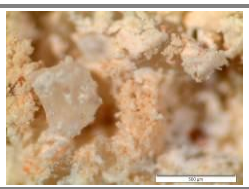	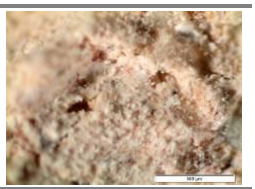
Description		No crystallization	No crystallization	Crystallization	Crystallization
Crystallization evaluation		(-)	(-)	(+)	(+)
Inside the holes (x70)	n.o.		-	-	
Description		Some crystallization /efflorescence			Some crystallization /efflorescence
Crystallization evaluation		(++)			(++)

*The crystallization evaluation range: (-) no crystallization; (+) some crystallization located as "hair crystals"/whitening of the surface; (++) crystallization generalized as "hair crystals" (fluffy efflorescence); (+++) dense crust crystallization (powdery fflorescence); (++++) dense crystallization associated with render sanding ; (+++++) dense crystallization associated with render crumbling

** n.o. - Not observed

At 0.3 m from the base, at the end of 2nd cycle some crystallization was observed on the outer surface and at the interface between outer and base layer on render systems FNH7 and NH. On both render systems FH7 and FNH7 crystallization as “hair crystals” was observed inside the vertical grooves.

Table 7.18 Optical microscope observations: salt crystallization in the several layers of the render systems and traditional lime render in the masonry wall, at the end of the 3rd cycle of absorption/drying

	Side A - reference	**Side B - Render system**			
	AL	**FH7**	**H**	**NH**	**FNH7**
					
					
Description	Generalized efflorescence as “dense crust” and render sanding and crumbling	Localized efflorescen-ce as “dense crust” and sanding	Localized efflorescen-ce as “dense crust” and sanding	Localized efflorescen-ce and dense crust associated to sanding and render delamina-tion (evaporation zone)	Localized efflorescence and dense crust associated to sanding and render delamination (evaporation zone)
Crystallization evaluation	(+++++)	(++)	(+++)	(++++)	(++++)

Table 7.18 (Cont.) Optical microscope observations: salt crystallization in the several layers of the render systems and traditional lime render in the masonry wall, at the end of the 3rd cycle of absorption/drying

	Side A - reference	Side B - Render system			
	AL	**FH7**	**H**	**NH**	**FNH7**
Optical microscope observation at 1.2 m from the base					
Outer layer (x7)	n.o.	n.o.			n.o.
Outer layer (x70)	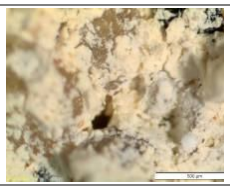	n.o.		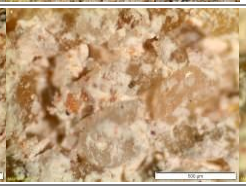	
Description	No crystallization	-	No crystallization	No crystallization	No crystallization
Crystallization evaluation	(-)	-	(-)	(-)	(-)
Interface between outer and base layers (x70)	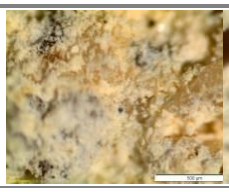				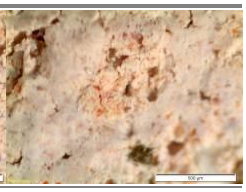
Description	No crystallization	No crystallization	No crystallization	No crystallization	No crystallization
Crystallization evaluation	(-)	(-)	(-)	(-)	(-)
Inside vertical grooves (x70)	-		-	-	
Description	No crystallization	No crystallization	No crystallization	No crystallization	No crystallization
Cryst. evaluation	(-)	(-)	(-)	(-)	(-)

Table 7.18 (Cont.) Optical microscope observations: salt crystallization in the several layers of the render systems and traditional lime render in the masonry wall, at the end of the 3rd cycle of absorption/drying

Side A - reference	Side B - Render system			
AL	**FH7**	**H**	**NH**	**FNH7**
Optical microscope observation at 0.6 m from the base				
Outer layer (x7)	n.o.				
Outer layer (x70)					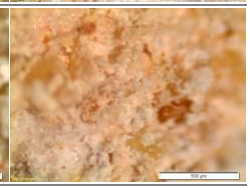
Description	Crystallization as “hair crystals”	No crystallization	No crystallization	Crystallization as “hair crystals”	Crystallization as “hair crystals”
Crystallization evaluation					
Interface between outer and base layers (x70)	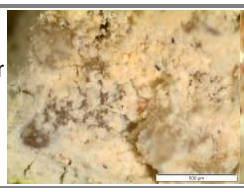			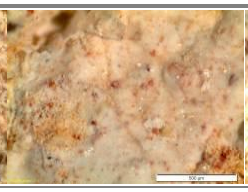	
Description	Generalized agglomeration of crystals	Generalized crystallization	Generalized crystallization	Crystallization as “dense crust”	Generalized crystallization “as dense crust and hair crystals”
Crystallization evaluation	(+++)	(++)	(++)	(+++)	(+++)
Inside vertical grooves (x70)	-		-	-	
Description		Generalized crystallization			Dense crust
Crystallization evaluation		(++)			(+++)

Table 7.18 (Cont.) Optical microscope observations: salt crystallization in the several layers of the render systems and traditional lime render in the masonry wall, at the end of the 3rd cycle of absorption/drying

	Side A - reference	Side B - Render system			
	AL	FH7	H	NH	FNH7
Optical microscope observation at 0.3 m from the base					
Outer layer (x7)					
Outer layer (x70)		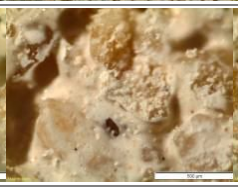	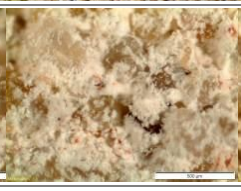		
Description	Generalized efflorescence as “hair crystals” and dense crust	Localized efflorescence (dense appearance)	Localized efflorescence	Generalized efflorescence as “dense crust”	Generalized efflorescence as “dense crust”
Crystallization evaluation	(+++++)	(++)	(+++)	(++++)	(++++)
Interface between outer and base layers (x70)	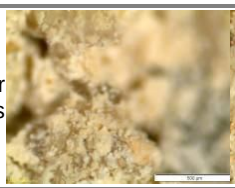	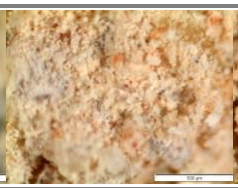			
Description	Generalized crystallization (dense appearance	Some crystallization (pulverulent crystallization)	Generalized crystallization (pulverulent crystallization)	Generalized crystallization (dense appearance)	Generalized crystallization (dense appearance)
Crystallization evaluation	(++)	(++)	(++)	(++)	(++)
Inside vertical grooves (x70)	-		-	-	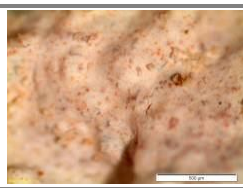
Description		Crystallization as “hair crystals and dense crust” (pulverulent appearance)			No crystallization observed (dense appearance)
Crystallization evaluation		(++)			(-)

*The crystallization evaluation range: (-) no crystallization; (+) some crystallization located as “hair crystals”/whitening of the surface; (++) crystallization generalized as “hair crystals” (fluffy efflorescence); (+++) dense crust crystallization (powdery efflorescence); (++++) dense crystallization associated with render sanding ; (+++++) dense crystallization associated with render crumbling
** n.o. - Not observed

No damage or salt crystallization was observed in render systems at 1.2 m from the base of the masonry until the end of the tests.

At 0.6 m damage associated to salt crystallization was observed at the end on 3rd cycle: at the outer surface crystallization “hair crystals” were observed in render systems FNH7, NH and AL; at

the interface, all studied render systems presented crystallization but more intense on render systems FNH7, NH and AL; a dense crust was observed inside the vertical grooves on render system FNH7 and generalized efflorescence on FH7.

At 0.3 m, damage due to salt crystallization was observed at the end of the 3rd cycle: at the outer surface on render systems FNH7, NH and AL generalized efflorescences as dense crust and localized efflorescence on render systems FH7 and H; at the interface between base and outer layer denser crystallization on render systems FNH7, NH and AL and less on FH7 and H; inside vertical grooves dense crust crystallization was observed on both FNH7 and FH7 render systems, but denser in FNH7 render system.

The vertical grooves are observed to allow salt crystallization inside them; presence of water repellent in the outer layer of FH7 and H render system does not seem to increase the salt accumulation between base and outer layer when compared with render systems without water repellent (FNH7 and NH); efflorescences as dense crust were observed in the surface of render systems without water repellent (FNH7 and NH) and the presence of vertical grooves in FNH7 render system does not seems to have influence on salt accumulation in the surface; in render systems with water repellent (FH7 and H) localized efflorescences were observed in the outer surface and the existence of vertical grooves seems to reduce the surface damage area (in the localized damage zones the type of crystallization was observed to be similar in FH7 and H render systems).

7.5.4 Location of crystallization - Scanning Electron Microscopy analysis (SEM/EDS)

Based on results obtained from previous sections, 7.52 and 7.53, render system FH7 and H show less damage due to salt crystallization when submitted to the severe action of salt laden water. Samples from these render systems were selected to be investigated by scanning electron microscopy (SEM/EDS) at the end on the 2nd cycle. The samples were removed at 0.30 m height from damaged and non damaged zones. The study of the type and location of crystallization was deeply investigated in the outer layer surface, in the middle of the outer layer and at the interface between outer and base layer. Analyzing these samples, a large variety of morphologies of NaCl crystals can be observed with SEM.

SEM observations were performed, for microstructure examination, with an energy dispersive spectrometer Si(Li) X-ray detector (EDX), on freshly fractured surfaces of different hardened mortars that were sputtered with gold. ESEM analyse was chosen to minimize preparation and damage to the samples. The pressure in the SEM chamber varied between 0.3 and 1.0 Torr, corresponding to a RH of 1.7-5.7% at 20 °C. This means that with dry samples introduced in the SEM, no change in the structure of the salt would occur during the SEM investigation. With SEM an

accelerated beam of electrons is focused on the sample to be analysed. Mortars analysis at SEM/EDS showed that all samples have a compact matrix, typical of lime mortars, with aggregates which are well involved in the calcitic binder.

Outer layer

Outer layer – surface

FH7 render system (damage zone) | H render system (damage zone)

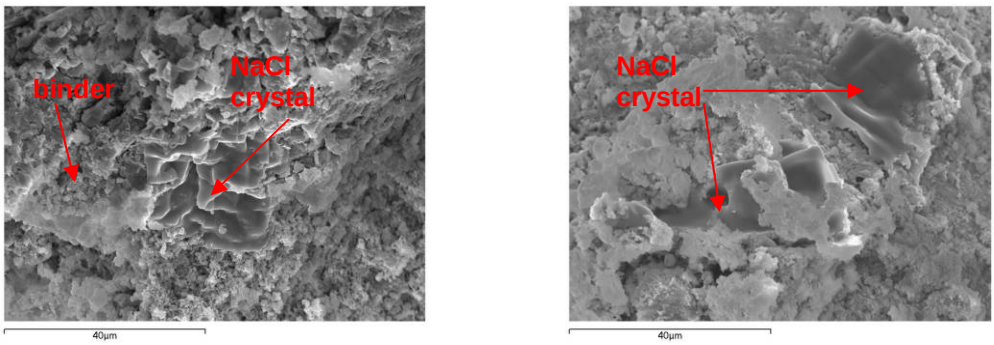

Fig. 7.25 SEM photograph of NaCl crystals in the outer layer surface: (magnification x1500) in FH7 render NaCl crystals are disperse and crystallize in the middle of the binder (left); (magnification x1500) in H render the NaCl crystals are localized and crystallize in voids in the middle of the binder (right).

In some areas, both in FH7 and H render system, a structure of salt and de-cohesioned binder is present (Fig.7.25), confirming damage in the outer surface: localized zones in FH7 and H render system (see section 7.5.1). Higher concentration of NaCl crystals seems to be observed in FH7 render system when compared with H render system.

Outer layer – 3/5 mm from the surface

FH7 render system (damage zone)

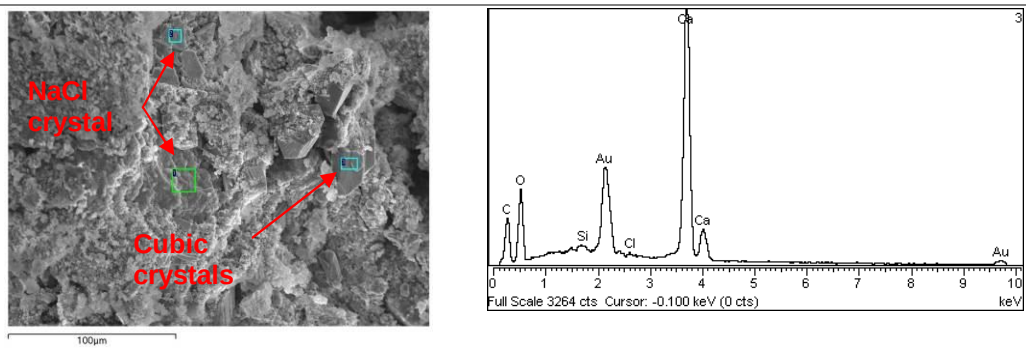

Fig. 7.26 SEM photograph of base layer: (magnification x500) in FH7 render system NaCl and carbonate crystals disperse in the middle of the binder (left); EDS photograph - carbonate (right)

Around 3/5 mm from the surface of the outer layer of FH7 render system there is evidence of salt filling the pores mixed in the middle of the binder (Fig. 7.26). Cubic crystals are present; this NaCl crystallization shape has already been referred in the literature [Lub06] and has been associated to the crystallization from solution.

Outer layer – 5 mm from the surface	
H render system (non damage)	H render system (damage)

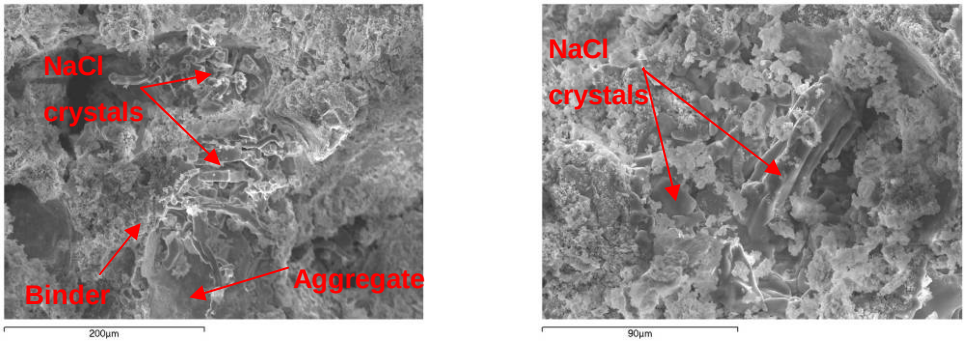

Fig. 7.27 SEM photograph of base layer: (magnification x300) NaCl crystals in voids; seems like the aggregates have drop down from the voids (in non-damage zone) (left); SEM photograph of base layer: (magnification x650) NaCl crystals disperse in the middle of the binder (in damage zone) (right).

Around 5 mm from the surface of the outer layer of H render system, the salts have crystallized in the form of needles, at the binder/aggregate interface (in non-damaged zones) and later they seem to have caused the de-cohesion of the binder (in damaged zones) (Fig. 7.27). The presence of NaCl with needle shape has already been referred in the literature [Lub06] due to repeated RH cycles on a restoration plaster, leading later to the detachment of the aggregate particles.

Interface between outer and base layers

Outer layer – interface base and outer layers	
FH7	

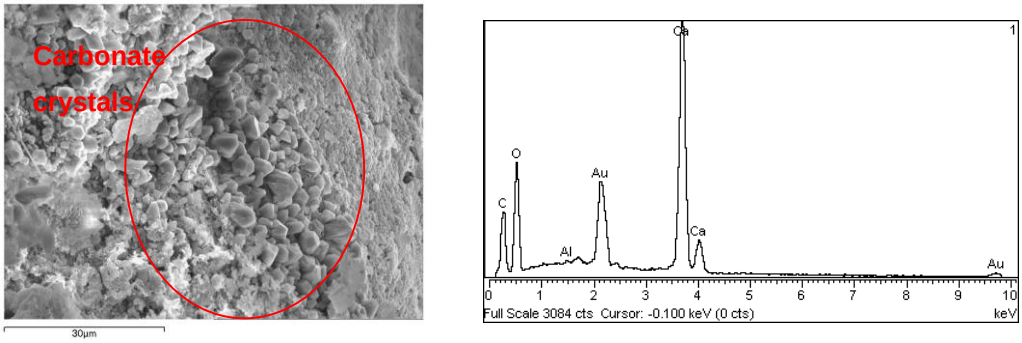

Fig. 7.28 SEM photograph of the interface between base layer and external layer: (magnification x1600) in FH7 render system zone of carbonate crystals well defined, seems like there was dissolution and re-crystallization; EDS photograph - carbonates (right).

Outer layer – interface base and outer layers

FH7

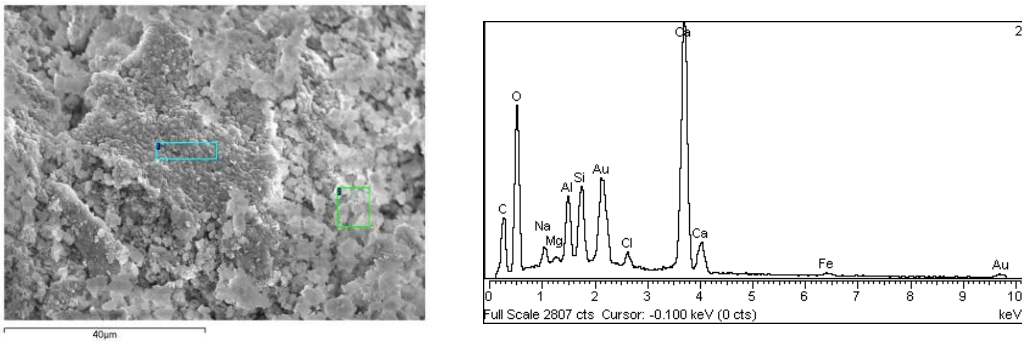

Fig. 7.29 SEM photograph of the interface between outer and base layers: (magnification x1500) Carbonate crystals and de-cohesion of the binder; EDS photograph - carbonates (right).

At the interface between outer and base layer in FH7 render system no NaCl crystallization was observed. There is generalized presence of carbonate crystals denoting a well carbonated paste (Figs 7.28 and 7.29).

Outer layer – interface between base and outer layers

H

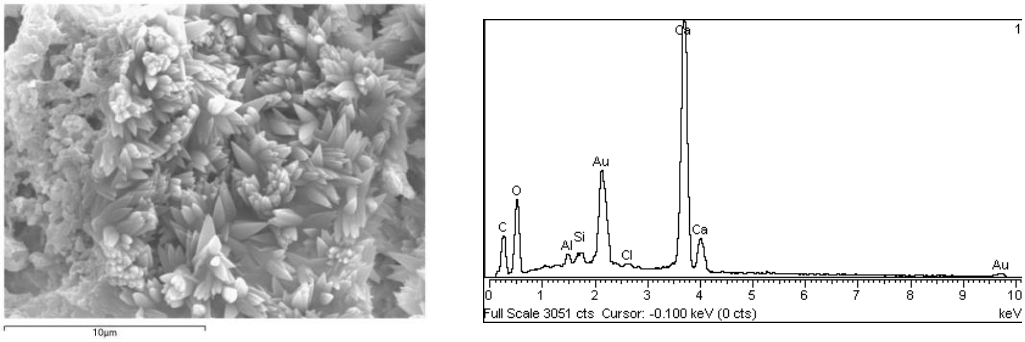

Fig. 7.30 SEM photograph of interface: (magnification x6000) in H render system although there is not so much carbonation is observed, the carbonate crystals seems like flowers; EDS photograph - carbonates (right)

Also in FH7 render system, at the interface between outer and base layers, there is no evidence of the presence of NaCl crystals. In Fig. 7.30 well carbonated materials are present, evident by the presence of carbonate crystals.

7.5.5 Salt distribution - chlorides quantification

Samples were removed from the render systems for salt content (in terms of chloride content) determination at the end of 2nd and 3rd cycles, after contamination with NaCl. The method is used to determine the total chloride % present. The samples were removed from the wall at different heights. Drilling was carried out at different heights (30, 60 and 120 cm) taking into consideration the whole thickness (from the external layer until the substrate), at low rotations per minute to prevent the disaggregation of the sample. The different layers of each sample (outer and base render layers) were taken into consideration.

The fraction analyzed was the fraction corresponding to the render layer as collected, designed overall fraction and obtained by reducing to powder the samples until they pass through a 106 µm sieve. The method used to determine the total chloride % percentage consists of extraction with diluted nitric acid and determination of chlorides by potentiometric titration, performed in NMM at LNEC. Extraction was made with diluted nitric acid and the determination of chlorides by potentiometric titration. The determined acid-soluble chloride was equivalent to total chloride content.

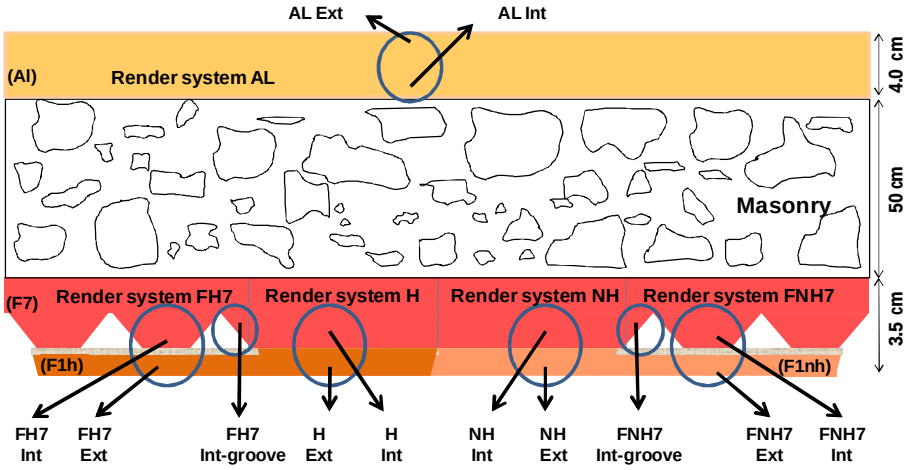

Fig. 7.31 Schematic representation of the location of the samples removed from render systems FH7, H, NH and FNH7.

In render systems FH7 and FNH7, the samples were removed at 0.30 m from the base of the masonry wall, in 4 different places (Ext, Int and Int-groove); in render systems H and NH at 0.30 and 0.60 m at the end of 2nd cycle and at 0.30 m at the end of 3rd cycle in 2 different places (Ext and Int) (Fig. 7.31). The samples removed from 1.2 m were considered as before contamination, as they didn't present salt contamination.

The chloride (Cl^-) content in the render systems layers, as a function of sample height, before contamination (defined as initial) and after contamination (defined as 2nd and 3rd cycles), is reported in Figs. 7.32 to 7.36. The chloride content for all render systems before contamination was almost zero and after contamination the salt distribution was very different depending on the location on the render system, sample removal height and number of cycles.

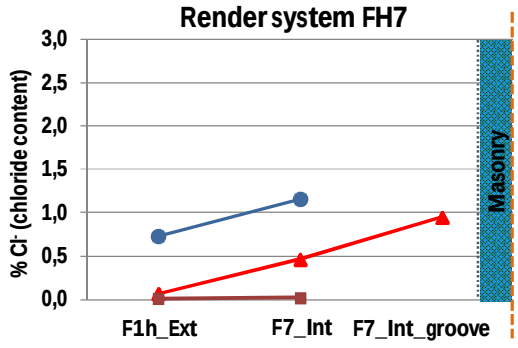

Fig. 7.32 Results of chloride content in render system FH7 in 2nd and 3rd cycles, at 0.30 m of height.

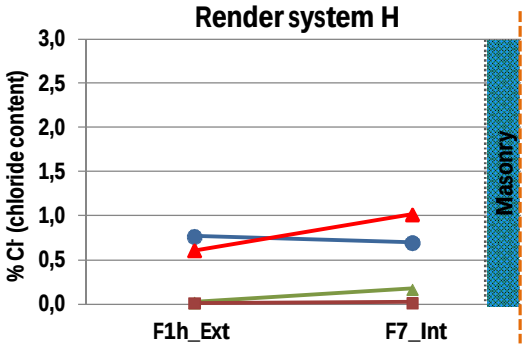

Fig. 7.33 Results of chloride content in render system H in 2nd and 3rd cycles, at 0.30 m and 0.60 m of height.

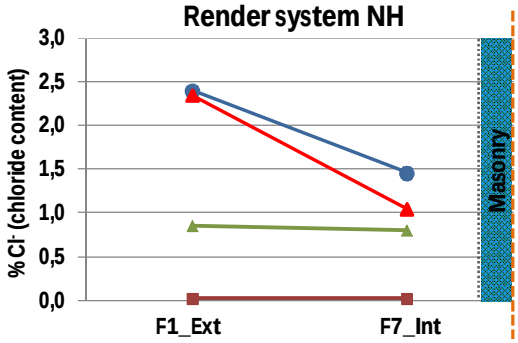

Fig. 7.34 Results of chloride content in render system NH in 2nd and 3rd cycles, at 0.30 m and 0.60 m of height.

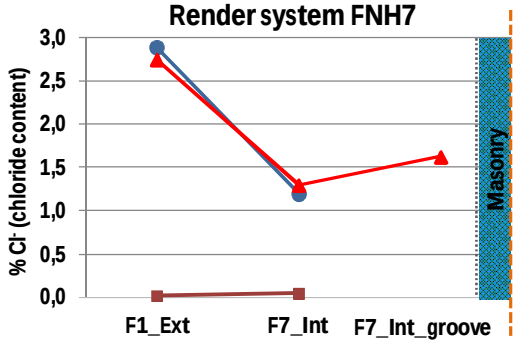

Fig. 7.35 Results of chloride content in render system FNH7 in 2nd and 3rd cycles, at 0.30 m of height.

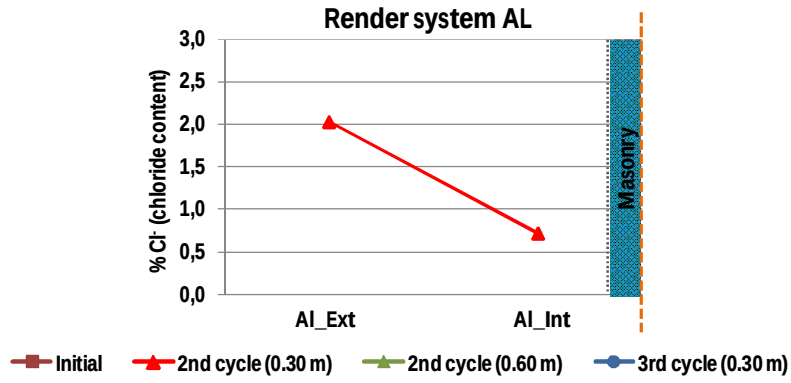

Fig. 7.36 Results of chloride content in render system AL in 2nd and 3rd cycles, at 0.30 m of height.

Effect of the height

Samples removed from render systems H and NH (both without vertical grooves) at the end of 2nd cycle, show higher chloride content at 0.30 m than at 0.60 m from the base, both in outer (Ext) and base layer (Int). At 0.30 m in NH render system the chlorides content of the base layer is a bit higher than at 0.60 m although in the outer layer the chlorides content is much higher; in H render system both base and outer layer the chlorides content is considerably higher than at 0.60 m. In H

render system base and outer layers show similar chlorides content as initial (before testing) and NH render system the base and outer layer show much higher chlorides content than initially.

Effect of the presence of water repellent

Both base and outer layers on FH7 and H render systems (with water repellent in the outer layer) show lower chloride content than on FNH7 and NH render systems (without water repellent in the outer layer) at the end of 2^{nd} and 3^{rd} cycles. On FH7 and H render systems lower chloride content was found in outer layer (Ext) when compared with the base layer (Int); on FNH7 and NH render systems higher chloride content was found in the outer layer (Ext) when compared with the base layer (Int), at the end of 2^{nd} and 3^{rd} cycles.

The results point out to the reduction of the evaporation/moisture transport through the outer layer (with water repellent) of render systems FH7 and H and leading to much lower chlorides content in this layer due to the existence of water repellent, when comparing with the outer layer (without water repellent) of NH and FNH7 render systems. The base layer of all render systems seems to be able to accumulate salts, with similar chlorides content. The existence of water repellent in the outer layer seems to reduce a bit the salt content in the vertical grooves (Int-groove).

Effect of the presence of vertical grooves

At end of 2^{nd} cycle, higher concentration of chlorides in the vertical grooves (F7_int_groove) than in outer layer (F1_ext) of FH7 render system is observed, while the opposite seems to happen with FNH7 render system.

In render systems with water repellent (FH7 and H), the presence of vertical grooves in FH7 render system seems to reduce the chlorides content in the outer layer at the end of 2nd cycle although at the of the 3rd cycle the chlorides content in outer layer was similar for both render systems. A tendency for higher salt accumulation in the base layer of FH7 render system at the end of the 3rd cycle is observed. Besides the interpretation of the results from the chlorides content, it was observed that the evaporation front in the outer surface of FH7 render system (with water repellent and grooves) occurs localized in some vertical grooves, while in the H render system (with water repellent) is generalized through the outer surface of the outer layer. The presence of vertical grooves associated with the presence of water repellent in the outer layer reduces the damage due to salt crystallization of outer surface on render system FNH7

In render systems without water repellent (FNH7 and NH7), the presence of vertical grooves seems to increase the chloride concentration in outer layer; similar chloride content was observed in the base layer of both render systems. The visual observations on those render systems on section 7.5.2 show that damage was generalized through the outer surface in both render systems

and taking into consideration these observation, besides the chlorides quantification, the vertical grooves do not seem to have a great influence in this case.

Effect of the cycles

The effect of the cycles in chloride concentration is significant in the render systems with water repellent in the outer layer. Higher difference in chloride content was found in NH and FNH7 render systems than in FH7 and H, comparing the initial, 2nd cycle and 3rd cycles results, in outer and base layers. FH7 render system shows a high difference from 2nd to 3rd cycle in chlorides content in base and outer layer, while this difference on the other render systems (FNH7, NH and H) was not significantly.

7.5.6 Influence of pore characteristics on salt uptake and distribution

To study the influence of pore characteristics on salt crystallization, the total connected porosity (P_c) and pore size distribution were determined by Mercury Intrusion Porosimetry (MIP) (Figs. 7.37 and Table 7.19). Pore size distribution was performed using Quantachro AutoScan 60 mercury porosimeter with a total range of pressure between 0.17 and 344 MPa. Pressure, pore diameter and intrusion volume were automatically registered.

The pore size distribution was studied for each sample, removed from the test wall at 0.30 m from the base of the wall on base layer and outer layer of render systems FH7 (F7-FH7 and F1h-FH7 respectively) and FNH7 (F7-FNH and F1-FNH respectively). The samples removed before testing are named pre-experiment, and at the end of the 3rd cycle are named post-experiment.

The introduction of water repellent mixed in the lime-based mortars may show a reduction of larger pores producing a more uniform pore size distribution characterized by a lower pore diameter. This behaviour is described by Izaguirre et al. [Iza09] explaining that total porosity increases due to large air content and water absorption by capillarity decreases due to the air bubbles introduced that might block the capillary network contributing also to the decrease of larger pores.

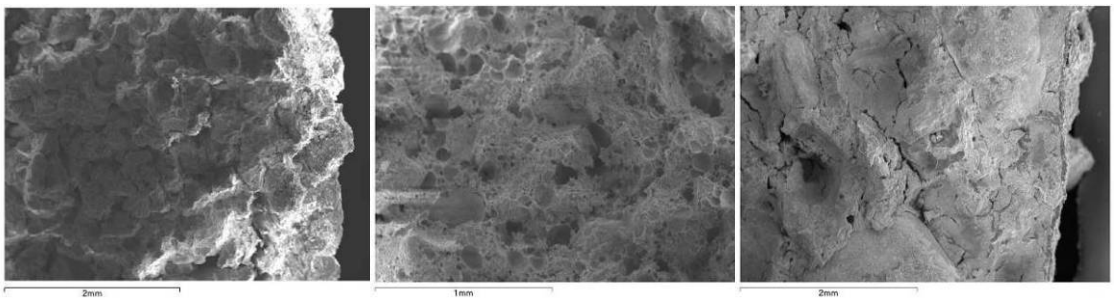

Fig. 7.37 SEM photograph on the material structure of: a) outer surface of FNH7 render system (left); b) outer surface of FH7 render system (middle); c) render systems base layer (right).

The way water enters and moves through render and masonry mortars depends on the material characteristics, especially porosity and porosimetric structure, but also on the number and thickness of coats applied and on the finishing material or technique [Vei09a]. The structure of the render layers was investigated by scanning electron microscope (SEM), showing the presence of large voids in outer surface of render system FH7 compared with the outer surface of FNH7 render system and the base layer of all render systems in the masonry wall (Fig. 7.36).

The lower open porosity of the new render systems tested (FH7, H, NH, FNH7) was determined , considering two samples for each evaluation, in the outer layer F1h of FH7 render system (with water repellent in the outer layer) (Fig. 7.37).

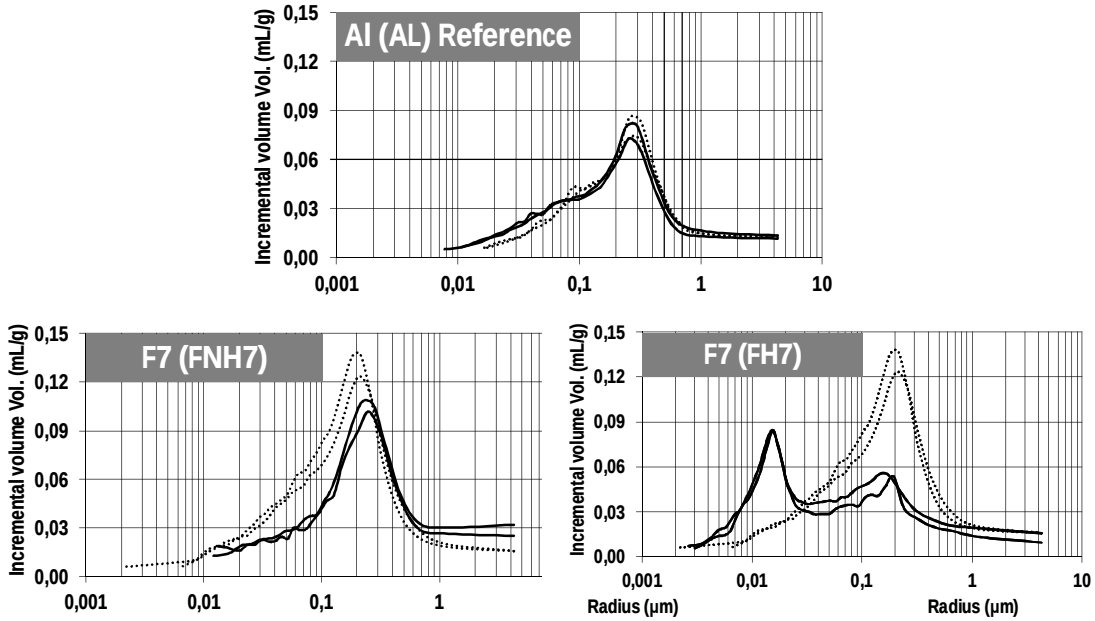

Fig. 7.38 Pre-experiment and post-experiment pore size distribution of the different layers of the render systems: traditional lime render – AI(AL); base layers - F7(FNH7) and F7(FH7); outer layers - F1(FNH7) and F1h(FNH7).

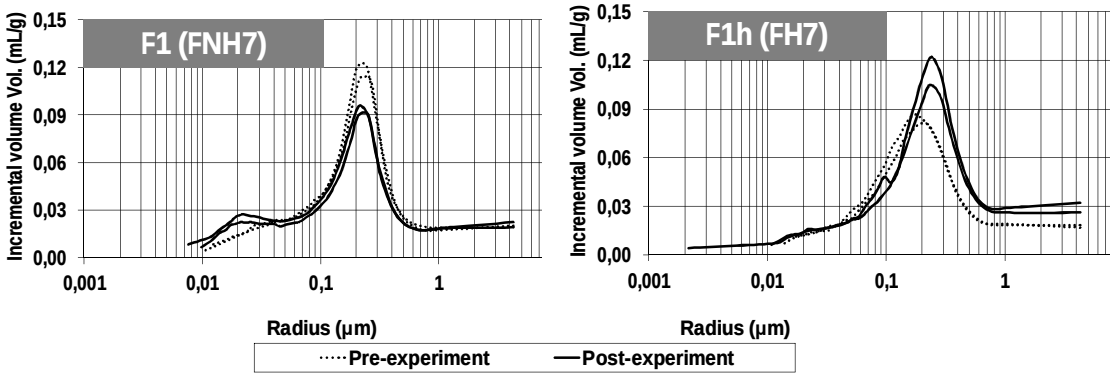

Fig. 7.38 (Cont.) Pre-experiment and post-experiment pore size distribution of the different layers of the render systems: traditional lime render – AI(AM); base layers - F7(FNH7) and F7(FH7); outer layers - F1(FNH7) and F1h(FNH7).

Izaguirre et al. [Iza09] confirms that the action mechanism of the addiction of water repellent is the incorporation of air bubbles into the whole mass of the mortar, leading to the blocking of pores and, therefore, reducing water intake.

The samples show a small range of connected porosity (Pc) ranging from 15.9 % to 24.7 %. To evaluate the pore size relative influence on salt crystallization and damage, five microporosities were calculated (from Mercury Intrusion Porosimetry data) by setting five upper limits of micropore size, which were attributed in previous studies to salt damage. The microporosities (P<5 μm to P<0.01 μm) in Table 7.19 represent the volume percentages of pores radius smaller than 5, 1, 0.1, 0.05 and 0.01 μm.

Table 7.19 Connected porosity and pore size distribution on the render layers of render systems FH, FNH and AL – pre-experiment and post-experiment.

Render layer properties	Sample								
Render system	FNH7/FH7	FH7	FNH7	FH7		FNH7		AL (reference)	
Render layer	F7	F7	F7	F1h		F1		Al	
Pore size distribution (μm)	Pre-exp.	Post-exp.	Post-exp.	Pre-exp.	Post-exp.	Pre-exp.	Post-exp.	Pre-exp.	Post-exp.
5-1	8.26	8.95	16.53	12.73	17.12	13.23	15.21	10.56	10.13
1-0.1	58.39	33.51	61.38	60.14	62.07	63.01	55.29	64.28	58.27
0.1-0.05	15.49	11.48	9.92	15.23	10.25	10.22	10.03	15.04	15.34
0.05-0.01	15.39	42.19	10.99	10.06	8.97	11.97	16.75	8.32	14.78
Connected porosity P_c (%)	24.7	22.23	20.97	17.3	20.6	19.1	17.5	15.9	16
Microporosity, $P_{<5\mu m}$ (%)	24.57	22.11	20.85	17.07	20.37	18.83	17.31	15.75	15.81
Microporosity, $P_{<1\mu m}$ (%)	22.53	20.12	17.38	14.87	16.84	16.30	14.65	14.07	14.19
Microporosity, $P_{<0.1\mu m}$ (%)	8.11	12.67	4.51	4.46	4.05	4.27	4.97	3.85	4.87
Microporosity, $P_{<0.05\mu m}$ (%)	4.29	10.12	2.43	1.83	1.94	2.31	3.22	1.46	2.41
Microporosity, $P_{<0.01\mu m}$ (%)	0.49	0.74	0.12	0.13	0.12	0.04	0.4	0.22	0.08

Note: $P_{<5\mu m}$, $P_{<1\mu m}$, $P_{<0.1\mu m}$, $P_{<0.05\mu m}$, $P_{<0.01\mu m}$ are the microporosities of pores smaller than 5, 1, 0.1, 0.05 and 0.01 μm in radius, respectively; *Pre-exp. - Pre-experiment; **Post-exp. - Post-experiment.

More than 55 % of the connected porosity was found in a pore range between 0.1 and 1 μm for all specimens and more than 20% was found between 0.1 and 0.01 μm.

Before experiment F1h, F1 and Al showed similar connected porosity as well as pore size distribution; the highest connected porosity is found in F7. F7 presents the highest percentage of pore range radius between 0.1-0.01 μm and lowest in pore range 5-0.1 μm. The higher porosity percentage, almost 25%, of base layer render F7 can be associated to fine porosity (large percentage of pores below 0.1 μm) when compared with Al mortar (Table 7.19); it is supposed to favour the moisture/solution extraction from the masonry to the base layer and may allow the salt accumulation. The presence of higher percentage of very small pores in base layer determines its higroscopicity and sensitivity to RH changes.

After experiment the pore size distribution seems to move towards smaller pores, between 0.05 and 0.01 μm (exception F1h and F7 on FNH7 render system, that shows a tendency for pore size distribution to move towards coarse pores). Yu and Oguchi [Yu10] observed that pore range between 0.1 and 5 μm seems to be the most effective in solution/salt absorption in stones; this is referred the range where salt crystallization mostly occurs; if the porous materials presents substantial amounts of larger microporosities (0.1 - 5 μm) they become more susceptible to salt crystallization attack. Zehnder and Arnold [Zeh89] also confirms that salt crystallization occurs mainly in pore range between 0.5 and 5 μm. In F1h a tendency for the pore size distribution to shift towards coarse pores (between 5 and 0.1 μm) was observed, maybe due to the presence of water repellent that may inhibit the salt solution uptake in pores higher than 0.1 μm and thus inducing salt crystallization in pores lower than 0.1 μm. Another complementary explanation may be the salt solution uptake in some large pores (higher than 0.1 μm) that may disrupt the layer formed by the water repellent, increasing the porosity in this range as well as the connected porosity.

After experiment the connected porosity decreases, except in F1h; the presence of water repellent in this sample and the reduced crystallization observed at the end of the 3rd cycle are a possible explanation for this exception, although pores smaller than 0.1 μm were noticeable to be also filled with salts. The equilibrium between salt distribution and pore size distribution may be achieved in F7 (on FH7 render system). This render layer presents highest pore size reduction on pore sizes between 1-0.1 μm and the highest increase in pore size range 0.05-0.01 μm. Also the highest connected porosity decrease was observed on F7 (on FH7 render system) that can be attributed to salt crystallization occlusion of some pores in salt crystallization range due to the presence of F1h render solution in the outer surface, forcing the salt to accumulate in the base layer. At the end, in F7 (from FNH7 render system) was observed a tendency for the pore size distribution to shift towards coarse pores (between 5 and 0.1 μm) due to the salt crystallization on the pore range radius between 0.1 and 0.01 um.

7.5.7 Discussion on the effect of the severe action of salt laden water–damage evaluation

Damage due to salt crystallization was observed on the outer surface of render systems. The damage extent was different among render systems: render systems without water repellent in the outer layer (FNH7 and NH) show generalized crumbling and sanding until 0.90 m; Al (reference render system) shows even higher damage at the end of the tests; in render systems with water repellent (FH7 and H) localized scaling and efflorescence, between 0.30 and 0.60 m, were observed.

The crystallization at the interface between base and outer layer and inside the vertical grooves was deeply investigated by means of optical microscope at 0.3, 0.6 and 1.2 m. In all render systems the salt crystallization was mainly observed at 0.3 m while at 1.2 m there is no evidence of

salt crystallization. This discussion will be focused at 0.30 m height. In render systems FNH7, NH and AL dense crystallization was observed. At the interface on render system FH7 significant crystallization was not observed, although inside vertical grooves there was crystallization. The higher crystallization in the vertical grooves seems to be found in FNH7 compared with FH7 render system. In outer layers of FNH7, NH and AL render systems dense crust crystallization was observed while in render systems FH7 and H the crystallization is localized and appears as "pulverulent" crystallization. No significant damage was observed on the outer surface of FH7 and H attributed to the presence of water repellent that reduces the salt solution uptake and doesn't allow salt crystallization from the solution, when compared with the other render systems. Some localized damage observed on render systems FH7 and H can be attributed to some salt solution absorption trough the base and outer layer, inducing the preferential salt crystallization. Comparing systems with and without water repellent, no significant difference in damage was observed.

The main objective of this experimental work is to focus on the development of a durable and efficient render system for historic buildings when there is the presence of moist due to rising damp together with soluble salts. Based on the discussed results until now, FH7 render system is the one that fulfilled these objectives, showing less damage due to salt crystallization in the outer layer and at the same time allowing salt accumulation in the base layer (in vertical grooves).

SEM investigations on type and location of crystallization may explain some of the differences observed on damage patterns of render systems FH7 and H. Based on the referred above, investigation was made in the outer layer and at the interface between outer and base layers of these render systems. The samples were removed at the end of 2nd cycle at 0.30 m from both damaged and non-damaged zones. They were selected from 2nd cycle, because in the 3rd cycle the damaged zones were not resistant enough to be investigated by SEM. At the interface between base and outer layer no evidence of NaCl crystallization is observed; on its place defined carbonate crystals are observed denoting a well carbonated render. This can be explained by the presence of the vertical grooves in FH7 render system at the interface that increases the ventilation and as consequence higher degree in carbonation is achieved. Based on that, the detachment of the outer layer due to salt crystallization at the interface was not a possibility, until the end of the 3rd cycle. On the outer layer surface, on localized zones, of FH7 and H7 render solutions NaCl crystals grow as an agglomeration of crystals that are not strongly attached to the material. Similar crystallization behaviour was observed in chapter 5 section 5.5.2. Deeper in the outer layer of FH7 render solution some cubic crystals present may induce that salt solution is absorbed through the outer layer where it then evaporates and crystallizes; on H7 render solution in some areas a structure of salt (as needles shape) can be associated to repeated RH cycles, the de-cohesion of the binder is present, denoting the occurrence of damage (see section 7.5.3).

The chlorides quantification was made in all render systems. Render systems with water repellent (FH7 and H) show lower chloride content in the outer layer than in base layer; render systems

without water repellent (FNH7 and NH) show higher chloride content in outer layer than in base layer. Higher chlorides content were found in vertical grooves of FNH7 than of FH7, which is in accordance with the optical microscope observations. In FH7 and H render system fewer chlorides were found in the outer layer and higher in base layer; comparing both render systems, the vertical grooves influence salt crystallization by its reduction in the base layer. The render systems without water repellent show higher chlorides content in all layers than in the ones with water repellent. At the end of the tests similar chlorides content was determined in the base layer of render systems FH7 and FNH7.

The study concerning the pore structure shows that the base layer of render systems favour the salt solution uptake from the masonry to this layer due to the high percentage of very small pores (below 0.1 μm). This layer shows highest percentage of pores in this range size as well as the connected porosity. After experiments, the existence of water repellent in the outer layer moves pore range of base layer to pore size range below 0.1 μm and the highest connected porosity decrease is observed. The highest decrease in connected porosity is attributed to this layer, when the outer layer has water repellent, due to salt crystallization occlusion of pores in salt crystallization range. When there is no water repellent in the outer layer, after experiments a tendency of pore range to move towards coarser pores (above 0.1 μm) is observed. After experiments, in outer layer F1h there is a tendency of pore range to move towards coarser pores (above 0.1 μm) while in outer layer F1 and in render layer Al it moves towards smaller pores (below 0.1 μm).

The similar connected porosity and pore size distribution found in the outer layer of FNH7, NH and AL render systems can be the cause of the similar damage of their outer layer due to salt crystallization (disintegration, detachment, lacunae and efflorescence). At the end of the experiments similar salt crystallization concentration was observed on F1 and Al and a similar reduction on pore range 1-0.1 μm and a similar increase in pore range 0.05-0.01 μm.

7.6 Classification of render systems – working principle and performance

Based on the results obtained from the experimental work in this chapter, it is possible to define the category of each render system in the masonry when submitted to the severe action of salt laden water.

Table 7.20 describes the classification of each render system tested, taking into consideration the working principle (transporting, accumulating, blocking and sealing) and performance (no decay, slow decay, moderate decay and fast decay), considering the influence the whole system (full-scale masonry wall and render system).

Table 7.20 Category attributed to each render system at the end of the study

Render system	Classification
FH7	Accumulating (slow)
H	Accumulating (moderate)
NH	Transporting (fast)
FNH7	Transporting (fast)

7.7 Conclusions

With this experimental program it was proved that: i) the vertical grooves increase the durability of the system due to the high amount of salts crystallization inside it and to not allowing their crystallization on the outer surface (comparison with and without grooves); ii) the water repellent in the outer layer does not allow the salts coming to the outer surface (no visual de-characterization), when compared with the system without water repellent in the outer layer and iii) none of the tested render systems contributes to salt crystallization inside the wall as salt solution transport was allowed through the render systems, mainly due to the presence of F7 formulation in the base layer.

In all render systems both render layers (base and outer layer) show physical and mechanical properties appropriate for their application in old masonries, resulting in compatible render systems;

The render systems were carefully executed with 2 cm thickness and no shrinkage was observed after their execution or at the end of the cycles.

The damage in the outer surface of the other render systems without water repellent in the outer layer (FNH7, NH, and H) is observed to be at a much higher extent than in FH7 render system, as they act as transporting systems where soluble salts can crystallize in the outer surface, while FH7 acts as an accumulating render system.

The contribution of the grooves in the base layer and water repellent in the outer layer was observed to reduce salt damage in the render system FH7, where at the end only some damage was observed just in small zones in the outer surface near the grooves; in H render system a greater damage zone in the outer surface was observed compared with FH7 render system; in render systems FNH7 and NH, the vertical grooves have no influence on surface damage and both render systems show high surface salt damage.

The artificial ageing tests simulated the severe action of salt laden water in the real-size masonry, allowing the study of salt damage and testing the durability and efficiency of the render systems (FH7, H, NH and FNH7) compared with traditional renders (AL).

The 3rd cycle of the test simulates a very aggressive stage with severe degradation for the render systems (specially FNH7, NH and AL), pointing out that the results obtained at this stage really affects the further behaviour of render systems.

From this experimental research the most significant general conclusions can be drawn:

- In ventilated render system (FH7) it might perhaps not be necessary to apply the vertical grooves along all wall height. The necessary height is dependent on: the use of more or less impermeable renders in the opposite side of the wall and on the presence or not of active rising damp. In case of using permeable renders, the vertical grooves until 0.9 m from the base of the wall could be enough; however it is important to garantee the ventilation with well placed holes;

-In the FH7 render system the water repellency of the outer layer reduces the moisture evaporation through the outer layer (although this layer is of course not fully water proof), preventing salt solution transport through the surface and as consequence salt damage and loss of material in the outer surface;

- FH7 render shows less superficial damage, localized in correspondence to the grooves as efflorescence, because salt solution transport in the second layer to the surface was low; detachment of the outer layer due to salt crystallization at the interface was not observed, until the end of the tests;

-In FH7 render system the salts are induced to crystallize in the vertical grooves of the base layer and not in the substrate or in the outer layer, working as a salt accumulating render system as is was the main objective of this work;

-The vertical grooves in FH7 render system, in contact with the surrounding ambience promoting the air circulation inside them, are shown to allow moisture evaporation and salt accumulation inside them;

-The base layer with brick powder as additive promotes a good adherence to the substrate and allows salt crystallization inside the pore system, as well as salt solution transport until the vertical grooves (in FH7 and FNH7 render systems) and to the outer surface where salt crystallization occurs as efflorescence (in FNH7 render system);

-The base layer was observed to be very salt-resistant without damage at the end of the tests when submitted to the severe action of salt laden water and shows high strength underlined by the difficulty associated to sample removal.

The higher performance of render system FH7 when compared with the other render systems, in the presence of the severe action of salt laden water, has been proven. This render system should be used in old masonries with high moisture (continuous capillary rise) and salt content, when no

damage in the outer surface is allowed, showing the following characteristics: i) compatibility with old substrates; ii) allow the salt solution transport to the render, without increasing salt crystallization in the substrate; iii) allow salt crystallization in the vertical grooves, working as accumulating render system; iv) good bonding to the substrate even in the presence of damp substrates; v) high resistance on damp and salt loaded masonries; vi) in mass water repellent in the outer layer; vii) brick powder in the base layer; viii) easy application, execution and long lasting.

8. CONCLUSIONS

8.1 Results of the research

This thesis is focused on the improvement of renders durability when submitted to severe action of water by the:

- Definition of a maintenance action to improve renders and masonry durability and;
- Study of replacement renders in order to be able to design and develop a compatible, efficient and durable renders and test its performance .

The research started with a literature review on damage mechanisms and on the evaluation of the viability of renders to be used as replacement renders, i.e. salt accumulation and transport systems referred to in other studies (Chapter 2).

The observation of the damage occurring in field due to the presence of moisture and salt loads in substrates and of the damage evolution is crucial for the understanding of the critical variables that originate the walls deterioration. The understanding of the damage phenomena in the case studies constitutes a starting point for the design of a high performance replacement render system, in the presence of damp and salt loaded masonries, as well as a base of comparison with the damage observed in the general Portuguese works and a tool to validate laboratory experiments. This comparison may allow, at first instance, to assess whether the testing conditions in laboratory can be used efficiently to test the system. For this reason a research approach based on the combination of the main problems observed in field due to the presence of damp and salt loaded masonries of Portuguese case studies (Chapter 3), the definition of the main characteristics of the render system and the laboratory experiments (Chapter 5, 6 and 7) was adopted in this work for the development of a high performance render system for damp and salt loaded masonries of historic buildings.

The investigation of Portuguese case studies (Chapter 3) revealed that rising damp is one of the main sources of moisture in old buildings. The presence of moisture associated with soluble salts in most of the case studies, was found to be the main cause for damage. Besides the surrounding conditions, the use of an adequate render formulation and application considering the substrate is necessary in order to avoid premature damage and to create an increase in durability.

The use of an effective diagnosis methodology during the inspections in old buildings can help to eliminate or minimize the origin of the anomalies observed, and help in the prescription of the adequate conservation technology and definition of the most adequate repair solutions, including a substitution render. The visual observation of the anomalies is necessary for the definition of the state of conservation of the renders, but by itself does not conclude about the origin of the indeed

anomalies. (sources of moisture, inadequate render solutions, soluble salts, etc.). When moisture and soluble salts are present, damage may appear as salt efflorescence, delamination, scaling, spalling, sanding, crumbling and detachment of the outer layer.

The expedite identification of the type of salts and the monitoring of moisture distribution, using simple tools like a humidimeter, by experts, can be helpful and of importance towards the definition of the sources of moisture. Also the assessment of mechanical characteristics with the use of a durometer and a esclerometer can give valuable in situ information on the resistance of the renders allowing the comparison with other results obtained from previous studies and concluding about the state of conservation.

From the results obtained from the case studies (Chapter 3) arises the necessity of defining efficient and compatible actions able to improve renders durability by: i) maintenance of existent renders (Chapter 4) and application of replacement renders (Chapters 5, 6 and 7).

The study of a maintenance action to improve renders and masonry durability, preventing renders premature replacement was developed in Chapter 4. The electrokinetic desalination applied to rendered masonries to increase the durability of the existent renders, as maintenance procedure to delay its replacement, was an innovation. From laboratory work, salt reduction both in renders and support was observed. In this work the application of this method for both render and support desalination was an innovation, especially efficient in cases of active moisture/salt solution sources and salt loaded masonry (severe action of water).

The study of replacement renders under severe action of water, was performed in Chapters 5, 6 and 7. This part of the work allowed the design and development of ventilated render form Fradical, as well as its performance evaluation.

In Chapter 5 render solutions with extreme characteristics (cement based and air lime based mortars) where applied on perforated bricks and tested in laboratory. The dissolution/crystallization cycles conditions were defined to simulate rising damp followed by drying in laboratory conditions in order to: i) reproduce the degradation patterns observed in field in the design extreme render mortar mixes tested in laboratory, and ii) compare the degradation patterns between the tested solutions. This chapter allowed the definition of small scale specimens able to simulate a rendered brick masonry and simulate the effects of severe action of water by dissolution/crystallization cycles, with good correspondence to in situ observations.

Another part of the laboratory research was the design of the substitution render system to be studied (formulations and execution) concerning the development of a high performance render system able to be durable, efficient and compatible with masonry in historic buildings, when high moisture content and soluble salts are present (Chapter 6). Several render systems based on similar formulations with lime putty but with different layers were applied on solid bricks and

compared between them after the dissolution/crystallization cycles in conditioned environment. The designed substitution render system is composed by two layers, base and outer layers, in which the base layer has brick powder as additive and vertical grooves.

The results obtained prove: the adherence to the substrate in moist conditions was guaranteed by using powdered brick in the base layer; this render seems to be very resistant when compared with the other tested renders; this render works as a transport system, transporting the soluble salts until the evaporation surface (vertical grooves in base layer or outer surface in case of inexistence of vertical grooves). The vertical grooves were efficient on the accumulation of the soluble salts in all tested render systems. The outer layer was formulated with and without water repellent and some differences were observed after experiments: the water repellent prevents the salt transport through it and as a result the salt crystallization in this layer; the outer layer without water repellent was observed to be very damaged after several cycles of dissolution/crystallization with NaCl solution. The render system FH7, denominated as "emboço ventilado" (with brick powder in the base layer and vertical grooves and water repellent in the outer layer) seemed to be the most effective and durable render system. None of the tested render systems were observed to induce the salt accumulation in the support. The cycles reproduced in laboratory seem to be very damaging and several differences on damage patterns, due to salt crystallization, were observed. Besides that, all tested formulations were durable until the 6^{th} cycle, after which the degradation became more evident and some render systems collapsed (fell down).

To assess the efficiency and durability of the render system "emboço ventilado" this render system and three more render systems for comparison with "emboço ventilado", were selected. These render systems were applied on a full scale masonry wall (Chapter 7) and deeply studied. The render systems carefully executed and cured and after 90 days were submitted to dissolution/crystallization cycles under ambient conditions in the Wall Covering Laboratory of National Laboratory of Civil Engineering (LNEC) in Lisbon. From the obtained results it is possible to conclude that: damage in the outer layer of the render system was located where salt crystallization accumulation was observed; the presence of water repellent in the outer layer and the vertical grooves in the base layer completely modifies damage patterns compared with the other three render systems studied in this chapter; in the render system FH7 "emboço ventilado", salt accumulation in the vertical grooves and less damage in the outer layer were observed, compared with the other tested render systems, when submitted to the severe action of salt laden water (capillary rise with water and NaCl); the presence of water repellent in the outer layer of the render, in contact with exterior atmosphere, strongly influences the location of salt accumulation, inhibiting salt solution transport to the surface of the render and preventing the surface damage, in "emboço ventilado" render system; the vertical grooves in "emboço ventilado" seem to increase the durability of the system due to the salts crystallization inside the grooves and significantly reduces their crystallization in the outer surface. The base layer in all render systems (F7 mortar) was

observed to be very salt-resistant, presenting high strength and allowing salt crystallization inside the pore system without damaging it, as well as salt solution transport to the vertical grooves and to the outer surface where salt crystallization occurs as efflorescences, this case specially in FNH7 and NH render systems, and some located crystallization in H render system (executed without vertical grooves).

The ventilated render system from Fradical – FH7 - was designed for salt loaded masonry in the presence of rising damp (severe action of water) and was proved to be: i) compatible with salt loaded masonry, ii) efficient on salt accumulation in grooves and base layer and preventing its accumulation in the support and durable as surface salt damage was reduced. The ventilated render system – FH7 – has been proved to be an innovative high performance accumulating replacement render.

As final remarks:

The developed render system "ventilated render" can be used in historic walls especially when exposed to severe action of salt laden water (under conditions of rising damp where water contains soluble salts). This "ventilated render" (FH7 render system) possesses the following characteristics:

- Compatibility with the historic masonry, enabling salt transport from the masonry to the render system, and as result preventing the salt accumulation in the masonry;
- Efficiency in salts accumulation in the surface of the vertical grooves within the base layer F7 (formulated with brick powder additive and very resistant);
- Durability as it avoids visible efflorescences and superficial damage to the surface of the outer render layer F1h (formulated with water repellent additive in mass);
- Two-layer render system (base and outer layer) acting as an accumulating render system;
- Better bounding to the masonry when compared with traditional lime render (AL).

This "ventilated render" system has been designed for the most difficult cases, under the severe action of salt laden water in old buildings masonry, when good external appearance is required without damage to the outer surface.

8.2 Future work

Based on these main conclusions, investigations must be carried out using scanning electron microscopy (SEM) to better understand the deposition of the salts in greater detail and the influence of render formulations on salt crystallization and possible decay.

It is also important to study the porous structure of the bricks and of the mortars applied, and to compare them, in order to establish a link to the degree and location of salt damage.

The electrokinetic desalination of salts was proved to be efficient in laboratory, however, in future work, it should be tested in real cases.

It is desirable that the salt resistant render system “ventilated render” (*emboço ventilado,* in Portuguese) from Fradical Lda., that allows controlling the anomalies due to salt crystallization in historic buildings due to capillary rise associated to the presence of soluble salts, be tested in real cases.

In the future testing the mechanical ventilation within the groves of ventilated render system would be also desirable, in order to improve the render system efficiency.

9. REFERENCES

[Adr07a] Adriano P., Santos Silva A., Veiga R., Mirão J., Candeias A. - Microscopic characterization of old mortars from the Santa Maria church in Évora. Proceedings of the 11th Euroseminar on Microscopy Applied to Building Materials, ed. I. Fernandes, A. Guedes, 2007.

[Arn82] Arnold A. - Rising damp and saline materials. Proceedings of the 4th International Congress on Deterioration and Preservation of Stone Objects, ed. K.L. Gauri and J.A. Gwinn. Louisville, Ky.: University of Loiisville, p.11-28, 1982.

[Arn87] Arnold A., Zehnder K. – Monitoring wall paintings affected by soluble salts. Proceedings of The conservation of wall paintings symposium. London, 1987.

[Aug90] Auger, Fernand - World limestone decay under marine spray conditions. The conservation of monuments in the Mediterranean Basin: the influence of coastal environment and salt spray on limestone and marble. Proceedings of the 1st International Symposium, Bari, 7-10 June 1989, p. 65-69, 1990.

[Bak09] B.H. Abu Bakar, M.H. wan Ibrahim, M.A. Megat Johari - A Review: Durability of Fired Clay Brick Masonry Wall due to Salt Attack. International Journal of Integrated Engineering (Issue on Civil and Environmental Engineering), vol.1, n.2, 2009.

[Bar95a] Baronio G., L. Binda, Saisi A. - Analisi di malte antiche e comportamento di malte riprodotte in laboratorio. Convegno Nazionale L'ingegneria sísmica in Itália. Siena, 25–28 September, 1995. Studies on mortars sampled from historic buildings. Selected papers 1983–1999. Milan, Italy: Polytechnic of Milan, Strctural Engineering Department.

[Bed05] Beddoe R.E., Dorner H.W. - Modelling acid attack on concrete: Part I. The essential mechanisms. Cement Concrete Research 35, p. 2333-2339, 2005.

[Ben04] - Benavente D., García del Cura M.A., Fort R., Ordóñez S. - Durability estimation of porous building stones from pore structure and strength. Engineering Geology 74, p. 113-127, 2004.

[Bor99a] Borreli, E. - Conservation of Architectural heritage, historic structures and materials salts. Roma: International Centre for the Study of the Preservation and the Restoration of Cultural Property (ICCROM), 1999.

[Bos01] Bosiljkov, Violeta Bokan - The use of industrial and traditional limes for lime mortars. Historical Constructions, P.B. Lourenço, P. Roca (Eds.), Guimarães, 2001

[Cha00a] A. E. Charola - Salts in the deterioration of porous materials: An overview. Journal of the American Institute for Conservation, 39, p. 327-343, 2000.

[Cal00a] Callebaut K., W. Viaene, K. van Balen - Production of historic lime mortars: evidences from old mortar analyses and laboratory tests. In Proceedings of the 12th International Masonry Conference, p. 363–372. Madrid, Spain: J. M. Adell, 2000.

[Cor49] C.W. Correns - Growth and dissolution of crystal under linear pressure, Discussion of the Faraday Society 5, p. 267-271, 1949.

[Cru10] Cruz, Claúdio - Comportamento e durabilidade de telhas cerâmicas em ambiente marítimo. PhD Thesis. Universidade de Aveiro. 2010.

[Dei99] Luigi Dei, Marcello Mauro, Piero Baclioni - Growth of Crystal Phases in Porous media. American Chemical Society, Langmuir, 15, p. 8915-8922, 1999.

[Doe02] E. Doehne - Salt weathering: a selective review, Geological Society Publication, Natural Stone, Weathering Phenomena, Conservation Strategies and Case Studies, Vol 205, p. 51-64, 2002.

[Far04] Rodrigues, M. Paulina – Argamassas de revestimento para alvenarias antigas: Contribuição para o estudo da influência dos ligantes. PhD Thesis, Universidade Nova de Lisboa, Faculdade de Ciências e Tecnologia, 2004 (Render mortars for historic masonry: study of binder influence, in Portuguese).

[Far12a] Faria P., Silva V., Carneiro J., Branco, T., Mergulhão, D., Aantunes, R. - Argamassas compatíveis com alvenarias históricas com base em cal hidráulica natural. CIRea 2012 - Conferência Internacional sobre Reabilitação de Estruturas Antigas de Alvenaria, p. 28-38. Lisboa, Universidade Nova de Lisboa, 4 de Maio de 2012 (*Natural hydraulic lime mortars for historic masonry, in Portuguese*).

[Far12b] Faria, P., Silva, V., Flores-Colen I. - Argamassas de cal hidráulica natural e pozolanas artificiais: avaliação laboratorial. APFAC 2012 – 4º Congresso Português de Argamassas de Construção, sob a Égide da Inovação (CD-ROM). Universidade de Coimbra, Coimbra, 29 e 30 de Março de 2012 (Natural hydraulic lime mortars and artificial pozzolans: laboratory evaluation, in Portuguese).

[Fra07a] Fragata A., Veiga M.R., Velosa A.L., Ferreira V.M. - Incorporação de resíduos de vidro em argamassas de revestimento: avaliação da sua influência nas características da argamassa. In Proceedings of the 2nd Congresso Nacional Argamassas de Construção, APFAC. Lisbon, Portugal, 2007 (Incorporation of glass residues in renders: evaluation of their influence on mortars properties, in Portuguese).

[Fra07b] Fragata A., Paiva H., Velosa A.L., Veiga M.R., Ferreira V.M. - Application of crushed glass residues in mortars. In International Conference on Sustainable Construction, Materials and Practices. Challenges of the Industry for the New Millenium, ed. L. Bragança, M. Pinheiro, S. Jalali, R. Mateus, R. Amoeda and M. C. Guedes. Lisbon, Portugal, 2007.

[Fra10a] Fragata A., Velosa A.L., Veiga M.R. – Salt crystallization in substitution renders for historical constructions. In 2nd Historic Mortars Conference & RILEM TC 203-RHM repair Mortars for Historic Constructions – Final workshop, p. 983-992. Praga, República Checa, 22 a 24 de Setembro de 2010.

[Fra10b] Fragata A., Velosa A., Veiga M.R., Ottosen L. – Renders study: Sodium chloride crystallization and application of an electric field DC for their removal. In: 8th International Symposium on the Conservation of Monuments in the Mediterranean Basin (MONUBASIN8). Grécia, Patras, 31 de Maio a 2 de Junho de 2010.

[Fra10c] Fragata A., Velosa A.L., Veiga M.R. - Salt crystallization in substitution renders for historical constructions, in Proceedings of HMC2010: 2nd Historic Mortars Conference & RILEM TC 203-RHM Repair Mortars for Historic Masonry Final Workshop. Praga, Check Republic, 22 a 24 de Setembro de 2010.

[Fra10d] Fragata A., Veiga R. – Air lime mortars: the influence of calcareous aggregate and filler addition. Materials Science Forum, Vols. 636-637, p. 1280-1285, January 2010.

[Fra10e] Fragata, Ana - Relatório de Progresso da Tese de Doutoramento de Ana Fragata. Lisboa: LNEC, Abril de 2010. I&D EDIFÍCIOS, Relatório Confidencial (Proc.º 0803/11/17797) (Ana Fragata's Doctoral Thesis Progress Report, in Portuguese).

[Fra10f] Fragata A., Velosa A.L., Veiga M.R., Ottosen L. – Application of electric DC field for sodium chloride removal from rendered bricks. Conference on Electrochemical Desalination Science and Technology. Denmark, Technical University of Denmark (DTU), 30th September to 1st October, 2010.

[Fra11a] Fragata A., Veiga M.R., Velosa A.L, Tavares M. – Casos de estudo: metodologia de diagnóstico e soluções de reparação para revestimentos com problemas de humidade em edifícios antigos. SBTA: IX Simpósio Brasileiro de Tecnologia de Argamassas. 17 a 20 de Maio de 2011 – Brasil, Belo Horizonte, Minas Gerais (Case studies: diagnosis methodology and repair measures for historic buildings with moisture problems, in Portuguese).

[Fra11b] Fragata A., Veiga M.R., Velosa A.L., Tavares M. – Cases studies: Substitution renders and other measures to prevent capillary water rise in historical buildings. 12th International Conference on Building Materials and Components (XII DBMC). FEUP, Porto, 12 a 15 de Abril de 2011.

[Fra12a] Fragata A., Veiga R. Velosa A., Cartaxo F. - Soluções de revestimento para alvenarias históricas sujeitas à ação da água. Jornadas LNEC, Engenharia para a Sociedade Investigação e Inovação: Cidades e Desenvolvimento. Lisboa, Portugal, LNEC, 18 a 20 de Junho de 2012 (Renders for historic masonry submitted to severe action of water, in Portuguese).

[Fra13a] Fragata A., Veiga M.R., Velosa A.L. - Render system “emboço ventilado”: a substituion render for historic constructions. 3rd Historic Mortars Conference (HMC13). Glasgow, Scotland, 11 to 13 September, 2013.

[Fre02a] Freitas, V.P., Torres, M.I., Ascensão A., Gonçalves, P.F. - Tratamento da humidade ascensional na Igreja de Vilar de Frades. Património Estudos, 3, p. 54-62, 2002 (Rising damp tretament in Church of Vilar de Frades, in Portuguese).

[Gam12a] Gameiro A., Santos Silva A., Veiga R., Velosa A. – Lime-metakaolin hydration products: a microscopy analysis. Materiali in tehnologije / Materials and Technology 46 (2), p.145-148, 2012.

[Gam12b] Gameiro A., Santos Silva A., Veiga R., Velosa A. – Hydration products of lime-metakaolin pastes at ambiente temperature with ageing. Thermochimica Acta 535, p. 36-41, 2012.

[Gui10] Guimarães A.S., Delgado J.M.P.Q., Freitas V.P. – Mathematical analyses of the evaporative processo of a new technological treatment of rising damp in historic buildings. Building and Environment 45, p. 2414-2420, 2010.

[Gon97] Gonçalves, Teresa - Capacidade de impermeabilização de revestimentos de paredes à base de ligantes minerais. Desenvolvimento de um método de ensaio com base na resistência eléctrica. Lisboa, LNEC, Tese de Mestrado em Construções pela Universidade Técnica de Lisboa, 1997 (Impermeabilization capacity of mineral binder mortars, in Portuguese).

[Gon06a] Gonçalves T.D., Rodrigues J.D., Abreu M.M., Esteves A.M., Santos Silva A. - Causes of salt decay and repair of plasters and renders of five historic buildings in Portugal. In Proceedings of Heritage, Weathering and Conservation HWC 2006, ed. Fort, A. de Buergo, Gomez-Heras and V. Calvo, p. 273–284. Madrid, Spain, 2006.

[Gon07] Gonçalves, Teresa - Salt crystallization in plastered or rendered walls. PhD Thesis, Tecnical University of Lisbon, Lisbon, 2007.

[Gro00a] Groot C., Bartos P., Hughes J. - Characterisation of old mortars with respect to their repair. In Proceedings of the 12th international brick/block masonry conference, p. 815–827. Madrid, Spain, 2000.

[Gro09a] Groot C., van Hees R., Wijffels T. - Selection of plaster and renders for salt laden masonry substrates. Construction and Building Materials, Vol.23, p. 1743-1750, 2009.

[Gui10] Guimarães A.S., Delgado J.M.P.Q., Freitas V.P. – Mathematical analyses of the evaporative processo of a new technological treatment of rising damp in historic buildings. Building and Environment 45, p. 2414-2420, 2010.

[Gro12] Groot, Caspar; van Balen, Koen; Bicer-Simsir, Beril; et al. RILEM TC 203-RHM: Repair mortars for historic masonry Performance requirements for renders and plasters Materials and Structures Volume: 45 Issue: 9 Pages: 1277-1285 Published: 2012. DOI: 10.1617/s11527-012-9916-0.

[Hee95] R.P.J. van Hees, J.A.G. Koek, Treatment of Rising Damp. A Laboratory Evaluation Method, Proceedings of the International Colloquium on Methods of Evaluating Products for the Conservation of Porous Building Materials in Monuments, Rome, pp 403-418, June 1995

[Hee96] R.P.J. van Hees, Koek J.A.G., Treatment of Rising Damp. Evaluation of six chemical products, Proceedings 8th International Congress on Deterioration and Conservation of Stone, Berlin, pp 1435-1446, 1996.

[Hee03a] van Hees R.P.J. - Zoutschade Curaçao, fase IV, TNO report 2003-BS-R0014, 2003.

[Hee07a] van Hees R.P.J., Naldini S. - Compatibility of plasters and renders with salt loaded substrates in historic buildings, Comunity research - Compass final report, p. 8-23, Contract n. EVK4–CT–2001–0047, 2007.

[Hee09a] van Hees R.P.J., Naldini S., Rodrigues J. D. - Plasters and renders for salt laden substrates, Construction and Building Materials, 23 (5), p. 1714-1718, 2009.

[Hee09a] van Hees R.P.J., Lubelli B. - Desalination of historic masonry. In: Proceedings of the 8th International Symposium on the Conservation of Monuments in the Mediterranean Basin, Patras, 2010, Vol III, pp 308-317, Technical Chamber of Greece, 2013

[Hee12] van Hees R.P.J. – Repair mortars for historic masonry. From problem to intervention: a decision process. Materials and structures, RILEM TC 203-RHM: Repair mortars for historic masonry, 45, pp 1295-1302, 2012.[Hen01] Henriques, Fernando – Humidade em paredes (2ª edição). Lisboa: LNEC, 2001.

[Hug03a] Hughes J., VÁLEK J. - Mortars in historical buildings. A review of the conservation, technical and scientific literature. Edinburgh, Scotland: Technical Conservation, Research and Education Division—Historic Scotland, 2003.

[Hug02a] Hughes D.C, Sugden D.B. - The use of brick dust as a pozzolanic addition to hydraulic lime mortars. International RILEM Workshop on Historic Mortars: Characteristics and Tests. Proceeding PRO12, Eds. P. Bartos, C. Groot, J.J. Hughes, p. 351-359, 2000.

[Hui07] Henk Huinink, Jelena Petkovic, Leo Pel, Klaas Kopinga - Water and salt transport. Final Report, COMPASS project EVK4-CT-2001-00047: Compatibility of plasters with salt loaded substrates in historic buildings, Edit R.P.J. van Hees, S. Naldini, 2007.

[Iza09] Izaguirre A., Lanas J., Álvarez J.I. - Effect of water-repellent admixtures on the behaviour of aerial lime-based mortars. Cement and Concrete Research 39, p.1095-1104, 2009.

[Lan03a] Lanas J.; Alvarez J.I. - Masonry repair lime-based mortars: Factors affecting the mechanical behaviour. Cement and Concrete Research, 33, p. 1867-1876, 2003.

[Lub06a] Lubelli Barbara - Sodium chloride damage to porous building materials. PhD Thesis. Delft University of Technology, Delft 2006.

[Lub06b] Lubelli B., van Hees R.P.J., Groot C.J.W.P. - Sodium chloride crystallization in a salt transporting restoration plaster. Cement and Concrete Research, 36, p.1467–1474, 2006.

[Lub07] Lubelli B., Van Hees R., Huinink H. - Effect of NaCl on Hydric and Hygric behaviour of lime-cement mortar. In C.J.W.P. Groot, R.P.J. van Hees eds., Special Issue COMPASS, Heron, volume 51, no. 1, 2006 (publ. 2007).

[Lub08a] Lubelli B., Van Hees, Rob P.J. - Sodium chloride damage to porous building materials: effect of RH changes. International Conference: SWBSS - Salt Weathering on Buildings and Stone Sculptures, October 22-24, The National Museum, Copenhagen, Denmark, 2008.

[Lub09] Lubelli B., Rooij M.R. - NaCl crystallization in restoration plasters. Construction and Building Materials, 23, p. 1736-1742, 2009.

[Lub09] Lubelli B., Hees van R.P.J. - Desalination of masonry structures. Fine tuning of poultice pore size distribution to substrate properties, Journal of Cultural Heritage (2009), on line: http://dx.doi.org/10.1016/j.culher.2009.03.005

[Lub13] Lubelli B., van Hees R.P.J., Hacquebord A. (2013), Experimental study of the distribution of chemical products against rising damp in substrates with different water saturation degrees, Construction and Building Materials 40 891–894.

[Lux07a] Luxán M., Dorrego F., Dorrego J. – Render and plaster system with new designed water-repelling mortars to prevent damage caused by moisture and salt loaded substrates. Final Report COMPASS: Compatibility of plasters with salt loaded substrates in historic buildings, Edit R.P.J. van Hees, S. Naldini, p. 44-54, 2007.

[Mag02a] Magalhães, Ana Cristian - Patologia de rebocos antigos. Cadernos de Edifícios, nº 2. Lisboa: LNEC, Outubro 2002 (Old renders pathology, in Portuguese).

[Mag05a] Magalhães A.C., Veiga M.R. - Estudo comparativo de possíveis soluções de argamassas para revestimentos de paredes de edifícios antigos. In 1º Congresso Nacional Argamassas de Construção, Lisboa, Portugal: APFAC, 2005 (Comparative study concerning renders for historic buildings, in Portuguese).

[Mag06a] Magalhães A.C., Veiga M.R., Cartaxo F. – Characterization of lime mortars with water repellent for use on ancient buildings. 7th International Brick Masonry Conference (7 IBMAC). London, October 30 to November 1, 2006.

[Mag08a] Magalhães A.C., Veiga M.R., Santos D. – Caracterização experimental de argamassas de reboco com aditivo pozolânico para paredes de edifícios antigos. Lisboa: LNEC, Relatório

171/2008 – NRI, 2008 (Experimental characterization of mortars with pozzolanic addition to be use in historic masonries, in Portuguese).

[Mag08b] Magalhães A.C., Veiga M.R., Pina dos Santos C. – Metodologia de diagnóstico de anomalias devidas à humidade em paredes antigas. Lisboa: LNEC, Relatório 115/2008 – NRI, 2008 (Humidity diagnosis methodology for historic masonry, in Portuguese).

[Mag09a] Magalhães A., Veiga M.R. – Physical and mechanical characterisation of ancient mortars. Application to the evaluation of the state of conservation. Materiales de Construcción, Vol 59 (295), p. 61-77, 2009 (doi: 10.3989/mc.2009.41907).

[Mal88a] Malinowski R. – Durable prehistoric ancient mortars and concretes. In Geopolymer 88, vol. 2. Compiègne, France: Université de Technologie de Compiègne, 223, 1998.

[Mar03a] Maravelaki-Kalaitzaki P., Bakolas A., Moropoulou A. - Physico–chemical study of Cretan ancient mortars. Cement and Concrete Research 33:651–661, 2003.

[Mar97a] Margalha, Goreti - O uso da cal em argamassas no Alentejo. University of Évora Master's thesis. Évora, Portugal, 1997.

[Mar06a] Margalha M.G., Veiga M.R., Brito J. - Algumas vantagens do uso da cal em pasta em revestimentos. PATORREB 2006, V. Peixoto Freitas, V. Abrantes and C. D. Goméz, p. 283–293. Porto, Portugal, 2006 (Advantages of lime putty based renders, in Portuguese).

[Mar09] Margalha M.G. - Ligantes aéreos minerais. Processos de extinção e o factor tempo na sua qualidade. PhD Thesis. Universidade Tecnica de Lisboa, Instituto Superior Tecnico, 2009 (Mineral binders: importance of extinsion processes and time for their quality, in Portuguese).

[Mas93] Massari, Giovanni and Ippolito – Damp Buildings. Old and new. Roma: International Centre for the Study of the Preservation and the Restoration of Cultural Property (ICCROM), 1993.

[Mat07a] Matias L., Magalhães A.C., Vilhena A., Pina dos Santos C.A., Veiga M.R. – Ensaio de capilaridade e análise termográfica para visualização da secagem de um murete de alvenaria de pedra. Lisboa, LNEC: Relatório 22/2007 – NRI, 2007 (Capillarity test and termografy for the analyses of drying of a small scale masonry, in Portuguese).

[Mat10a] Matias, Luís; Magalhães,Ana; Pina dos Santos, C.A.; Veiga, M.R. - Estudo de avaliação do estado higrotérmico de uma parede de alvenaria de pedra utilizando sondas miniaturas termohigrométricas e um humidimetro. Lisboa: Laboratório Nacional de Engenharia Civil (I&D EDIFÍCIOS, NRI Report 138/2010 – NRI), 2010 (Study for hygrotermal evaluation of a full scale masonry wall using hygrothermal and humidimeter probes, in Portuguese).

[Mor98a] Moropoulou A., Bakolas A. - Range of acceptability limits of physical, chemical and mechanical characteristics deriving from the evaluation of historic mortars. In Proceedings of the Compatible Materials Recommendations for the Preservation of European Cultural

heritage, ed. G. Biscontin et al, p. 165–178. Athens, Greece: National Technical University, 1998.

[Mor04a] Moropoulou A., Bakolas A., Aggelakopoulou E. - Evaluation of pozzolanic activity of natural and artificial pozzolans by thermal analysis. Thermochimica Acta, 2004, 420, p. 135-140, 2004.

[Mor05a] Moropoulou, A., Bakolas A., Moundoulas P., Aggelakopoulou E. - Reverse Engineering: a proper methodology for compatible restoration mortars. In Proceedings of Workshop Repair Mortars for Historic Masonry, TC RMH. Delft, The Netherlands: RILEM, January 25–28, 2005.

[Mor05b] Moropoulou A., Bakolas A., Moundoulas P., Aggelakopoulou E., Anagnostopoulou S. - Strength development and lime reaction in mortars for repairing historic masonries. Cement and Concrete Composites 27, p. 289–294, 2005.

[Mos06a] Mosquera M.J., Silva B., Prieto B., Ruiz-Herrera - Addition of cement to lime–based mortars: Effect on pore structure and vapour transport. Cement and Concrete Research 36, p. 1635–1642, 2006.

[Oli06a] Oliveira D.V., Silva R., Garbin E. – Comportamento de paredes antigas de alvenaria de panos múltiplos. Guimarães: Universidade do Minho, Relatório 06-DEC/E-14, 2006 (Behaviour of historic masonry with several render layers, in Portuguese).

[Ott07a] Ottosen L., Pedersen A. Rörig-Dalgaard – Salt-related problems in brick masonry and electrokinetic removal of salts. Journal of Building Appraisal, 0, p. 1-14, 2007.

[Ott07b] Ottosen L., Rörig-Dalgård I. - Electrokinetic removal of (CaNO3)2 from bricks to avoid salt induced decay. Electrochim Acta 52 (10), p. 3454-3463, 2007.

[Ott08a] Otossen L., Rorig-Dalgaard I., Villumsen A. - Electrochemical removal of salts from masonry: Experiences from pilot scale. International Conference on Salt Weathering on Buildings and Stone Sculptures (SWBSS). Copenhagen, Denmark, National Museum, 22 to 24 October, p. 341-350, 2008.

[Ott08b] Ottosen L., Chrostensen I., Rörig-Dalgaard I., Jensen P.E., Hansen H.K. - Journal of Environmental Science and Health Part A, 43, p. 795-809, 2008.

[Ott09a] Ottosen L., Ferreira C., Christensen, I. - Electrokinetic desalination of glazed ceramic tiles – preliminary results. International Seminar on Conservation of Glazed Ceramic Tiles. Research and Practice, April 15-16, National Laboratory of Civil Engineering, Lisbon, Portugal, 2009.

[Ott09b] Ottosen L., Rörig-Dalgaard II. - Desalination of a brick by application of an electric DC field. International Journal of Materials and Structures, Vol. 42, p. 961–971, 2009.

[Ott12a] Ottosen L., Christensen I. - Electrokinetic desalination of sanstones for NaCl removal – Test of different clay poultices at the electrodes. Electrochimica Acta, 86, p. 192-202, 2012.

[Pal92] Palma J., Leite D. – Aparelho Detector de Humidade no Betão com Base na Variação da Condutibilidade. Lisboa, LNEC, Report 56/92-GEEt, 1992 (Equipment for humidity detection in concrete, based on the conductivity variation, in Portuguese) .

[Pal95] Palma, J. – Incorporação de capacidades de Data-Logging no aparelho detector de humidade no betão. Lisboa, LNEC, Report 355/95-CPCE, 1995 (Incorportaion of data-logging in the equipment for humidity detection for concrete, in Portuguese), .

[Pal01] Palma, J. – Novo sistema de aquisição de dados para sondas de penetração de humidade em argamassa e betão. Lisboa, LNEC, Report 355/01-CPCE, 2001 (System for data assessment for humidity probes used on concrete, in Portuguese).

[Pap98a] Papayianni I. - Criteria and methodology for manufacturing compatible repair mortars and bricks. In Proceedings of the Compatible Materials Recommendations for the Preservation of European Cultural Heritage, ed. G. Biscontin et al, p. 179–190. Athens, Greece: National Technical University, 1998.

[Pap03a] Papayianni I., Stefanidou M. - Mortars for interventions in monuments and historic buildings. Advances in Architecture 15, p. 57–64, 2003.

[Pap08] Papayianni I., Pachta V. - Damages of old Lighthouses and their repair. Medachs - Construction heritage in coastal and marine environments: Damage, diagnostics, maintenance and rehabilitation. Lisbon, Portugal: Laboratório Nacional de Engenharia Civil (LNEC), january 2008.

[Pel04] L. Pel, H. Huinink, K. Kopinga, R.P.J. van Hees, O.C.G. Adan - Efflorescence pathway diagram: understanding salt weathering. Construction and Building Materials 18, p. 309–313, 2004.

[Pen08a] Penas F., R. Veiga, and A. Gomes - Hydraulic lime mortars to use in old buildings: advantages and drawbacks. In HMC08—1st Historical mortars conference 2008: Characterization, diagnosis, conservation, repair and compatibility, Lisbon, Portugal, Lisbon, Portugal: Laboratório Nacional de Engenharia Civil (LNEC), September 24–26, 2008.

[Pet10] Petković J., Huinink H.P., Pel L., Kopinga K., van Hees R.P.J. - Moisture and salt transport in three-layer plaster/substrate systems. Construction and Building Materials, 24, p. 118-127, 2010.

[Rie94] Riecke E. - Ueber das Gleichgewicht zwischen einem festen, homogeny deformirten Koeper und einer flussigen Phase, insbesondere uber die depression des Schmelzpunctes durch eiseitige Spannung, Nachrichten von der (koniglichen) gesellschaft der wissens, p. 278-284, 1894.

[Rij04] Rijniers L.A. - Salt crystallization in porous materials: an NMR study. PhD Thesis. Technical University of Eindhoven, 2004.

[Rod98a] Delgado Rodrigues, J. - In the search for tentative recommendations regarding compatible restoration mortars. In Proceedings of Pact 56: Compatible Materials for the Protection of European Cultural Heritage. Athens, Greece: Technical chamber of Greece, p. 141–147, 1998.

[Rod99] Rodriguez-Navarro C., Dohene E. - Salt weathering: influence of evaporation rate, Supersaturation and crystallization pattern. Earth Surface Processes and Landforms 24, p. 191-209, 1999.

[Rod05a] Delgado Rodrigues J., Gonçalves T., Luxan M.P., Vergès-Belmin V., Wijffels T., Lubelli B. - A proposal for classification of salt crystallization behavior of plasters and renders. End reports COMPASS project EVK4-CT-2001-00047, 2005.

[Rod07a] Delgado Rodrigues J., Gonçalves T., Luxán M.P., Vergès-Belmin V., Wijffels T., Lubelli B. - A proposal for classification of salt crystallization behaviour of plasters and renders, in Compatibility of plasters and renders with salt loaded substrates in historic buildings, Final report EU Contract no. EVK4-CT-2001-00047, (Ed. R.P.J. van Hees and S. Naldini), p. 172-186, 2007.

[Rör08a] Rörig-Dalgaard I., Ottosen L.M. - Method and Devise for Removing an Ionic Impurity from building structures (Pub. No. WO/2009/124890), 2008.

[Rör09a] Rörig-Dalgaard I. - Preservation of masonry with electrokinetics - with focus on desalination of murals, Ph.D Thesis, Department of Civil Engineering, Technical University of Denmark, 2009.

[Sab01a] Sabir S.S., Wild S., Bai J. - Metakaolin and calcined clays as pozzolans for concrete: a review, CEm. Concr. Compos., 23, p. 441–454, 2001.

[San02a] Santos Silva A. - Caracterização de argamassas antigas – casos paradigmáticos, eds Cadernos de Edifícios, Lisboa, 2, p. 87-101, 2002 (Historic mortars characterization – paradigmátic cases, in Portuguese).

[San06a] Santos Silva A., Ricardo J.M., Salta M., Adriano P., Mirão J., Estevão Candeias A. - Characterization of Roman mortars from the historical town of Mértola. In Proceedings of the International Conference on Heritage, Weathering and Conservation, ed. Fort, A. de Buergo, Gomez-Heras and V. Calvo, p. 85–90. Madrid, Spain, 2006.

[San10] A. Santos Silva,G. Borsoi, R. Veiga, A. Fragata, M. Tavares, F. Llera, B. Barreiros, T. Teixeira - Physico-chemical characterization of the plasters from the church of Santissimo Sacramento in Alcântara, Lisbon. 2nd Conference on Historic Mortars – HMC 2010 and RILEM TC 203-RHM final workshop (Ed. J. Válek, C. Groot and J.J. Hughes), RILEM Book series, p. 345-357, 2010.

[Saw08a] Sawdy A., Heritage A.,Pel L. - A review of salt transport in porous media, assessment methods ans salt reduction treatments. International Conference on Salt Weathering on Buildings and Stone Sculptures (SWBSS). Copenhagen, Denmark, National Museum, 22 to 24 October, p. 1-28, 2008.

[Ser87] Serry M.A., El-Didamong H., El-Kader A.A.A.Abd – Influence of calcinations conditions on the hydration of metakaolin-lime, Silic. Ind. 5-6, p. 83-87, 1987.

[Sch04] Scherer G. W. - Stress from crystallization of salt, Cement and concrete research, 34, p. 1613-1624, 2004.

[Sch06] Scherer G.W. – Internal stress and cracking in stone and masonry. Measuring, Monitoring and Modeling Concrete Properties, p. 633–641, 2006.

[Sch99] Scherer G. W. - Crystallization in pores. Cement and Concrete Research 34, p. 1613-1624, 1999.

[Sil93] Silva P.S., Glasse F.G. – Phase relation in the system CaO-Al2O3-SiO2-H2O relevant to metakaolin-calcium hydroxide hydration, Cem. Concr. Res., 23 (3), p. 627–639, 1993.

[Ste05a] Steiger M. - Crystal growth in porous materials – II: Influence of crystal size on the crystallization pressure. Journal of Crystal Growth 282, p. 470-481, 2005.

[Ste05b] Steiger M. - Crystal growth in porous materials - II: influence of crystal size on the crystallization pressure. Journal of Crystal Growth 282, p. 470-481, 2005.

[Ste05c] Stefanidou M., Papayianni I. – The role of aggregates on the structure and properties of lime mortars. Cement and Concrete Composites, 27, p. 914-919, 2005.

[Ste08] Steiger M., Asmussen S. – Crystallization of sodium sulphate phases in porous materials: The phase diagram Na2SO4-H2O and the generation of stress. Geochimica et Cosmochimica Acta 72, p. 4291-4306, 2008.

[Ste11] Steiger M., Charola A.E., Sterflinger K. - Weathering and deterioration. In:Siegesmund S., Snethlage R. (eds.) Stone in architecture: Properties, durability,Springer, Heidelberg, p. 227-316, 2011.

[Tav08a] Tavares M., Veiga M.R., Fragata A., Aguiar J. - Consolidation of renderings simulating stone in the façade of LNEC's building. In: International Symposium, EU-ARTECH: Stone consolidation in cultural heritage - Research and practice. Lisboa: LNEC, Lisbon, Portugal, May 6–7, 2008.

[Tav08b] Tavares M., Magalhães A.C., Veiga M.R., Velosa A.L., Aguiar J. 2008b, 'Repair mortars for a maritime fortress of the XVII century'. Proc. Medachs - Construction heritage in coastal and marine environments: Damage, diagnostics, maintenance and rehabilitation. Lisbon, Laboratório Nacional de Engenharia Civil (LNEC), Portugal, January 2008.

[Tav07a] Tavares, M. and Veiga, M.R. – A conservação de rebocos antigos - restituir a coesão perdida através da consolidação com materiais tradicionais e sustentáveis. (Conservation of old renders – restitution of cohesion by consolidation with traditional and sustainable materials). VII SBTA, Recife, Brasil, 2007 (Conservation of historic mortars – cohesion restituion through the use of traditional and compatible products, in Portuguese).

[Tav09a] Tavares, Martha – A conservação e o restauro de revestimentos exteriores de edifícios antigos: Uma metodologia de estudo e reparação. PhD thesis, Technical University, Architectural Faculty of Lisbon, 2009 (Conservation and restaur of historic renders: a methodology for their sutyd and repair, in Portuguese).

[Tho62] J. Thomson - On crystallization and liquefaction, as influenced by stress tending to change of forms in crystals, Philosophical Magazine 24, (162), p. 395-401, 1862.

[Tor07] Torres, M. Isabel; Freitas, Vasco P – Treatment of rising damp in historical buildings: wall base ventilation. Building and environment 42, p. 424-435, 2007.

[Val00a] Valek J., Hughes J.J., Bartos P.J.M. - Compatibility of historic and modern lime mortars. In Proceedings of the 12th International Masonry Conference, p. 1839–1851, Madrid, Spain, 2000.

[Vel01a] Velosa A.L., Veiga M. R. - The use of pozzolans as additives in lime mortars for employment in building rehabilitation. In International Seminar Historical Constructions 2001. Guimarães: Universidade do Minho, November 2001.

[Vel05a] Velosa A.L., M.R. Veiga - Pozzolanic materials. Evaluation of mechanical properties. In International building lime symposium. Orlando, FL., 2005.

[Vel05b] Velosa A., Coroado J., Veiga M.R., Rocha F. - Characterisation of Roman mortars from Conímbriga in view to their repair. 10th Euroseminar on microscopy applied to building materials, p. 1208–1216. Paisley, Scotland, June 21–25, 2005.

[Vel06a] Velosa, Ana Luísa - Argamassas de cal com pozolanas para revestimento de paredes antigas. University of Aveiro Doctoral thesis. Aveiro, Portugal, 2006 (Lime mortars with pozzolans for historic masonry walls, in Portuguese).

[Vel07a] Velosa A.L., Coroado J., Ferreira V., Veiga R. - Monitoring of pozzolanic reaction of different pozzolanic materials in lime–pozzolan pastes. Materiais 2007. Porto, Portugal, April 1–4, 2007.

[Vel07b] Velosa A., Veiga M.R. - Utilização de um sub–produto industrial como aditivo em argamassas de cal. VII Seminário Brasileiro de Tecnologia de Argamassas, Recife, Brasil: SBTA, 2007 (Use of na industrial sub-product as additive for lime mortars, in Portuguese).

[Vel09a] Velosa A.L., Rocha F., Veiga M.R. – Influence of chemical and mineralogycal composition of mekaolin on mortars characteristics. Acta Geodyn. Geomater., Vol. 6, No. 1 (153), p. 121–126, 2009.

[Vei94a] Veiga M.R., Carvalho F. - Argamassas de revestimento na reabilitação do património urbano. In 2nd ENCORE Enc. Conservação e Reabilitação de Edifícios, vol. 1, Lisbon, Portugal: Laboratório Nacional de Engenharia Civil (LNEC), p. 195–206, 1994 (Renders for built heritage conservation, in Portuguese).

[Vei98] Veiga M.R., Carvalho F. - Some performance characteristics of lime mortars for use on rendering and repointing of ancient buildings. Proceedings of the 5th International Masonry Conference. London, October 1998.

[Vei00] Veiga, M.R. - Protecção contra a água de paredes de edifícios antigos. Avaliação experimental da capacidade de protecção de argamassas de reboco com base em cal. Proceedings of Encontro Nacional sobre Conservação e Reabilitação de Estruturas – REPAR 2000. Lisboa, LNEC, June 2000 (Protection against moisture in historic buildings: experimental evaluation of the protection capacity of lime based renders, in Portuguese).

[Vei01a] Veiga M.R., Aguiar J., Santos Silva A., Carvalho F. - Methodologies for characterisation and repair of mortars of ancient buildings. International seminar historical constructions, ed. P. Lourenço and P. Roca, p. 353–362. Guimarães, Portugal, Universidade do Minho, 2001.

[Vei02a] Veiga M.R., Carvalho F. – Argamassas de reboco para paredes de edifícios antigos. Requisitos e características a respeitar. Caderno de edifícios n.º 2, Lisbon, LNEC, 2002 (Renders for historic buldings: requirements and characteristics, in Portuguese).

[Vei02b] Veiga M.R., Tavares M. - Características das paredes antigas. Requisitos dos revestimentos por pintura (Characteristics of ancient walls. Requirements of the render painting), Lisbon, eds APTETI, October 2002 (Historic walls characteristics: requirements of paint as finishing, in Portuguese).

[Vei04a] Veiga M.R. – Conservação e renovação de revestimentos de paredes de edifícios antigos. Lisboa: LNEC, Colecção Edifícios, CED9, Julho de 2004 (Conservation and replacement of renders for historic buildings, in Portuguese).

[Vei05a] Magalhães A.C., Veiga M.R., Costa D.– Caracterização do estado de conservação de revestimentos de paredes antigas através de ensaios in situ. Dois casos de estudo. VI Simposio Brasileiro de Tecnologia de Argamassas. Florianopolis, Brasil, 23 a 25 de Maio de 2005 (Characterization of the conservation state of render by in situ tests, in Portuguese).

[Vei07a] Veiga M.R., Velosa A.L., Magalhães A.C. - Evaluation of mechanical compatibility of renders to apply on old walls based on a restrained shrinkage test. Materials and Structures 10(40), p. 1115–1126, 2007.

[Vei07b] Veiga M.R., Tavares M., Magalhães A.C. - Restauro da fachada em marmorite de cal do Laboratório Nacional de Engenharia Civil, em Lisboa. Materiais, métodos e resultados. Conference. In VII Simposio Brasileiro de tecnologia de argamassas (SBTA). Recife, Brasil: SBTA, 2007 (Restoration of “marmorite” facade of National Laboratory for Civil Engineering, in Portuguese).

[Vei07c] Veiga, Maria do Rosário – Conservação e reparação de revestimentos de paredes de edifícios antigos: Métodos e materiais. Programa de Investigação e Programa de Pós-graduação apresentados para a obtenção do título de Habilitação para o Exercício de Funções de Coordenação de Investigação Científica. Lisboa, LNEC, I&D Programa de Investigação Edifícios, 2007 (Conservation and restoration of historic mortars: methods and materials, in Portuguese).

[Vei08a] Veiga M.R., Fragata A., Velosa A., Magalhães A.C., Margalha G. - Substitution mortars for application in historical buildings exposed to the sea environment. Analyses of the viability of several types of compositions. Proceedings of MEDACHS 08—Construction Heritage in Coastal and Marine Environments, January 28–30. Lisbon, Portugal: LNEC, 2008.

[Vei09a] Veiga M.R. - Characteristics of repair mortars for historic buildings concerning water behaviour. Quantification and requirements. Actas do Workshop Repair Mortars for Historic Masonry, TC RMH. Delft, RILEM, 25-28 de Janeiro de 2005. RILEM, 2009, p. 305-315, e-ISBN: 978-2-35158-083-7.

[Vei09b] Veiga R., Fragata A., Tavares M., Magalhães A.C., Ferreira N. - Inglesinhos Convent: Compatible renders and other measures to mitigate water capillary rising problems. Journal of Building Appraisal, 5, No 2, p. 171-185, 2009.

[Vei09c] Veiga M.R., Velosa A.L., Magalhães A.C. - Experimental applications of mortars with pozzolanic additions: Characterization and performance evaluation. Construction and Building Materials 23, p. 318–327, 2009.

[Vei09e] Veiga M.R., Fragata A., Tavares M. - Gama de valores obtidos em argamassas de cal aplicadas na EENRevPa – LNEC, Lisboa, 2009 (Relatório não editado) (range of values for lime mortars at EENRevPa – LNEC, in Portuguese).

[Vei09f] Veiga R., Fragata A., Tavares M., Magalhães A.C., Ferreira N. - Inglesinhos Convent: Compatible renders and other measures to mitigate water capillary rising problems. 3º Encontro sobre Patologia e Reabilitação de Edifícios (PATORREB), Porto, FEUP, 2009.

[Vei10a] Veiga M.R., Fragata A., Velosa A.L., Magalhães A.C., Margalha G. - Lime based mortars: discussion of their viability to be used as substitution renders in historical buildings. International Journal of Arquitectural Heritage: Conservation, analysis and restoration, vol. 4, issue 2, p. 177-195, 2010.

[Vei10b] Veiga M.R., Tavares M. – Pousada de Tavira: Parecer sobre as anomalias construtivas nos revestimentos exteriores de paredes (in Portuguese). Lisboa: LNEC, Março 2010. Confidential Report 98/2010 – NRI (Tavira Charming Hotel: Report concerning the renders anomalies, in Portuguese).

[Ver07a] Vergès-Belmin V., Wijffels T., Gonçalves T., Nasraoui M. - The compass salt crystallization test (compass-test) as a way to figure out how salts migrate and accumulate in renovation plasters, Compass end-report, p. 160-171, 2007.

[Ver08] V. Vergès_Belmin (ed.), ICOMOS Illustrated glossary on stone deterioration patterns, ICOMOS International Scientific Committee for Stone (ISCS), 2008.

[Vil07a] Vilhena A., Matias L.M., Magalhães A.C., Pina dos Santos C.A., Veiga M.R. – Análise termográfica para visualização da absorção de água salina e da secagem de murete de alvenaria de pedra: ensaio de capilaridade. Lisboa: LNEC, Relatório 241/2007 – NRI, 2007 (Thermographic analysis for salt solution absorption and drying of a small scale masonry, in Portuguese).

[Von97a] Von Konow T. - Reliable restoration mortars— requirements and composition. In Proceedings of the 4th International Symposium on the Conservation of Monuments in the Mediterranean, vol. 3, eds. A. Moropoulou, F. Zezza, E. Kolias, and I. Papachristodoulou, Rhodes, Greece, p. 415–425, 1997.

[Wel65] Wellman H., Wilson W. - Salt weathering, a neglected geological erosive agent in coastal and arid environments, “Nature”, no. 4976, , pp.1097-1098, March 1965.

[Wij07a] Wijffels T., Groot C., van Hees R.P.J. - Risk factors: practical priorities and a selection tool for the application of restoration plasters. Final Report, COMPASS: Compatibility of plasters with salt loaded substrates in historic buildings, Edit R.P.J. van Hees, S. Naldini, 2007.

[Wij05] Wijffels T., Lubelli B. - Development of a new accelerated crystallization test. End reports COMPASS project EVK4-CT-2001-00047, 2005.

[Wij02] Wijffels T.J., van Hees R.P.J. - Salt transport in restoration plaster, TNO report 2001-BS-R0400, 2002.

[Wij97a] T.J. Wijffels, C.J.W.P. Groot, R.P.J. van Hees - Performance of restoration plasters in: 11th International brick/block masonry conference, Shangai, p. 1050-1062, 1997.

[Yu10] Yu S., Oguchi C.T. - Role of pore size distribution in salt uptake, damage, and predicting salt susceptibility of eight types of Japanese building stones. Engineering Geology, vol. 115, p. 226-236, 2010.

[You08] Young D. - Salt attack and rising damp: a guide for salt damp in historic and older buildings. Technical guide, Heritage Council of NSW, Heritage Victoria, South Australian Department for Environment and Heritage and Adelaide City Council, 2008.

[Zeh89] Zehnder K, Arnold A., Crystal Growth in salt efflorescence. American Chemical Society, Journal of Crystal Growth 97, p. 513-521, 1989.

Standards and Test specification

[IPQ2002] IPQ, NP EN 459-1:2002 - Cal de construção. Parte 1 - Definições, especifícações e critérios de conformidade. Monte da Caparica.

[IPQ2011] IPQ, NP EN 459-1:2011 - Cal de construção. Parte 1 - Definições, especifícações e critérios de conformidade. Monte da Caparica.

[LNEC1999] LNEC 26 FE Pa-38 - Test Specification Sheet Revestimentos de paredes: Caracterização da capacidade de impermeabilização. Laboratório Nacional de Engenharia Civil (LNEC). Lisbon, LNEC, May 1999.

[LNEC05] VEIGA, R. Regras para concessão de Documentos de Aplicação a revestimentos pré-doseados de ligante mineral com base em cimento para paredes. Lisbon, LNEC, December 2005. Report 427/05-NRI.

[RILEM1980] RILEM – Water absorption under low pressure. Pipe method. Test Nº II.4, Tentative Recommendations. Paris: RILEM, 1980.

[ÖNORM1999] Österreichisches Normungsinstitut, ÖNORM B 3355-1, Trockenlegung von feuchten Mauerwerk-Bauwerksdiagnostik and Planungsgrundlagen, 1999.